

# **For Reference**

---

**NOT TO BE TAKEN FROM THIS ROOM**

Ex LIBRIS  
UNIVERSITATIS  
ALBERTAEISIS





Digitized by the Internet Archive  
in 2019 with funding from  
University of Alberta Libraries

<https://archive.org/details/Currie1984>







THE UNIVERSITY OF ALBERTA

RELEASE FORM

NAME OF AUTHOR

Ronald W. Currie

TITLE OF THESIS

An Investigation of the State of Water in Early  
Postmortem Beef Muscle

DEGREE FOR WHICH THESIS WAS PRESENTED Doctor of Philosophy

YEAR THIS DEGREE GRANTED Spring 1984

Permission is hereby granted to THE UNIVERSITY OF ALBERTA LIBRARY to reproduce single copies of this thesis and to lend or sell such copies for private, scholarly or scientific research purposes only.

The author reserves other publication rights, and neither the thesis nor extensive extracts from it may be printed or otherwise reproduced without the author's written permission.

~ ~



THE UNIVERSITY OF ALBERTA

An Investigation of the State of Water in Early Postmortem  
Beef Muscle

by

Ronald W. Currie

A THESIS

SUBMITTED TO THE FACULTY OF GRADUATE STUDIES AND RESEARCH  
IN PARTIAL FULFILMENT OF THE REQUIREMENTS FOR THE DEGREE  
OF Doctor of Philosophy

IN

Food Chemistry

Department of Food Science

EDMONTON, ALBERTA

Spring 1984



THE UNIVERSITY OF ALBERTA  
FACULTY OF GRADUATE STUDIES AND RESEARCH

The undersigned certify that they have read, and recommend to the Faculty of Graduate Studies and Research, for acceptance, a thesis entitled An Investigation of the State of Water in Early Postmortem Beef Muscle submitted by Ronald W. Currie in partial fulfilment of the requirements for the degree of Doctor of Philosophy in Food Chemistry.



## ABSTRACT

The state of water in muscle is important to all aspects of meat handling. The strength of water binding by the muscle proteins is of great importance for the quality of meat and meat products, as almost all procedures for the storage and processing of meat are influenced by the water holding capacity (WHC). As important as water is to the quality of meat, the factors immobilizing the water in muscle are not clearly understood.

The major thrust of this thesis has been to introduce and apply some new techniques to the study of changes in the muscle water of early postmortem beef. These techniques may assist in understanding some of the factors immobilizing the water in muscle. The principal method in this regard has been the examination of changes in the spin lattice relaxation times ( $T_1$ ) of the water protons as the muscle enters rigor. It has been found that the  $T_1$  measurement can detect changes in the muscle water during rigor development. Although there is a similarity in the  $T_1$  profile obtained from each carcass, there is a considerable carcass-to-carcass variability in the initial  $T_1$ , peak  $T_1$ , time to the peak  $T_1$ , and postpeak  $T_1$  slope. This variability in muscle water properties has been interpreted in terms of the rate of rigor development as measured by pH fall, ATP metabolism (as measured by an HPLC method developed during the course of the work), and isometric tension development.



Included in this study has been the development of a method in which the changes in the extracellular space are used to reveal the intrafibre water affinity of the early prerigor muscle. A term ECS app is used to describe the intrafibre water affinity. The smaller the value, the greater is the intrafibre water affinity of the muscle. Unfortunately, this method is only applicable to the early prerigor muscle since the membrane loses its functionality near rigor and cannot exclude the extracellular marker (inulin) which is needed to reliably measure ECS app. In the early prerigor period the ECS data suggest that the initial loss of intrafibre water affinity by the muscle is reversed, leading to an improvement in the intrafibre water affinity before it is lost again. Often this leads to a bimodal appearance of the ECS app versus time postmortem plot. This alteration in the muscle water properties has been used to explain some of the changes observed in the mechanical properties (tensile and adhesive) of early postmortem beef.

The variation in the isometric tension profile, in particular the maximum isometric tension, between carcasses has been interpreted as indicating differences in the inter-filamentous spaces of the muscle fibre. This observation has lead to the conclusion that factors affecting the inter-filamentous spacing have a pronounced affect on the WHC of meat. It has also been observed that the effect of ATP on muscle water properties is variable and supports the view that the hydrolysis of ATP itself is not the main reason for



postmortem alteration in WHC, but rather it is the development of rigor mortis initiated by the depletion of ATP that alters the postmortem WHC of muscle.



## ACKNOWLEDGEMENTS

I am very grateful to all those who provided assistance in the research and preparation of this thesis. First, I must thank Dr. F.H. Wolfe, my supervisor, for the direction, assistance and discussion provided during the course of this work. I am most appreciative of his interest in the development of my career over the past 15 years. Meat research in Dr. Wolfe's laboratory has lead to the investigation of many areas of meat science. One of the most interesting areas has been the role of water in meat, and thus the topic of this thesis.

I have appreciated and gained much from the contacts I have had with members of my supervisory examining committee [Dr. C.M. Kay (Biochemistry), Dr. R. Jordan (Chemistry), Dr. J.R. Thompson (Animal Science), and Dr. P. Sporns (Food Science)], whether it be through course work or through their assistance in the research performed. I am most grateful to Dr. R. Jordan for his early mornings and late nights to start and maintain the NMR portion of the experiments on the carcasses. I also appreciate his assistance in training me on the use of the NMR for the model system studies. I have valued the assistance of Dr. P. Sporns in the development of the HPLC method for the ATP metabolites. I wish to thank my external examiner, Dr. D.W. Stanley (Univ. of Guelph) for his constructive criticism and comments which I believe have contributed to the quality of this thesis.



During the course of this research I must express deep appreciation to the Food Science Department, without whose cooperation I would not have been able to have completed the work reported in this thesis. I am most grateful to Drs. F.H. Wolfe, H. Jackson and D. Hadziyev, whose recommendations assisted in my obtaining a Natural Sciences and Engineering Research Council Postgraduate Award (1980/81). Such financial assistance allowed me to focus my attention full time on the research at hand. An additional source of funding that came just at the right time was the Farming for the Future Award, which not only allowed me to complete the research but eased the financial burden of preparing the thesis.

During the course of the work, many other people provided assistance. Sharon Dubetz assisted in the study by freezing the samples for ATP analyses and performing the expressed juice measurements during the day a carcass was analyzed. Ian Duncan provided me access to the liquid scintillation counter in Plant Science. Len Steele has assisted not only in several of the APL computer programs used in the course of this work, but also kindly agreed to type the thesis into the computer and has graciously accepted the changes to the text that have been repeatedly coming to him. Dr. Nathan Aboagye made time to discuss with me the most appropriate statistical approach to the treatment of this data. Ray Weingardt (Animal Science) has also been most accommodating with his knowledge of



statistics and provided access to the computer program available for this purpose. Art Bates assisted with the graphics and must be commended for the speed with which he met the deadline set to complete the graphics. I also wish to express appreciation to the NAIT Chemical and Industrial Process Department with whom I am now employed, in particular Ed Raypold and Gerry Wyard-Scott, for their cooperation in my attending meetings that have been necessary for the completion of this thesis and for the use of the HPLC and integrator needed to complete some of the analyses.

Finally, I must acknowledge with deep appreciation the support of my family. My wife, Germaine, has had to bear with me since 1978 in my construction of our home, my enrolment in graduate studies, and our introduction to the parenting of our children, Desireé and Levi. She has been most helpful in keeping me organized and in the graphics presented in this thesis. My wife's parents should be acknowledged for their baby sitting services when it was imperative that work be done. I also want to acknowledge my parents, who instilled within me a good work ethic and for their guidance given. I deeply regret that my mother cannot share in the completion of this work since she was suddenly killed on Dec. 2, 1981 in an automobile accident.



## Table of Contents

Chapter	Page
I. INTRODUCTION .....	1
A. Structure and Composition of Muscle .....	1
B. Biochemical and Physiological Events Associated with Rigor-mortis .....	4
C. Postrigor Meat Quality .....	7
D. Methods of Assessing Meat Quality .....	11
E. Protein-Water Interactions .....	14
F. Methods of Examining the State of Water in Meat .....	17
G. Statement of the Problem .....	23
II. MATERIALS AND METHODS .....	26
A. Introduction .....	26
B. Methods Used to Monitor Rigor Development .....	27
Animals, muscle and muscle treatment .....	27
Fibre typing .....	28
pH measurements .....	30
Sarcomere length measurements .....	30
Isotonic contraction measurements .....	31
Isometric tension followed by unrestrained contraction measurements .....	32
Isometric tension measurements .....	33
Mechanical measurements .....	36
Other physical measurements of texture ...	37
Photography of muscle strips stretched to initial yield .....	38
Measurement of ATP and its metabolites .....	39



Mobile phase and chromatographic procedure .....	40
Preparation of meat samples for injection .....	41
Quantitation and standardization of ATP metabolites .....	41
Elution profiles .....	42
C. Methods Used to Monitor the State of Water .....	47
Nuclear magnetic resonance spectroscopy .....	47
Introduction .....	47
NMR T <sub>2</sub> determinations .....	51
NMR T <sub>1</sub> .....	51
NMR of model systems .....	61
NMR of aged and cooked meat samples .....	61
Other physical and chemical measurements related to water .....	62
Swelling capacity .....	62
Water holding capacity .....	62
Differential scanning calorimetry .....	65
Moisture determinations .....	66
Extracellular space measurements .....	67
III. RESULTS AND DISCUSSION .....	78
A. Introduction .....	78
B. Biochemical and Physiological Effects of Rigor Development .....	78
Fibre typing .....	78
pH fall .....	81
Isometric tension .....	100
Sarcomere measurements .....	102



Isotonic contraction .....	102
Mechanical measurements .....	109
Photographs of muscle fibres at initial yield .....	123
Conclusion .....	136
<b>C. State of Water in Muscle .....</b>	<b>137</b>
NMR T <sub>1</sub> .....	137
Expressed juice .....	159
Swelling capacity .....	167
Differential scanning calorimetry (DSC) ....	181
Extracellular space (ECS) measurements ....	184
Conclusion .....	188
<b>D. Interrelation of the Biochemical and Physiological Events in the Carcass and the State of Water in the Muscle .....</b>	<b>189</b>
Carcass 15 ( $\Delta T_1=0.105$ sec) .....	190
Carcass 10 ( $\Delta T_1=0.065$ sec) .....	194
Carcass 16 ( $\Delta T_1=0.060$ sec) .....	197
Carcass 13 ( $\Delta T_1=0.052$ sec) .....	203
Carcass 11 ( $\Delta T_1=0.040$ sec) .....	205
Carcass 14 ( $\Delta T_1=0.038$ sec) .....	208
Carcass 12 ( $\Delta T_1=0.037$ sec) .....	210
Carcass 8 ( $\Delta T_1=0.035$ sec) .....	212
Carcass 9 ( $\Delta T_1=0.035$ sec) .....	214
Carcass 17 ( $\Delta T_1=0.031$ sec) .....	215
Carcass 18 ( $\Delta T_1=0.020$ sec) .....	215
Statistical Correlations .....	217
Conclusion .....	225



IV. REFERENCES	234
V. Appendices	248
A. Mobile phase	248
B. Treatment of acid extracts	251
C. ATP metabolites	253
D. Carcass 4 ( $\Delta T_1=0.098$ sec)	285
E. Carcass 5 ( $\Delta T_1=0.038$ sec)	288
F. Carcass 6 ( $\Delta T_1=0.038$ sec)	290
G. Carcass 7 ( $\Delta T_1=0.017$ sec)	292
H. Pearson's correlation coefficients from parameters obtained from carcasses 9-18	294



## List of Tables

Table		Page
II.1	Reproducibility of extraction and chromatography of a 0.6 hr postmortem meat sample.....	43
III.1	Fibre typing data.....	79
III.2	pH response in postmortem muscle.....	82
III.3	Isometric tension data.....	101
III.4	Isotonic contraction data.....	106
III.5	14 day postmortem ST data.....	120
III.6	pH at peak T <sub>1</sub> compared to ultimate pH.....	138
III.7	Percent moisture and initial and peak T <sub>1</sub> ,.....	145
III.8	Data obtained for parameters tested for 32 carcasses.....	155
III.9	Correlation coefficients for the parameters tested in Table III.8.....	156
III.10	Pearson's correlation coefficients of selected variables from carcasses 9-18.....	218
V.1	Retention times of ATP degradation products'.....	250
V.2	Pearson's correlation coefficients of 36 selected variables from carcasses 9-18.....	296



## List of Figures

Figure		Page
II.1	Clamping device with clamps.....	34
II.2	Lucite cell used to support the clamping device.....	35
II.3	Elution profile of ATP and metabolites of early prerigor beef muscle.....	44
II.4	Elution profile of ATP and metabolites of mid prerigor beef muscle.....	45
II.5	Elution profile of ATP and metabolites of postrigor beef muscle.....	46
II.6	Plot of $\log(I_\infty - I_\tau)$ vs $\tau$ (s) for an NMR $T_2$ determination of 54 h beef muscle.....	52
II.7	Plot of $T_1$ (s) vs temperature ( $^{\circ}$ C) of rehydrated myofibrils.....	54
II.8	Plot of $\log(I_\infty - I_\tau)$ vs $\tau$ (s) using short $\tau$ values and long $\tau$ values.....	55
II.9	Plot of $\log(I_\infty - I_\tau)$ vs $\tau$ using long and short $180^{\circ}$ pulse lengths.....	58
II.10	Plot of $T_1$ (s) vs time postmortem for duplicate determinations from carcass A and carcass B.....	60
II.11	Plot of ECS app (mL/100 g) vs time postmortem.....	68
II.12	Plot of ECS app (mL/100 g) vs time postmortem using HEPES buffer and phosphate buffer.....	71
II.13	Plot of ECS app (mL/100 g) vs incubation time for prerigor muscle.....	72
II.14	Plot of ECS app (mL/100 g) vs incubation time for postrigor muscle.....	73
III.1	Plot of pH vs time postmortem for carcass 3, carcass 4, carcass 5 and carcass 6.....	82



Figure	Page
III.2 Plot of pH vs time postmortem for carcass 7 and carcass 8. Plot of expressed juice (%) vs time postmortem for carcass 7 and carcass 8.....	84
III.3 Plot of pH vs time postmortem for carcass 9. Plot of isometric tension vs time postmortem for carcass 9. Plot of expressed juice (%) vs time postmortem for carcass 9.....	85
III.4 Plot of pH vs time postmortem for carcass 10. Plot of isometric tension vs time postmortem for carcass 10. Plot of expressed juice (%) vs time postmortem for carcass 10.....	86
III.5 Plot of pH vs time postmortem for carcass 11. Plot of isometric tension vs time postmortem for carcass 11. Plot of expressed juice (%) vs time postmortem for carcass 11.....	87
III.6 Plot of pH vs time postmortem for carcass 12. Plot of isometric tension vs time postmortem for carcass 12. Plot of expressed juice (%) vs time postmortem for carcass 12.....	88
III.7 Plot of pH vs time postmortem for carcass 13. Plot of isometric tension vs time postmortem for carcass 13. Plot of expressed juice (%) vs time postmortem for carcass 13.....	89
III.8 Plot of pH vs time postmortem for carcass 14. Plot of isometric tension vs time postmortem for carcass 14. Plot of expressed juice (%) vs time postmortem for carcass 14.....	90
III.9 Plot of pH vs time postmortem for carcass 15. Plot of isometric tension vs time postmortem for carcass 15. Plot of expressed juice (%) vs time postmortem for carcass 15.....	91



Figure		Page
III.10	Plot of pH vs time postmortem for carcass 16. Plot of isometric tension vs time postmortem for carcass 16. Plot of expressed juice (%) vs time postmortem for carcass 16.....	92
III.11	Plot of pH vs time postmortem for carcass 17. Plot of isometric tension vs time postmortem for carcass 17. Plot of expressed juice (%) vs time postmortem for carcass 17.....	93
III.12	Plot of pH vs time postmortem for carcass 18. Plot of isometric tension vs time postmortem for carcass 18. Plot of expressed juice (%) vs time postmortem for carcass 18.....	94
III.13	Plot of sarcomere length vs time postmortem for an off-carcass sample and an on-carcass sample.....	103
III.14	Plot of % isotonic contraction vs time postmortem for muscle strips at several different loadings.....	104
III.15	Plot of % contraction vs time postmortem following the removal of the restraint to contract.....	108
III.16	Typical tensile response of a prerigor muscle strip.....	110
III.17	Typical tensile response of a near rigor muscle strip.....	111
III.18	Typical tensile response of a 14 day postrigor muscle strip.....	112
III.19	The tensile profile due to longitudinal stretch vs time postmortem.....	114
III.20	Tensile extensibility profile due to longitudinal stretch vs time postmortem.....	116
III.21	Adhesive profile due to stretch perpendicular to the fibre axis vs time postmortem of early postmortem beef muscle undergoing slow pH fall.....	117



Figure		Page
III.22	Adhesive profile due to stretch perpendicular to the fibre axis vs time postmortem of early postmortem beef muscle undergoing rapid pH fall.....	118
III.23	Adhesive extensibility profile due to stretch perpendicular to the fibre axis vs time postmortem of early postmortem beef muscle undergoing slow pH fall.....	121
III.24	Adhesive extensibility profile due to stretch perpendicular to the fibre axis vs time postmortem of early postmortem beef muscle undergoing rapid pH fall.....	122
III.25	A phase contrast micrograph of a muscle fibre (pH 6.25) fixed at initial yield.....	124
III.26	A phase contrast micrograph of a muscle fibre (pH 6.10) fixed at initial yield.....	125
III.27	A phase contrast micrograph of a muscle fibre (pH 5.95) fixed at initial yield.....	126
III.28	A phase contrast micrograph of a muscle fibre (pH 5.75) fixed at initial yield.....	127
III.29	A phase contrast micrograph of a muscle fibre (pH 5.65) fixed at initial yield.....	128
III.30	A phase contrast micrograph of a muscle fibre (pH 5.5) fixed at initial yield.....	129
III.31	A phase contrast micrograph of a muscle fibre (pH 5.6) fixed after stretching the fibre beyond initial yield.....	130
III.32	A phase contrast micrograph of a muscle fibre (postrigor) fixed at initial yield.....	131
III.33	A phase contrast micrograph of a muscle fibre (an on-carcass sample removed postrigor) fixed at initial yield.....	132
III.34	NMR T <sub>1</sub> profile for carcass 1, carcass 2, carcass 3, carcass 4, carcass 5 and carcass 6.....	139



Figure	Page
III.35 NMR T <sub>1</sub> profile for carcass 7, carcass 8, carcass 9, carcass 10, carcass 11 and carcass 12.....	140
III.36 NMR T <sub>1</sub> profile for carcass 13, carcass 14, carcass 15, carcass 16, carcass 17 and carcass 18.....	141
III.37 Plot of NMR T <sub>1</sub> vs pH of myofibrils at 82% moisture, 80% moisture and 78% moisture.....	148
III.38 Profile of NMR T <sub>1</sub> vs incubation time of myofibrils in the presence of ATP and 500 μM EGTA or 500 μM Ca <sup>2+</sup> .....	150
III.39 Plot of NMR T <sub>1</sub> vs pH for myofibrils in buffer, buffer plus EGTA and buffer plus Ca <sup>2+</sup> .....	153
III.40 Plot of planimeter area vs pH of meat homogenate for carcass 7.....	163
III.41 Plot of planimeter area vs pH of meat homogenate for carcass 8.....	164
III.42 Plot of planimeter area vs pH of meat homogenate for carcass 9.....	165
III.43 Plot of planimeter area vs pH of meat homogenate for carcass 10.....	166
III.44 Carcass 15. Plot of swelling capacity vs time postmortem. Plot of ECS dw vs time postmortem. Plot of ECS app vs time postmortem.....	168
III.45 Carcass 10. Plot of swelling capacity vs time postmortem. Plot of ECS dw vs time postmortem. Plot of ECS app vs time postmortem.....	169
III.46 Carcass 16. Plot of swelling capacity vs time postmortem. Plot of ECS dw vs time postmortem. Plot of ECS app vs time postmortem.....	170
III.47 Carcass 13. Plot of swelling capacity vs time postmortem. Plot of ECS dw vs time postmortem. Plot of ECS app vs time postmortem.....	171



Figure		Page
III.48	Carcass 11. Plot of swelling capacity vs time postmortem. Plot of ECS dw vs time postmortem. Plot of ECS app vs time postmortem.....	172
III.49	Carcass 14. Plot of swelling capacity vs time postmortem. Plot of ECS dw vs time postmortem. Plot of ECS app vs time postmortem.....	173
III.50	Carcass 12. Plot of swelling capacity vs time postmortem. Plot of ECS dw vs time postmortem. Plot of ECS app vs time postmortem.....	174
III.51	Carcass 8. Plot of swelling capacity vs time postmortem. Plot of ECS dw vs time postmortem. Plot of ECS app vs time postmortem...	175
III.52	Carcass 9. Plot of swelling capacity vs time postmortem. Plot of ECS dw vs time postmortem. Plot of ECS app vs time postmortem...	176
III.53	Carcass 17. Plot of swelling capacity vs time postmortem. Plot of ECS dw vs time postmortem. Plot of ECS app vs time postmortem.....	177
III.54	Carcass 18. Plot of swelling capacity vs time postmortem. Plot of ECS dw vs time postmortem. Plot of ECS app vs time postmortem.....	178
III.55	Plot of % nonfreezable water vs time postmortem for carcass 8, carcass 9, carcass 10 and carcass 18.....	182
V.1	Concentration profile of ATP metabolites for carcass 7.....	254
V.2	Concentration profile of ATP metabolites for carcass 7.....	255
V.3	Concentration profile of ATP metabolites for carcass 8.....	256
V.4	Concentration profile of ATP metabolites for carcass 8.....	257



Figure		Page
V.5	Concentration profile of ATP metabolites for carcass 9.....	258
V.6	Concentration profile of ATP metabolites for carcass 9.....	259
V.7	Concentration profile of ATP metabolites for carcass 10.....	260
V.8	Concentration profile of ATP metabolites for carcass 10.....	261
V.9	Concentration profile of ATP metabolites for carcass 11.....	262
V.10	Concentration profile of ATP metabolites for carcass 11.....	263
V.11	Concentration profile of ATP metabolites for carcass 12.....	264
V.12	Concentration profile of ATP metabolites for carcass 12.....	265
V.13	Concentration profile of ATP metabolites for carcass 13.....	266
V.14	Concentration profile of ATP metabolites for carcass 13.....	267
V.15	Concentration profile of ATP metabolites for carcass 14.....	268
V.16	Concentration profile of ATP metabolites for carcass 14.....	269
V.17	Concentration profile of ATP metabolites for carcass 15.....	270
V.18	Concentration profile of ATP metabolites for carcass 15.....	271
V.19	Concentration profile of ATP metabolites for carcass 16.....	272
V.20	Concentration profile of ATP metabolites for carcass 16.....	273
V.21	Concentration profile of ATP metabolites for carcass 17.....	274



Figure		Page
V.22	Concentration profile of ATP metabolites for carcass 17.....	275
V.23	Concentration profile of ATP metabolites for carcass 18.....	276
V.24	Concentration profile of ATP metabolites for carcass 18.....	277
V.25	Carcass 4. Plot of swelling capacity vs time postmortem. Plot of ECS dw vs time postmortem. Plot of ECS app vs time postmortem...	286
V.26	Carcass 5. Plot of swelling capacity vs time postmortem. Plot of ECS dw vs time postmortem. Plot of ECS app vs time postmortem...	289
V.27	Carcass 6. Plot of swelling capacity vs time postmortem. Plot of ECS dw vs time postmortem. Plot of ECS app vs time postmortem...	291
V.28	Carcass 7. Plot of swelling capacity vs time postmortem. Plot of ECS dw vs time postmortem. Plot of ECS app vs time postmortem...	293



## I. INTRODUCTION

The introduction to this report on the state of muscle water consists of seven parts. These are: (1) a discussion of the structure and composition of muscle; (2) a review of some of the biochemical and physiological events associated with rigor-mortis; (3) a consideration of some of the factors affecting postrigor meat quality; (4) a discussion of several methods used to assess meat quality; (5) a review of factors affecting protein-water interactions; (6) an examination of methods being used to examine the state of water in meat; and, finally, (7) a statement of the problem, including the reasons for the work performed.

### A. Structure and Composition of Muscle

Each of the muscles in the carcass is attached to the bone by tendons, and all connective tissue components of the muscle cells are continuous with the tendons. Connective tissue components include the epimysium, perimysium and the endomysium. The epimysium is the large connective tissue sheath that encircles the muscle. The perimysium divides the muscle into groups of muscle fibres or fasciculi. The arteries and blood vessels carrying nutrients and waste to and from the cell lie within this structure. The endomysium contains the capillaries of the blood supply system and surround each muscle fibre. This interrelated structure allows the force generated by contraction of the muscle fibre to be transmitted to the tendons through the



connective tissue components.

The sarcolemma, lying under the endomysium, surrounds each fibre and is attached to the endomysium by a spiral collagenous structure (Lawrie, 1979). The sarcolemma consists of three layers: the plasma membrane; a middle layer (the basement membrane) consisting primarily of glycoprotein; and an outer layer of collagen fibres. The T-system is a continuation of the plasma membrane and comes into intimate contact with the sarcoplasmic reticulum (SR). Thus, the extracellular space (ECS) comes deep within the muscle fibre. The SR is a membranous structure which surrounds each myofibril.  $\text{Ca}^{2+}$  is retained within the SR by an ATPase pump. It is the release of this  $\text{Ca}^{2+}$ , as the depolarization wave from a nerve impulse travels down the sarcolemma, that initiates contraction.

The myofibril consists of the A band, with a central clear H-zone; and the I band, with a central division, the z-line. The distance between the two adjacent z-lines is the functional unit of the myofibril, called the sarcomere. The reason for the banding is seen from a high magnification of the myofibril. Within the region of the A band are filaments consisting primarily of myosin, which traverse the A band and are relatively thick. Extending from the z-line to the edge of the H-zone are relatively thin filaments (composed primarily of actin, tropomyosin and the troponin complex). Therefore, the I band consists of only the thin filaments but the A band is composed of both thick and thin filaments.



Within the H-zone, where thin filaments are absent, an M line can be seen. The M substance serves to link and maintain the proper spatial arrangements of the thick filaments.

When  $\text{Ca}^{2+}$  is released from the SR, the  $\text{Ca}^{2+}$  combines with troponin C (Tn-C) of the troponin complex. This initiates conformational changes in the troponin complex which inhibits the function of blocking the interaction of myosin and actin. Once the inhibitory action of the Tn complex is removed, contraction can occur. The contraction cycle requires ATP. When ATP combines with myosin, the rigor complex between myosin and actin dissociates. The myosin-ATP complex formed becomes activated by the cleavage of the terminal phosphate, forming myosin-ADP- $\text{Pi}^*$ . This activated complex can form a crossbridge with actin of the thin filament if the blocking action of the Tn complex has been removed. Upon the release of ADP and  $\text{Pi}$  from myosin, a conformational change in the myosin head occurs which results in a movement of the thin and thick filaments relative to each other. ATP may again bind with the myosin head, dissociating actin and myosin, and the cycle may be repeated.



## B. Biochemical and Physiological Events Associated with Rigor-mortis

In beef, bleeding is effected by severing the carotid artery and the jugular vein. This stoppage of the circulation of blood, at death, initiates several changes. Perhaps the most obvious is cessation of the oxygen supply to the cells, cessation of nervous and hormonal regulation and destruction of the osmotic equilibrium of the cells (Lawrie, 1979). The absence of oxygen is perhaps the most detrimental circumstance since it prevents the aerobic synthesis of ATP. In an attempt to meet the energy demands of the cell, glycolysis proceeds, converting glycogen in the muscle to lactic acid. This leads to a drop in pH. Lawrie (1979) discussed the final pH attained, and whether due to a lack of glycogen, inactivation of glycolytic enzymes or because the glycogen is insensitive or inaccessible to attack, it is generally about pH 5.4-5.5.

Bendall (1973) has suggested that the principal source of ATP utilization in early postmortem muscle is the noncontractile ATPase activity of myosin. Whiting (1980) has shown the SR ATPase activity to be quite high in the temperature range of 20-30°C. This activity leads to a reduction in ATP levels of the postmortem muscle.

In early postmortem muscle the level of ATP can be maintained for some time by a resynthesis from ADP and creatine phosphate (CP). But when CP is used up, glycolysis alone cannot maintain adequate ATP levels and, eventually,



rigor bonds form, resulting in rigid chains of actomyosin. Honikel *et al.* (1981) reported that these rigid chains of actomyosin begin forming when the ATP level falls to about 1  $\mu$ mole/g or when the pH falls to 5.9. This is the pH and ATP concentration required for initiation of rigor contraction. Bendall (1973) has shown that rigor contraction is a weak contraction and appears to involve only a fraction of the fibres. However, this contraction can significantly affect the sarcomere length of muscles in the postrigor carcass. Hostetler *et al.* (1972) examined the effect of various methods of carcass suspension on sarcomere length and found that the final length was related to the load on that muscle. For example, the postrigor sarcomere length of the semitendinosus (ST) varied between 2.4 and 3.3  $\mu$ m, depending upon the method of suspension. If the muscle bore more of the load of the carcass, rigor contraction was too weak to contract the sarcomere length and at some extreme loads stretching of the fibre actually occurred.

One of the most visible affects of rigor development and the associated biochemical and physiological changes is a change in the water holding capacity (WHC) of the muscle. Hamm (1960, 1974) has discussed several factors contributing to the loss of WHC.

As glycolysis proceeds and the pH falls, the isoelectric point of actomyosin (pH 5.0) is neared. Since at the isoelectric point the charge on the proteins is minimum, a maximum number of intermolecular salt linkages between



positively and negatively charged groups develops. This tightens the structure of the fibre and reduces the amount of water that can associate with the proteins. Lawrie (1979) has indicated that the rate of postmortem pH fall can affect the WHC. The more rapid the pH fall, the greater the loss in WHC. This is thought to be a result of a greater denaturation of the sarcoplasmic proteins (Scopes, 1964), which can precipitate on the myofibrillar proteins. In addition to this, Bendall (1960) showed an increased tendency for rigor contraction when the pH fall is rapid. This would tighten the myofibrillar structure, reducing the WHC. Penny (1977) found if the rapid pH fall occurs at a high temperature, an increased denaturation of the muscle proteins leads to a fall in the WHC.

While pH fall affects WHC, the major factor contributing to the loss in WHC is the formation of crossbridges between the thick and thin filaments. As ATP levels fall and crossbridges form, the interfilamental spacing of the fibre is reduced. This lowers the amount of water that can be associated with the myofibrils (Goldman *et al.*, 1979). The fact that pH fall is not a major contributor to the loss in WHC was shown by Hamm (1960). He reported that two-thirds of the hydration drop in beef postmortem is due to the breakdown of ATP and one-third to the fall of pH. Honikel *et al.* (1981) do not think that this was due to the hydrolysis of ATP itself, but rather a result of the formation of rigor bonds due to the reduction in ATP.



The general consensus among most authors (Hamm, 1974; Offer and Trinick, 1983) is that once the repulsive forces between the thick and thin filaments are reduced, if constraints to swelling (the M- and Z-lines and crossbridges) prevent a large interfilamentous spacing, the WHC will be low.

Heffron and Hegarty (1974) have measured an increase in the ECS during rigor development. Pearson *et al.* (1974) determined from their NMR  $T_2$  data that approximately 17% of the muscle water was being transferred from the intracellular space to the ECS as rigor developed in porcine muscle. Penny (1977) found that for a given muscle when the ECS was large, the drip loss was greater. For this reason he concluded that the increased water in the ECS was responsible for the increase in drip at temperatures between 20-30°C. At higher temperatures denaturation of the myofibrillar proteins was viewed as the major cause of increased drip. Note that such movement of water into the ECS would reduce the intrafibre water.

### C. Postrigor Meat Quality

Locker (1960) found evidence for a positive correlation between sarcomere length and tenderness. Hostetler *et al.* (1972), in their studies of carcass suspension, found some improvement in meat quality when the sarcomere lengths were increased in the range between 2.0-2.5 $\mu\text{m}$ . On the other hand, when the sarcomere was stretched beyond 2.5 $\mu\text{m}$ , little improvement in tenderness occurred. But the amount of



actin-myosin overlap is not the sole reason for toughness. Bouton *et al.* (1975) found that adhesive forces, which they view as reflecting the connective tissue component, were higher in contracted fibres. In support of this, Rowe (1974; 1977a,b) showed that the angle between the connective tissue and the muscle fibre varies with the state of contraction. He views this to be the major factor relating the toughness of the meat sample with contraction state.

Hamm (1974) indicated the WHC of meat is closely related to tenderness, juiciness and colour. In particular, he showed that an improved tenderness and an increase in WHC were associated with a loosening of the protein structure and a rise in the ultimate pH. Bouton *et al.* (1971) have published data which confirm Hamm's findings. On the other hand, shortened fibres have been shown to have a reduced WHC and tenderness (Behnke *et al.*, 1973; Bouton *et al.*, 1972).

The importance of WHC to meat quality and meat products has been emphasized by Hamm (1974), who listed meat industry procedures that are sensitive to WHC of the tissue or that change the WHC of the muscle. These procedures include transportation, storage, mincing, salting, curing, canning, cooking, freezing, thawing, drying and aging. For these reasons the study of factors affecting the binding of water in meat and meat products is of considerable importance to the meat industry.



Conditioning or aging of the postrigor carcass has been observed to improve the quality of the resultant meat. One of the earliest explanations proposed for this increase in meat quality with aging was from Arnold *et al.* (1956). They felt that the increase in WHC observed during conditioning was the main reason for an improved tenderness. They found that  $\text{Na}^+$  and  $\text{Ca}^{++}$  were being released into the sarcoplasm as the muscle aged and that  $\text{K}^+$  was being absorbed. This change in the ion-protein relationship contributed to an increased charge and thereby an improvement in the WHC.

In the postrigor period a small rise in pH, after the ultimate pH has been attained, is often seen. This rise in pH may be thought to contribute to an increase in the WHC since a high pH has been associated with a higher WHC (Lawrie, 1979). However, Hamm (1960) has shown that the increase in pH postrigor could only impart a small improvement in WHC. Later, Hamm (1974) suggested that the increase in WHC during conditioning is due to the loosening of the myofibrillar structure caused by the attack of proteolytic enzymes in the region of the Z-line. It is his view that proteolysis would not have to be extensive to increase the WHC. A disruption of only a few bonds is all that may be needed to increase the WHC, if the Z-line is viewed as the myofibrillar organizational centre and the anchor point for the contractile filaments (Franzini-Armstrong, 1973; Gard and Lazarides, 1979). Nagainis and Wolfe (1982) have described an actin-like



component in the Z-line which is hydrolysed by a calcium activated neutral protease (CANP). The hydrolysis of the actin-like protein may be responsible for deterioration of the Z-line observed during aging (Stromer *et al.*, 1967; Goll *et al.*, 1970; Hay *et al.*, 1973).

The disruption of the Z-line may also be responsible for the improvement in tenderness during aging. The fragmentation index, which measures the susceptibility of myofibrils to undergo breaking during homogenization has been correlated with organoleptic tenderness (Takahashi *et al.*, 1967; Moller *et al.*, 1973) and is thought to be due to changes in the structure of the Z-line. The importance of the Z-line structure on water retention by the myofibril has been confirmed by the work of Offer and Trinick (1983). They observed considerable differences in the response of freshly prepared myofibrils from different preparations to swelling in solutions of increasing salt concentrations. This was most observable in the appearance of the Z-lines. At times the Z-line would be weakened by the salt treatment and would expand appreciably, while the Z-line from other myofibrillar preparations would not expand at all. The variability in the integrity of the Z-line influenced the appearance of the remainder of the myofibril. If the Z-line expanded, the A and I bands also expanded to a greater extent. Thus the integrity of the Z-line influences the expansion of the A band as well as the I band. For this reason the postulate of Hamm (1974), in which the disruption of a few key bonds



could loosen the structure of the myofibril, seems to be supported by the above results and may be the major reason for the improvement in WHC during the postrigor period.

#### D. Methods of Assessing Meat Quality

Harris (1976) reviewed several methods used to assess meat quality. The methods were examined in relation to their ability to discriminate between the strength of the different structural components of meat and their ability to reflect organoleptic tenderness.

During shear force measurements, such as the Warner Bratzler, the sample is subjected to a combination of tensile, compression and shear stresses. The tensile stress is considered to correlate best with the myofibrillar component of toughness (basically the degree of actin-myosin interdigitation) being assessed. In the force deformation curve, the initial yield point is affected most by the treatments that can influence the muscle fibres, such as aging, cooking and myofibrillar contraction. The final yield point is affected by changes in the connective tissue due to animal age and muscle connective tissue differences. Unfortunately, correlations of these measurements with taste panel assessments have been inconsistent.

The tensile stress applied parallel to the fibre axis using the Instron Universal Testing Machine was first examined by Stanley *et al.* (1971, 1972). They found the method to be capable of determining variations in the



tensile properties of uncooked meat which were highly correlated with meat tenderness. Bouton *et al.* (1975) showed that the contraction state has little effect on the tensile peak force, but increases in contraction lead to an increase in the elongation required before the sample breaks. Eino and Stanley (1973) showed that this pattern can change with aging. They observed a fall in the breaking strength which stabilized 4 days postmortem. Also the break elongation pattern was different. It was at a minimum by day two, but increased by day eight to about 65% of its former value.

Locker and Wild (1982) have hand loaded (100 g increments) muscle strips and have recorded yield points. An initial yield was recorded at the weight which contributed to an extension of 7% in about 10 min. They concluded from their results that the mechanism of yielding differs between unaged and aged meat samples. In unaged samples the yield is viewed as a failure of actin filaments or their attachments, followed by elastic extension of gap filaments within the I-band. In aged samples both actin and gap filaments have been weakened by proteolysis and fail together at low loads, resulting in a clean break at the I-band.

These results imply that a tensile force applied parallel to the fibre axis is responsive to both postmortem aging effects and the contraction state, but the relationship between elongation and tensile force can be quite complex.



Tensile stress measurements on cooked meat made perpendicular to the fibres (adhesion measurements) show effects which Bouton *et al.* (1975) believe are an index of the connective tissue strength. The adhesion values are larger when the myofibrillar contraction state is increased. This supports the results of Rowe (1977b), who showed with adhesion measurements that fibres made up of short sarcomeres are stronger than fibres made up of long sarcomeres. The swelling of the muscle fibre upon contraction increases the angle between the collagen sheath and the muscle fibres, thus increasing the strength of the fibre. Carroll *et al.* (1978) examined changes in the ultrastructure of 10 day muscle fibres. They used a video camera to record the effects of tensile stress applied parallel to the fibre axis and observed a rupture of the muscle fibre components followed by a tensioning of the connective tissue components. Approximately twice the force was necessary to rupture the strands as was required to rupture the muscle fibres. When the force was applied perpendicular to the fibre axis, rupture occurred at the endomysial - perimysial connective tissue junction and the muscle fibres remained relatively undisturbed. This observation supports the Bouton *et al.* (1975) conclusion that adhesive measurements primarily reflect the connective tissue components in the muscle.



Taste panel assessment of meat (subjective evaluation) is the most reliable means of assessing meat quality. However, such assessments are slow, time consuming and very expensive. Harris (1976) thinks that judgement implies interpretation by the human brain of all the physical or physiological information reaching it. Since human interpretation is involved, unavoidable variations in judgement between taste panelists will exist. For this reason the correlation between subjective and objective methods may never be very high.

#### E. Protein-Water Interactions

Chou and Morr (1979) reviewed the factors which contribute to protein-water interactions. The degree of hydration of protein molecules depends upon the number of molecules that can associate with the amino acid groups in the protein. The amino acid residues have been classified into three groups: (1) polar amino acids with ionized side chains which bind the greatest amount of water; (2) nonionized polar amino acids which bind an intermediate amount of water; and (3) hydrophobic groups which bind little or no water.

Another order of water binding that has been suggested reflects the type of polar side chain and the water activity ( $Aw$ ) at which the binding can occur. At low  $Aw$  conditions, the sequence of the polar groups in order of decreasing water binding is: amino, carboxyl and hydroxyl groups. At



intermediate Aw, binding of the water can be facilitated by peptide linkages, and at high Aw there is formation of multilayers of water.

Although the polar amino acids are the primary sites for protein-water interactions, it is necessary that these binding sites be sterically available for interaction with water. If a polar side chain interacts with other amino acid side groups or is buried within the protein molecule, it will be unable to interact with the same number of water molecules. As well, alteration in the charge of ionized groups by changing the pH will influence the net charge on the protein, which in turn alters its attractive and repulsive forces. For example, at or near the isoelectric point the repulsive forces between the proteins in meat are reduced and salt bridges are enhanced, which dramatically reduces the WHC of the meat.

Solutes at high concentrations can enhance ("salting-in") protein-water interactions or reduce these interactions ("salting-out") as a result of a competition of the solutes and proteins for the available water. In meat the addition of salt enhances the WHC. Chloride ions are believed to bind to the filaments (likely the cationic amino groups) and enhance their negative charge, and thus the electrostatic repulsion between the filaments. This should increase the amount of water that can enter between the filaments (Offer and Trinick, 1983). The response of the protein to water binding may also involve the type of



solute. Ling and Peterson (1977) have shown that the fixed anions in the cell ( $\beta$ - and  $\gamma$ -carboxyl groups) have different affinities for different cations. The same is true for the fixed cations ( $\epsilon$ -amino, guanidyl and imidazole groups) for anions. They have shown that  $K^+$  is preferred over  $Na^+$  for the fixed anions in the cell. Thus  $K^+$  will tend to break salt bridges better than  $Na^+$ . Also,  $Cl^-$  is preferred by the fixed cations over  $SO_4^{2-}$ . For this reason salts containing  $Cl^-$  enhance swelling more than those containing  $SO_4^{2-}$ . Thus the nature of the ions can effect differences in the water imbibed by the tissue. Godt and Maughan (1977) suggested that the counterions surrounding the charged filaments in the muscle may contribute to a swelling of the fibre due to a Donnan osmotic force, where water enters the filament lattice, diluting the excess concentration of counterions. Clearly, different levels of protein-water interactions exist. Chou and Morr (1979) define the different types of water which are interacting with or under the influence of proteins as follows:

Structural water: engages in hydrogen bonding to the protein molecules and stabilizes the native structure of the protein.

Monolayer water: is the first absorbed layer of water around the protein molecule and is attached to specific water-binding sites (through hydrogen bonding or dipole interaction). A typical protein will have between 4 and 9% monolayer water.



Unfreezable water: does not freeze at a sharp transition temperature and may represent the total water molecules clustered around each polar group of the protein molecules (thus includes structural and monolayer water). This type may account for up to 45% of the water present in some protein systems.

Capillary water: is held physically or by surface forces on the protein molecule. It is the major portion of the water in meat and meat emulsions, and is freely available for chemical reactions as well as for solvent functions. However, considerable force is required to remove it from the protein mass.

Hydrodynamic hydration water: would mainly apply to proteins in solution and would be water that would diffuse with or be transported along during movement of the proteins.

Hydrophobic hydration water: is in the vicinity of protein hydrophobic groups. It is believed to adopt a clathrate type structure.

#### F. Methods of Examining the State of Water in Meat

The principal method of examining the water properties of meat has been WHC measurement. Hamm (1960) defined WHC as the ability of meat to hold fast its own or added water during the application of any force (pressing, heating, grinding, etc.). Thus, the water expressed from the tissue is the most loosely bound water within the muscle cell or



within the tissue. WHC is a very imprecise term since the value of WHC measured depends upon the method chosen.

Hamm (1960, 1974) identified several methods that have been used. Most consist of an application of pressure to the muscle tissue, and involve centrifugal methods, filtration or a pressing of the tissue between plates. Offer and Trinick (1983) discussed variability in the results achieved at different pressures. At a pressure near  $4 \times 10^6$  Pa most of the water of the meat is expressed and there is little distinction between samples. At lower pressures (about  $10^5$  Pa) a variation in the WHC between samples is more likely to be detected. The water expressed is thought to be both the extracellular water and that part of the intracellular free water that is situated between the myofibrils.

A second group of WHC methods measure some relevant technologically important property of the meat, such as drip or cooking loss or weight of water absorbed by the meat.

Ranken (1976) stated that, when the different measures of WHC are compared or related to such parameters as color or pH, significant correlations are achieved, but no absolute figures for the immobilized part of the water can be determined.

One of the more powerful tools being used to examine the state of water in muscle is NMR. Belton *et al.* (1972) measured the spin-spin relaxation times ( $T_2$ ) of water in frog muscle. They observed a nonexponential decay, caused by more than one kind of water state. They considered the long



relaxation ( $T_2 = \approx 240$  msec) component (approximately 15%) to be derived from the water in the extracellular space. They thought that the water in this environment would be the closest in its physical properties to a dilute aqueous solution, but because of the water's interaction with connective tissue components, the  $T_2$  value would be shortened. A more rapidly relaxing ( $T_2 = \approx 10$  msec) water proton fraction (about 20%) was thought to be strongly bound to proteins. This factor could be detected upon freezing the muscle to  $-8^{\circ}\text{C}$  at which point 80% of the signal was lost. This was attributed to the freezing of 80% of the water, leading to a  $T_2$  of the magnitude of ice, too short to be seen in their spectrophotometer. This would be a nonfreezable water fraction. The remainder of the muscle water (65%) was assigned to water associated with the myofibrils and SR and was viewed as an intermediate relaxing fraction ( $T_2 = \approx 40$  msec).

Hazlewood *et al.* (1974) provided a similar interpretation of their  $T_2$  results. The water associated with the macromolecules was found to be about 8% of the total tissue water and did not exchange rapidly with the rest of the intracellular water. The water in the myoplasm was a second fraction (82% of the tissue water), while a third and final fraction (about 10%) was confined to the ECS.



Since those early interpretations of the state of water in muscle, views of  $T_2$  data have become more controversial and complex. According to Fung and Puon (1981) the short  $T_2$  ( $\approx 24 \mu\text{sec}$ ) is due to protons on proteins and other macromolecules. The next fastest (0.4-10 msec) fraction is attributed to relatively mobile proteins in tissue protein and lipid. However, Peemoeller and Pintar (1979) and Peemoeller *et al.* (1980) proposed that the decay in this time period is due to protons in large molecules ( $\approx 30\%$ ) plus protons in water ( $\approx 70\%$ ). Fung and Puon (1981) did argue that the  $T_2$  at 140 msec could not entirely be attributed to organic molecules as the above authors had suggested, but had to reflect in part the tissue water. However, Fung and Puon (1981) argued that the slow decaying part of the proton spin echoes is not due to extracellular water as previously reported.

Very few studies examining changes in NMR signal as rigor develops have been performed, however one of the more interesting was conducted on porcine muscle by Pearson *et al.* (1974). They observed a single exponential decay from immediately postmortem to 1.5 hr postmortem. Then, for 5.7 hr, nonexponentiality was observed in the spin-spin relaxation decay. This was interpreted in terms of two water fractions which were physically separated. The more rapidly relaxing fraction was intracellular and the development of nonexponentiality was attributed to water being transferred from the intracellular to the extracellular space. It is



interesting that one of the reasons Fung and Puon (1981) dismissed the ECS as the source of the slow fraction was the fact the contribution of the slow fraction increased as rigor developed. They stated they knew of no evidence to show that there is a postmortem redistribution of the water into the ECS. For this reason they discounted the results of Pearson *et al.* (1974). This must have been an error, as Heffron and Hegarty (1974) and Penny (1977) have both observed the ECS increasing with postmortem rigor development.

Pearson *et al.* (1974) also examined the spin-lattice relaxation times ( $T_1$ ) but viewed them to be invariant during rigor development. Chang *et al.* (1976) confirmed that others have made similar observations. However, Chang *et al.* (1976) found that when they measured the spin-lattice relaxation in a large time domain,  $T_1$  was sensitive to the postmortem changes in the muscle. In reviewing the literature an interesting observation was made concerning the work of Belton *et al.* (1973), who had examined the variation of  $T_1$  with load on the muscle tissue. The experimental design consisted of placing the muscle in the probe immediately after excision and measuring  $T_1$  under no load. After this, successive loads were placed on the muscle. Inexplicably, to them, the  $T_1$  rose and fell. The results appear surprisingly similar to those of Chang *et al.* (1976) and those in this study. It is likely that the experiment extended over a few hours, allowing the frog muscle to enter rigor, which could



have caused the results they reported.

Another approach that has been used to examine the water in muscle is that of laser Raman spectroscopy. Pezolet *et al.* (1978) used this technique in examining the muscle fibres of the barnacle. They concluded that no more than 5% of the water can be "structured" intracellular water. They arrived at this conclusion because they found no appreciable differences in the spectra in the region of the O-H (or O-<sup>2</sup>H) stretching modes of water between unfrozen fibres and pure water. This agrees with the observations of Hamm (1960), where adsorption isotherms, vapor pressure, freezing point and dissolving power experiments were used to show that not more than 4-5% of the total muscle water can be tightly bound to muscle proteins.

However, Pezolet *et al.* (1978) also found, when the Raman spectra of frozen fibres were taken, they could calculate that approximately 20% of the intracellular water remained unfrozen. This agrees with the results obtained by Belton *et al.* (1972). Thus the distinction between monolayer water and the unfreezable water reported by Chou and Morr (1979) is supported by these results.

Differential scanning calorimetry was used by Aubin *et al.* (1980) to examine the state of water in muscle. From the shapes of the melting curves, three types of water were identified: (a) unfrozen water; (b) free or bulk water which shows a melting point close to that of pure water; and (c) intermediate water which shows a large depression in melting



point and was considered to be partly retained on protein molecules. They examined muscle at various water contents and concluded that the water bound to the protein does not change with water content. The variation in water content is almost exclusively confined to a variation in the amount of free water.

#### G. Statement of the Problem

The state of water in muscle has been shown by Hamm (1960, 1974) to be important to all aspects of meat handling. He indicated the strength of water binding by the muscle proteins is of great importance for the quality of meat and meat products, as almost all procedures for the storage and processing of meat are influenced by the WHC. As important as water is to the quality of meat, Hamm (1974) clearly showed that the factors immobilizing the water in muscle are not clearly understood.

A few key papers created the interest in this project. The Pearson *et al.* (1974) paper presented data which showed NMR was capable of detecting differences in the properties of the muscle water as the muscle enters rigor. The proposal that the ECS was taking up the water lost by the fibre could help to explain differences in the WHC of meat if different amounts of water were being translocated to the ECS during rigor development. In support of the concept of water entering the ECS, Heffron and Hegarty (1974) measured an increase in the size of the ECS as rigor developed, but no



differences in ECS were measured between carcasses. Penny (1977) measured changes in the ECS and produced evidence that, for a given carcass, the amount of drip increased as the ECS and temperature of the meat sample increased. However, the results were puzzling in that the carcass with the lowest drip loss had the largest percentage of ECS and, conversely, the carcass with the highest drip loss had the smallest percentage of ECS. The observations of Chang *et al.* (1976) that  $T_1$  was sensitive to changes in the muscle water as rigor developed in rat muscle, prompted an interest in this technique to monitor the muscle water. Additionally, their statement, "It would be interesting to find out what mechanism(s) are responsible for the rise and fall in  $\Delta T_1$ ", encouraged examination of these changes in  $T_1$  with beef, since it takes longer to enter rigor and provides time to more carefully assess changes in the  $T_1$  profile as rigor develops.

A comparison of the  $T_1$  and ECS data may help to explain if water movement into the ECS would contribute to the  $T_1$  profile. With the possible translocation of water within the muscle during rigor development, it was felt that the mechanical properties of the muscle may also change. Bendall (1973) reported on the measurement of extensibility using hand loading methods or a mechanical loading and unloading of the muscle strip. However, Stanley *et al.* (1971, 1972) and Bouton *et al.* (1975) demonstrated better ways to monitor changes in the mechanical properties of muscle. The



advantage of tensile and adhesive measurements is that both the strength of the yield points and extensibility can be measured simultaneously.

As a result of the foregoing, the objectives of the study were to:

1. Examine the T<sub>1</sub> profile of several carcasses to see if that measurement can detect changes in the muscle water during rigor development, and also measure carcass to carcass variations in muscle water properties.

2. Develop a method of measuring the ECS which may help explain the T<sub>1</sub> profile, as well as provide information regarding the proposal that translocation of water to the ECS is occurring during rigor development.

3. Determine if changes in the mechanical properties of the muscle may be related to water translocation during rigor development.



## II. MATERIALS AND METHODS

### A. Introduction

The materials and methods section has been divided into two parts. The first part, "Methods used to monitor rigor development", details the methods which were used to characterize the muscles and measure those selected biochemical and physiological properties of muscle which changed during rigor development. The data generated from these measurements monitor the rate of rigor development and the time needed to reach rigor maximum. Other tests described here were used to measure the response of the muscle to mechanical stress. These measurements are needed to correlate the onset of rigor mortis to the state of water in the muscle. The fiber typing was used to aid in defining the complex nature of the muscle sampled. The extra detail included under "Measurement of ATP and metabolites" is included to clearly explain this new HPLC method for nucleotides.

The second part, "Methods used to monitor the state of water", deals with those methods used to measure properties of the intra and extra muscle fibre water. NMR T<sub>1</sub> values were measured during rigor onset and resolution in order to determine water mobilities. Other physical and chemical measurements were undertaken to reveal the factors affecting the mobility of the water.



## B. Methods Used to Monitor Rigor Development

### Animals, muscle and muscle treatment

Musculus semitendinosus (ST), obtained from steers and heifers slaughtered at Gainers Ltd (Edmonton, Alberta), was the principal muscle examined in this study due to its ease of removal at the abattoir. Since the outer and inner portions of the ST differ considerably in their fibre types (Hunt and Hedrick, 1977a), the large central portion of the ST was sampled, unless stated otherwise in the text. Most samples were from Grade A animals aged between 1.5 to 2 years, although some of the muscle samples (as specified) were from older animals.

In the portion of this study where the mechanical properties of early postmortem muscle were being examined, two conditions were maintained for comparison purposes. The first condition refers to those muscles removed within one hour of slaughter, brought to the laboratory and allowed to enter rigor unrestrained. These samples were labelled off-carcass (OFC) and were stored in a Labline temperature controlled room. The temperature in the room was regulated to conform to the temperature decrease (measured at a depth of 2 cm) within a carcass hanging in the chill cooler. For the second condition samples were removed from the carcasses at the packing plant at regular intervals during the development of rigor mortis and brought to the lab. These samples would be restrained from contraction due to the load



placed on the muscle by the weight of the carcass, and were labelled on-carcass (ONC).

In subsequent studies where NMR was one of the methods used to examine early postmortem muscle, muscles were removed from the carcass and allowed to enter rigor at room temperature unrestrained. These samples would be similar to the OFC samples examined above but without the temperature control corresponding to the cooling rate in the packing plant.

#### *Fibre typing*

The fibre typing method used was the procedure of Guth and Samaha (1969) for differentiation of muscle fibre types based on difference in ATPase activity. A muscle sample was removed, wrapped in tin foil, labelled and frozen rapidly in isopentane cooled in liquid nitrogen. For fibre typing of muscles also to be used for NMR studies, the sample was taken from a site adjacent to the location of the NMR sample. At the time of sectioning the frozen muscle was removed from the tin foil and embedded in dimethyl cellulose on the microtome chuck. The muscle was oriented as an upright cylinder so that transverse sections could be cut and the dimethyl cellulose supporting the muscle was then frozen in the liquid nitrogen-cooled isopentane. Sections (14 µm) were then cut in an American Optical Cryostat (model 845). The sections were lifted from the knife with a brush and placed on a room temperature slide. The sections were air dried for approximately 30 min and



then placed in a fixing solution (5% formaldehyde, 200 mM sodium cacodylate, 68 mM CaCl<sub>2</sub> and 340 mM sucrose). This step was found to be necessary to prevent loss of the sections during the subsequent staining procedure. The fixative was removed by two 1 min rinses in 0.1 M Tris-HCl, 18 mM CaCl<sub>2</sub> (pH 7.8). The staining procedure consisted of: 15 min alkali preincubation (0.1 M 2-amino-2-methyl-1-propanol, 18 mM CaCl<sub>2</sub>, pH 10.4); rinsing in two changes of 0.1 M Tris-HCl, 18 mM CaCl<sub>2</sub> pH 7.8; 60 min incubation in 0.1 M 2-amino-2-methyl-1-propanol, 18 mM CaCl<sub>2</sub>, 2.7 mM ATP (pH 9.4) at 37°C; three 30 sec washes in 70 mM CaCl<sub>2</sub>; one 4 min rinse in 2% cobaltous chloride; 30 sec rinsing in four changes of 0.1 M 2-amino-2-methyl-1-propanol pH 9.4; one 3 min rinse in 1% yellow ammonium sulfide; finished by washing in water for 3-5 min. The sections were then dehydrated in graded alcohol solutions (70, 85, 95, 98% ethanol) and then after 5 min of clearing in xylene, were mounted in Permount. They were then photographed using Tri-X Kodak film and the prints were counted. The method of Guth and Samaha (1969) reveals three fibre types (white, intermediate and red). Differentiation between the white and intermediate fibre types proved to be quite variable. The shades of grey characteristic of the intermediate fibres made it difficult to decide whether some fibres should be classified as white or intermediate. If the intermediate and white fibres were counted together, good reproducibility between photographed microscope fields



could be achieved. The results were expressed as percent white-intermediate and percent red fibres.

#### *pH measurements*

In those studies where mechanical properties and isotonic contraction of muscle were examined, the pH was measured by inserting a combination glass electrode into a small slit that had been cut in the muscle with a scalpel. That method had the advantage of accuracy because the surface was freshly cut. However, since slight variations occurred between regions of the muscle, several readings were taken and averaged.

In those studies where the muscle entered rigor at room temperature and where comparisons of the rate of pH fall were of greater importance than individual pH measurements, a Corning surface combination electrode was gently pressed against the surface of the muscle. The muscle was put in a plastic bag, which was closed with a tie about the electrode. A Fisher Accumet Model 320 Expanded Scale Research pH Meter was attached to a recorder and the pH monitored continuously for at least a 24 hr period at room temperature.

#### *Sarcomere length measurements*

Muscle samples (250 mg) were homogenized in a 50 mL container of the Sorvall omnimixer at an intermediate speed for 10 sec with 10 mL of a Ringer-Locke solution containing 5 mM EDTA, pH 7.2 according to the procedure of Heffron and



Hegarty (1974). About 20 different fibres were photographed using an Olympus Model BH phase contrast microscope (40 $\times$  objective). The developed negative film (Tri-X, 400 ASA) was projected onto a screen and the sarcomere lengths measured. The magnification factor of the microscope onto the film was obtained by photographing a graded etched slide. The magnification of the film onto the screen was obtained by puncturing the film with the fine points of a caliper set at 1 cm and then measuring the separation on the screen.

#### *Isotonic contraction measurements*

Muscle strips were cut to about 5 cm in length and trimmed to a measured circumference of from 2.2 to 2.3 cm, giving a range of cross-sectional areas from 0.38 to 0.42 cm $^2$ . The cross-sectional area calculated from the measured circumference was used to calculate the load in g/cm $^2$  placed on the muscle by suspended weights. The circumference (C) was measured by wrapping a flat nylon string about the muscle strip, marking it and measuring the distance between the marks with a dial caliper. The cross-sectional area (A) was calculated from  $A = C^2 \times 0.0795$ . The muscle strips were tied at each end 3.5-4.0 cm apart with silk surgical suture (size 0), leaving a loop on one end to attach a weight. For most determinations 2, 5 and 10 g weights were attached to give load values of approximately 5, 12.5 and 25 g/cm $^2$ . The string on the nonweighted end was tied to a glass rod



spanning the top of a hydrometer jar and the muscle strip and weight were suspended in the jar, which was filled with liquid paraffin to prevent dehydration of the muscle over the period during which the muscle contraction was measured. Paraffin oil was chosen to bathe the muscle since none of the water soluble components of the muscle are leached, nor is the pH fall of the muscle altered, as it might be by aqueous buffers (Bendall, 1975). Contraction was determined by measuring the length of the muscle strip at regular time intervals, reading directly against a strip of graph paper taped to the side of the hydrometer jar. The muscle was allowed to contract at room temperature unless otherwise indicated. Results are expressed as the percentage of contraction versus time, using the extended length (an initial stretching of the muscle due to the weight tied to the muscle strip occurred) as the zero time length, to which either the initial extension or rigor contraction was compared.

*Isometric tension followed by unrestrained contraction measurements*

The muscle strips were cut, measured and tied as described in the methods for isotonic contraction. In this experiment, however, rather than allowing the muscle strips freedom to contract, they were tied at both ends to a rigid horizontal frame. Thus, isometric tension could develop for predetermined lengths of time, whereupon cutting the string allowed the muscle to contract. No loading of the muscle



was done in these experiments.

### *Isometric tension measurements*

Isometric tension development was measured using an Instron Universal Testing Instrument (model 1132) and a 500 g tension load cell. A muscle strip (circumference about 1.5 cm; length, 5 cm) was removed from the ST. The muscle strip was clamped in the upper stainless steel clamp of the support device (Fig. II.1). This device was built by the Technical Services Machine Shop at the University of Alberta. The clamps were designed to exert a force of 70 g, which was found necessary to restrain the muscle from slipping in the clamp. After zeroing the Instron and the external recorder, the upper clamp holding the muscle strip was attached to the load cell. The muscle strip and clamp were then immersed in a beaker of paraffin and the Instron was balanced to this load. The muscle strip and upper clamp were mounted in the clamp support device and the muscle strip clamped in the lower clamp such that the two clamps were spaced 3 cm apart on the muscle strip. The muscle strip and clamping device were then placed in the liquid paraffin filled lucite cell (Fig. II.2) bolted to the Instron base. A preload tension was placed on the muscle strip to prevent sagging. The cross-sectional area was measured in the same manner as that indicated under isotonic contraction methods.



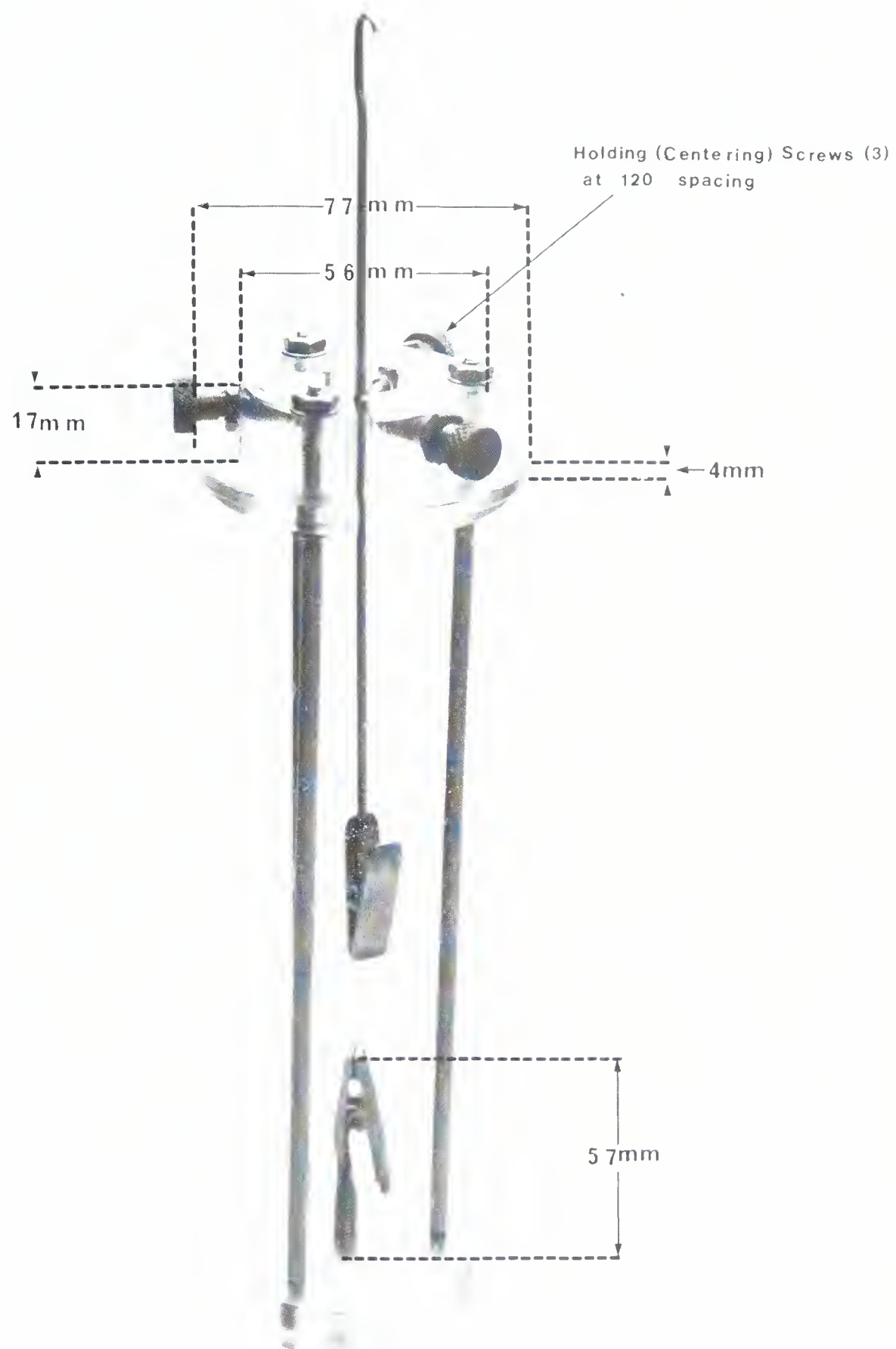


Figure 11.1 Clamping device with clamps



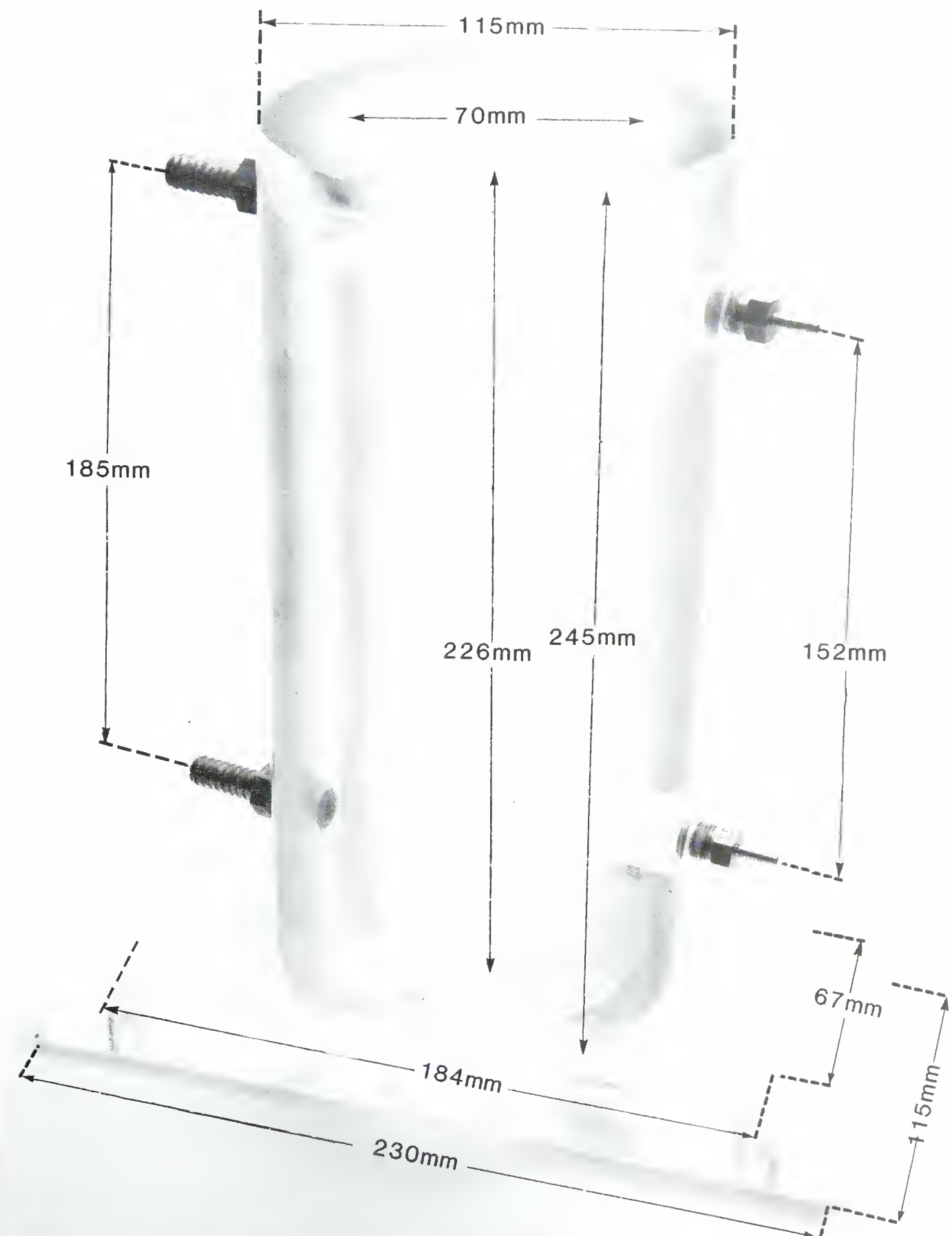


Figure 11.2 Lucite cell used to support the clamping device



### *Mechanical measurements*

The tensile properties and the extensibility of raw muscle strips were examined using the Instron Universal Testing Instrument (model 1132). Muscle strips (5 cm) were cut parallel to the fibre axis and were formed into dumbbell shapes (Bouton and Harris, 1972a,b) to prevent breakage of the sample when mounted in the jaws of the clamps. The narrowest point was cut to have a circumference of between 0.8-1.1 cm and was measured using the same technique outlined under isotonic contraction methods. After the muscle samples were cut they were immediately covered with a plastic film to prevent dehydration before mounting in the clamps. The sample was placed in the same lucite cell described under the isometric tension methods. The test was performed in the air at room temperature since the test was rapid and little drying of the muscle could occur between preparation of the sample and completion of the measurement. After the muscle strips were clamped in the stainless steel clamps (3 cm apart), the crosshead was set to move at 2 cm/min by means of a decade reducer and the chart was set to run directly proportional to the crosshead (5 times greater). As the crosshead rose, the tensile properties of the muscle could be measured from the response of the 500 g tension load cell and the extensibility measured by determining the distance the crosshead moved. The crosshead was elevated until the muscle parted or exhibited a "final yield".



The adhesive properties of the muscle were measured in the same way as those above except that the muscle strips were cut and mounted so that the forces developed were perpendicular to the fibre axis and the circumference was increased to the range of 0.9-1.3 cm. Extreme care was taken in the preparation of the muscle strips to avoid the major perimysial sheets of muscle mentioned by Rowe (1977a) which can result in significant within-sample variability. All the mechanical measurements were run in triplicate.

#### *Other physical measurements of texture*

The Warner Bratzler shear test was performed according to the procedure of Hawrysh *et al.* (1979). The semitendinosus was cooked to an internal temperature of 65°C as measured by a thermocouple inserted into the midpoint of the muscle. After measurements were made of the cooking loss, the meat was cut into .5 inch slices parallel to the fibre axis. Two scalpels fixed .5 inches apart were then used to cut the first slices into strips .5 inch wide. This provided a strip of .5 x .5 inches and as long as the depth of the muscle. Those strips near the core of the muscle, where the uniformity in cooking proved to be the most consistent, were chosen. The Ottawa Texture Measuring system, equipped with a 50 lb load cell set on the most sensitive range, was used to measure the shear force of 10 strips from each sample. The peak heights from a chart recorder were measured and the mean of these measurements was recorded.



*Photography of muscle strips stretched to initial yield*

In an attempt to examine the appearance of the muscle fibres at initial yield, muscle strips of approximately the same dimensions as those for the tensile tests were tied at both ends with silk surgical suture at a distance of 3 cm apart and stretched to the same length as at the initial yield in the Instron. The stretched muscle strips were fixed for 2 hr in modified Karnovsky's fixative (dissolve 2 g paraformaldehyde in 25 mL 0.05 M cacodylate buffer pH 7.2, on a hotplate; clear solution by adding 1-2 drops 1 N NaOH; cool; add 10 mL 25% EM-grade glutaraldehyde; dilute to 50 mL with 0.05 M cacodylate buffer pH 7.2). The fixed muscle fibres were disrupted in a 50 mL container of the Sorvall omnimixer at an intermediate speed for about 30 seconds in 50 mM cacodylate buffer and were photographed using the Olympus Model BH microscope equipped with phase contrast optics. In taking the photographs of a given fibre, to observe the effect at the yield point, the stage had to be moved along the length of the fibre to the point where the yield effect was evident. It appears that only a small part of a fibre, likely corresponding to the narrowest portion of the muscle strip, shows evidence of yield. The remainder of the muscle fibre appears "normal" with respect to the sarcomere lengths and the alignment of the structural units of the sarcomere across the muscle fibre.



## Measurement of ATP and its metabolites

ATP metabolites in meat were reported by Bendall and Davey (1957) and Davey (1961). A rapid method to measure these metabolites was developed in this lab during the course of this work. Previously, attempts at using thin layer chromatography, elution of the nucleotides after scraping of the plate and quantitation by uv absorbance proved tedious and unreliable. Enzyme assays, although reliable, could not conveniently be used to analyze all the ATP metabolites present during rigor development. The method of Khan and Frey (1971), using the uv absorbance ratios at 258 nm and 250 nm [recently reappraised by Attrey *et al.* (1981)], measures the conversion of adenosine to inosine containing components. It does not reveal the changes that IMP is undergoing during postmortem aging nor the exact levels of ATP, AMP and ADP present in the muscle, hence it was unsatisfactory. A high performance liquid chromatographic method (Currie *et al.*, 1982) was developed which has proved to be both reliable and rapid in providing quantitative results for inosine, hypoxanthine, NAD (nicotinamide adenine dinucleotide), AMP (adenosine 5'-monophosphate), IMP (inosine 5'-monophosphate), GMP (guanosine 5'-monophosphate), IDP (inosine 5'-diphosphate), ADP (adenosine 5'-diphosphate), ATP (adenosine 5'-triphosphate), and GTP (guanosine 5'-triphosphate).

Two different HPLC instruments were used during the course of this work. The procedure was developed utilizing a



Beckman Gradient Liquid Chromatograph (model 332) equipped with a Tracor model 970 variable wavelength detector and a Hewlett Packard model 3388A Integrator. Most of the analytical work was performed on a Varian 5100 liquid chromatograph with a fixed wavelength (254 nm) detector and a Hewlett Packard 3380 integrator. The HPLC was fitted with a Whatman Solvecon precolumn which is essential to prevent dissolution of the silica in the analytical column. The strong anion exchange column was a Whatman Partisil-10/25 SAX protected by a Whatman AS Pellionex SAX guard column.

The analytical column was not suitable for immediate use in that uv impurities were eluted during the upper part of the gradient. The regeneration procedure outlined by Whatman in its booklet on column care resulted in a stable baseline.

#### *Mobile phase and chromatographic procedure*

Buffers (A and B) were prepared from  $\text{KH}_2\text{PO}_4$  using water from a Millipore Milli Q system. Buffer A was .015 M  $\text{KH}_2\text{PO}_4$ , .001 M KCl at pH 4.1. The KCl concentration was obtained by adding 1 mL of 1 N HCl to 1 L of the  $\text{KH}_2\text{PO}_4$  buffer and adjusting the pH to 4.1 with KOH. Buffer B was a 0.5 M  $\text{KH}_2\text{PO}_4$  solution at pH 4.5 (see Appendix A). All solutions were filtered through a .45  $\mu\text{M}$  membrane filter (Millipore) before use. The HPLC was programmed to elute the compounds of interest and be ready for reinjection within 60 min. The flow rate was 1.5 mL/min. The program consisted of Buffer A for 7 min, a gradient from 0-100%



Buffer B in 10 min, 100% Buffer B for 18 min and a gradient from 100% to 0% Buffer B in 5 min. After 20 min of Buffer A, the next sample (20  $\mu$ L) was injected.

#### *Preparation of meat samples for injection*

The meat samples (3-4 g) were collected at various times postmortem, wrapped in tin foil, labelled with the Scotch C-31 labelling device, frozen and stored in liquid N<sub>2</sub> until the time of extraction of the nucleotides. During the development of the procedure, ATP and its degradation products were extracted either by pulverizing the meat sample to a powder with a stainless steel mortar and pestle cooled in dry ice or by shaving small pieces off the sample and weighing 1.0-1.5 g into the 50 mL container of the Sorvall omnimixer. The nucleotides were extracted by adding 10 mL of cold (2°C) 0.5 M HClO<sub>4</sub> to the sample and then homogenizing for 60 sec with the homogenizer container immersed in an ice bath. The content of the homogenizer was filtered to remove the precipitated proteins, and the filtrate extracted with an equal volume of 0.5 M tri-N-octylamine/Freon 113 to remove HClO<sub>4</sub> from the nucleotides (see Appendix B).

#### *Quantitation and standardization of ATP metabolites*

In preparing the standard solutions 10-15 mg of the appropriate standard were dissolved in water and made up to a 50 mL volume. Dilutions of these standards were made to provide solutions giving values of 0.1-15 nmoles/injection.



The concentrations of the ATP degradation products were calculated from the integrated peak areas of the absorbing materials eluting from the column. The factors used to convert the areas into concentrations were the regression coefficients obtained from the calibration curves of the standard solutions. All calibration curves were linear in the 0.1-15 nmole/injection (20  $\mu$ L) range.

### *Elution profiles*

Figures II.3-II.5 present the elution profiles of a meat sample at various times postmortem. Inosine and hypoxanthine were not completely resolved, but reproducible results were obtained in repetitive runs (Table II.1). The column must be freed of impurities from the phosphate buffers to prevent interference of these components eluted on the gradient with IDP. IDP and ADP do not show baseline separations at equivalent concentrations, however the ADP peak is very sharp and the IDP is generally in low concentration so that quantitation of IDP is possible.

Injections of standard NAD (oxidized) and NADH (reduced) showed that both forms have identical retention times. An NAD/NADH ratio would be valuable in determining the oxidative state of the cell. Unfortunately, when scans of NADH in water and 0.5 M HClO<sub>4</sub> were compared, the acid was observed to oxidize the NADH to NAD. If a method to extract the nucleotides without oxidizing NADH were possible, a shift in the detector wavelength to 340 nm or a simultaneous multiple wavelength detector would allow an



Table II.1 Reproducibility of extraction and chromatography  
of a 0.6 hr postmortem meat sample

Compound	Extract:	Concentration ( $\mu$ mole/g muscle wet weight)		
		1.07 g	1.61 g	Repeat 1.61 g
Inosine		0.08	0.08	0.07
Hypoxanthine		0.07	0.08	0.07
Nicotinamide adenine dinucleotide		0.59	0.60	0.61
Adenosine 5'-monophosphate	trace	trace	trace	
Inosine 5'-monophosphate	0.76	0.80	0.77	
Adenosine 5'-diphosphate	0.71	0.76	0.75	
Adenylosuccinic acid - GDP	trace	trace	trace	
Adenosine 5'-triphosphate	4.10	4.34	4.24	

Figure II.3. Elution profile of ATP and metabolites of early prerigor beef muscle. The numbered peaks are: inosine (1), hypoxanthine (2), NAD (3), AMP (4), IMP (5), GMP (6), IDP (7), ADP (8), adenylosuccinic acid and GDP (9), UDP and CTP (10), ATP (11), GTP (12).

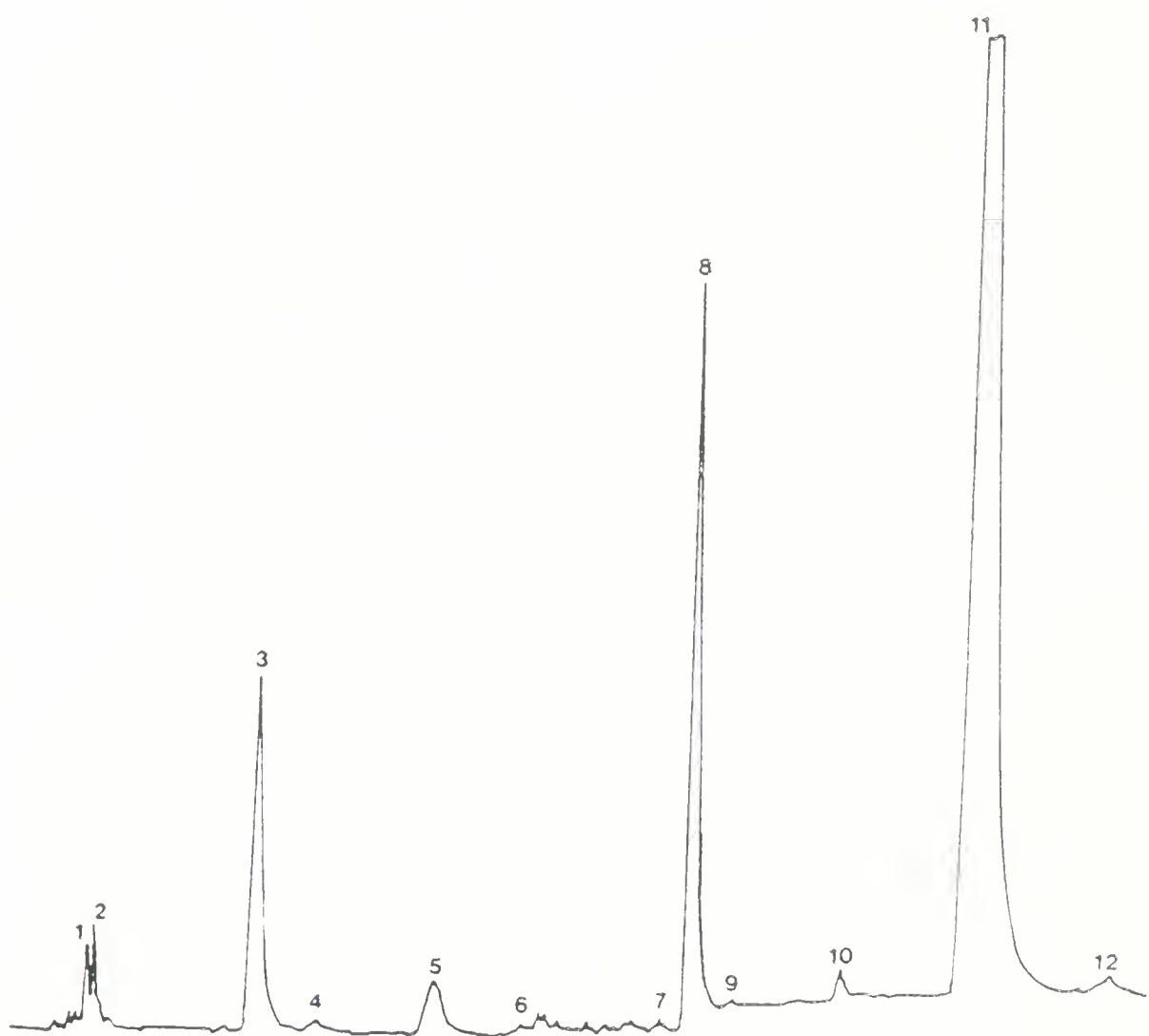


Figure II.4. Elution profile of ATP and metabolites of mid prerigor beef muscle. The numbered peaks are: inosine (1), hypoxanthine (2), NAD (3), AMP (4), IMP (5), GMP (6), IDP (7), ADP (8), adenylosuccinic acid and GDP (9), UDP and CTP (10), ATP (11), GTP (12).

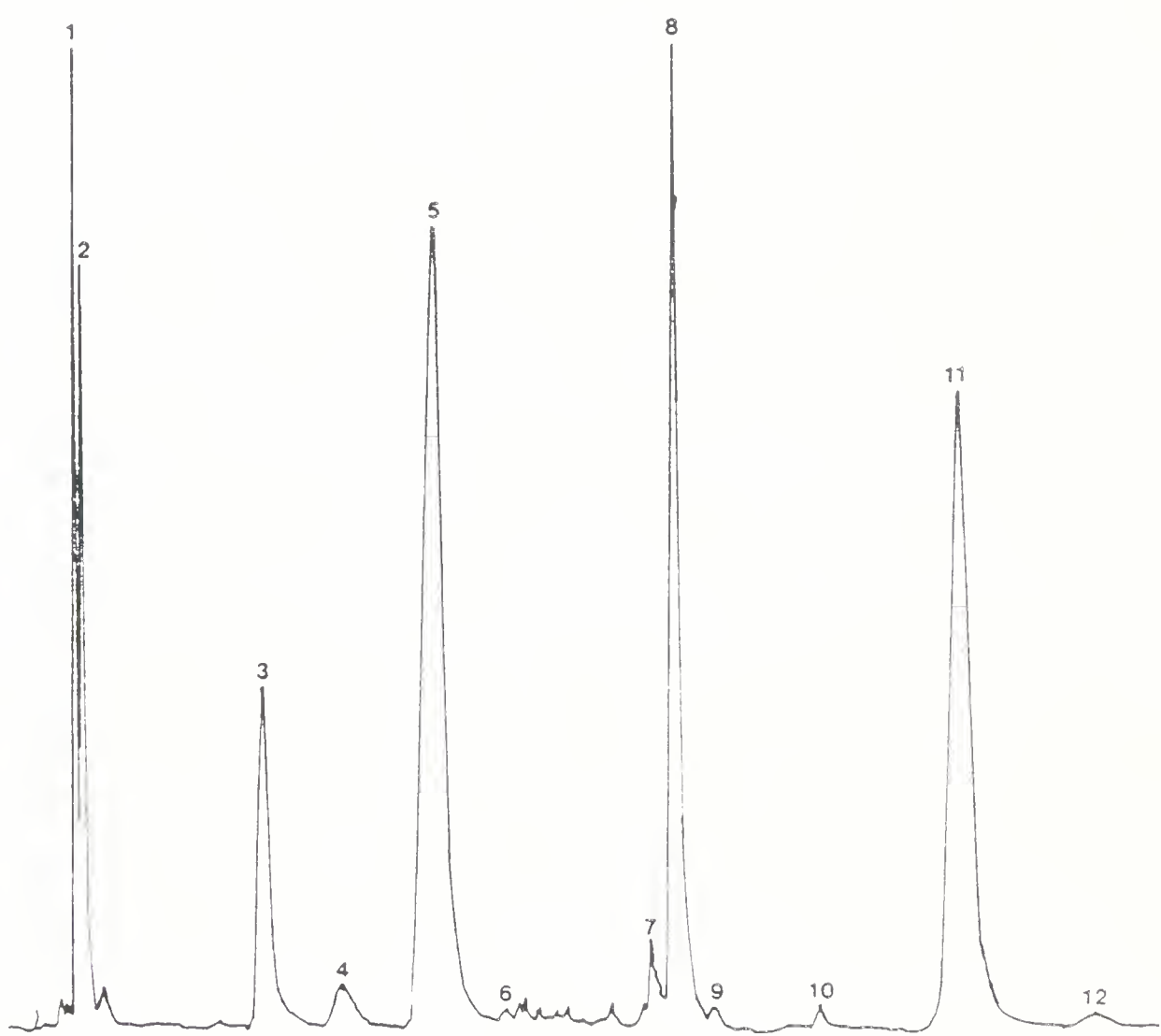
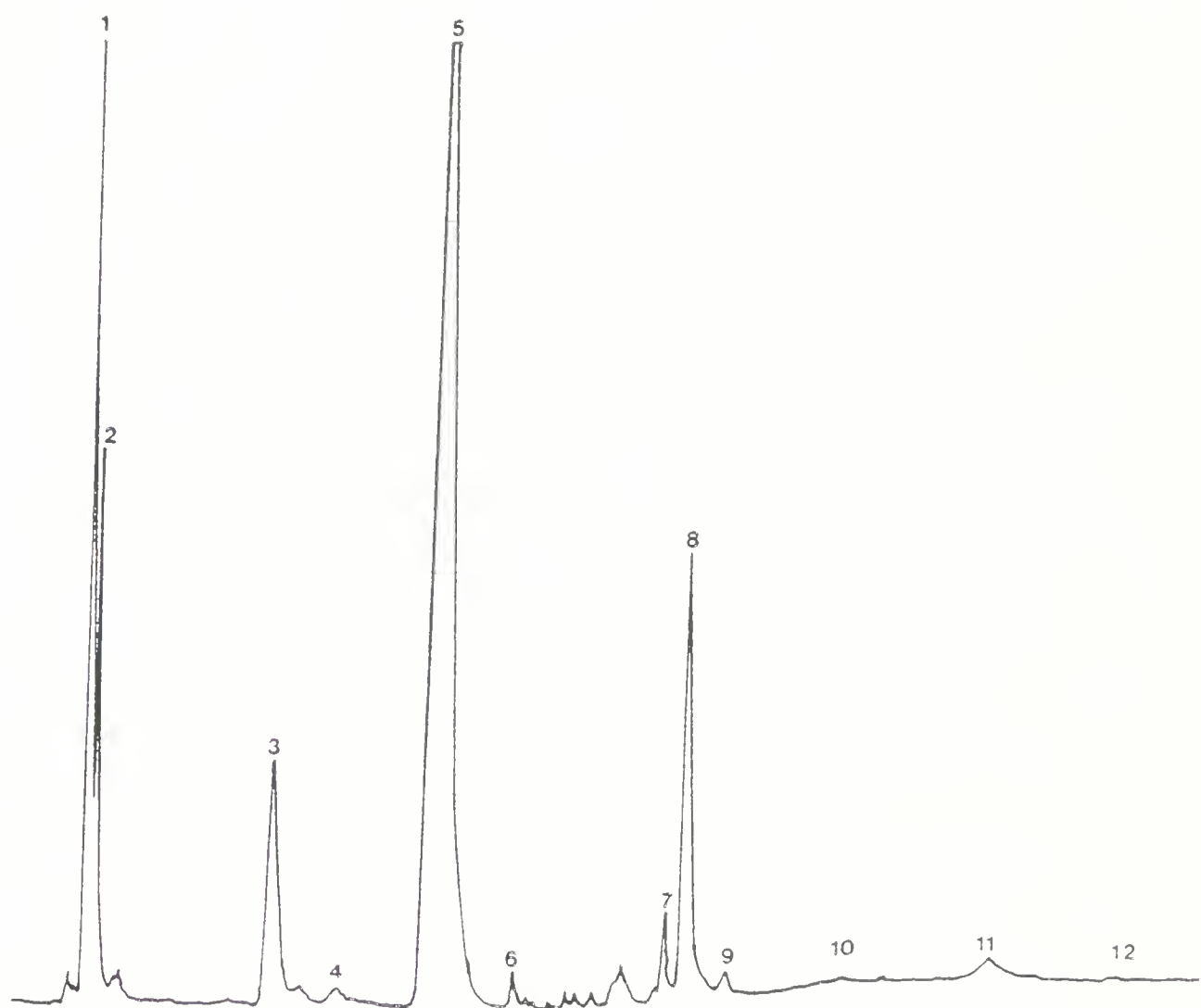


Figure II.5. Elution profile of ATP and metabolites of postrigor beef muscle. The numbered peaks are: inosine (1), hypoxanthine (2), NAD (3), AMP (4), IMP (5), GMP (6), IDP (7), ADP (8), adenylosuccinic acid and GDP (9), UDP and CTP (10), ATP (11), GTP (12).





easy measure of the NADH in this peak.

### C. Methods Used to Monitor the State of Water

#### Nuclear magnetic resonance spectroscopy

##### *Introduction*

The experiments were performed on a Bruker SXP4-100 NMR spectrophotometer operating at 60 MHz using a 14 KG Varian electromagnet and V3506 flux stabilizer. The experiments were controlled by a Nicolet 1180 computer and 293A programmable pulser. The muscle sample was cut into a small cylinder (8 mm x 10 mm) as soon as the muscle was brought into the lab from the meat packing plant. The sample was inserted into the NMR tube (10 mm x 83 mm) by placing the muscle into the top of the tube, capping the tube and then centrifuging about 20 sec in a small table top centrifuge. This procedure oriented the fibres vertically in the tube.

The nature of the NMR experiments performed in the current study can be best described in terms of the behavior of the nuclear magnetization in a rotating 3-axis coordinate system. The spectrometer magnetic field  $H_0$  is applied along the z axis and the x' and y' axes rotate around the z axis at the carrier frequency of the spectrometer. Because of the fact the ensemble of nuclei (e.g. water protons) is characterized by an excess population aligned with  $H_0$  (lower energy state) and



randomly distributed about  $H_0$ , a residual magnetization or net macroscopic magnetization ( $M_z$ ) along the z axis exists.

In the pulse Fourier transform experiment a high power radiofrequency (rf) pulse of short duration ( $H_1$ ) is applied along the x' axis. This rf pulse will cause  $M_z$  to rotate about the x' axis. The angle of rotation ( $\alpha$ ) is given by Equation 1:

$$\alpha = \gamma H_1 t_w \quad (1)$$

where  $\gamma$  is the magnetogyric ratio of the nucleus being investigated,  $H_1$  the intensity of the rf pulse, and  $t_w$  the length of the pulse (generally in the range of microseconds).

The NMR signal is detected along the y' axis. Thus when the nuclei under investigation are at equilibrium the signal is 0 since there is no residual magnetization on the y' axis. With an appropriate combination of  $H_1$  and  $t_w$ ,  $M_z$  can be rotated through  $90^\circ$  so that it becomes colinear with the y' axis, giving rise to a signal which is equivalent to  $M_z$ . However, this situation is a nonequilibrium condition, and the system returns to equilibrium by two relaxation processes. The magnetization in the x'y' plane relaxes by spin-spin relaxation ( $T_2$ ) which arises from molecular interactions which cause the individual nuclei to precess at slightly different frequencies and thus get out of phase with each other in the x'y' plane. The time constant for relaxation in the x'y' plane is given by Equation 2:

$$M_t^{x' y'} = M_z e^{-t/T_2} \quad (2)$$



The magnetization returns to equilibrium along the z axis by spin lattice relaxation ( $T_1$ ). The energy gained by the nuclei during the  $H_1$  pulse is exchanged with the lattice.

The time constant for relaxation along the z axis is given by Equation 3:

$$M_t^z = M_z (1 - e^{-t/T_1}) \quad (3)$$

In order to measure each of these relaxation processes multiple pulse techniques are utilized. The  $T_2$  relaxation is measured using a "spin echo" technique. This consists of applying a  $90^\circ$  pulse followed by a succession of  $180^\circ$  pulses. A single  $90^\circ$  pulse can not be used to measure  $T_2$  since  $H_0$  field inhomogeneities also contribute to the nuclei precessing at slightly different frequencies. Thus the loss of phase coherence by the nuclei in the x'y' plane would not be due to  $T_2$  mechanisms only. The sequence of  $180^\circ$  pulses used in the spin echo experiment is to cancel out the contribution of  $H_0$  field inhomogeneities to the measured  $T_2$ .

The  $T_1$  relaxation is measured using an inversion recovery sequence. The first  $180^\circ$  pulse inverts  $M_z$  into the negative z direction. After different times ( $\tau$ ) the size of  $M_z$  upon its return to its equilibrium position is obtained using a  $90^\circ$  pulse to bring the magnetization into the y' axis so that the NMR signal can be measured.

Mathur-DeVré (1979) indicated that biological macromolecules induce a characteristic water structure in their close vicinity due to weak macromolecular-water



interactions. As a result there is a hydration layer associated with macromolecules. The water molecules contributing to the hydration layer are dynamically oriented, and exhibit restricted motion due to a significant decrease in the translational and rotational modes of motion caused by macromolecular-water interactions. Consequently, the mobility and the extent of ordering of the hydration water molecules are distinctly different from those characterizing the fast and random motion of the bulk water.

The relaxation rates of water molecules are governed by the strength of local magnetic interactions between water nuclei and molecular motion and proton exchange rates. Since the hydration water differs from the bulk water in these properties, the relaxation rates of each of these water fractions differ. In determining the  $T_1$  of muscle sample the relaxation rate of the hydration water can not be measured independently of the bulk or free water. For this reason the  $T_1$  observed is actually given by Equation 4:

$$(T_1)_{obs} = X_f(T_1)_f + X_h(T_1)_h \quad (4)$$

$X_f$  is the fraction of free water with the spin lattice relaxation time  $(T_1)_f$ .  $X_h$  is the fraction of hydration water with the spin lattice relaxation time  $(T_1)_h$ . Although the fraction of free water  $X_f$  is much greater than the fraction of hydration water  $X_h$  the term  $X_h(T_1)_h$  can be an important contributor to  $(T_1)_{obs}$  since the  $(T_1)_h$  is very



short due to the restricted motion of water molecules in the hydration layer.

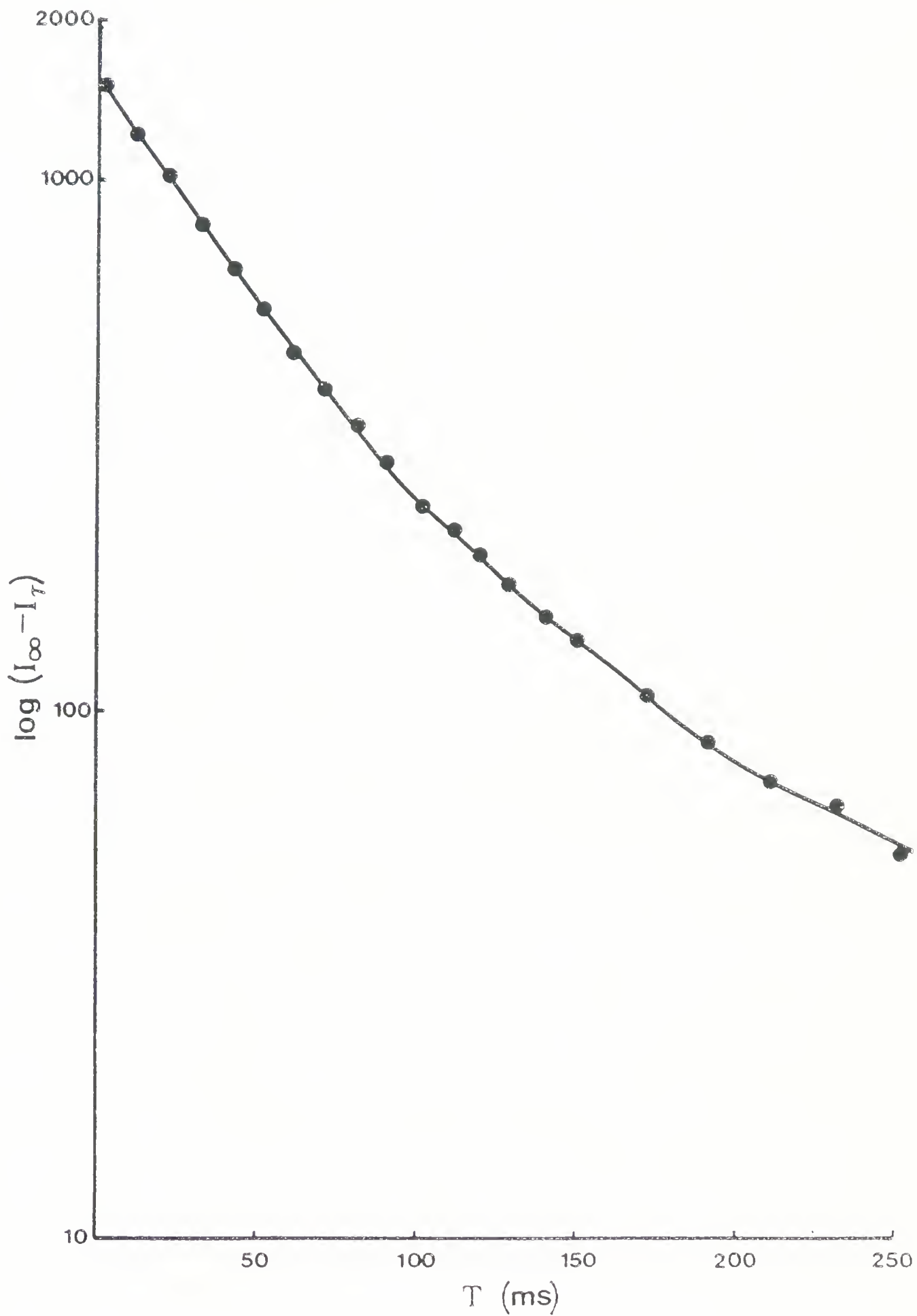
#### *NMR $T_2$ determinations*

The spin-spin relaxation times ( $T_2$ ) were measured using the Carr-Purcell-Meiboom-Gill Method ("spin echo" experiment). This consists of applying a  $90^\circ$  pulse followed by a succession of  $180^\circ$  pulses. Figure II.6 presents the results of one such experiment on postmortem muscle (54 h). The curve exhibits the nonexponentiality characteristic of meat samples, suggesting more than one fraction of water. The problem with this method is how to draw a best fit line that reflects the  $T_2$  associated with these different water fractions. This problem makes the accurate assessment of  $T_2$  difficult and for this reason the determination of  $T_2$  was abandoned.

#### *NMR $T_1$*

The spin lattice relaxation times ( $T_1$ ) are determined by applying a series of pulse sequences of the type  $180^\circ-\tau-90^\circ$ . By repeating this pulse sequence at differing  $\tau$  values, the exponential regrowth of magnetization ( $M_z$ ) can be detected. The  $\tau$  values generally were varied from 1 sec to 3.5 sec in 100 msec increments. The  $T_1$  was determined by least square fitting and gave a standard error of 0.3-0.5%. Typically, the experiment was repeated at 15 min intervals over the first 26-28 hr postmortem period. The measurements were at an ambient probe temperature of  $24 \pm 1^\circ\text{C}$ . These

Figure II.6. Plot of  $\log(I_{\infty} - I_t)$  vs  $t$  (s) following the Carr - Purcell - Meiboom - Gill Method for an NMR  $T_2$  determination of 54 h beef muscle.





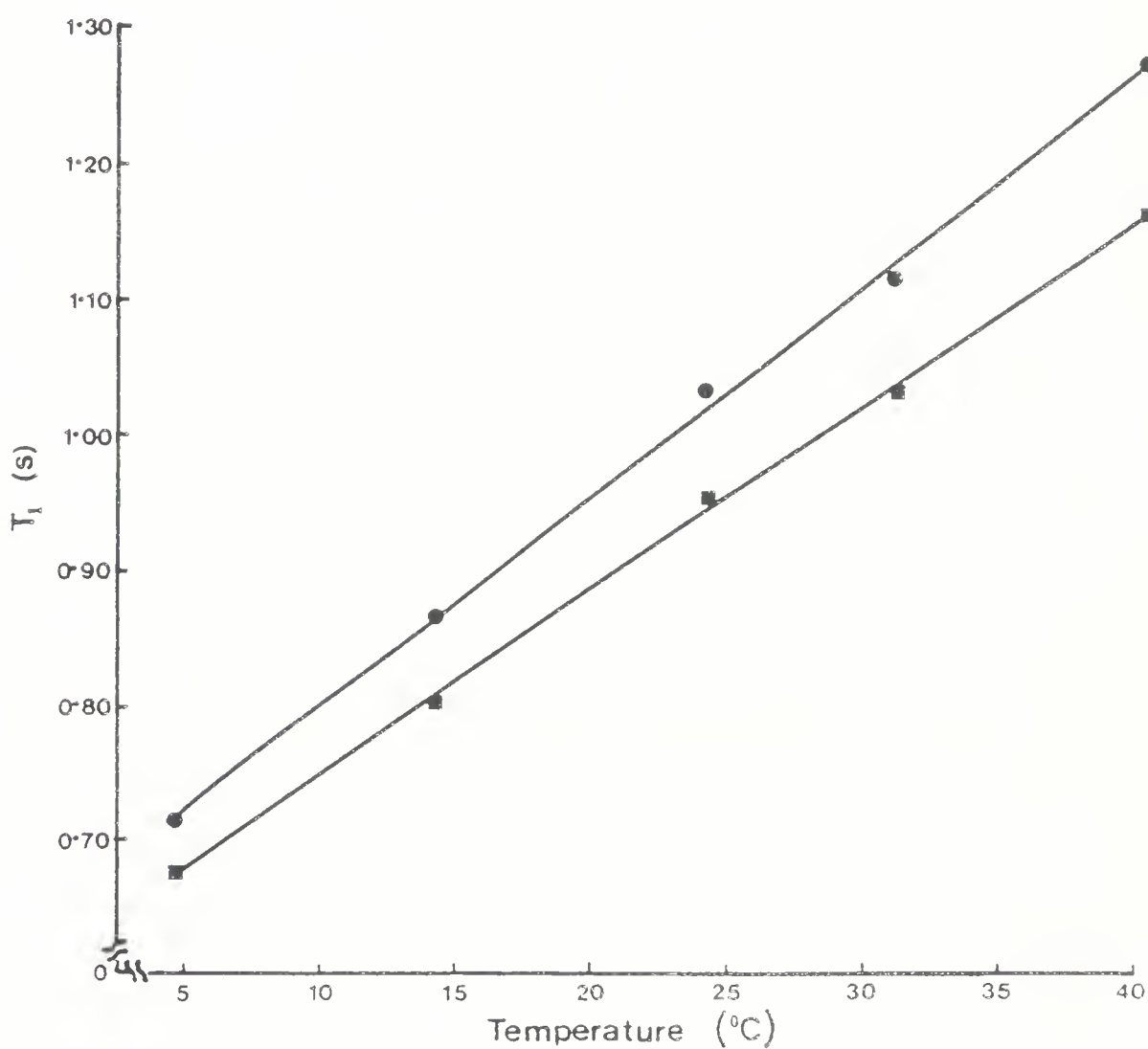
parameters were chosen as a result of the following observations.

The temperature of the meat was maintained at a constant value ( $24 \pm 1^\circ\text{C}$ ). In one experiment where the temperature was varied to examine temperature effects upon  $T_1$ , a Bruker B-ST100/700 temperature controller was used. The actual temperature was measured by a thermocouple in a glycerol-containing probe. Figure II.7 represents the effect of temperature change on the  $T_1$  values of myofibrils rehydrated to 82% moisture. It is evident that varying temperature causes a change in  $T_1$ . Therefore, constant temperature was used in all other muscle  $T_1$  experiments.

Chang *et al.* (1976), studying rat muscle entering rigor, reported nonexponentiality in their plots of  $\log(I_\infty - I_\tau)$  vs  $\tau$ . The slope of this curve equals  $1/2.303T_1$ . They suggested that only the latter part of the curve (values obtained from  $\tau$  values greater than 1 sec) were sensitive to the water in postmortem muscle. The  $T_1$  from this part of the curve was referred to as  $T_{1B}$ . However,  $T_{1A}$  (measured with short  $\tau$  values) remained practically unchanged with time postmortem. They considered  $T_{1A}$  to reflect the weighted average of all the water protons.

During the development of the  $T_1$  methodology several muscle samples at various times postmortem were examined to see if  $T_{1A}$  and  $T_{1B}$  could be measured successfully using the instrument in this study. In these studies, the nonexponentiality of the  $\log(I_\infty - I_\tau)$  vs  $\tau$  plots reported by Chang

Figure II.7. Plot of  $T_1(s)$  vs temperature ( $^{\circ}\text{C}$ ) of rehydrated myofibrils (82% moisture) at pH 6.0 (•-•-•) and pH 8.0 (■-■-■). The standard error of each point plotted is  $\pm 0.3\text{-}0.5\%$ .

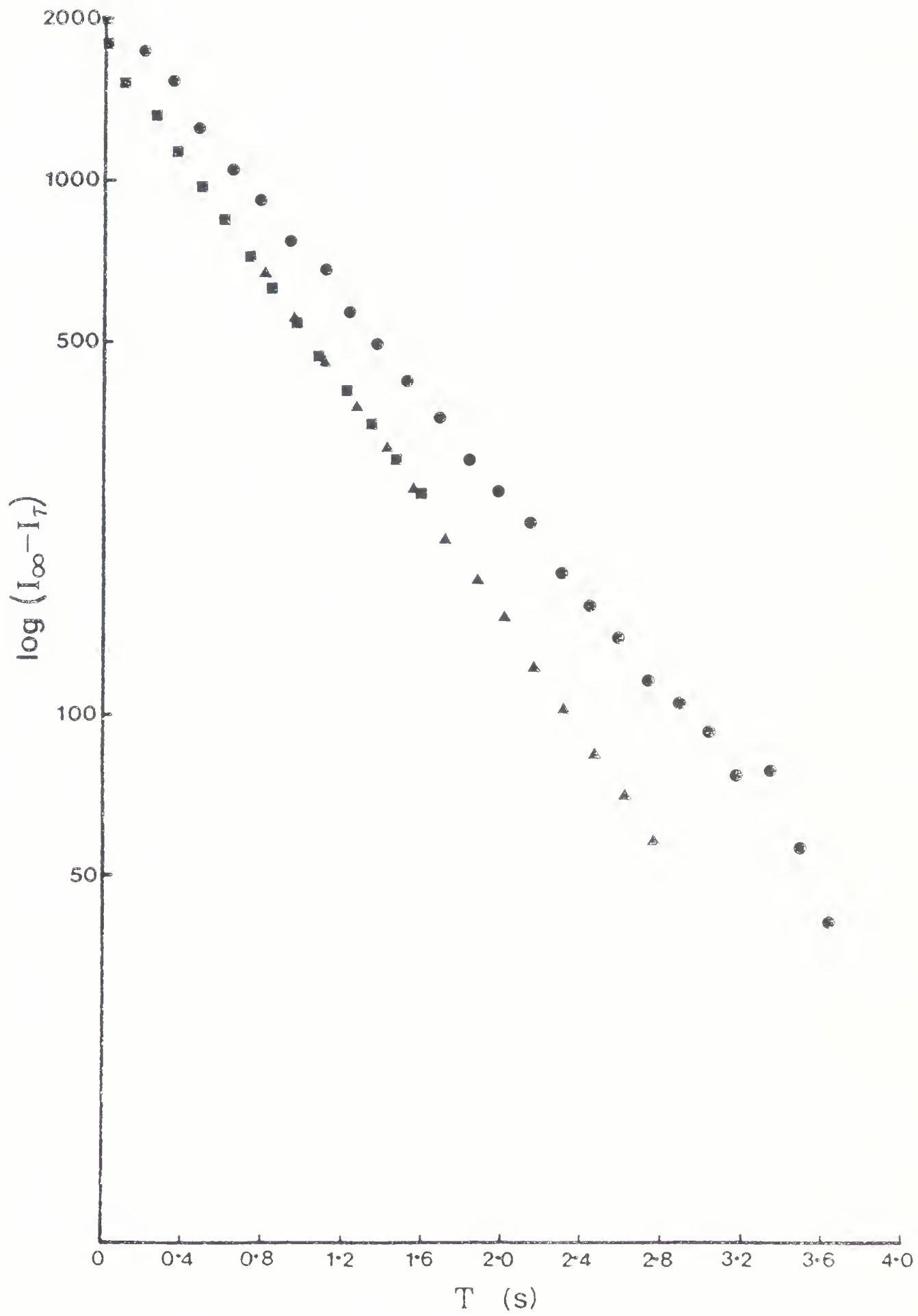




*et al.* (1976) was not observed. Figure II.8 shows one such plot of a late prerigor sample. Such a sample should show maximum differences between T<sub>1A</sub> and T<sub>1B</sub>. The plot using both short and long  $\tau$  values for the experiment reveals no nonexponentiality. Myofibrils at varying water contents and pH values were examined over the same range of  $\tau$  values and, as indicated in Figure II.8, a representative sample at pH 6.0 and 82% moisture exhibited no nonexponentiality. The differences between the results of Chang *et al.* (1976) and those reported in this thesis cannot be explained. The longer  $\tau$  values (1 sec to 3.5 sec) have been used in these NMR experiments to be certain that the greatest sensitivity to alterations of the water in the muscle was achieved. Additionally, the longer  $\tau$  values allow the diode mode of the spectrophotometer to be used wherein an averaging of the signal leads to a greater precision of the points being plotted.

Edzes and Samulski (1978) developed a selective hydration inversion technique in which the contribution of cross relaxation (a transfer of spin energy between a bound water proton and a proton at the macromolecular surface) to the relaxation process can be assessed. The method is based on a difference in the length of the 180° pulse. A strong 180° pulse (high amplitude, short pulse length) results in the complete inversion of both the water and macromolecular magnetization. However, a weak 180° pulse (low amplitude, long pulse length) will completely invert the water

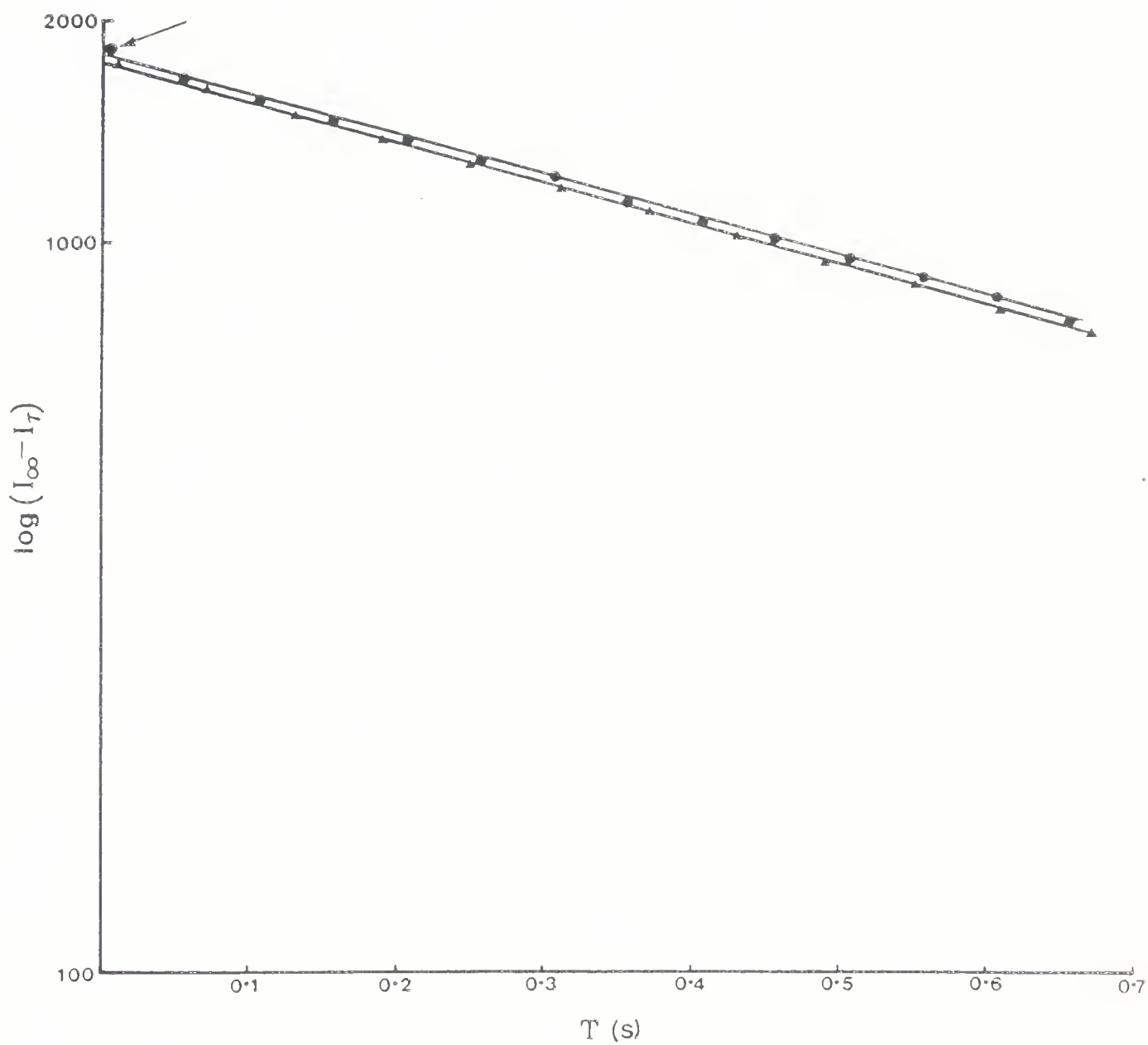
Figure II.8. Plot of  $\log(I_\infty - I_\tau)$  vs  $\tau$  (s) on (a) late prerigor meat using short  $\tau$  values (0.005 s - 1.6 s; ■-■-■) and long  $\tau$  values (0.8 s - 2.75 s; ▲-▲-▲); (b) myofibrils at pH 6.0 and 82% water (●-●-●) using a wide range of  $\tau$  values (0.2 s - 3.6 s).





magnetization but it no longer inverts the macromolecular magnetization. The 90° measuring pulse length is the same in both cases. Such experiments, especially in low water content samples, show considerable deviations from exponentiality when using a long 180° pulse length. The deviation is particularly evident for short  $\tau$  values. Edzes and Samulski (1978) calculated that cross relaxation may contribute as much as 40% of the observed water relaxation rate in chicken muscle meat. The macromolecular and water magnetizations were measured from the free induction decay (FID) amplitudes at 10 and 200  $\mu$ sec after the pulse. This was near the dead time of the spectrophotometer detector used in this study and so such early measurements could not reliably be made. Edzes and Samulski (1978) reported that, although the macromolecular magnetization decreases rapidly in the initial part of the decay (indicating cross relaxation), both phases decay with approximately the same relaxation rates at longer  $\tau$  values. In Figure II.9 the magnetization was plotted vs  $\tau$  values ranging from 5 msec to 700 msec for both long (108.5  $\mu$ sec) and short (4.056  $\mu$ sec) 180° pulse lengths. The first datum point (see arrow) using the long 180° pulse length has the greatest deviation, suggesting a cross relaxation process as one of the mechanisms of relaxation. The computer printout of the least squares fit of the data using the long (108.5  $\mu$ sec) 180° pulse indicated (in the "observed" minus "calculated" column) a positive deviation of all points up to  $\tau$  values

Figure II.9. Plot of  $\log(I_\infty - I_r)$  vs  $\tau$  using long (108.5  $\mu$ s;  $\bullet-\bullet-\bullet$ ) and short (4.056  $\mu$ s;  $\blacktriangle-\blacktriangle-\blacktriangle$ )  $180^\circ$  pulse lengths.

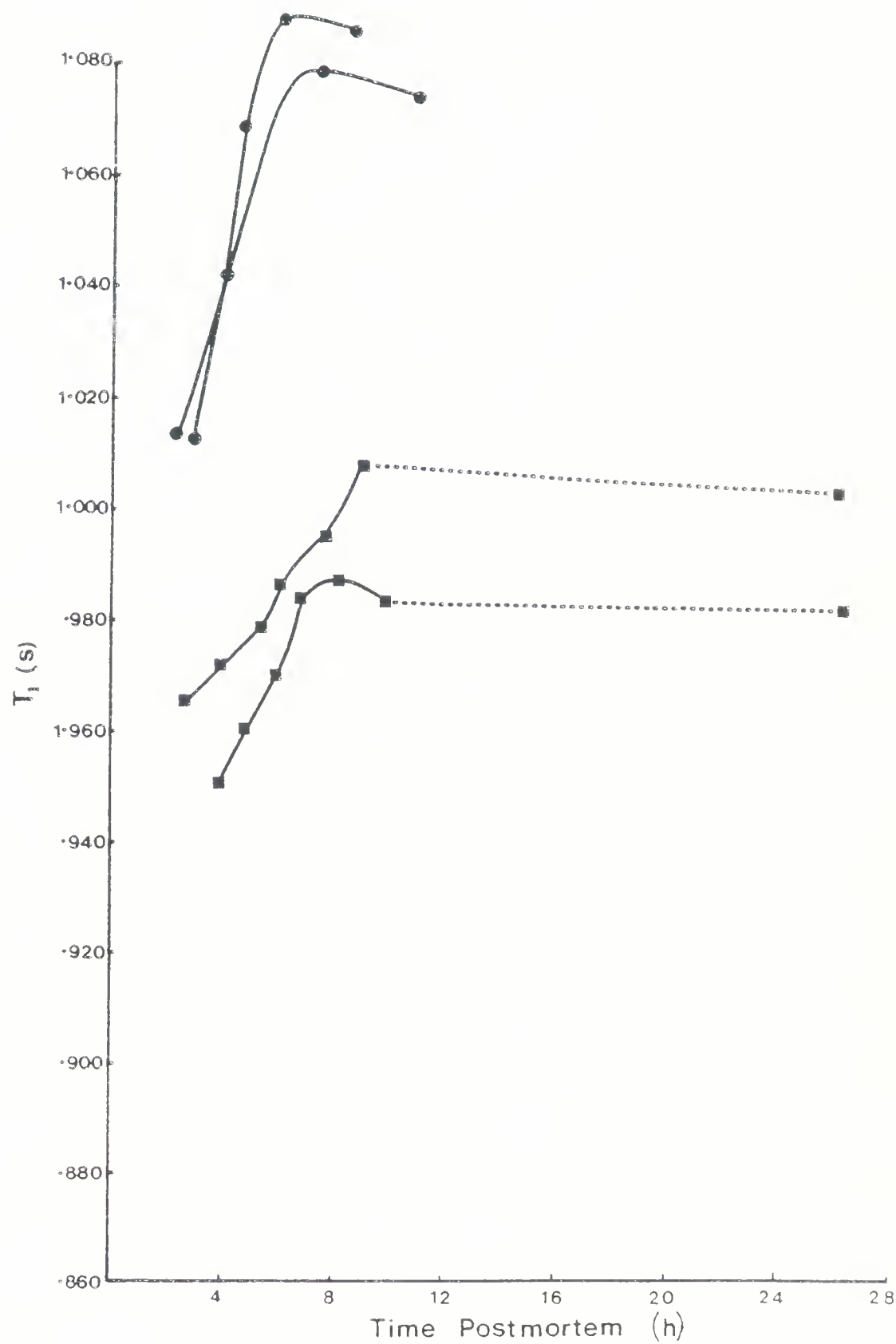




of 450 msec. The deviation was very small but may in fact support the conclusion that some cross relaxation was observed. The results presented in Figure II.9 do, however, confirm the observations of Edzes and Samulski (1978) that the  $T_1$  observed is similar when either short or long 180° pulse lengths are used in meat samples. Cross relaxation would not be expected to be a major factor in meat where the water content is near 75%.

In Figure II.10 two different muscle sources with 2 samples from each source were run to determine reproducibility in the  $T_1$  profile of a given muscle with time postmortem. The intention of the experiment was to determine the reliability of the sample run on the NMR as being representative of the muscle as a whole. Although some differences do exist between samples of a muscle from each muscle source, the general appearances of the plots are comparable and were viewed as reflecting the postmortem properties of the muscle in question. The vertical displacement of the recorded  $T_1$  values for samples from the same muscle may reflect variation in sample preparation. The actual  $T_1$  value is influenced by water content. The samples that were cut out were not immediately inserted into the sealed NMR tubes and thus may have lost slightly differing amounts of moisture due to some surface dehydration.

Figure II.10. Plot of  $T_1(s)$  vs time postmortem (h) for duplicate determinations from carcass A (•-•-•) and carcass B (■-■-■). The standard error of each point is  $\pm 0.3\text{--}0.5\%$ .





### NMR of model systems

Myofibrils from aged *semitendinosus* were prepared according to the procedures of Hay et al. (1973) from an initial 300 g of meat. A portion of the preparation was washed thoroughly with water to remove the salts and then the myofibrils were suspended in water and freeze dried. Solutions, having a pH range from 5.5 to 8.5, were prepared, consisting of .15 M KCl, 50 mM Tris-maleate, 1 mM NaN<sub>3</sub>, and at times 500 μM EGTA or Ca<sup>2+</sup>. This would provide Ca<sup>2+</sup> or EGTA concentrations of approximately 0.4 μmole/g in the final myofibril preparation. Approximately 75 mg of freeze dried myofibrils were added to an NMR tube (10 mm x 83 mm) followed by an appropriate amount of buffer to obtain the desired moisture content. The myofibrils and the buffer were then mixed with a glass rod within the NMR tube. The contents were allowed to equilibrate for a minimum of 24 hr at room temperature before measurements were made. This step was found necessary to improve reproducibility of T<sub>1</sub> values between duplicates of the same sample treatment. In experiments where ATP (.25 g) was added to the myofibrils in the NMR tube, the NMR readings were begun immediately after mixing without any equilibration time.

### NMR of aged and cooked meat samples

The aged meat samples (7 days) obtained from the Department of Animal Science, University of Alberta, courtesy of Dr. Hawrysh of the Department of Home Economics



and Dr. Price of the Department of Animal Science, were primarily from beef possessing a high ultimate pH. Many of the samples exhibited the properties of dark-firm-dry beef.  $T_1$  values were determined for these samples in both the raw and cooked (internal temperature, 65°C) states.

Additional meat samples possessing a "normal" range of ultimate pH were obtained from local supermarkets. Only the  $T_1$  values of the raw meat were assessed for these samples.

#### Other physical and chemical measurements related to water

##### *Swelling capacity*

The swelling capacity of meat has been defined by Hamm (1974) as the spontaneous uptake of fluid from any surrounding fluid resulting in an increase of weight and volume of the muscle. He indicated that swelling capacity usually shows a close correlation with WHC. The swelling capacity was determined from the muscle strips incubated in the ECS buffer and was calculated using the following formula:

$$\text{Swelling capacity (\%)} = \frac{\text{Ma (mg)} - \text{Mb (mg)}}{\text{Mb (mg)}} \times 100\%$$

where:

Mb = muscle weight before incubation in the ECS buffer  
Ma = muscle weight after incubation in the ECS buffer

##### *Water holding capacity*

Two methods of measuring the water holding capacity were examined. The filter paper press method of Grau and Hamm (1957) consisted of placing 300±5 mg of the tissue on



6.5 x 6.5 cm piece of filter paper (Schleicher and Schull, 2040b) in triplicate. The filter paper and muscle were stacked between plexiglass sheets (1 x 8 x 8 cm) which were placed in a lab press and a pressure of 250 pounds per square inch was applied for 5 min. The filter paper was kept at a constant moisture content by storing the paper over a saturated solution of KCl in a desiccator. The applied pressure results in the muscle being squeezed into a circular patty. The juices resulting from the compression are absorbed by the filter paper and a round, brown colored spot is formed. The area reflects the WHC of the sample. A large ring represents a low WHC. The actual area of the spot left by the water release is obtained by marking the outer ring with a pencil immediately after its removal from the press and the total area measured with a planimeter. The area of the spot left by the patty is also measured and subtracted from the total area to give an area which is proportional to the weight of water lost from the sample. The areas obtained in this manner from meat at various stages of rigor were plotted versus time postmortem to observe the changes in WHC.

The effect of pH variation upon the WHC of meat removed at various times postmortem was also examined. This procedure consisted of homogenizing the muscle sample in a Waring blender with an equal weight of water for approximately 2 min. A portion of this homogenate was placed in the Sorval Omnimixer and the pH was adjusted by



the addition of solid Tris (tris hydroxymethylaminomethane) or trifluoroacetic acid (concentrated) and the sample homogenized. Using this approach, approximately 7 homogenates were obtained spanning a range in pH of approximately 3-8. An aliquot (300 mg) of these homogenates was weighed and the filter paper press method, outlined above, was followed to measure the water holding capacity at each of the homogenate pH's. The planimeter area was plotted versus pH..

The second method was a centrifugation procedure in which the weight of expressed juice was calculated as a percentage of the initial weight. The procedure of Bouton *et al.* (1971) was followed in which muscle samples in duplicate (approx. 2 g) were placed in polycarbonate tubes and centrifuged at 28,000 rpm for 1 hr in the #30 rotor of the Beckman L2-65B ultracentrifuge. The expressed juice was removed from the muscle sample by inserting Kimwipes into the tube to soak up the juice. A high percentage of expressed juice is indicative of a sample having a low WHC.

The centrifugal technique was used for the results reported in this thesis since the sample manipulation and the area measurements using the planimeter were very time consuming. Additionally, the press method did not have any apparent advantages over the centrifugal technique in obtaining an indication of the WHC of the muscle.



### Differential scanning calorimetry

Approximately 10 mg of the muscle at various times postmortem were hermetically sealed in a capsule and frozen by pouring liquid N<sub>2</sub> into the cooling tower of the Dupont Model 910 DSC. The freezing rate of the sample was determined to be 0.5 C°/sec. After equilibration at -50°C, the temperature was increased at a rate of 10 C°/min up to 140°C. The two pen recorder was set to run at a time base of 1.0 min/cm and the sensitivity of the pens was adjusted to 50 mV/cm and 20 mV/cm in order to detect the major and minor transitions, respectively. The major transition was the endothermic peak corresponding to the fusion of ice. This peak area was measured by a planimeter. The mg of freezable water in the sample was calculated by comparing the measured area of the endothermic peak near 0°C to a plot of planimeter area of pure water vs mg water from previous determinations. The differences between the mg of total water in the muscle sample and the freezable water obtained from the endothermic peak gave the nonfreezable water content of the tissue. This nonfreezable water was expressed as a percentage of the total tissue weight.

The minor transitions examined were the endothermic peaks observed in the 50-80°C range. These peaks reflect transitions occurring in the protein components of the meat.



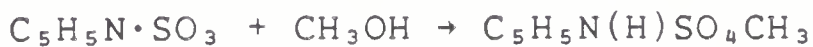
### *Moisture determinations*

Two methods of moisture determination were used. The first was simply weighing triplicate samples into disposable aluminum dishes and then heating at 110°C overnight. The loss in weight represented moisture and was expressed as a percentage of the initial wet weight. Additional moisture data were obtained from the drying of the muscle strips used in the extracellular space determinations.

The second method examined was the Karl Fischer method found in sections 32.046-32.049 of the Official Methods of the Association of the Official Agricultural Chemists (AOAC). Surprisingly, the method using N,N-dimethyl-formamide (DMF; reagent grade) as the solvent for the titration could not be used since no reaction between the Karl Fischer reagent and the water in the extract occurred. If methanol was substituted for formamide in the titration, a normal titration could be performed. Thus, the AOAC method for extraction of water from a meat sample using DMF was followed, but the solvent in the titration was methanol, dried by distillation over magnesium metal. The Karl Fischer reaction takes place in two steps:



and



As shown by the above reactions, for each mole of water, 1 mole of iodine, 1 mole of sulfur dioxide, 3 moles



of pyridine and 1 mole of methanol are required. An explanation for the problems with the titration using DMF as the solvent may be that insufficient methanol was present to carry the reaction to completion.

The most reliable results were obtained with the oven method. The high moisture content of the meat sample resulted in such a large dilution factor that a 0.1 mL variation in Karl Fischer reagent would relate to a  $\pm 1\%$  variation in the moisture content of the meat.

#### *Extracellular space measurements*

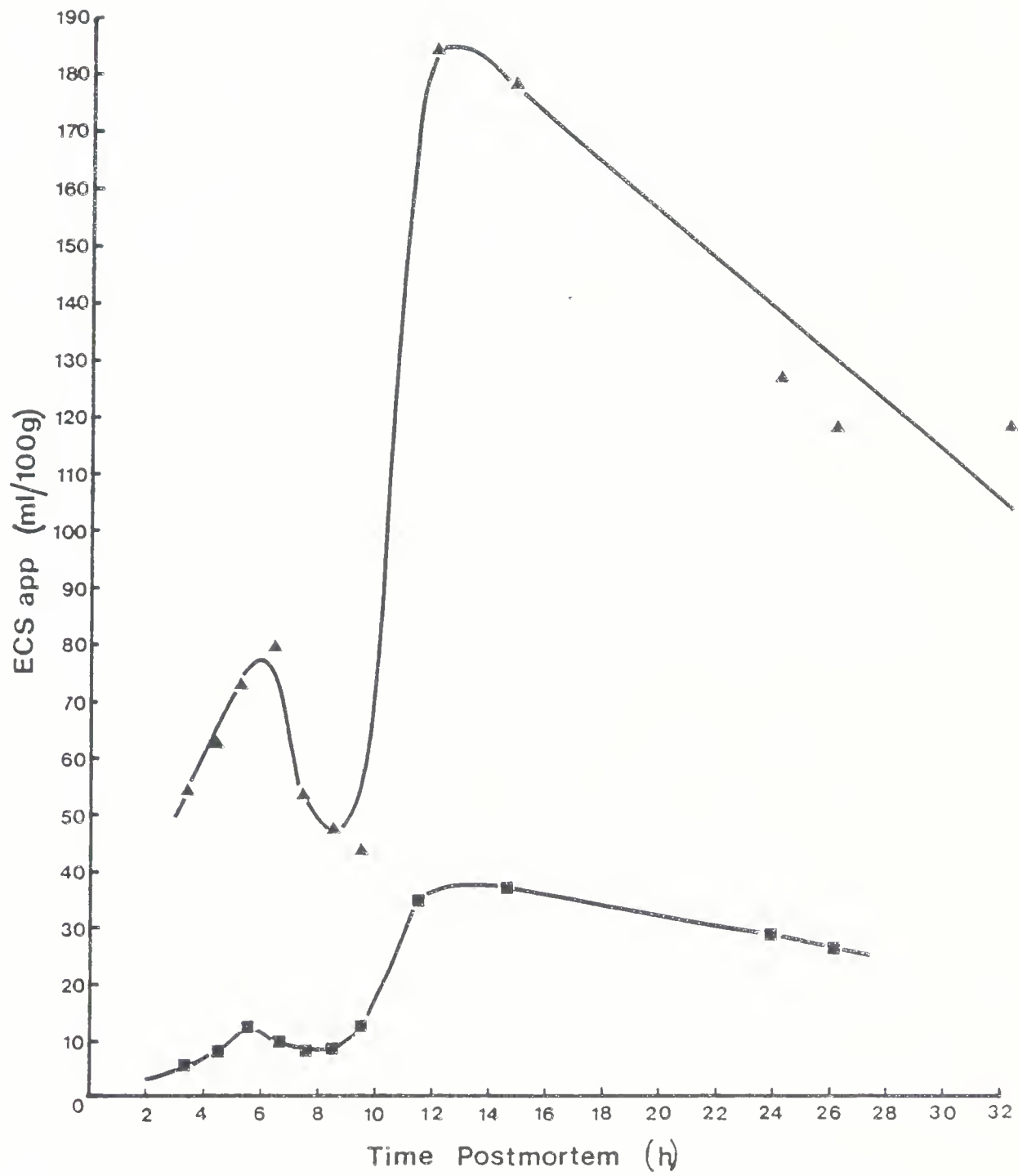
Heffron and Hegarty (1974) measured the extracellular space (ECS) of muscle entering rigor using a Ringer-Locke solution containing 0.3% inulin. The size of the ECS they measured steadily increased to a maximum at rigor. The experiments reported in the present study employed their method with minor modifications. The pH was maintained at 7.2, rather than incubating at the pH of the muscle strip, so that a comparison of the ECS could be made at different times postmortem without adding another variable (pH). The incubation buffer prepared for the preliminary studies on changes in the ECS consisted of 3.0 g inulin, 9.0 g NaCl, 0.42 g KCl, 1.0 g glucose, 0.5 g NaHCO<sub>3</sub>/1000 mL adjusted to pH 7.2. The inulin was measured by the method of Pappius and Elliott (1956), which involved homogenization of the blotted muscle strip in 6% TCA, centrifuging the precipitated proteins and determining the inulin content using resorcinol. The sample containing the inulin (1.0 mL)



was added to a solution of 0.125% resorcinol in ethanol (1.0 mL), 30% HCl (3.0 mL). The solution was incubated in a 80°C bath for exactly 10 min. Following a cooling period of exactly 10 min, the absorbance was read at 450 nm. The results, plotted in Figure II.11, show that the size of the ECS is not reasonable. It appears that inulin or other resorcinol-positive contaminants were being absorbed into the sarcolemma or resorcinol-positive substances were passing through the membrane and increasing the amount of inulin apparently in the muscle. When the procedure of Heffron and Hegarty (1974) was followed in which the muscle strip (following incubation in inulin) was extracted using the Ringer-Locke solution for 18 hr at 4°C and the extracted inulin determined, more reasonable values for the ECS were obtained (Figure II.11).

Obtaining reproducible color development using the resorcinol method for inulin proved difficult and the extraction procedure required several additional steps, so alternative methods were examined. Since the tissue would swell to a considerable extent in the Ringer-Locke buffer described above, some new buffers were examined. A HEPES buffer system similar to that used in the Animal Science Department for ion transport work (except for the addition of inulin) was tried. The buffers consisted of 1.0 mM CaCl<sub>2</sub>, 1.2 mM NaH<sub>2</sub>PO<sub>4</sub>, 1.2 mM MgSO<sub>4</sub>, 5.9 mM KCl, 10 mM NaHCO<sub>3</sub>, 20 mM HEPES, 116 mM NaCl, 5.0 mM acetate and 156 mM inulin (with 5 x 10<sup>4</sup> dpm/mL inulin [<sup>14</sup>C] carboxylic acid in

Figure II.11. Plot of ECS app (mL/100 g) vs time postmortem based on the resorcinol determination of inulin in a 6% TCA extract of an incubated muscle strip ( $\blacktriangle$ - $\blacktriangle$ - $\blacktriangle$ ) and the resorcinol determination of inulin in an 18 h Ringer - Locke solution extract of an incubated muscle strip ( $\blacksquare$ - $\blacksquare$ - $\blacksquare$ ).





the final solution). The other buffer system examined was taken from the procedure of Vaccari and Maura (1978) and included 107 mM NaCl, 6.0 mM KCl, 0.7 mM NaH<sub>2</sub>PO<sub>4</sub>, 3.75 mM Na<sub>2</sub>HPO<sub>4</sub>, 156 mM inulin (with 5 x 10<sup>4</sup> dpm/mL inulin [<sup>14</sup>C] carboxylic acid in the final solution), pH 7.4. The inulin [<sup>14</sup>C] carboxylic acid was from Amersham and was purified by gel exclusion chromatography and had a molecular weight of 5175±95. A comparison of the results obtained from the two buffers is shown in Figure II.12. It was observed that the swelling of the tissue was the same for both buffers but the tissue in the HEPES buffer contracted during the incubation step (particularly the early postmortem muscle strips). The contraction of the muscle strips may be the reason why there is a difference in the early postmortem ECS plots. The tissue in the HEPES buffer did not exhibit the drop (minimal ECS at 5 hr) in ECS app (see below) after the initial rise (peak near 2 hr) that was observed with the tissues incubated in the phosphate buffer. Perhaps the calcium added to the HEPES buffer promotes contraction of the muscle strip which in turn affects the ECS measurement.

As a result of these observations, the buffer of Vaccari and Maura (1978) was adopted except that the incubation times were increased to 75 min. Figures II.13 and II.14 show the incubation profiles of both prerigor and postrigor muscle strips. ECS dw (see below) reflects the amount of inulin taken up by the muscle strip. After 75 min of incubation in both the prerigor and postrigor muscle

Figure II.12. Plot of ECS app (mL/100 g) vs time postmortem using HEPES buffer (■-■-■) and phosphate buffer (●-●-●).

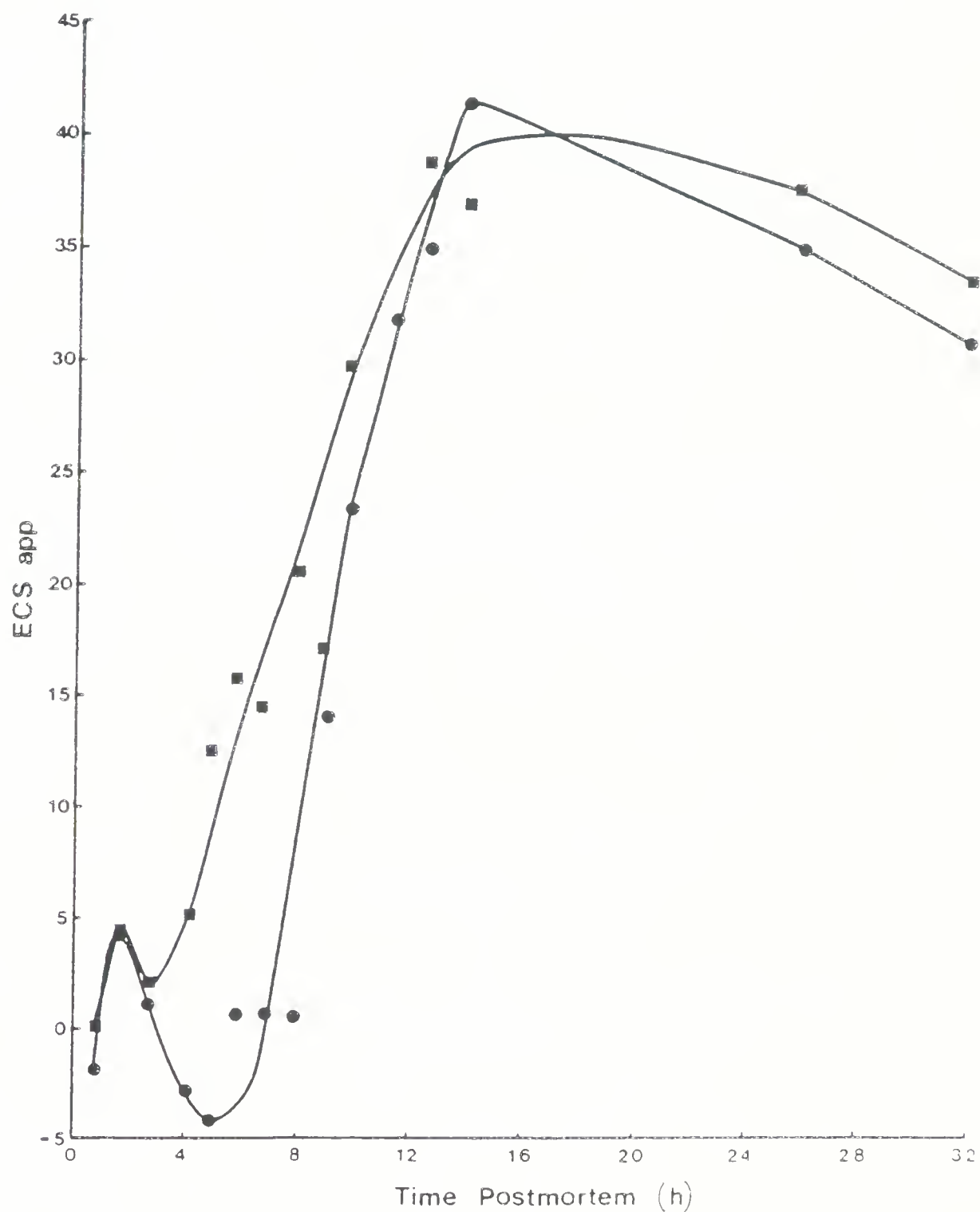


Figure II.13. Plot of ECS app (mL/100 g) vs incubation time (•-•-•) and ECS dw (mL/g dry weight) vs incubation time (■-■-■) for prerigor muscle.

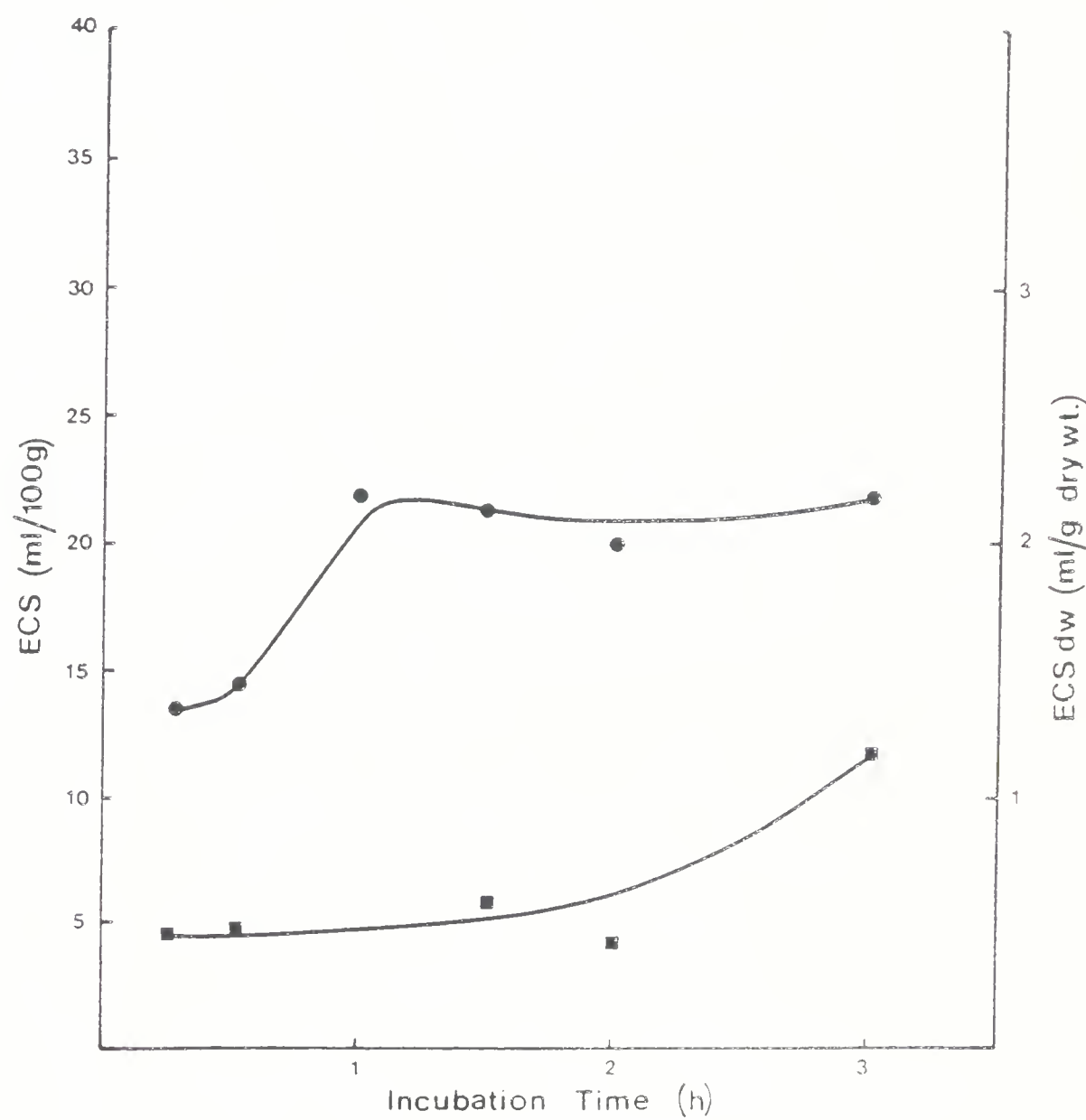
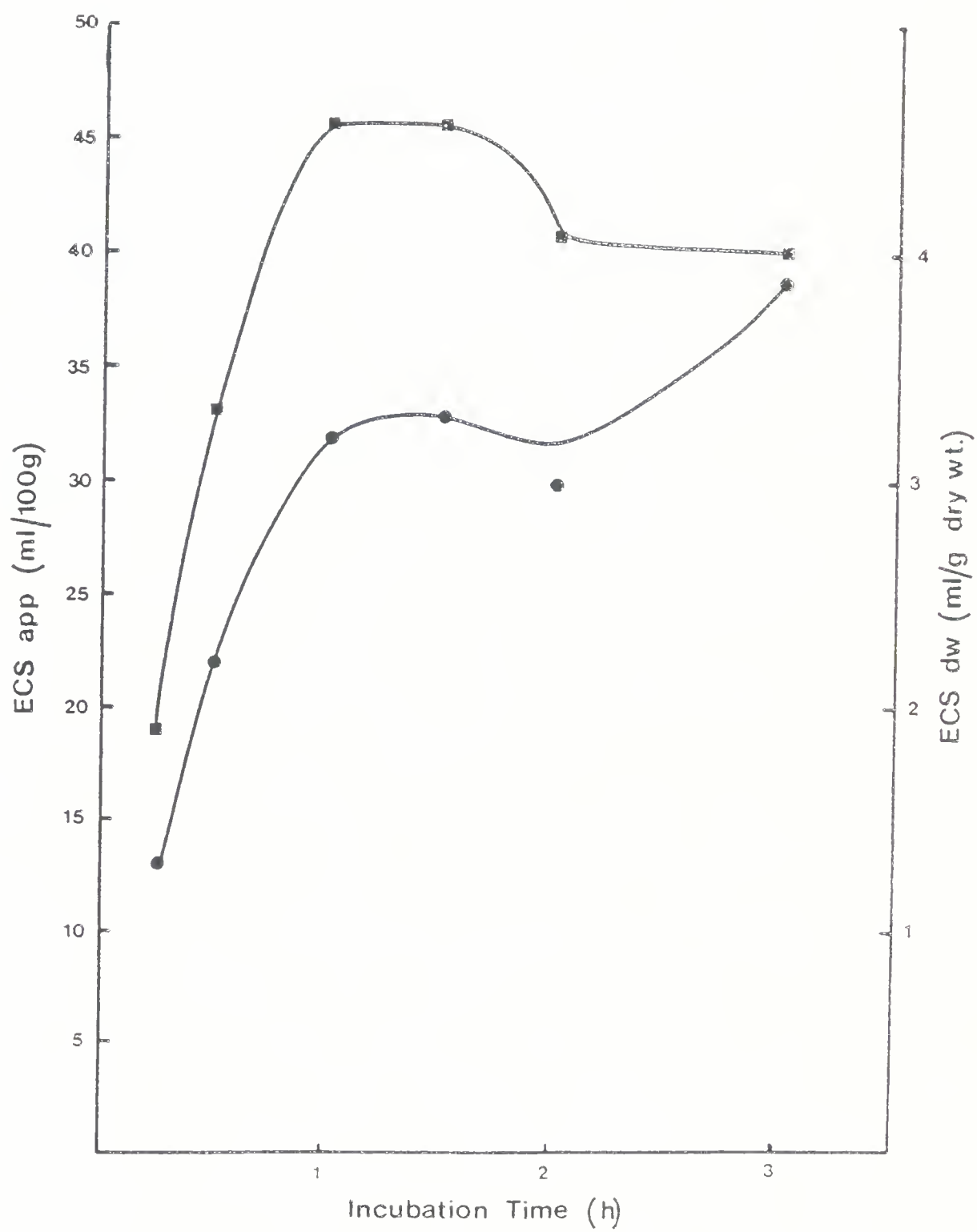


Figure II.14. Plot of ECS app (mL/100 g) vs incubation time (■-■-■) and ECS dw (mL/g dry weight) vs incubation time (●-●-●) for postrigor muscle.





strips, a plateau on the graphs has been reached, indicating the inulin has totally permeated the muscle strips. The differences in the appearance of the ECS app and ECS dw between the prerigor and postrigor samples in these incubation profiles will be discussed in the ECS results section.

For the above reasons, the following procedure for ECS measurements was followed. Approximately 75 mg of muscle was weighed out in triplicate and incubated for exactly 75 min in a buffer consisting of 107 mM NaCl, 6.0 mM KCl, 0.7 mM NaH<sub>2</sub>PO<sub>4</sub>, 3.75 mM Na<sub>2</sub>HPO<sub>4</sub>, 156 mM inulin (with 5 x 10<sup>4</sup> dpm/mL inulin [<sup>14</sup>C] carboxylic acid in the final solution), pH 7.4. After the incubation was completed at room temperature, the muscle strip was placed on a filter paper to remove the excess liquid and reweighed in a scintillation vial. The sample was dried at 110°C overnight and reweighed. The tissue was solubilized by adding 0.15 mL water and incubating the tissue at room temperature for a minimum of 6 hr, followed by addition of 1 mL NCS tissue solubilizer (Amersham). The vials were shaken overnight, after which time the tissue was solubilized. Glacial acetic acid (50 µL) was added to the vial contents to reduce a problem with chemiluminescence. After 10 mL of aquasol (New England Nuclear) were added, the contents were shaken and counted in the liquid scintillation counter. Quenched <sup>14</sup>C standards were used to obtain values relating percent efficiency vs channel ratio. These values were entered into



the computer and a quadratic equation computed which related the channel ratio to the efficiency of the count. The samples were counted for exactly 1 min. The channel ratio and the counts per minute (cpm) were entered into the computer and a program was developed in which the efficiency for each channel ratio was divided into the cpm, giving the disintegrations per minute (dpm). The dpm for each sample was then entered into the computer to calculate the ECS app and ECS dw outlined below.

The results were expressed in two ways. The first expressed the ECS as mL/g dry weight. The formula used to calculate the ECS in this way was:

$$(1) \quad \text{ECS dw} = \frac{\text{total dpm/g muscle (dry weight)}}{\text{dpm/mL incubating solution}}$$

A measure of the size of the ECS after swelling is given with this method of calculation.

The second method of calculation was based on the following reasoning. The muscle strip was incubated under conditions that prevented normal metabolism in the cell and as a result the tissue had a tendency to take up fluid from the incubating solution. This swelling could be due to the uptake of fluid by both the ECS and the intracellular space (ICS). The exact distribution of the fluid uptake between the two spaces is not known, but the  $\mu\text{L}$  of swelling could be expressed according to the following equation:

$$(2) \quad \mu\text{L swelling} = (\mu\text{L ECS}_s - \mu\text{L ECS}_t) + (\mu\text{L ICS}_s - \mu\text{L ICS}_t)$$

where:



$\mu\text{L}$  swelling = tissue weight (mg) after swelling - tissue weight (mg) before swelling (assuming the density = 1)

$\mu\text{L}$  ECS<sub>s</sub> =  $\mu\text{L}$  of extracellular space after swelling of the incubated tissue.

$\mu\text{L}$  ECS<sub>t</sub> = the true extracellular space of the tissue expressed in  $\mu\text{L}$ .

$\mu\text{L}$  ICS<sub>s</sub> =  $\mu\text{L}$  of intracellular space after swelling of the incubated tissue.

$\mu\text{L}$  ICS<sub>t</sub> = the true intracellular space of the tissue expressed in  $\mu\text{L}$ .

The marker (inulin [<sup>14</sup>C] carboxylic acid) should be unable to pass through the membrane and into the intracellular spaces and therefore should only be located within the extracellular space. As a result, the total dpm can be expressed according to the equation:

$$\begin{aligned} \text{Total dpm} &= \mu\text{L ECS}_s \times \text{dpm}/\mu\text{L incubating solution} \\ &+ (\mu\text{L ECS}_s - \mu\text{L ECS}_t) \times \text{dpm}/\mu\text{L incubating solution} \end{aligned}$$

Which can be simplified to:

$$(3) \quad \mu\text{L ECS}_s = \frac{\text{Total dpm}}{\text{dpm}/\mu\text{L incubating solution}}$$

Combining equations (2) and (3) and stating that  $(\mu\text{L ICS}_s - \mu\text{L ICS}_t)$  is equal to the change in the size ( $\mu\text{L}$ ) of the intracellular space ( $\Delta\text{ICS}$ ) in the tissue being studied, gives the following expression:

$$(4) \quad \mu\text{L ECS}_s - \Delta\text{ICS} = \frac{\text{Total dpm}}{\text{dpm}/\mu\text{L incubating solution}} - \mu\text{L swelling}$$



Since  $\mu\text{L ECS}_{\text{t}} - \Delta\text{ICS}$  equals the apparent ECS, the apparent extracellular space (ECS app) can be calculated on a volume/weight of tissue basis from the following expression:

$$(5) \quad \text{ECS app} = \frac{\mu\text{L ECS}_{\text{t}} - \Delta\text{ICS}}{\text{tissue weight (mg)}}$$

This value is plotted as ml/100 g tissue.



### III. RESULTS AND DISCUSSION

#### A. Introduction

The results and discussion section has been divided into three parts. The first part presents the data generated from each of the methods used to monitor rigor development. A discussion of the results obtained from each of these methods is included. The second part deals with the state of the water in muscle. The NMR  $T_1$ , extracellular space, swelling capacity, water holding capacity and the nonfreezeable water data are presented and discussed. In the third part the changes in the biochemical and physiological properties of muscle (part one) are discussed in relation to the changes in the state of water (part two) as the muscle from each carcass studied entered rigor.

#### B. Biochemical and Physiological Effects of Rigor Development

##### Fibre typing

Table III.1 contains the fibre typing data obtained from the *M. semitendinosus* (ST) of 9 carcasses, numbered 10 through 18. Carcasses 10 to 13, 17 and 18 were sampled from the large central portion of the ST. The percentages of white-intermediate and red fibres from the carcasses were similar (white fibre range 72-76%). Carcasses 14 and 16 were purposely sampled from the outer ST and contained 90 and 85%



Table III.1 Fibre typing data

Carcass Number	% White and Intermediate	% Red
10	74±5	26±5
11	76±0.2	24±0.2
12	74±0.7	26±0.7
13	73±2	27±2
14	90±4	10±4
15	62±0.7	38±0.7
16	85±5	15±5
17	72±5	28±5
18	74±8	26±8



white-intermediate fibres, respectively. These values compare very well with those reported by Nuss and Wolfe (1980/81) and Hunt and Hedrick (1977a) for the outer ST of 86.4 and 84%, respectively. The sample from carcass 15 was obtained from the inner ST and was high in its red fibre content (62% white-intermediate fibres). This value is similar to the findings of Hunt and Hedrick (1977a) for the same location in this muscle (63.9%).

The fairly narrow range in the fibre types of carcasses sampled normally (the central portion of the ST) indicate that the results reported in this study should not be significantly influenced by variations in fibre type.

Hunt and Hedrick (1977a) grouped the carcasses in their study as: (1) normal in color and exudation; (2) normal in color but soft and exudative; (3) pale, soft and exudative; and (4) dark cutting. They observed that carcasses in the latter three groupings had a greater content of intermediate ( $\alpha R$ ) fibres. Since it was not possible to distinguish between white ( $\alpha W$ ) and intermediate ( $\alpha R$ ) fibre types in this study, no correlations between the percentage of intermediate ( $\alpha R$ ) fibre types and other parameters measured could be assessed. A comparison between the percentage of white-intermediate fibres and the initial T<sub>1</sub> (a measure of water mobility) of the nine carcasses did not reveal a significant correlation ( $r=-0.086$ ; d.f.=7). Nor was a significant correlation ( $r=.142$ ; d.f.=4) between the percentage of white-intermediate fibres and expressed juice



of the six normally sampled carcasses found. These findings should not be viewed as conflicting with the results of Hunt and Hedrick (1977b). Firstly, ( $\alpha$ R) fibres were not compared and, secondly, none of the carcasses fibre-typed were viewed as soft and exudative or dark cutting. The latter point may be the major reason no correlations were found.

Hunt and Hedrick (1977b) reported that the rate and extent of glycolysis is directly associated with the variation in muscle quality. Although they indicated that glycolytic rate is related to the fibre type in postmortem muscle, the measurement of glycolytic rate (by pH and ATP measurements) would more likely correlate with exudation and water mobility than with fibre typing. Thus, in this study the relationship between glycolysis and exudation or water mobility is assessed using pH and ATP measurements rather than by predicting glycolytic rate by fibre type.

#### pH fall

Figures III.1 and III.2 depict the pH fall as a function of time for carcasses numbered 3 to 8. The pH profiles of carcasses 9-18 are presented in conjunction with the isometric tension data in Figures III.3 to III.12. Since complete pH profiles were not recorded for carcasses 1 and 2 only the ultimate pH's, of 5.65 and 5.55, respectively, are reported. Table III.2. indicates the pH at 1 hr, the initial rate of pH fall, the time to reach the ultimate pH and the ultimate pH for all carcasses 3 to 18. The pH at 1 hr was



Table III.2 pH response in postmortem muscle

Carcass Number	Rate of Initial pH Fall (pH units/h)	pH at 1 hr	Ultimate pH	Time (h) to Ultimate pH
1	---	---	5.65	---
2	---	---	5.55	14
3	0.46	6.50	5.50	20
4	1.33	6.20	5.42	16
5	0.36	6.40	5.46	11
6	0.36	6.36	5.42	16
7	0.42	6.26	5.52	10
8	0.86	6.02	5.67	20
9	0.97	6.10	<5.38	>28
10	1.33	5.85	<5.20	>36
11	0.53	6.46	5.12	18
12	0.23	6.18	5.46	18
13	0.42	6.74	5.42	23.5
14	0.23	6.11	5.38	21.5
15	0.29	6.82	5.52	17
16	0.38	6.41	5.42	15
17	0.28	6.68	5.27	10
18	0.46	6.85	5.65	8

Figure III.1. Plot of pH vs time postmortem for carcass 3  
(●-●-●), carcass 4 (▲-▲-▲), carcass 5 (■-■-■) and carcass 6  
(▼-▼-▼).

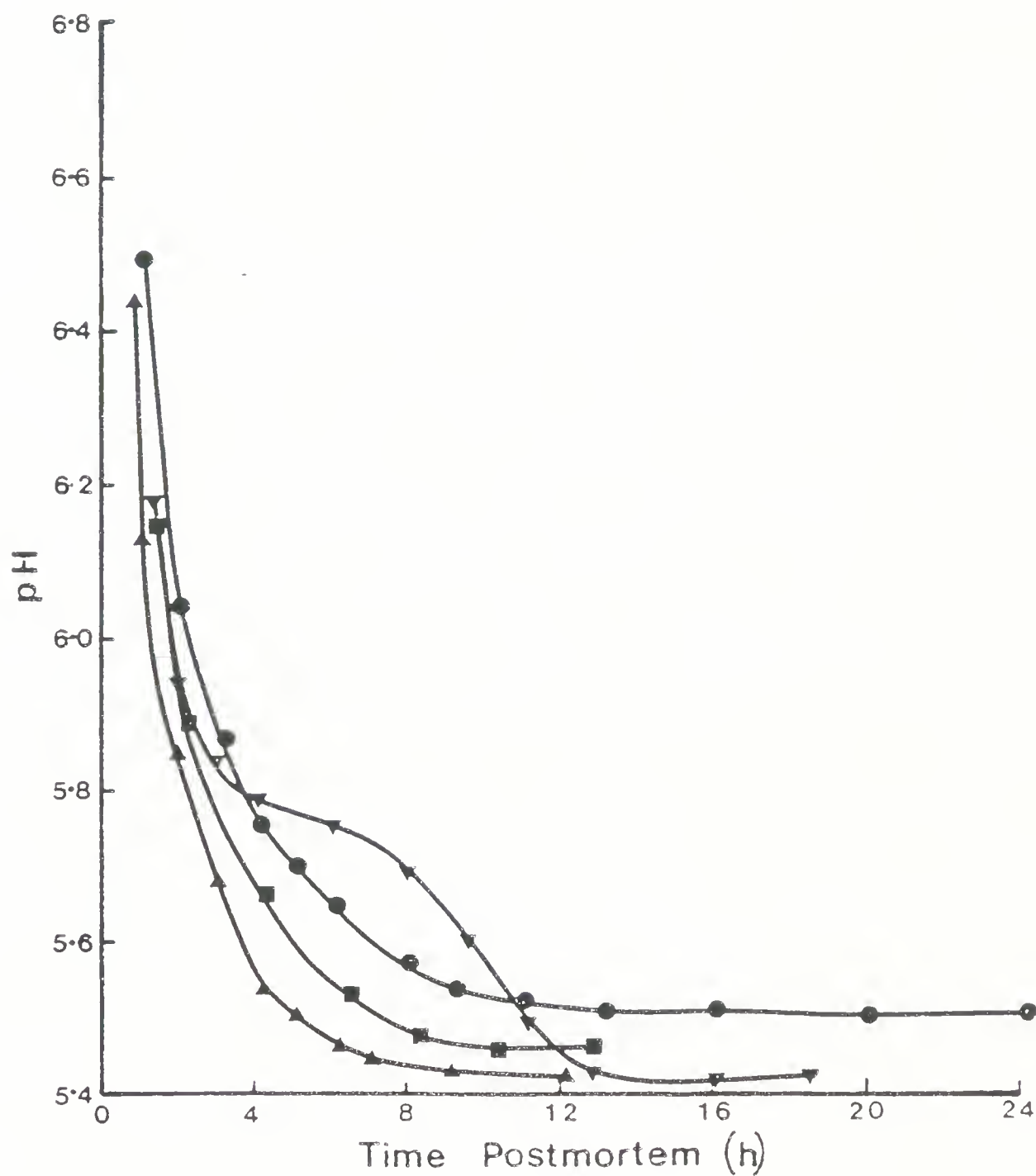


Figure III.2. Plot of pH vs time postmortem for carcass 7 (▼-▼-▼) and carcass 8 (■-■-■). Plot of expressed juice (%) vs time postmortem for carcass 7 (●-●-●) [standard deviation early prerigor  $\approx \pm 25\%$ ; standard deviation late prerigor and postrigor  $\approx \pm 11\%$  of the mean] and carcass 8 (▲-▲-▲) [standard deviation early prerigor  $\approx \pm 7\%$  of the mean; standard deviation late prerigor and postrigor  $\approx \pm 2\%$  of the mean].

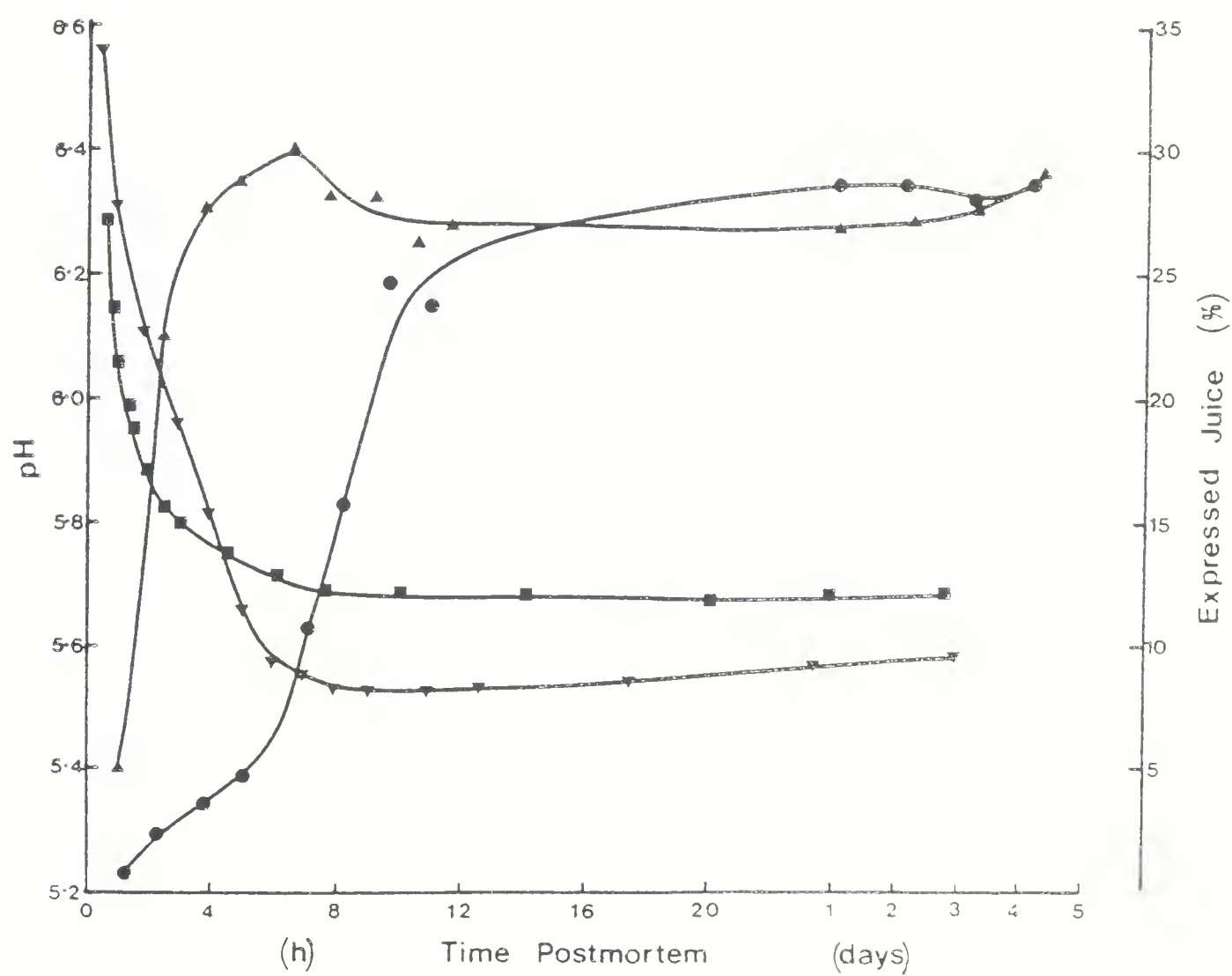


Figure III.3. Plot of pH vs time postmortem for carcass 9 (■-■-■). Plot of isometric tension vs time postmortem for carcass 9 (▲-▲-▲). Plot of expressed juice (%) vs time postmortem for carcass 9 (●-●-●). Standard deviation early prerigor  $\approx \pm 28\%$  of the mean; standard deviation late prerigor and postrigor  $\approx \pm 3\%$  of the mean.

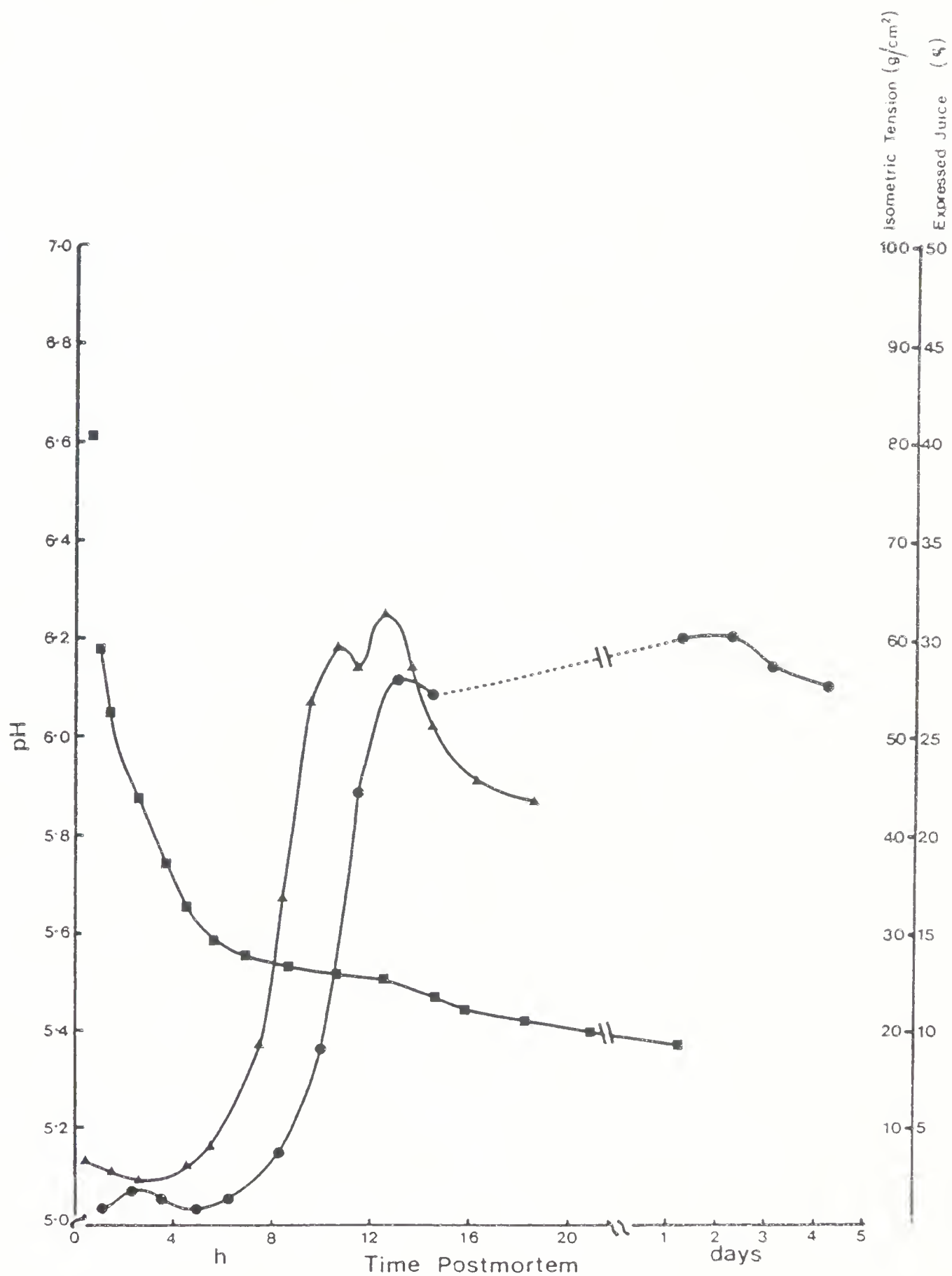


Figure III.4. Plot of pH vs time postmortem for carcass 10 (■-■-■). Plot of isometric tension vs time postmortem for carcass 10 (▲-▲-▲). Plot of expressed juice (%) vs time postmortem for carcass 10 (●-●-●). Standard deviation early prerigor  $\approx \pm 30\%$  of the mean; standard deviation late prerigor and postrigor  $\approx \pm 6\%$  of the mean.

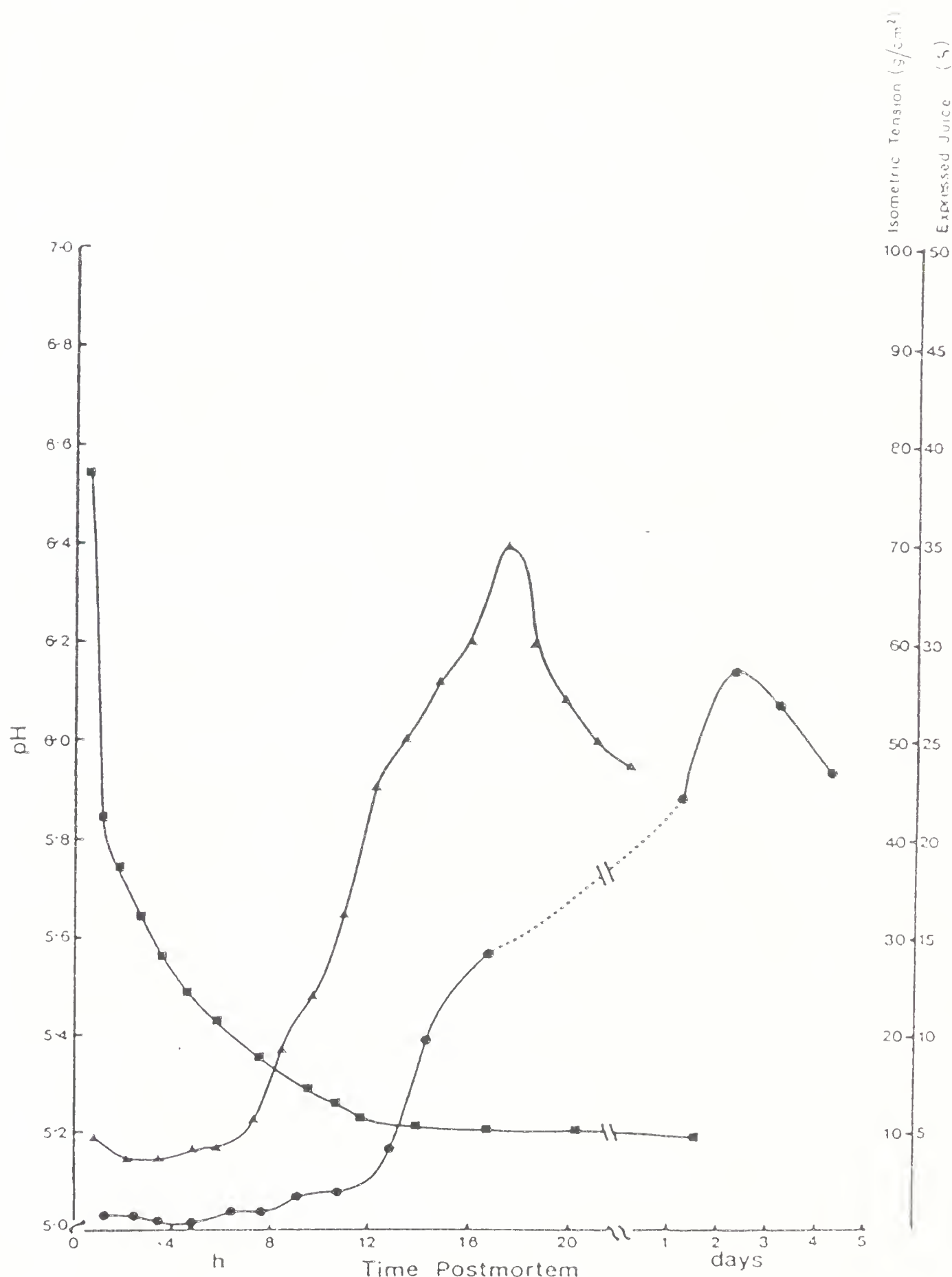


Figure III.5. Plot of pH vs time postmortem for carcass 11 (■-■-■). Plot of isometric tension vs time postmortem for carcass 11 (▲-▲-▲). Plot of expressed juice (%) vs time postmortem for carcass 11 (●-●-●). Standard deviation early prerigor  $\approx \pm 20\%$  of the mean; standard deviation late prerigor and postrigor  $\approx \pm 8\%$  of the mean.

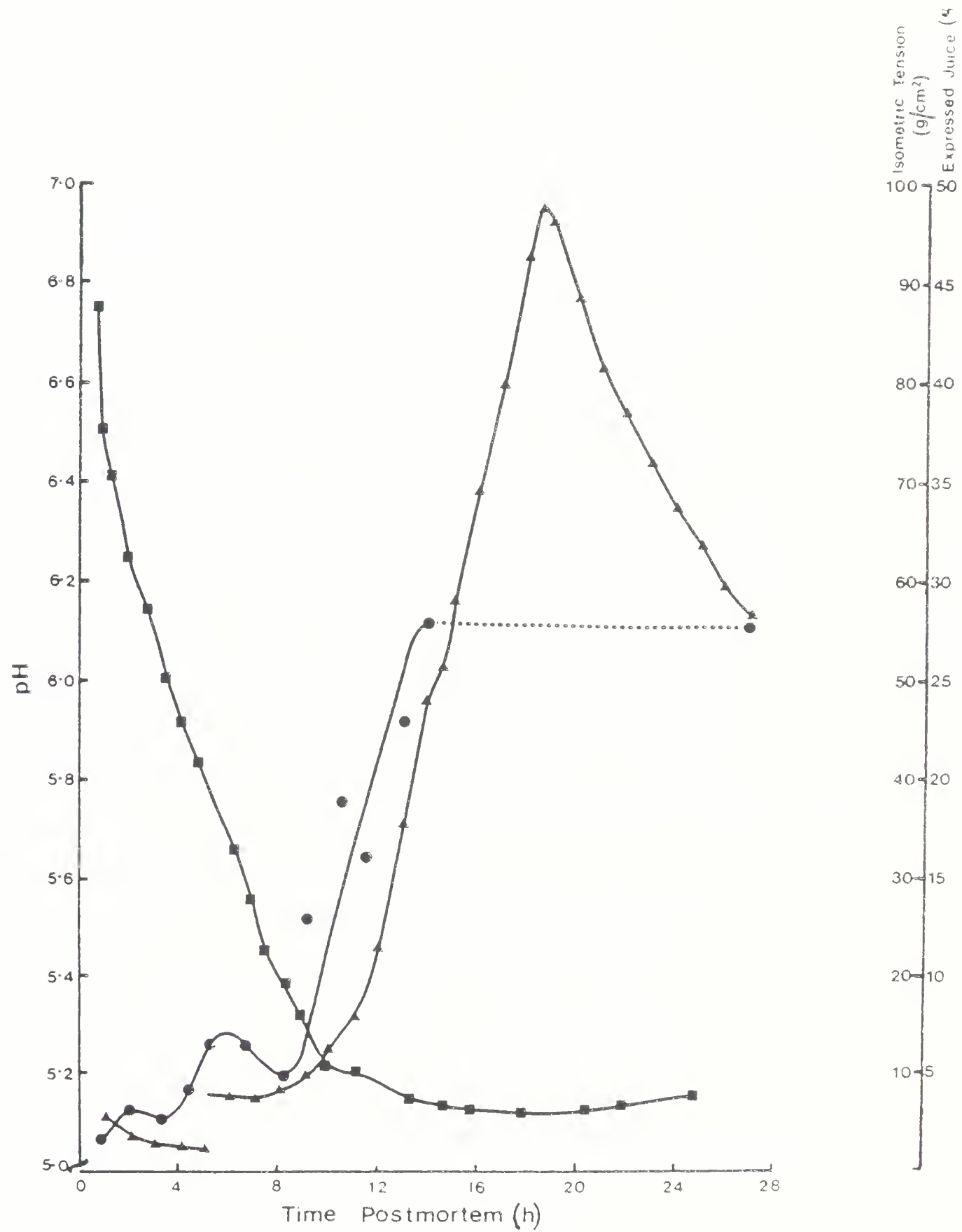


Figure III.6. Plot of pH vs time postmortem for carcass 12 (■-■-■). Plot of isometric tension vs time postmortem for carcass 12 (▲-▲-▲). Plot of expressed juice (%) vs time postmortem for carcass 12 (●-●-●). Standard deviation early prerigor  $\approx \pm 17\%$  of the mean; standard deviation late prerigor and postrigor  $\approx \pm 16\%$  of the mean.

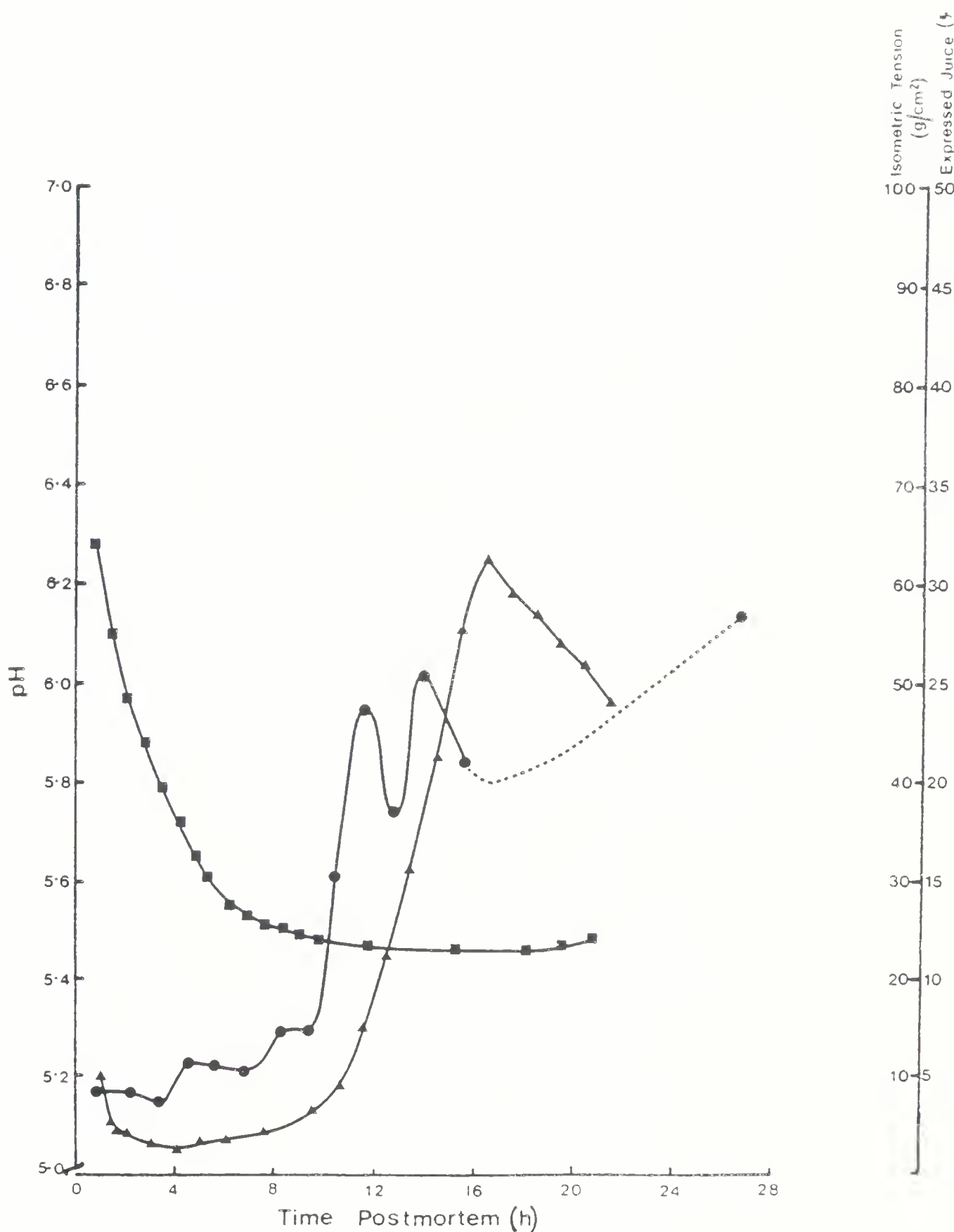


Figure III.7. Plot of pH vs time postmortem for carcass 13 (■-■-■). Plot of isometric tension vs time postmortem for carcass 13 (▲-▲-▲). Plot of expressed juice (%) vs time postmortem for carcass 13 (●-●-●). Standard deviation early prerigor  $\approx \pm 20\%$  of the mean; standard deviation late prerigor and postrigor  $\approx \pm 9\%$  of the mean.

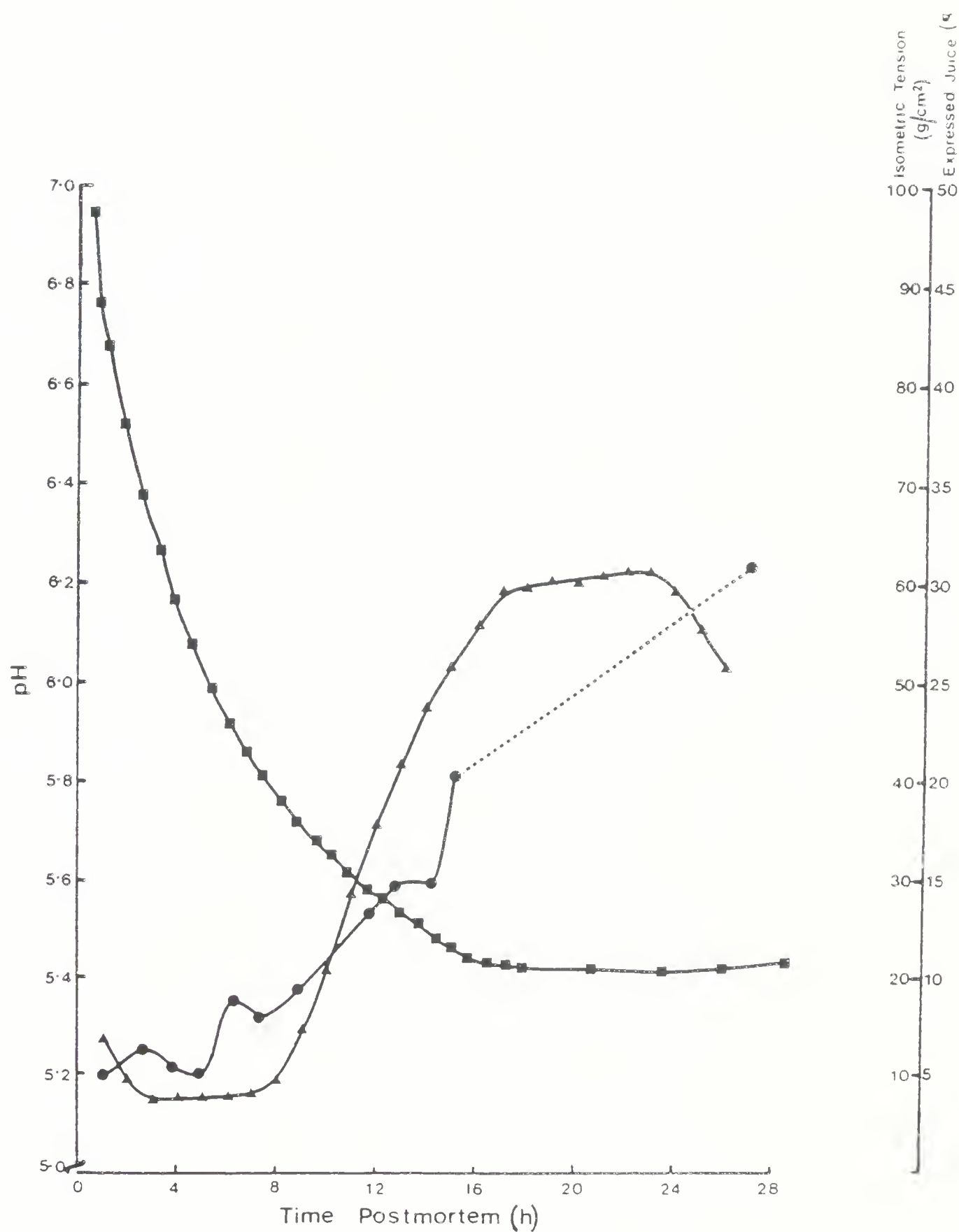


Figure III.8. Plot of pH vs time postmortem for carcass 14 (■-■-■). Plot of isometric tension vs time postmortem for carcass 14 (▲-▲-▲). Plot of expressed juice (%) vs time postmortem for carcass 14 (●-●-●). Standard deviation early prerigor  $\approx \pm 9\%$  of the mean; standard deviation late prerigor and postrigor  $\approx \pm 3\%$  of the mean.

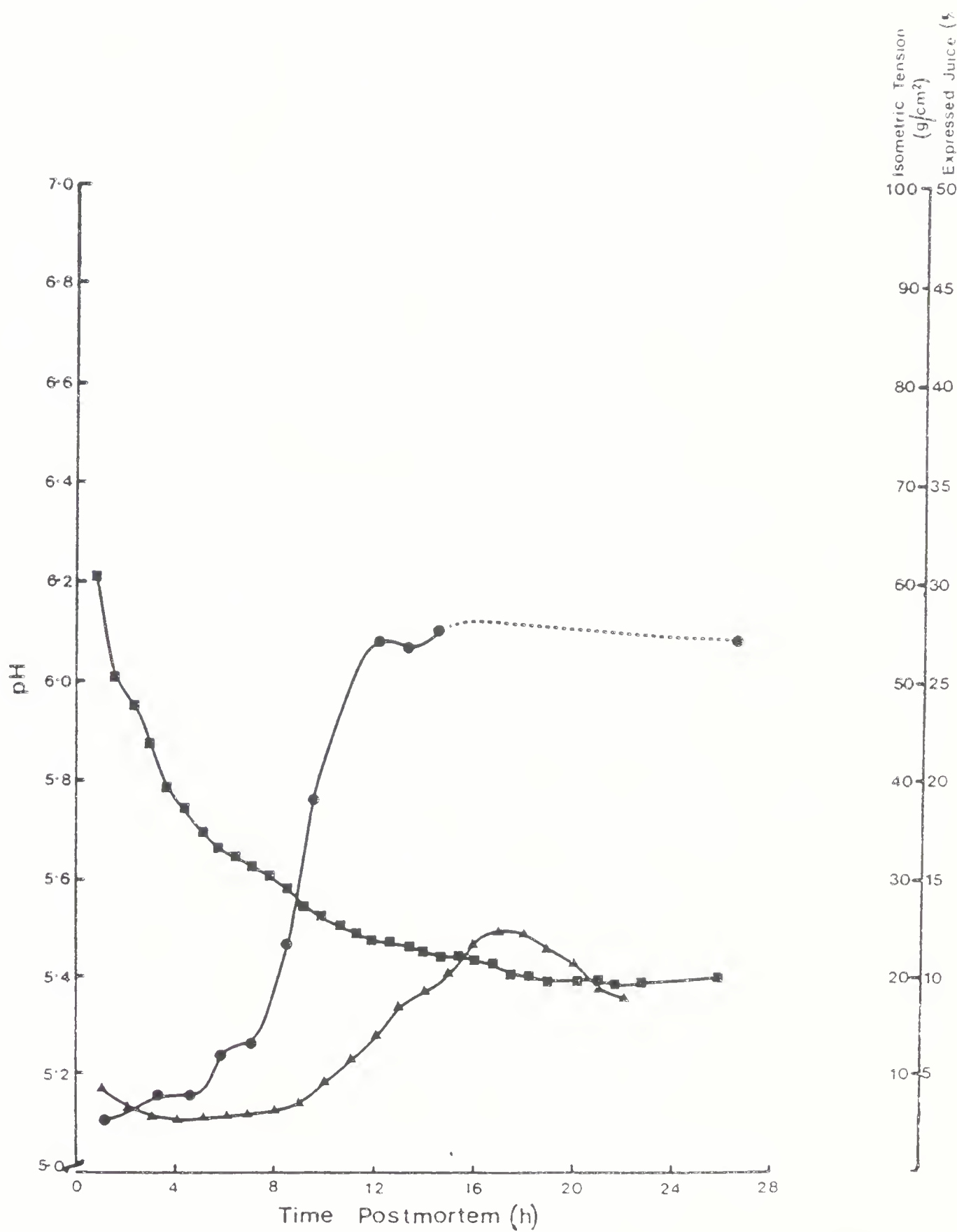


Figure III.9. Plot of pH vs time postmortem for carcass 15 (■-■-■). Plot of isometric tension vs time postmortem for carcass 15 (▲-▲-▲). Plot of expressed juice (%) vs time postmortem for carcass 15 (●-●-●). Standard deviation early prerigor  $\approx \pm 23\%$  of the mean; standard deviation late prerigor and postrigor  $\approx \pm 16\%$  of the mean.

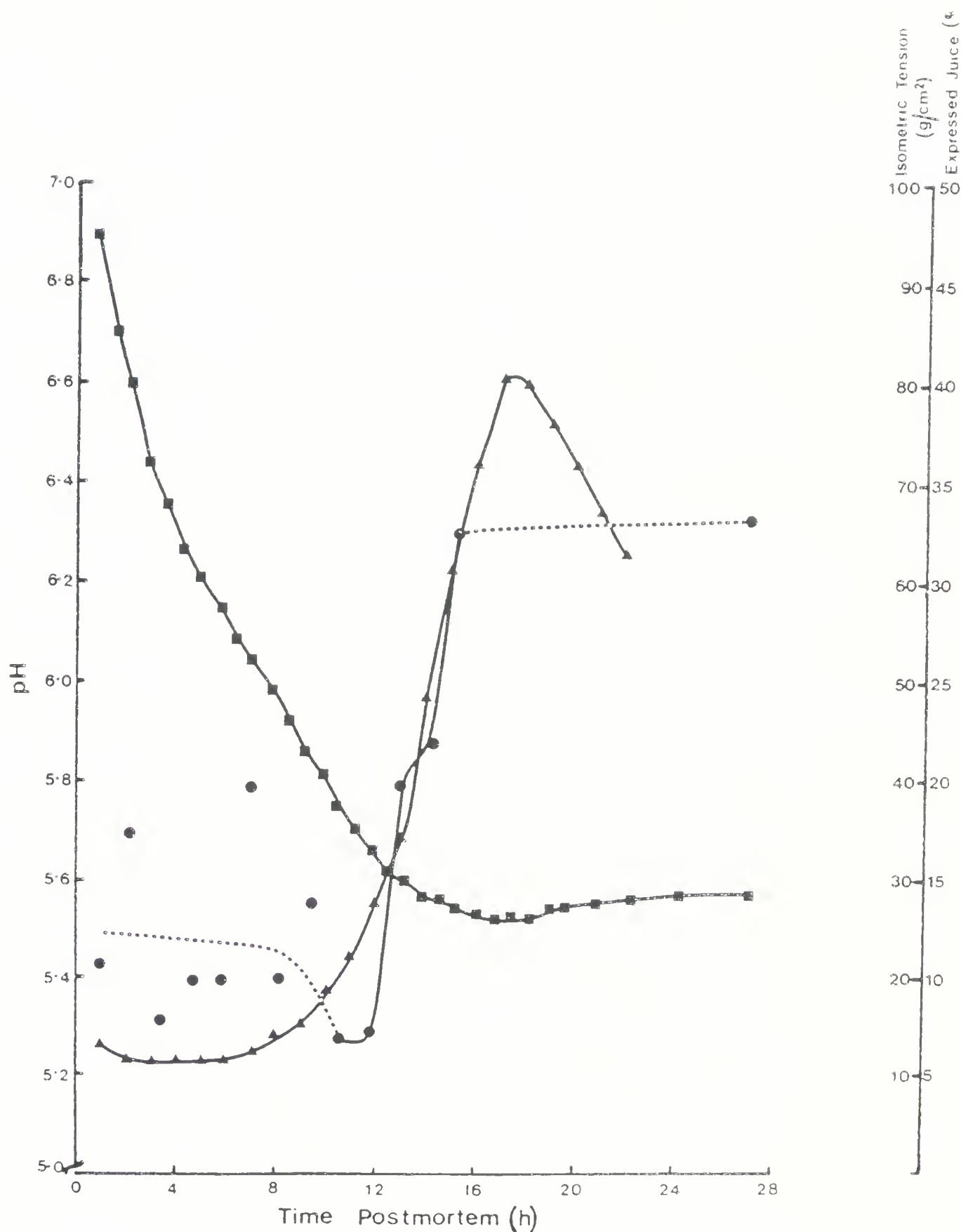


Figure III.10. Plot of pH vs time postmortem for carcass 16 (■-■-■). Plot of isometric tension vs time postmortem for carcass 16 (▲-▲-▲). Plot of expressed juice (%) vs time postmortem for carcass 16 (●-●-●). Standard deviation early prerigor  $\approx \pm 19\%$  of the mean; standard deviation late prerigor and postrigor  $\approx \pm 11\%$  of the mean.

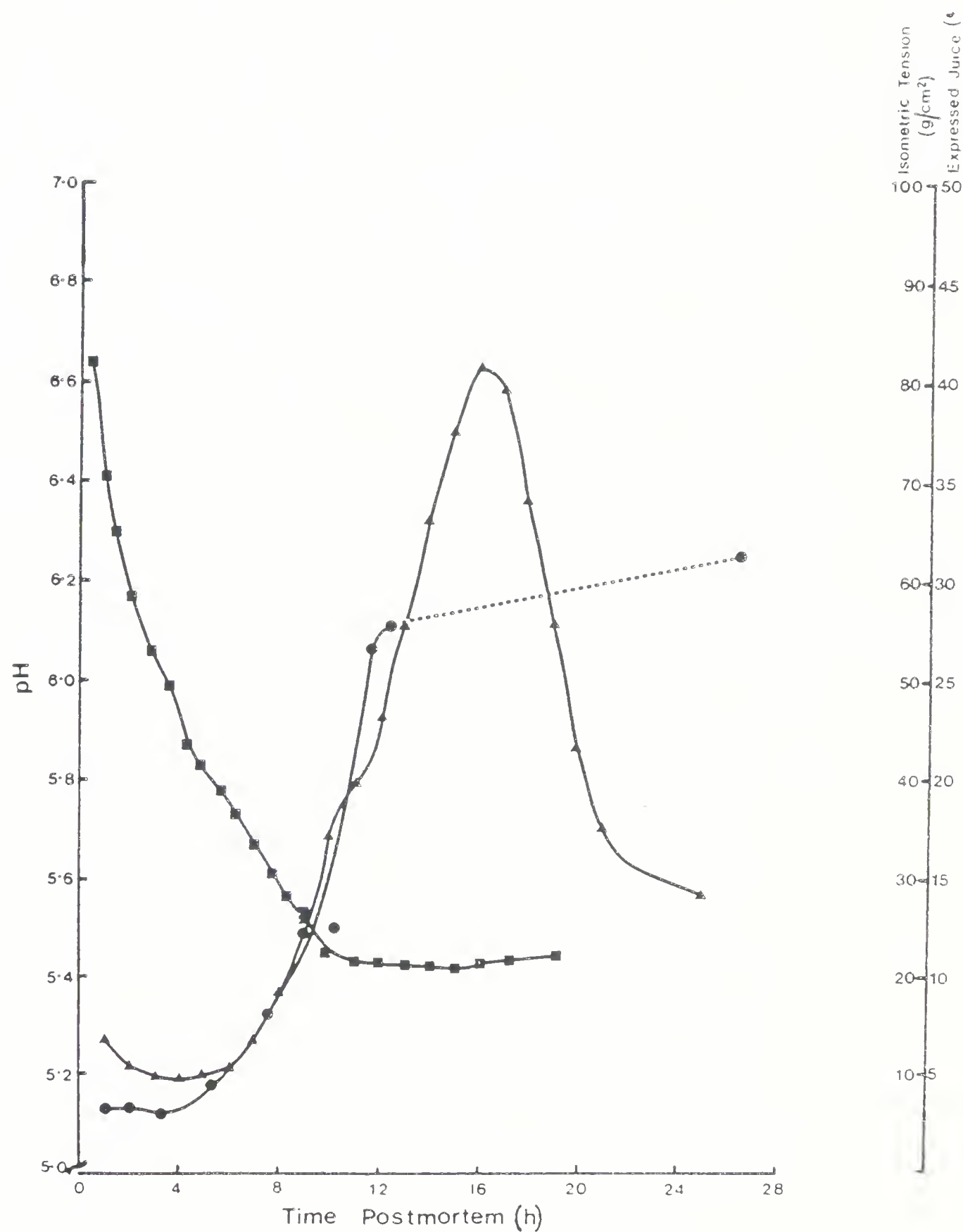


Figure III.11. Plot of pH vs time postmortem for carcass 17 (■-■-■). Plot of isometric tension vs time postmortem for carcass 17 (▲-▲-▲). Plot of expressed juice (%) vs time postmortem for carcass 17 (●-●-●). Standard deviation early prerigor  $\approx \pm 8\%$  of the mean; standard deviation late prerigor and postrigor  $\approx \pm 4\%$  of the mean.

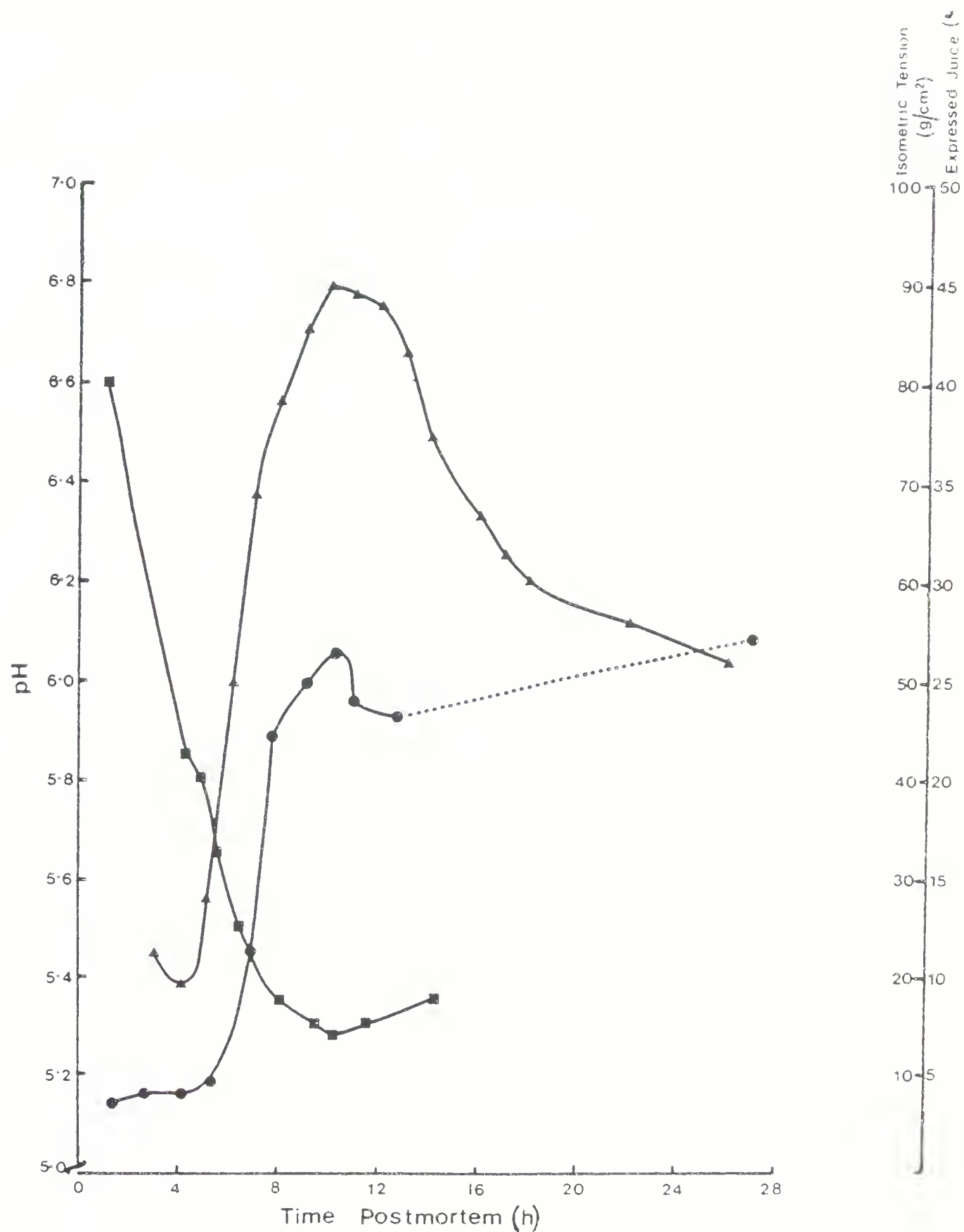
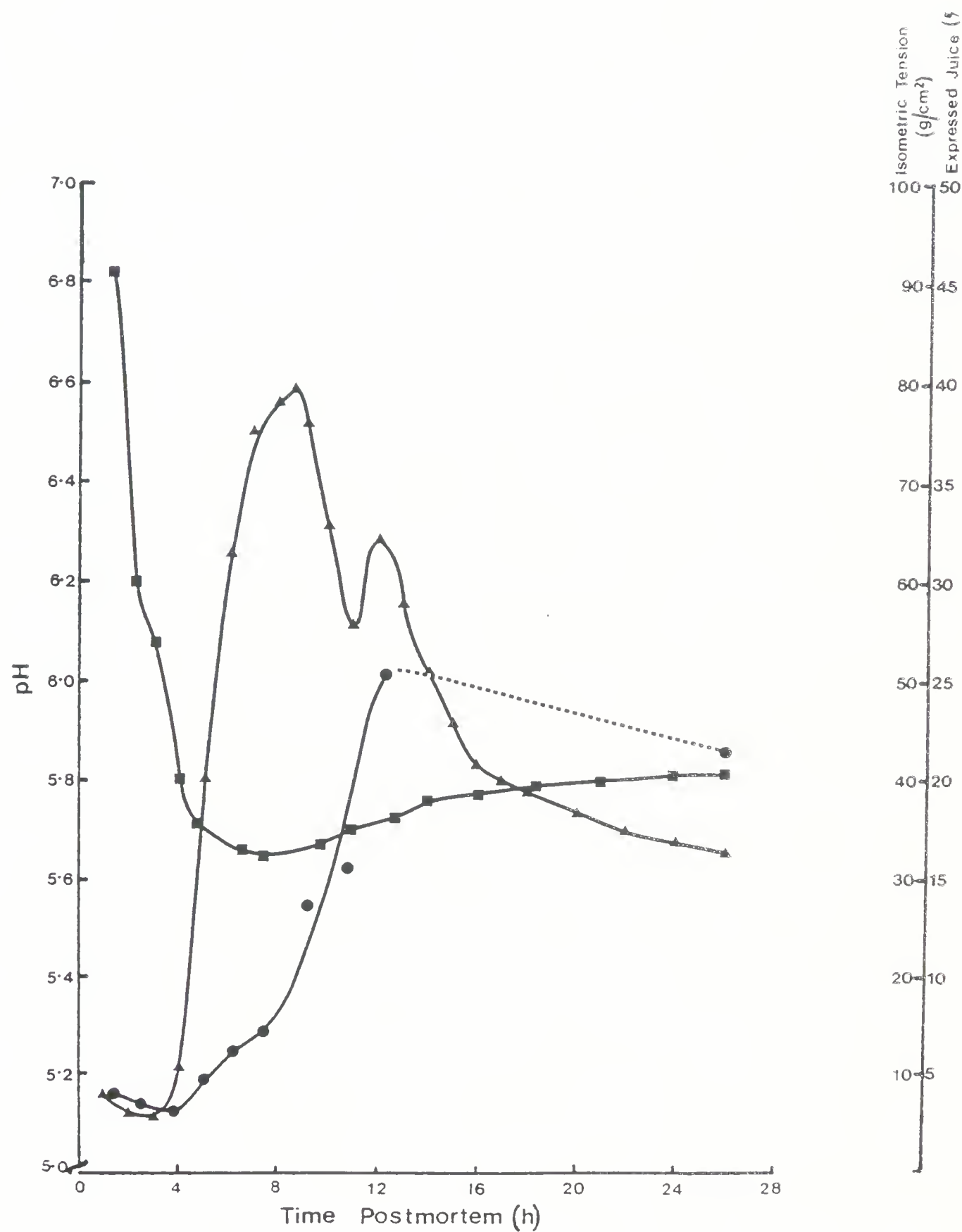


Figure III.12. Plot of pH vs time postmortem for carcass 18 (■-■-■). Plot of isometric tension vs time postmortem for carcass 18 (▲-▲-▲). Plot of expressed juice (%) vs time postmortem for carcass 18 (●-●-●). Standard deviation early prerigor  $\approx \pm 16\%$  of the mean; standard deviation late prerigor and postrigor  $\approx \pm 10\%$  of the mean.





variable, ranging from 5.85 for carcass 10 to 6.85 for carcass 18. The pH at 1 hr would be a function of acid production in the antemortem, at slaughter and 1 hr prerigor muscle. The initial rate of pH fall varied from 0.23 pH units/hr for carcasses 12 and 14 to 1.33 pH units/hr for carcasses 4 and 10. The initial rate of pH fall is a measure of the initial glycolytic rate. It was obtained from the pH data recorded over approximately the first 1.5 hr postmortem period. The ultimate pH was a high of 5.67 for carcass 8 and a low of 5.12 for carcass 11. The time to reach rigor was as early as 8 hr for carcass 18 and greater than 36 hr for carcass 10. No significant correlations between the pH at 1 hr and ultimate pH ( $r=-0.194$ ; d.f.=16) or initial rate of pH fall and ultimate pH ( $r=-0.178$ ; d.f.=16) were obtained. The lack of correlation in the above parameters is not unexpected, since the ultimate pH is thought to relate to lack of glycogen, inactivation of the glycolytic enzymes, or the glycogen being insensitive to attack (Lawrie, 1979). These factors would not be expected to influence the initial pH or rate of initial pH decline since the glycogen and pH levels will normally be quite high at this time and thus glycolytic activity would not be inhibited. The pH at 1 hr was significantly correlated with the time to reach ultimate pH ( $r=-0.574$ ; d.f.=16). This significant negative correlation indicates that a rapid pH fall to a low 1 hr postmortem pH will result in an extended time to reach the ultimate pH. This is supported by the positive significant



correlation ( $r=0.559$ ; d.f.=16) between the initial rate of pH fall and time to the ultimate pH. This correlation means that a rapid rate of pH fall would likely result in an extended time to reach the ultimate pH. A part of the explanation for these surprising correlations may be due to the continuous recording of pH. With this method, even the slightest glycolytic rate could be detected. This would increase the length of time measured to reach the ultimate pH since other techniques would be insensitive to these slight changes. Perhaps, because of this method, the results in this study do not totally agree with Khan and Lentz (1973). In their studies the pH's of the carcasses were measured by inserting an electrode directly into the muscle at the abattoirs. (As rigor proceeded, the temperature would drop and the glycolytic rate would be reduced, thus the time to rigor would increase compared to this study, where the meat samples were at room temperature.) The initial pH's of 10 carcasses were between 6.7 and 7.1, and another 10 carcasses were between 5.8 and 6.2. In those carcasses having a low initial pH it was found that the lactic acid formed by glycolysis was produced before and/or during slaughter rather than postmortem. Glycolytic changes were complete within 16 hr for some of these samples. In high post-slaughter pH meat, the major pH change occurred postmortem rather than before and/or during slaughter. In these carcasses the pH fall continued for up to 32 hr post-slaughter. There was no correlation coefficient



calculated between the initial pH and the time to ultimate pH to support the conclusion of Khan and Lentz (1973) that a rapid pH fall before and/or during slaughter results in a shortened time to rigor or that a high initial pH results in an extended time to the ultimate pH.

The results of Khan and Lentz (1973) are reasonable if the extent of glycolysis is similar from carcass to carcass. Under these circumstances, if glycolysis is initiated early (before and/or during slaughter), the initial pH is low and the time to reach the ultimate pH is shortened. Conversely, if the initial pH is high, the time to reach the ultimate pH will be extended before a comparable level of glycolytic activity has been obtained.

In this study a low 1 hr pH correlated with an extended time to the ultimate pH. These results imply that some carcasses possess a highly active glycolytic machinery. Carcasses of this type will be capable of glycolytic activity under conditions that would render carcasses possessing low level glycolytic activity inactive (perhaps low pH, low glycogen levels, etc.). For this reason, the time to reach the ultimate pH for highly glycolytic carcasses would be extended. Certainly, the results of Khan and Lentz (1973) and the results in this study (Figures III.1-III.12 and Table III.2) agree in that a variability in the pH decline does occur between carcasses.

In support of these observations, Martin and Fredeen (1974) reported differences in the initial pH and the rate



of pH fall between carcasses. Fischer and Honikel (1978) found that the ultimate pH and rate of rigor development reflected meat varying in quality between two extremes. Meat from carcasses exhibiting a rapid pH fall and low ultimate pH was similar to PSE (pale, soft and exudative) pork. The other extreme was meat from carcasses where the pH fall was very small, resulting in DFD (dark-firm-dry) beef. Hunt and Hedrick (1977a,b,c) attribute their classification of beef carcasses (normal in color, firmness and exudation; normal in color but soft and exudative; pale in color, soft and exudative; and dark in color, firm and dry), in part, to differences in the rate and extent of pH fall. Clearly, differences in the initial pH, rates of pH fall and ultimate pH should be expected in an examination of several carcasses. Additionally, the measure of pH is a useful tool for indicating differences in the biochemical activities between carcasses.

The early postrigor period also showed some differences in the pH recorded. Two carcasses (9 and 10) possessed such extensive glycolytic activity that the pH was still dropping at 28 hr and 36 hr, respectively, at which times the recording of pH was stopped. Thus, the pH response of these carcasses following the ultimate pH is not known. All other carcasses either exhibited a constant pH or a pH that slightly increased during the early postrigor period. This increase in pH postrigor was first reported by Wierbicki *et al.* (1956). Arnold *et al.* (1956) proposed that  $\text{Ca}^{++}$



released from the muscle proteins (due to K<sup>+</sup> displacement of the Ca<sup>++</sup>) reacts with free orthophosphoric acid from ATP breakdown. They suggested that the insoluble calcium orthophosphate salt could decrease the acidity of the muscle and thus raise the pH. This appears very unlikely.

Cassens *et al.* (1975) suggested that the trauma of excision of a prerigor muscle may contribute to the lowering of the initial pH. All samples measured in this study were excised from prerigor muscles and therefore a concern about the validity of the pH measurements may be raised. The fact that a significant negative correlation ( $r=-0.571$ ; d.f.=16) was found between the initial rate of pH fall and the initial pH should indicate that the initial pH measured was primarily a result of the inherent glycolytic activity of the carcass. This significant correlation may be a result of the muscle always being removed from the carcass at the same point on the kill line and in the same manner. All muscles suddenly contracted upon excision but were observed to relax and become pliable within a few minutes. Although excision may contribute to some reduction in the initial pH compared to the same nonexcised muscles, the uniformity in sampling should permit a meaningful comparison of pH fall from one carcass to the next. If a comparison of pH fall between carcasses were the only intent of this study, a more accurate recording of the pH could be made on the intact carcass. The other methods used required samples to be removed from the carcasses and so pH measurement of the



excised samples seemed more relevant to the study.

### Isometric tension

The isometric tension data for samples from ten carcasses are included with the pH profiles in Figures III.3 to III.12. Table III.3 shows a considerable divergence in the times required to attain maximum rigor tension (8.5 to 22.5 hr) and the values for maximum rigor tension (25-98 g/cm<sup>2</sup>). The initial tension ranged from 3.0 g/cm<sup>2</sup> (carcass 12) to 18 g/cm<sup>2</sup> (carcass 17). There was no significant correlation ( $r=0.52$ ; d.f.=8) between the initial loading and the maximum tension. This would imply that the initial loading did not significantly affect the maximum tension generated in the muscle. The maximum tension did not correlate with time to maximum tension ( $r=0.17$ ; d.f.=8) nor with ultimate pH ( $r=-0.216$ ; d.f.=8) nor with the initial rate of pH fall ( $r=0.046$ ; d.f.=8). These results confirm the observation of Nuss and Wolfe (1980/81) that maximum rigor tension is not related to the rate of pH decline nor the ultimate pH of the muscle.

There was a significant correlation ( $r=0.95$ ; d.f.=8) between the time to reach the ultimate pH and the time to reach maximum rigor tension. This correlation emphasizes the importance of continuously monitoring the pH fall during rigor development. This allows even a very small change in pH to be recorded. Without continuous monitoring, samples 12, 13, and 16 would not have been reported as having an



Table III.3 Isometric tension data

Carcass Number	Initial Tension (g/cm <sup>2</sup> )	Maximum Tension (g/cm <sup>2</sup> )	Time to Maximum Tension (hr)
9	5	63	12.4
10	7	70	17.5
11	7.5	98	18.5
12	3.0	63	16.5
13	7.5	62	22.5
14	5.5	25	17.0
15	11.5	80.5	17.5
16	9.5	82	16.0
17	18	91	10
18	6	79	8.5



ultimate pH at the times indicated. Other methods of measuring the pH probably would have resulted in the ultimate pH being assigned to a much earlier time. This observation may mean that as long as the pH is falling (due to glycolysis) sufficient ATP is being generated to maintain and in some instances increase tension in the muscle strip.

#### Sarcomere measurements

Figure III.13 depicts the sarcomere lengths of ST at various times postmortem following two different sampling procedures. Samples removed from the carcass shortly after slaughter and allowed to enter rigor unrestrained (OFC) contracted continuously, ceasing only when the sarcomere length was about 1.6-1.7  $\mu\text{m}$ . Samples removed from the carcass at the abattoirs at various times postmortem (ONC) and examined in the lab did not contract. Sarcomere lengths near 2.5-2.6  $\mu\text{m}$  were routinely measured throughout rigor development for these samples. This must mean that the ONC samples were prevented from contracting. The results reported here support those reported for *M. biceps femoris* (Currie and Wolfe, 1979). Most of the muscle samples examined in this study were OFC and would be expected to exhibit the same changes as described above.

#### Isotonic contraction

Figure III.14 shows the response of three prerigor muscle strips from one carcass to three different loadings.

Figure III.13. Plot of sarcomere length vs time postmortem for an off-carcass sample (●-●-●) and an on-carcass sample (■-■-■). The standard deviation of each data point is indicated on the graph.

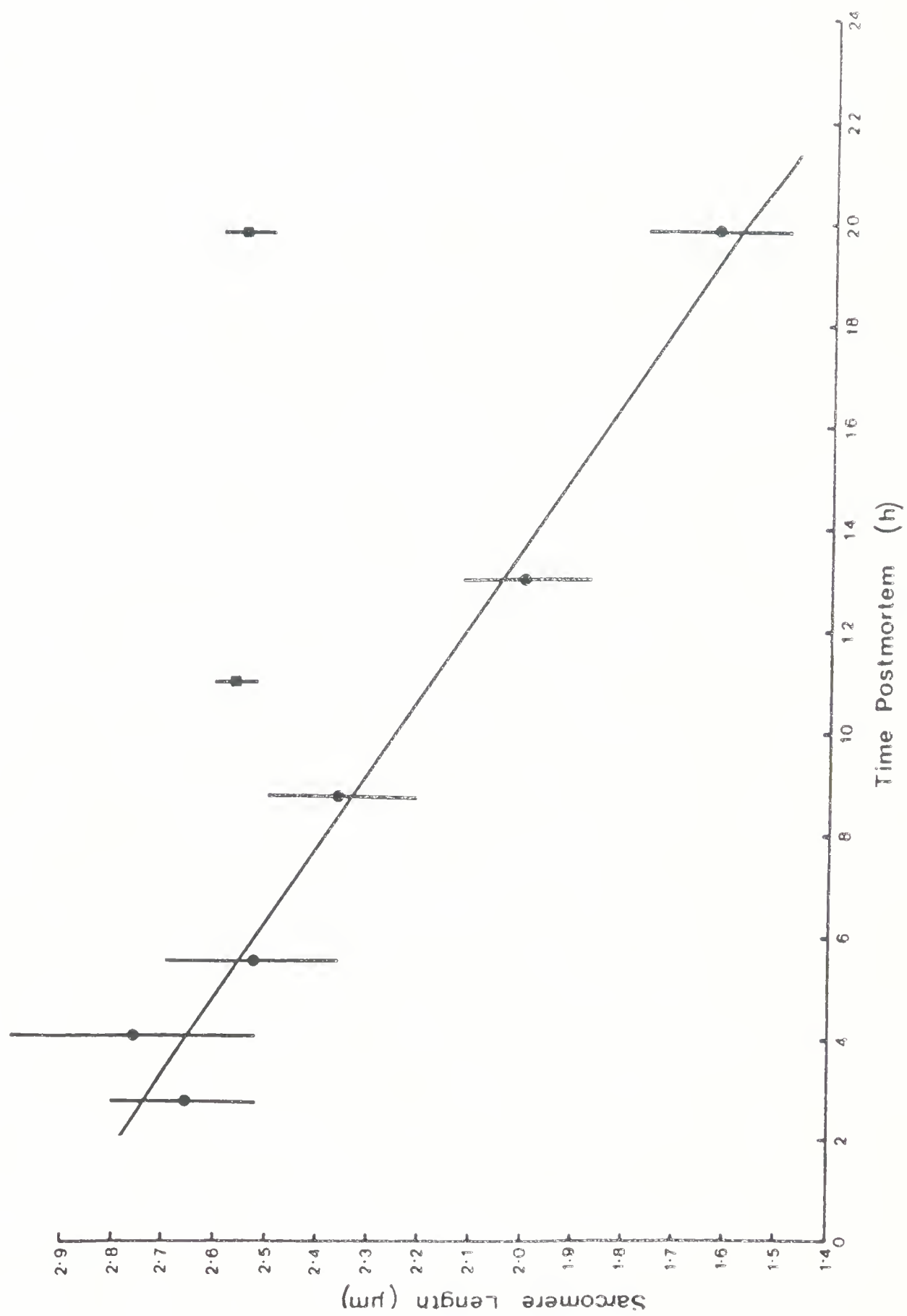
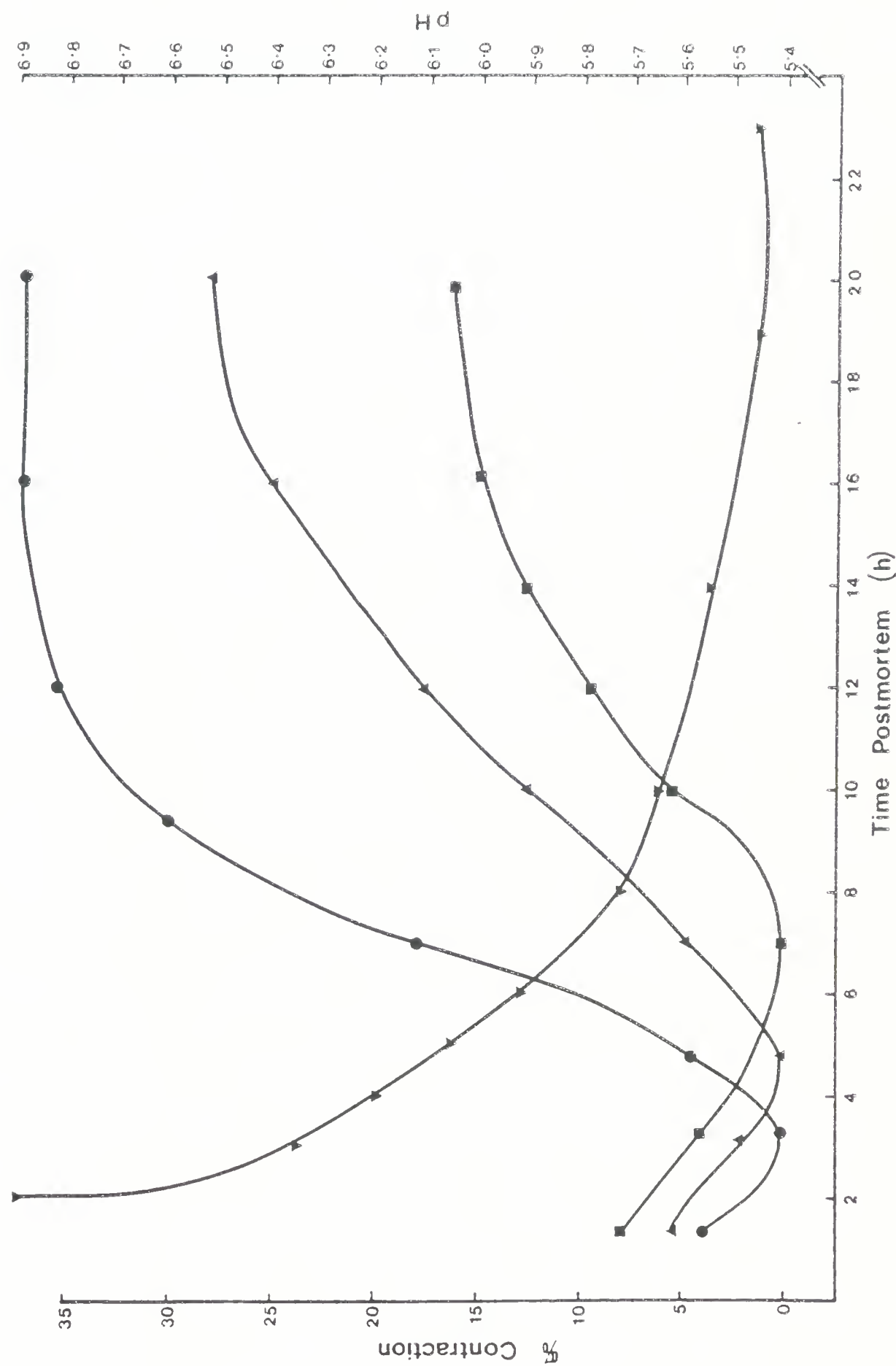


Figure III.14. Plot of % isotonic contraction vs time postmortem for muscle strips at several different loadings of  $5 \text{ g/cm}^2$  (●-●-●),  $12.5 \text{ g/cm}^2$  (▲-▲-▲) and  $25 \text{ g/cm}^2$  (■-■-■). These are data from one experiment. A plot of pH vs time postmortem (▼-▼-▼) is included for comparison between pH and the initiation of isotonic contraction at the various loadings. This figure has previously been published (Currie and Wolfe, 1979).





Initially the load placed on the strips at the time of mounting lead to an extension. This is represented by a reduction in the percentage contraction. Muscle strips which bore the greater loads extended the most initially and contracted the least when the contraction finally occurred. Lighter loads produced less extension and permitted more contraction. The results presented in Table III.4 show differences in the percentage contraction. A comparison of the percentage contraction for samples in the 5-7 g/cm<sup>2</sup> loadings showed values ranging from 15-35%. Thus the variability between maximum rigor tension for different carcasses using isometric tension measurements is supported by isotonic data as well. Unfortunately, the carcasses examined were not the same for isotonic and isometric measurements so direct comparison of the results can not be made. Table III.4 also reveals the pH at which the contraction under different loadings was initiated. These results reveal a correlation between the loading and the pH at which contraction was initiated ( $r=-0.948$ ; d.f.=15). For lightly loaded muscle strips (5-7 g/cm<sup>2</sup>), the contraction commenced at a pH range of 6.1-6.3; for intermediate loadings (10-16 g/cm<sup>2</sup>), the pH range was 5.9-6.1; and for heavy loadings (22-28 g/cm<sup>2</sup>), the pH was 5.8. The percent contraction is the greatest between this stage in rigor development (in the region of pH 5.8) and rigor maximum (see Figure III.14). The extent of the contraction likely depends upon the availability of ATP. When ATP is no longer being



Table III.4 Isotonic contraction data

Sample	Loading (g/cm <sup>2</sup> )	pH at which Contraction Initiated	Contraction (%)
5-7			
1		6.2	25.2
2		6.1	32
3		6.2	35
4		6.2	35
5		6.3	37
6		6.2	15
7		6.1	17.5
10-16			
8		6.0	24.5
9		6.1	21.8
10		6.1	28.5
11		6.0	11.0
12		5.9	11.5
22-28			
13		5.8	20
14		5.8	8.0
15		5.8	9.0
16		5.8	16.5
17		5.8	9.0

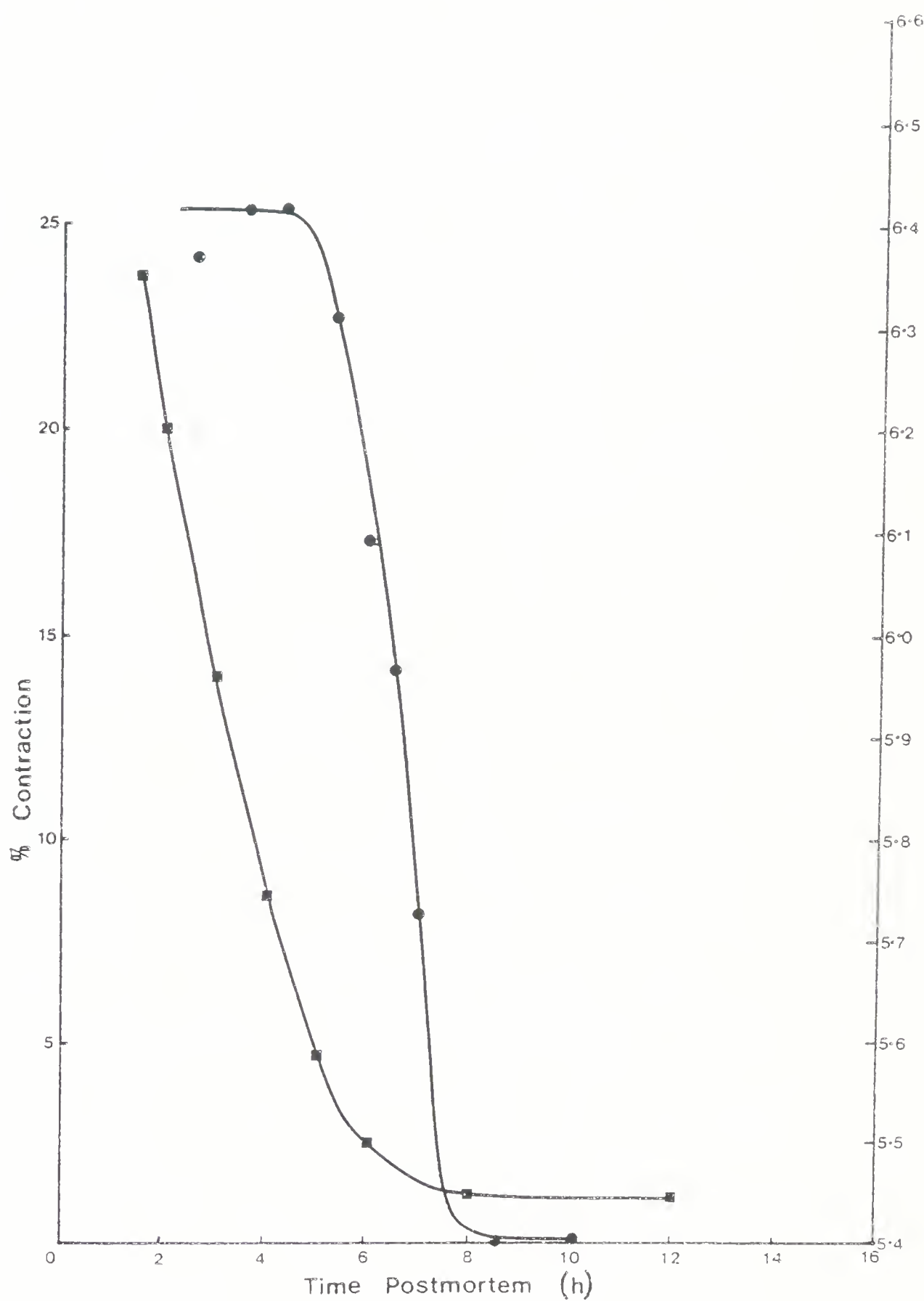


produced, no contraction occurs. The rigor bonds remain and are capable of supporting the loads tested without extending.

These observations (the delay in the initiation of contraction in relation to the load placed on the muscle) may be related to the number of crossbridges that exist during the different periods of rigor development. This hypothesis is supported by the fact that the ATP levels are often greater than 6.3  $\mu$ moles/g (in muscles that have an ultimate pH of 5.35-5.55). The ATP functions as a plasticizer, allowing extension of the muscle strip. As rigor development progresses, the ATP levels fall and the pH drops. Hay *et al.* (1973) observed that at low pH the  $\text{Ca}^{2+}$  sequestering ability of the sarcoplasmic reticulum is low, and thus free  $\text{Ca}^{2+}$  levels in the fibre rise (Nakamura, 1973). When the  $\text{Ca}^{2+}$  levels increase, crossbridges begin to form. The number of crossbridges would be few in the pH range of 6.1-6.3 and the load that could be lifted during the initiation of rigor contraction would be small. When the pH is 5.8, even the heaviest loads tested ( $45 \text{ g/cm}^2$ ) could be lifted since now the number of crossbridges is greater.

Figure III.15 presents the results obtained from prerigor muscle strips that were restrained from contraction (isometric tension). At different times postmortem this restraint on the muscle strips was released. All of the early prerigor muscle strips released from constraint contracted to the same extent. Then, the closer to rigor,

Figure III.15. Plot of % contraction vs time postmortem (●---●) for muscle following the removal of the restraint to contract at the time postmortem represented by the data points on the graph. A plot of pH vs time postmortem (■---■) is included to indicate the time rigor was attained. This figure has previously been published (Currie and Wolfe, 1979).





the contraction became smaller. This observation would be expected if the availability of ATP were the limiting factor contributing to contraction in late prerigor muscle. Contraction would only continue during the period of time ATP was being produced by the muscle strip. Thus, the muscle strips which were released in the early prerigor period would have sufficient ATP and  $\text{Ca}^{++}$  to contract maximally. The muscle strips released shortly before rigor maximum would have lost most of their ATP, partly a result of supporting an isometric tension during the time of muscle restraint. The contraction of these muscle strips upon release would be dependent upon the rate and duration of ATP production.

#### Mechanical measurements

Typical responses of muscle at three different postmortem periods are presented in Figures III.16-III.18. The early prerigor tensile response resulted in an initial yield at about 80% of the final yield tension and extension (Figure III.16). As the muscle neared rigor, the point of initial yield value dropped dramatically so that the yield point was about 20% of the final yield tension and extension (Figure III.17). When an aged sample (14 days) was examined by similar methods, the initial yield was again within 80-90% of the final yield tension and extension (Figure III.18). It can be inferred from the results that different mechanisms are involved in the tensile stretch response at

Figure III.16. Typical tensile response of a prerigor muscle strip. Initial yield (I.Y.) and final yield (F.Y.) points are indicated on the graph.

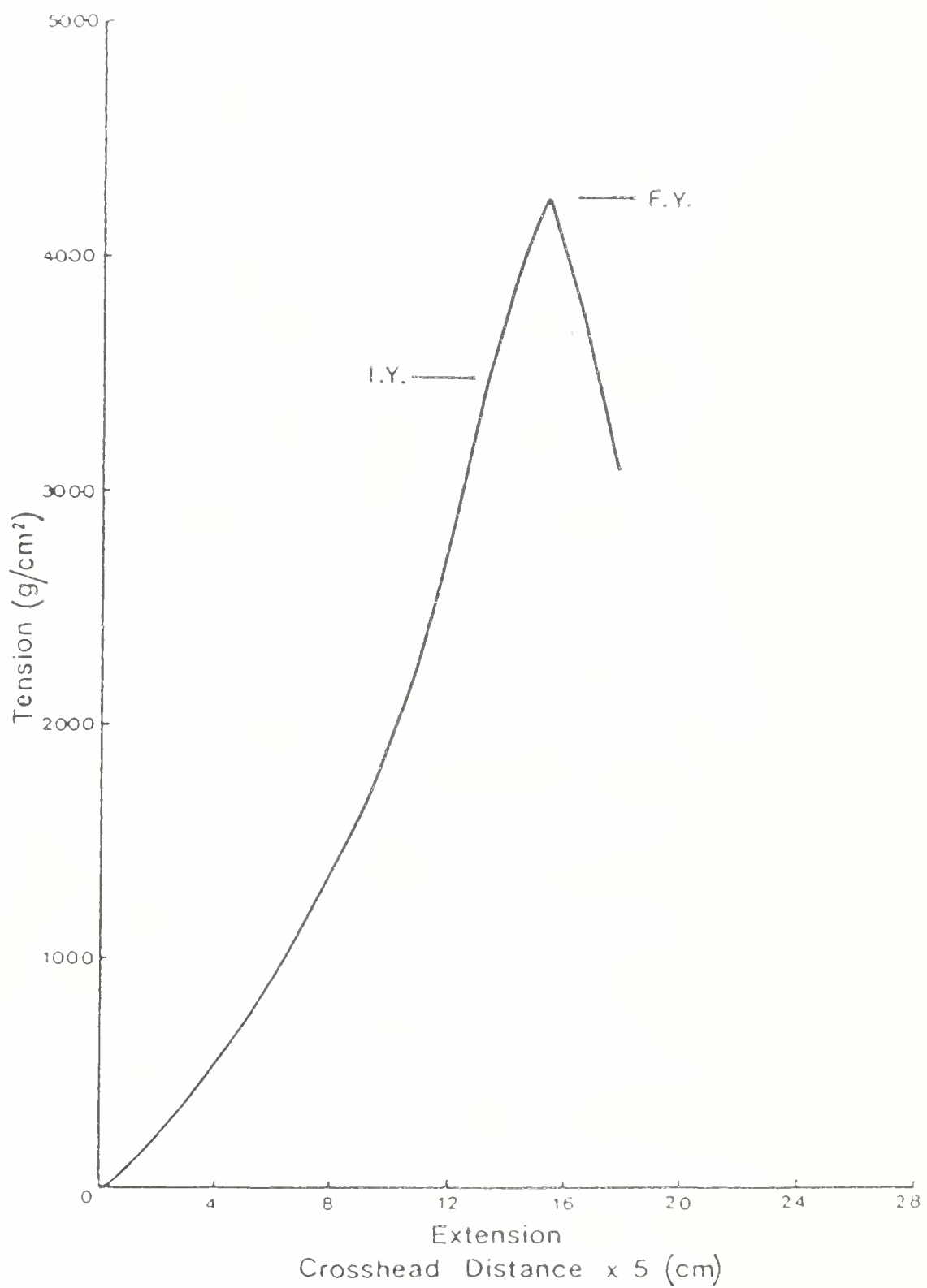


Figure III.17. Typical tensile response of a near rigor muscle strip. Initial yield (I.Y.) and final yield (F.Y.) points are indicated on the graph.

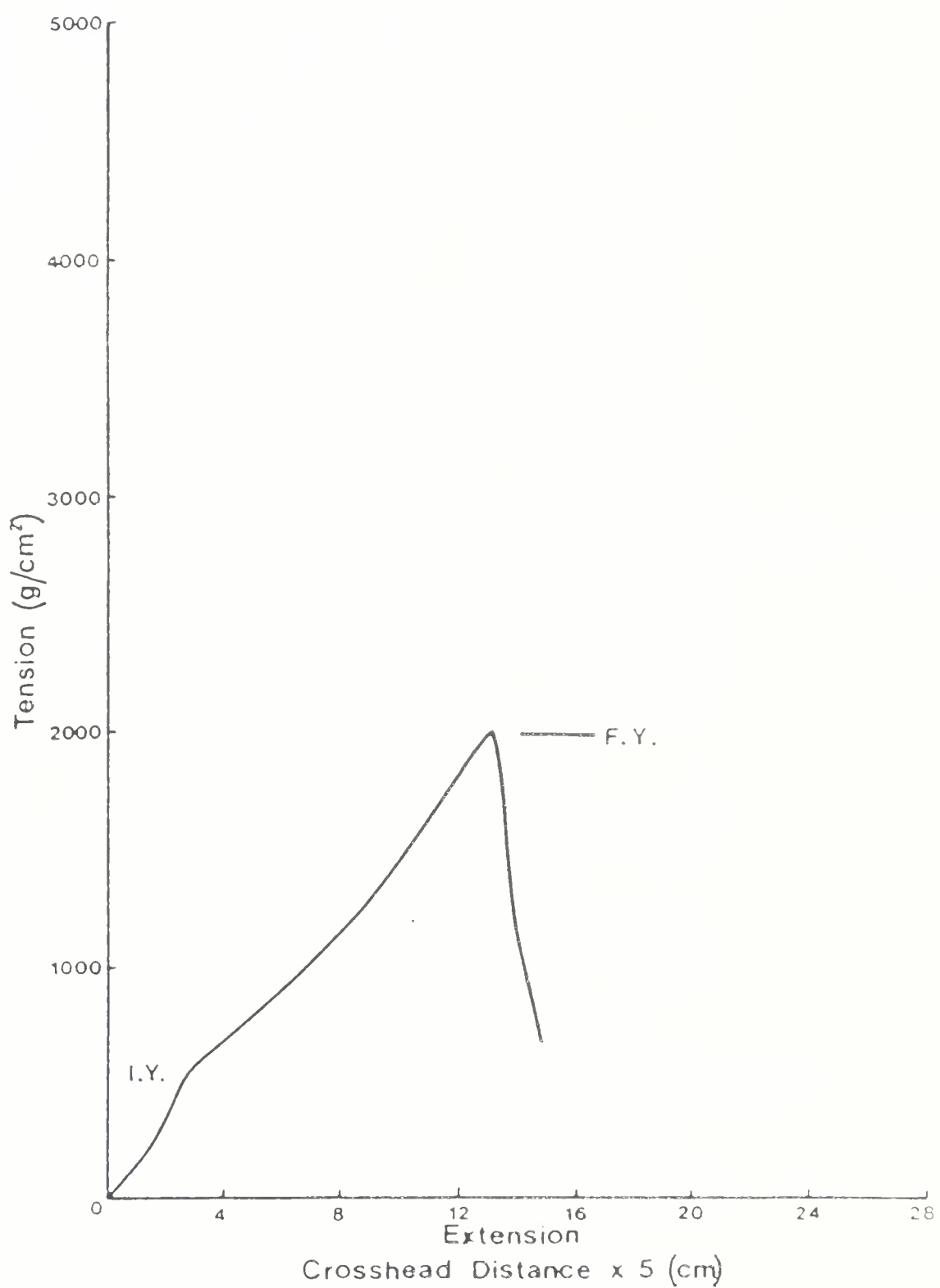
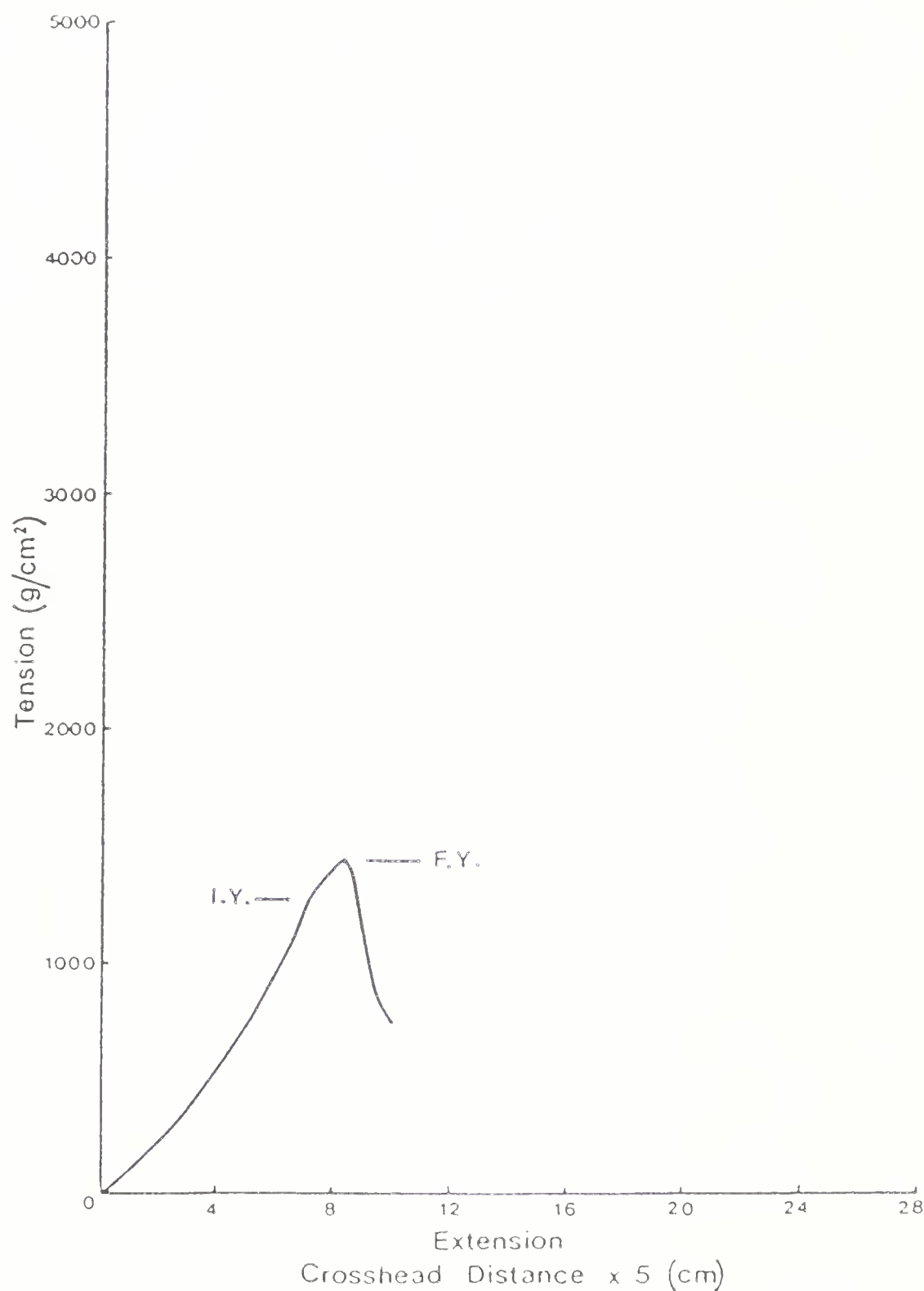


Figure III.18. Typical tensile response of a 14 day postrigor muscle strip. Initial yield (I.Y.) and final yield (F.Y.) points are indicated on the graph.



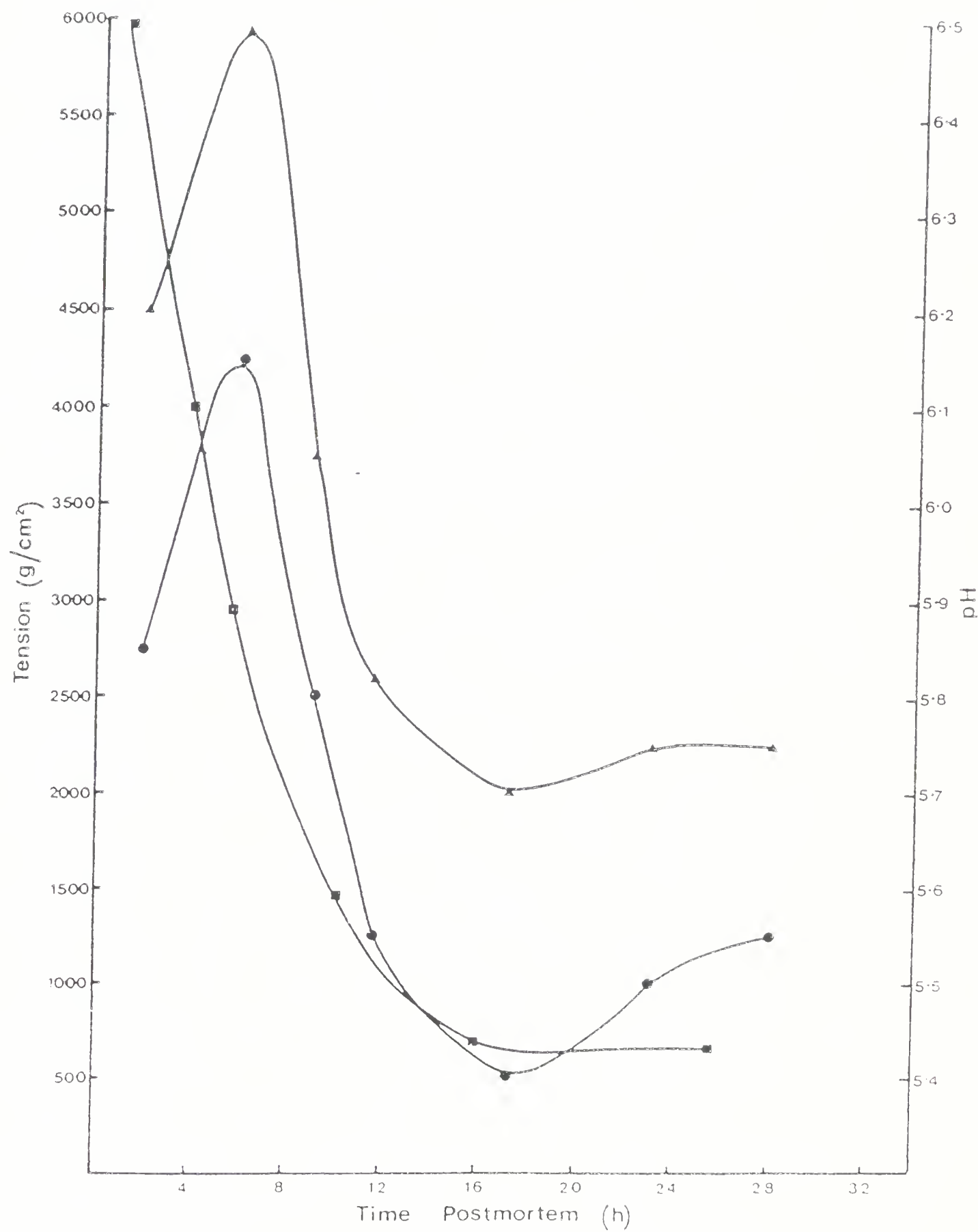


prerigor, rigor and postrigor postmortem periods.

Several muscles (biceps femoris, vastus lateralis, ST) were examined and, although the actual tension and extension values differed between muscle types and carcasses, the general profiles were the same. The meat samples reported here were not from the same carcasses as those examined using NMR. In order to simplify the results and discussion in this section, only one set of figures from the ST will be considered. The pH fall of the muscles entering rigor correlated with different features of the mechanical measurement profiles. Therefore, the mechanical measurements are plotted along with pH fall to simplify the presentation.

The changes in the tensile response of the muscle as it approached rigor are presented in Figure III.19. A plot of the tension at initial yield versus time postmortem revealed that the force to initial yield gradually increased to peak at about  $4250\text{ g/cm}^2$ . The pH of the muscle at this point was in the range of 5.85-5.95. Following this, a decrease in the tensile strength of the muscles was observed until the minimum values (about  $500\text{ g/cm}^2$ ) were recorded, coincident with rigor maximum. Samples analyzed beyond rigor maximum indicated some variability in the rise of the initial yield. With this sample the tension increased to level off at about  $1300\text{ g/cm}^2$ . The tensile strength of the muscle at final yield (Figure III.19) required greater force than the initial yield for failure. The final yield tension mirrored the initial yield profile except near rigor maximum where

Figure III.19. The tensile profile [tension at initial (•-•-•) and final yield (▲-▲-▲) generated due to longitudinal stretch vs time postmortem] of early postmortem beef muscle. The standard deviation of the points plotted is  $\approx \pm 10\text{-}15\%$  of the mean. pH (■-■-■) vs time postmortem is also plotted. This figure has previously been published (Currie and Wolfe, 1980).





the separation between initial and final yield tension was the most evident.

The extensibility of the muscle (Figure III.20), showed a similar profile to that of the tensile properties (Figure III.19). The extensibility of the muscle was greatest when the muscle pH was between 5.85-5.95. This correlates with the observation that the final yield or breaking point profile was also the highest at this point. After this the muscle rapidly became less extensible, with a sudden drop in the extension needed to exhibit initial yield. However, the extension needed for the final yield did not drop to as low a value as the initial yield extension. Even some of the postrigor samples did not lose the ability to extend once the initial resistance to stretch was overcome. This supports the results of Hegarty (1972), who showed that mouse muscle in rigor was partially extensible. Other postrigor samples which we examined did become very inextensible (such a sample is presented in Figure III.20).

The adhesive strength of the prerigor samples (Figures III.21 and III.22) changed with time, but a marked contrast between samples undergoing slow rigor development and fast rigor development was evident when different carcasses were compared. Both types of muscle samples showed an increase in their adhesive properties when the pH had dropped to the region of 5.85-5.95 (indicated by a rise in the tension needed to exhibit both initial and final yield). The adhesive strength of both samples also dropped as the pH

Figure III.20. Tensile extensibility profile [the extension at initial (•-•-•) and final yield (▲-▲-▲) due to longitudinal stretch vs time postmortem] of early postmortem beef muscle. The standard deviation of the points plotted is  $\pm 15\text{-}20\%$  of the mean. A typical value from an inextensible postrigor muscle strip is indicated in the graph (▼). pH vs time postmortem is also plotted. This figure has previously been published (Currie and Wolfe, 1980).

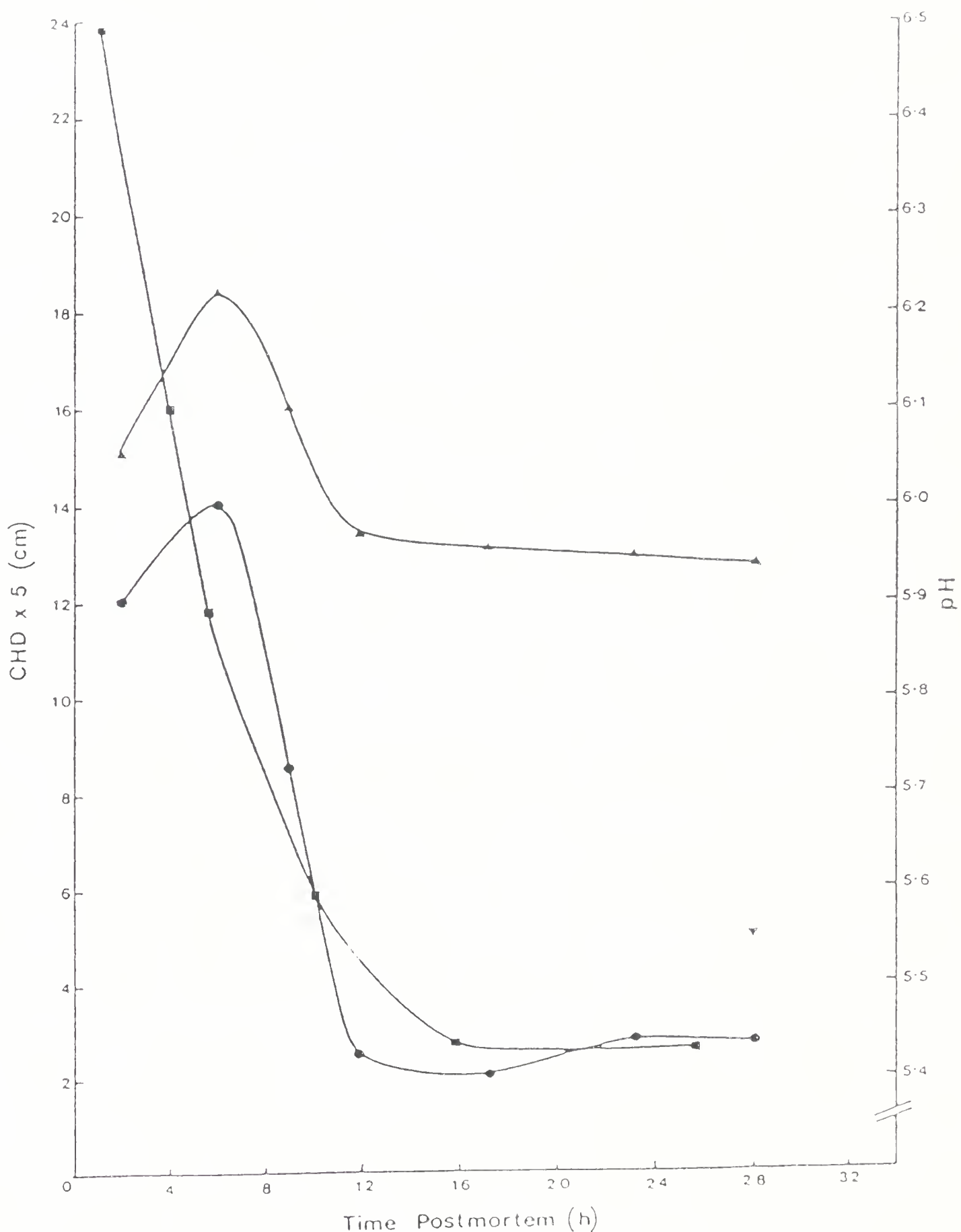


Figure III.21. Adhesive profile [tension at initial yield (•-•-•) and final yield (▲-▲-▲) generated due to stretch perpendicular to the fibre axis vs time postmortem] of early postmortem beef muscle undergoing slow pH (■-■-■) fall. The standard deviation of the points plotted is  $\pm 25\text{-}30\%$  of the mean. This figure has previously been published (Currie and Wolfe, 1980).

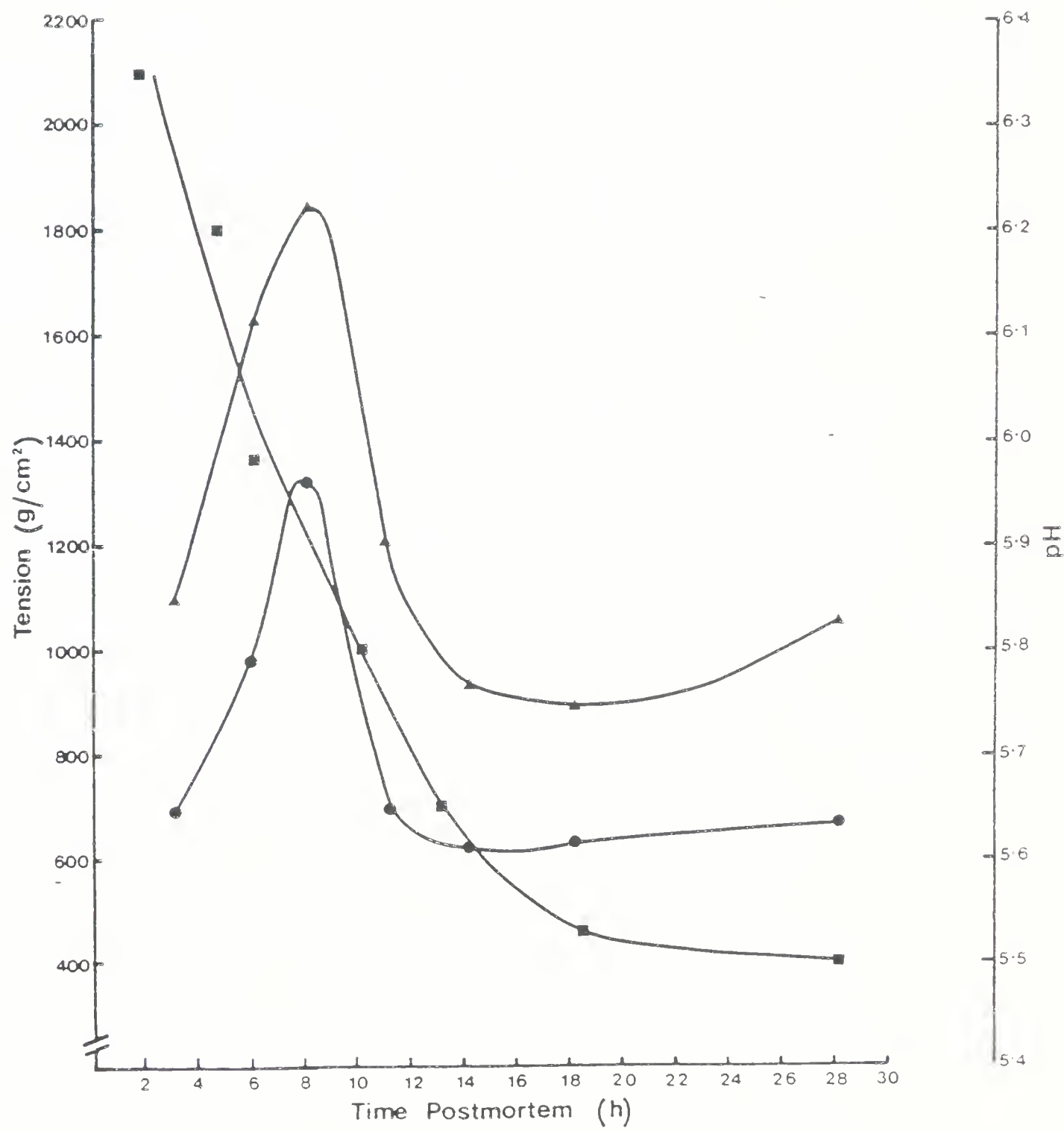
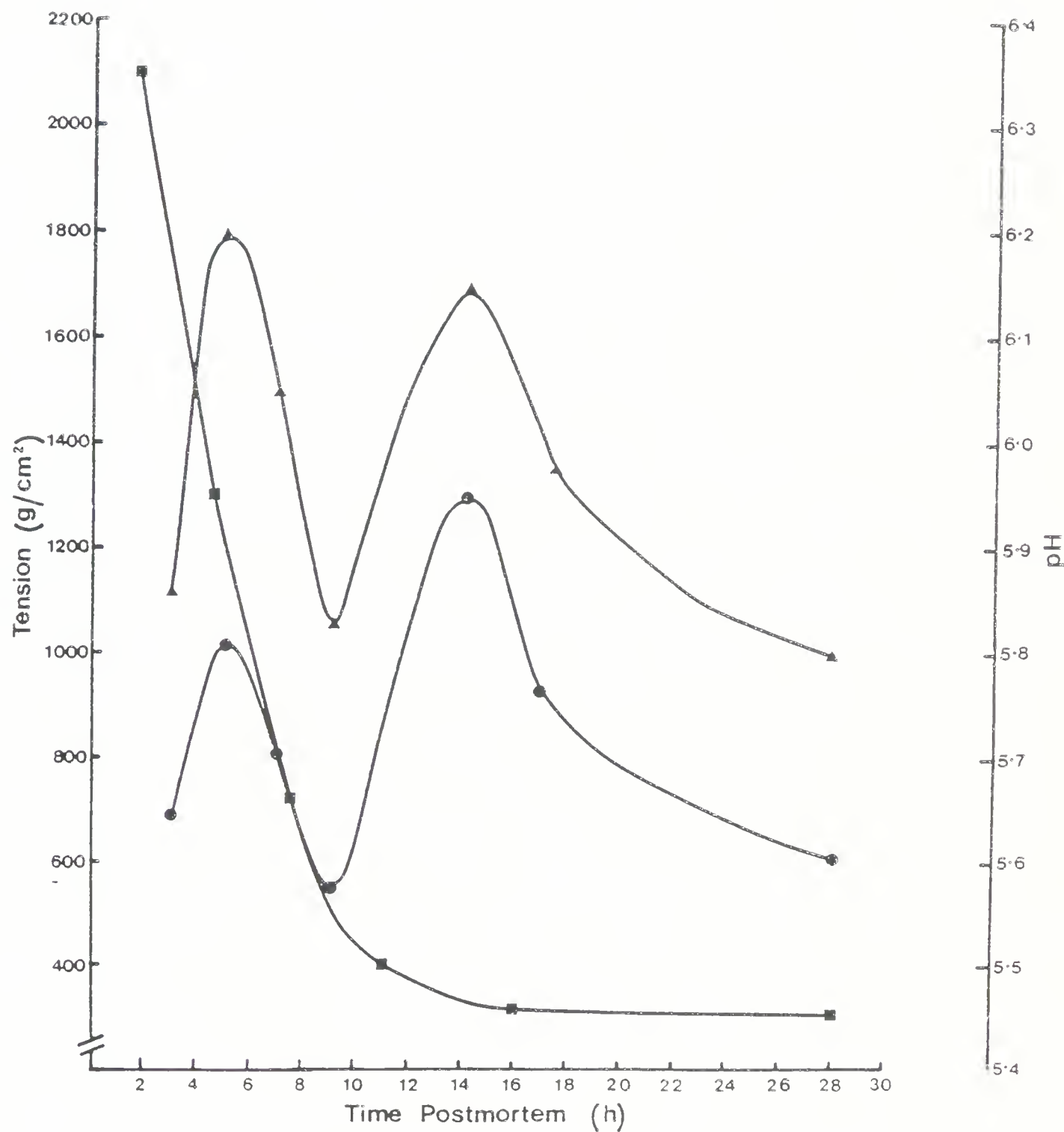


Figure III.22. Adhesive profile [tension at initial yield (•-•-•) and final yield (▲-▲-▲) generated due to stretch perpendicular to the fibre axis vs time postmortem] of early postmortem beef muscle undergoing rapid pH (■-■-■) fall. The standard deviation of the points plotted is  $\approx \pm 25\text{-}30\%$  of the mean. This figure has previously been published (Currie and Wolfe, 1980).





continued to fall, but near the point of rigor maximum the response to the stretch was different. The adhesive tension of muscle strips from samples experiencing a slow pH fall (Figure III.21) remained low throughout rigor, whereas samples undergoing rapid pH fall (Figure III.22) showed a new increase in strength, peaking at rigor. After rigor maximum the tension again dropped to lower values. In Figures III.23 and III.24 only the extension to initial yield is presented. The final yield profile has a greater magnitude but is identical. Both figures indicate that the adhesive extensibility of muscle undergoing slow and fast pH fall rises to a peak at rigor maximum. Although the bimodal curve is common to both sample types, it was also observed that the extensibility was greater for the samples undergoing slow pH fall (compare Figures III.23 and III.24).

The results from the 14 day postmortem samples of ST are included in Table III.5. The initial yield is within 80-90% of the final yield tension and extension for each sample. Carroll *et al.* (1978) examined the ST (10 days postmortem) during tensile stress using a video camera attached to a microscope (200x). Additional samples of the same muscle were fixed under stress to examine the fibres with a scanning electron microscope (SEM). Their estimated rate of extension (1.0-1.5 cm/min) compares well with our 2.0 cm/min crosshead movement on the Instron Universal Testing Machine. The SEM of the raw ST indicated an initial rupture at the muscle fibre level, concomitant with the



Table III.5 14 day postmortem ST data

	NMR T1 (raw)	Water Content	OTMS	Final Yield	Initial Yield	Cooking Loss	pH
1	0.744	73.8	0.105±.018	1076±203	948±164	15.4	5.69
2	0.750	75	0.133±.027	1302±382	1113±424	26.5	5.94
3	0.718	73.6	0.166±.018	1145±317	998±270	16.2	5.71
4	0.800	74.8	0.190±.027	1535±271	1142±343	15.8	5.75
5	0.772	75.2	0.132±.018	1444±301	1230±358	18.7	5.75
6	0.762	73.8	0.129±.015	1136±256	1108±372	15.7	5.64
7	0.778	74.6	0.100±.010	1133±183	884±313	15.6	5.72
8	0.874	75.3	0.102±.014	1219±505	1117±464	14.5	5.75
9	0.815	75.4	0.142±.016	1138±288	901±166	16.5	5.75
10	0.772	75.2	0.138±.013	1379±403	1113±486	16.2	5.71

Figure III.23. Adhesive extensibility profile (the extension at initial yield (●-●-●) due to stretch perpendicular to the fibre axis vs time postmortem) of early postmortem beef muscle undergoing slow pH (■-■-■) fall. The standard deviation of the points plotted is  $\approx \pm 15\text{-}20\%$  of the mean. This figure has previously been published (Currie and Wolfe, 1980).

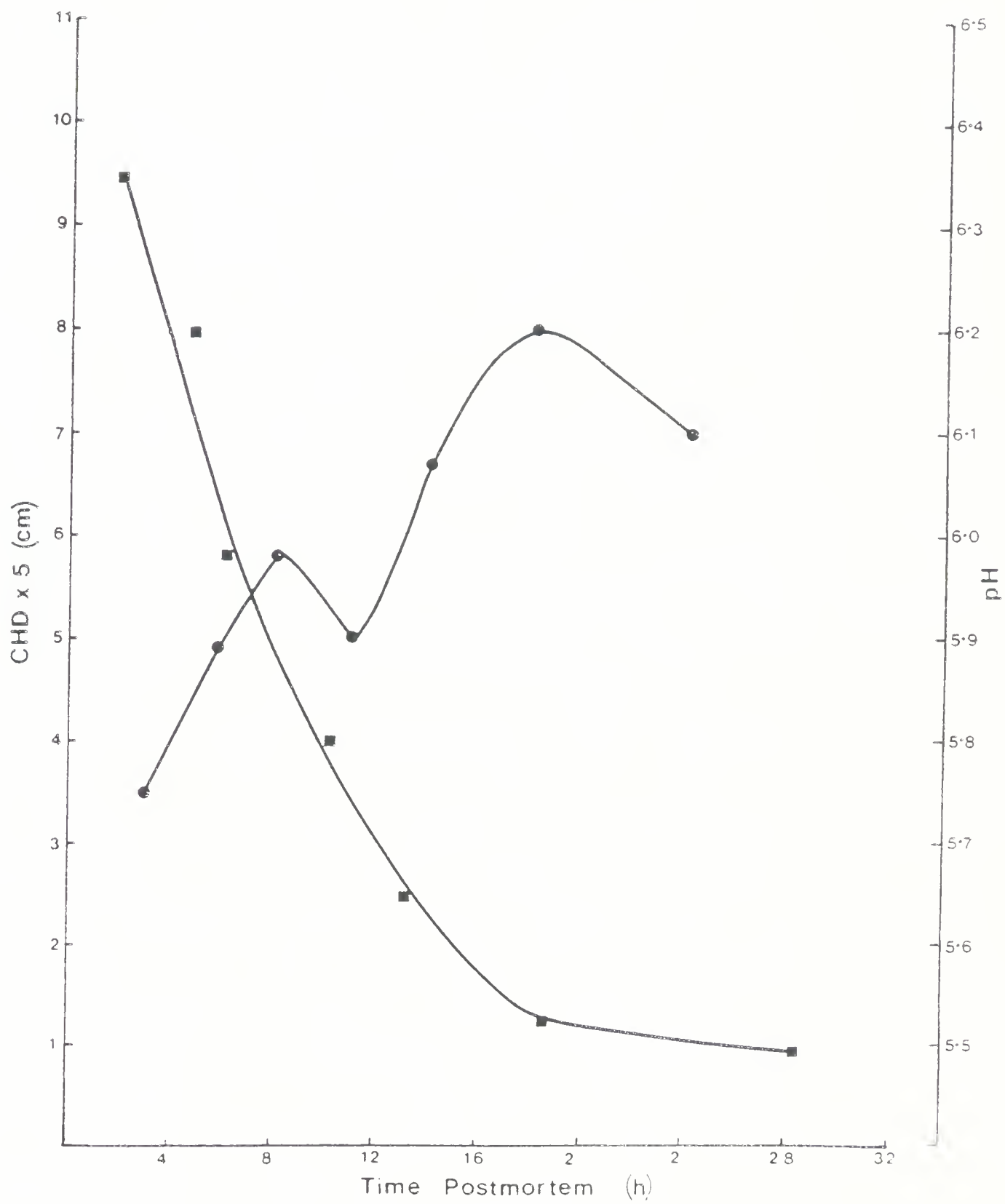
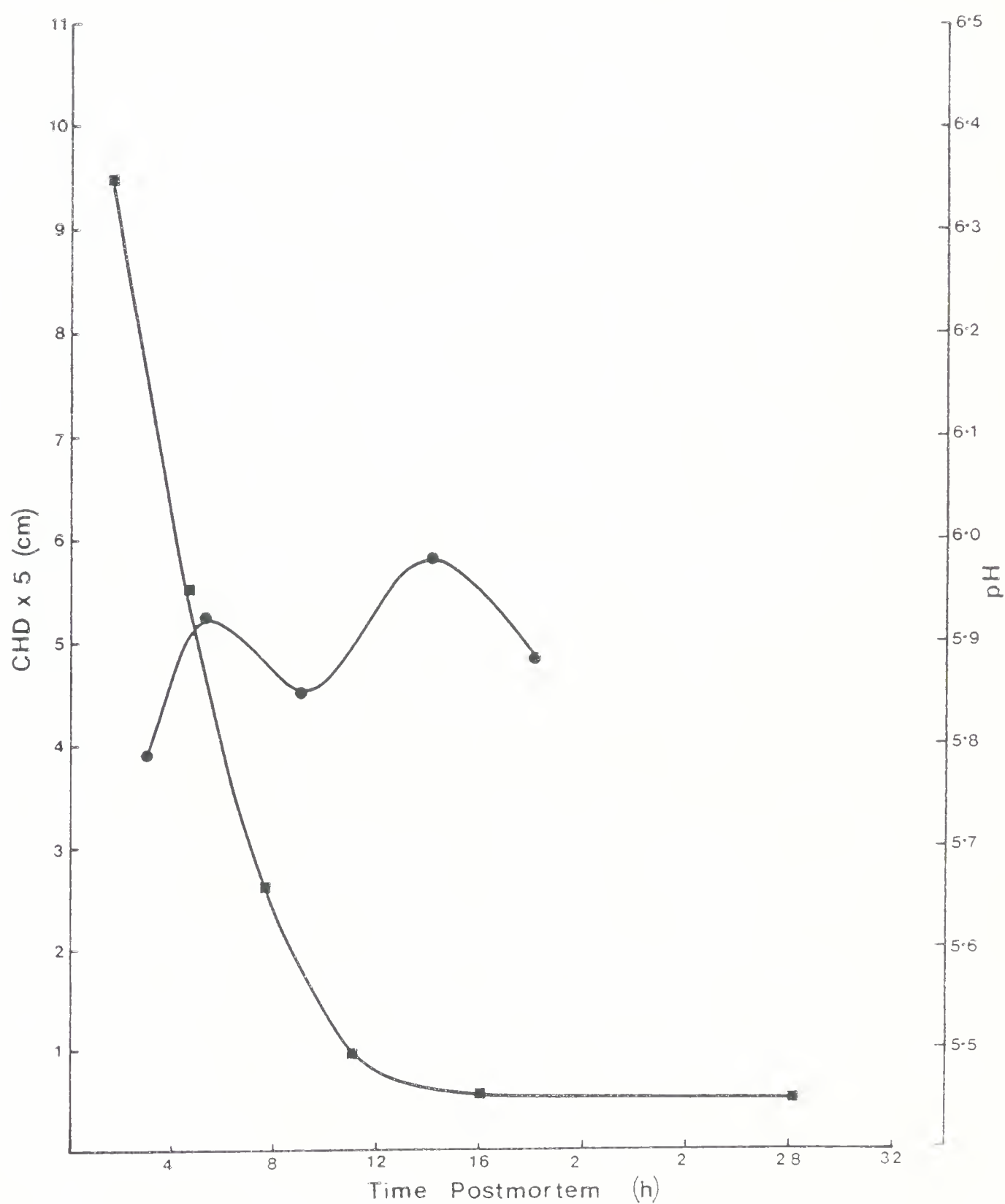


Figure III.24. Adhesive extensibility profile (the extension at initial yield (●-●-●) due to stretch perpendicular to the fibre axis vs time postmortem) of early postmortem beef muscle undergoing rapid pH (■-■-■) fall. The standard deviation of the points plotted is  $\approx \pm 15\text{-}20\%$  of the mean. This figure has previously been published (Currie and Wolfe, 1980).





appearance of strand material. It was observed, using the video camera, that as the stress was increased, the muscle fibres completely ruptured and only the stranded material (endomysium and perimysium) remained intact. It was found that approximately twice the force was necessary to rupture the strands as was required to rupture the muscle fibres. Unfortunately, the SEM and video tape photographs do not reveal the appearance of the sarcomeres at the point near the rupture of the fibre. As a result, the nature of the yield (breaks or extended sarcomeres in the fibre) can not be assessed. It would seem reasonable that rupture of the fibre before tensioning of the connective tissue components would be observed as an initial yield on the Universal Testing Machine with little extension. As would be predicted by the observations of Carroll *et al.* (1978), a low initial yield point at half the final yield (or lower, as observed in near rigor samples) was not observed. This suggests that the breakage of the raw myofibrillar component at this aging period occurs easily and thus could not be detected. It is probable that by this time the postmortem degradation of some of the structural myofibrillar proteins has occurred (e.g. CANP on Z-line actin), and the fibre fragments readily at low extensions.

#### Photographs of muscle fibres at initial yield

The phase contrast micrographs of muscle at the initial (tensile) yield, presented in Figures III.25 to III.33



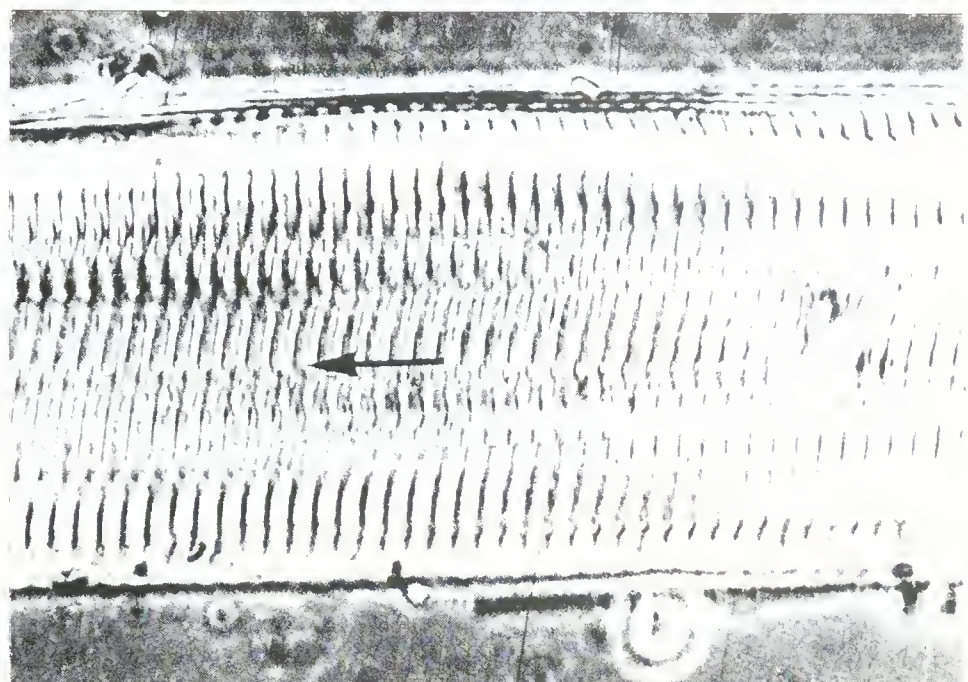


Figure III.25. A phase contrast micrograph of a muscle fibre (pH 6.25) fixed at initial yield (magnification 770x). The myofibrillar units within the fibre appear to be out of register.





Figure III.26. A phase contrast micrograph of a muscle fibre (pH 6.10) fixed at initial yield (magnification 850x). More of the myofibrillar units within the fibre appear to remain in register rather than slipping past one another as in Figure III.25.



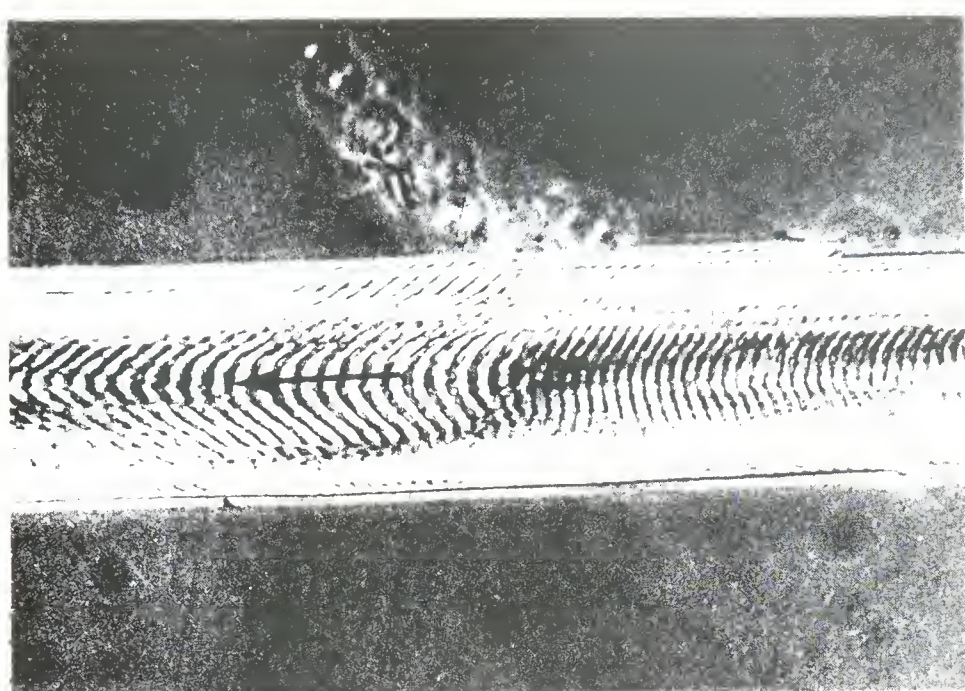


Figure III.27. A phase contrast micrograph of a muscle fibre (pH 5.95) fixed at initial yield (magnification 610x). Regions of the fibre are extended and the myofibrillar units appear in register.



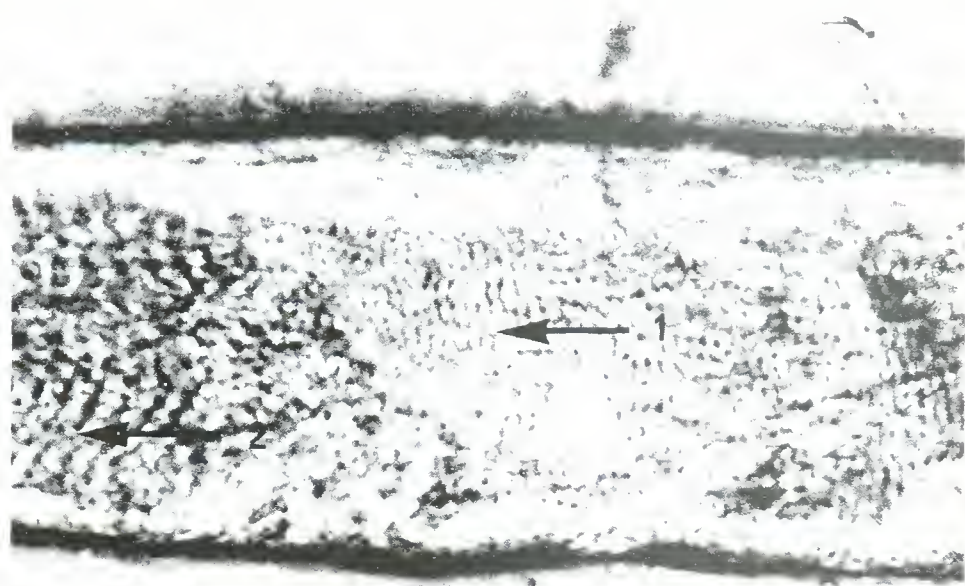


Figure III.28. A phase contrast micrograph of a muscle fibre (pH 5.75) fixed at initial yield (magnification 840x). Extensions of certain regions of the fibre (arrow 1) are presented, while other areas are free to extend (arrow 2).



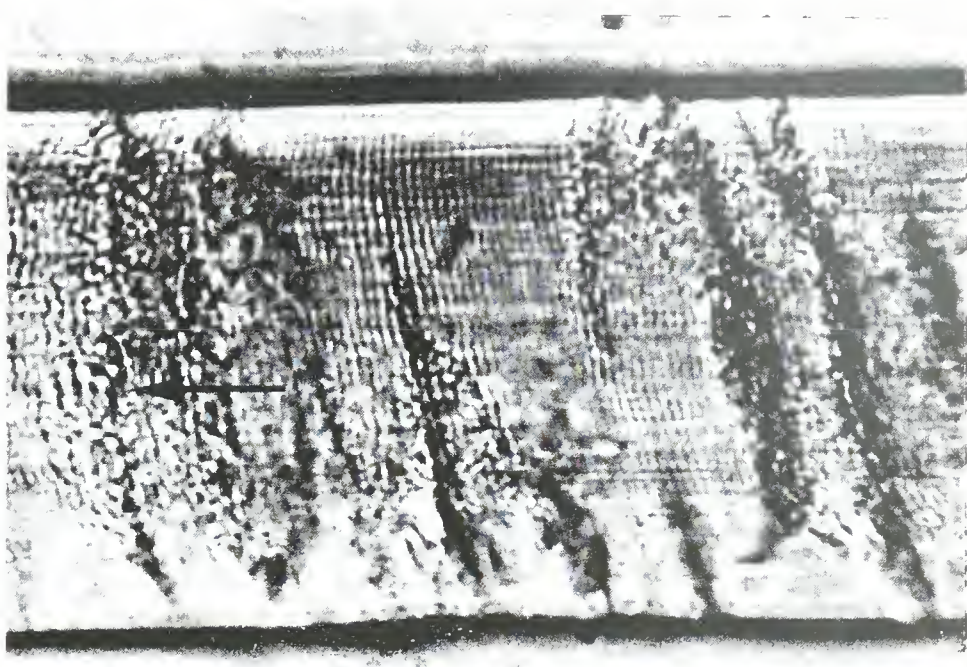


Figure III.29. A phase contrast micrograph of a muscle fibre (pH 5.65) fixed at initial yield (magnification 720x). Breaks across the fibre can be seen, suggesting actin-myosin interactions have been broken.





Figure III.30. A phase contrast micrograph of a muscle fibre (pH 5.5) fixed at initial yield (magnification 830x). Breaks across the fibre appeared sharper in most instances (than the breaks in fibres at pH 5.65), involving only a few sarcomeres.



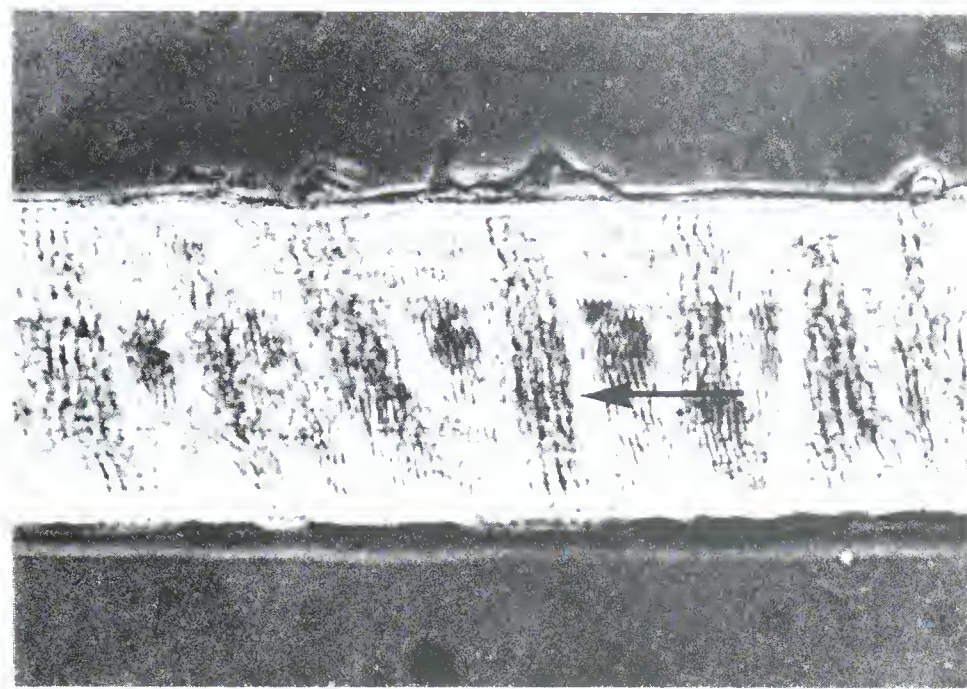


Figure III.31. A phase contrast micrograph of a muscle fibre (pH 5.6) fixed after stretching the fibre beyond initial yield (magnification 580x). It appears that the fibre will continue to extend where the breaks had occurred at initial yield.



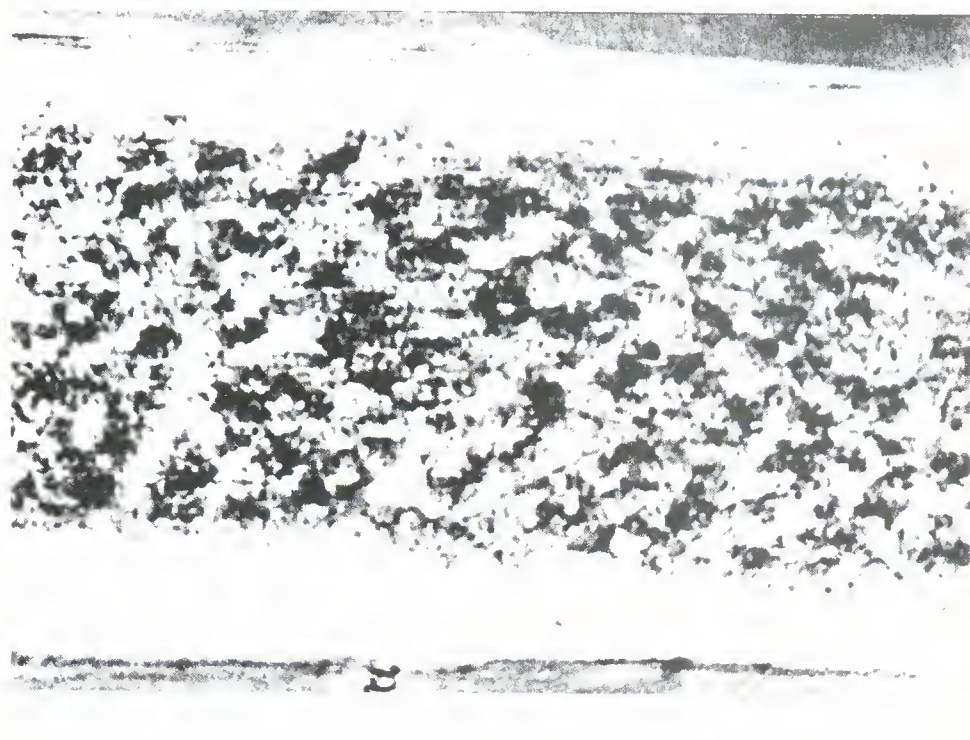


Figure III.32. A phase contrast micrograph of a muscle fibre (postrigor) fixed at initial yield (magnification 860x). Breaks do not appear across the fibre, but occur randomly, giving a very disordered appearance.



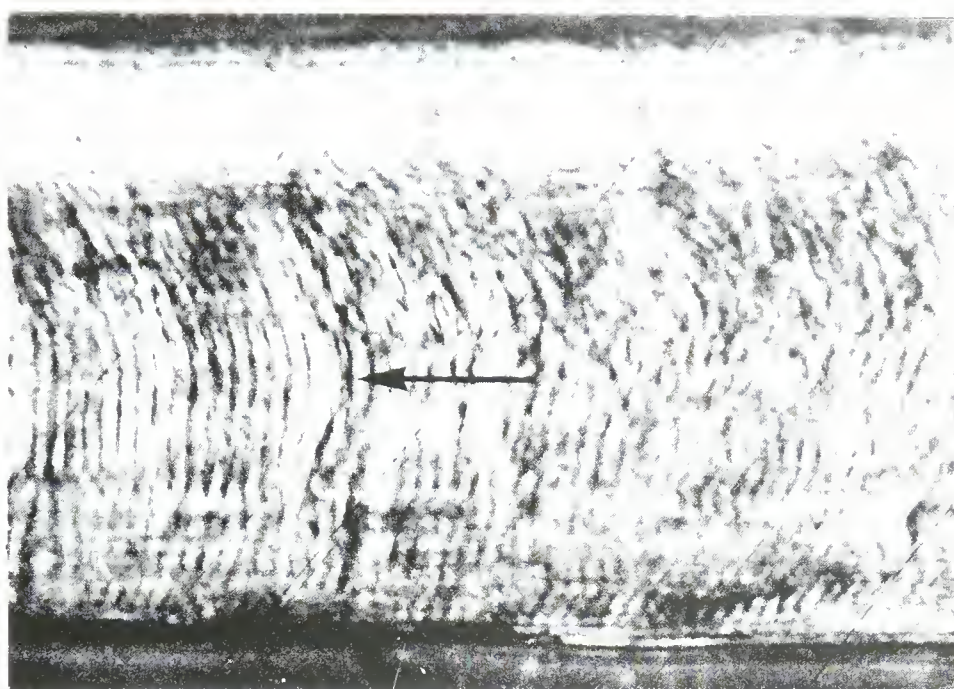


Figure III.33. A phase contrast micrograph of a muscle fibre (an on-carcass sample removed postrigor) fixed at initial yield (magnification 900x). Breaks appear to extend across the fibre. These fibres have a greater extensibility at final yield.



[previously published in Currie and Wolfe (1980); selected areas for detailed examination], help to explain the profiles observed in Figures III.19 and III.20. It is doubtful that these photographs represent the precise state of the muscle at initial yield since the time between stretching of the muscle and fixation would allow for some equilibration of the effects of stretch. However, examination of the photographs reveals a considerable difference between the early prerigor samples and those approaching rigor. The approximate pH of the muscle is indicated in the legends to these photographs to correlate the photographs with the profiles in Figures III.19 and III.20.

Figure III.25 depicts the state of the muscle following stretch in the early prerigor state. The sarcomeres are clearly stretched and units of myofibrils within the fibre are out of register with one another (i.e. not all A-bands and Z-lines are aligned across the fibre). Thus, it would appear, the initial yield at this point postmortem is not a reflection of the myofibrillar component, but an alignment of all the muscle components to the stretch. In Figure III.26 the myofibrils towards the interior of the fibre are stretched, but in comparison with those shown in Figure III.25, are more likely to stay in register before myofibrillar units slip past one another. Figure III.27 depicts the state of the fibre almost at the peak of the tensile profile. The sarcomere lengths become very long



( $>4.0 \mu\text{m}$ ) with all the myofibril units tending to remain in register (see arrow). As a result, instead of the myofibril units slipping past one another as in the previous photographs, they tend to break and be totally disrupted. It would appear that at this stage of rigor the myofibrillar component is increasing in its contribution to the initial yield. The myofibrils seem to resist alignment to the stretch due to a greater adhesive force between the myofibrils in the fibre. Figure III.28 presents the fibre at initial yield after the muscle begins to lose its extensibility. It is interesting to note that in certain regions of the fibre (see arrow 1) there are normal sarcomere lengths, which implies that the actin-myosin interactions are only minimally disrupted by stretch, whereas other regions (see arrow 2) freely extend until they are disrupted and exhibit the initial yield, suggesting a weakness in actin-myosin interactions or a small number of crossbridges. Subsequent photographs (Figures III.29 and III.30) reveal that more of the fibre is affected by strong actin-myosin interactions (perhaps a greater number of crossbridges) with the result that fewer regions of the fibre will extend as rigor maximum is approached. Some of the sarcomeres of myofibrils will yield, resulting in what appear to be breaks (see arrows) at rather regular intervals along the fibre. If the muscle is extended beyond the initial yield (and before the final yield), the regions of the fibre that have yielded will continue to extend, as



shown in Figure III.31, resulting in regions of extended sarcomeres (see arrow), interdispersed between regions of contracted unyielding myofibrils. Hamm *et al.* (1980) confirmed the report by Currie and Wolfe (1980) that rigor bonds between actin and myosin are beginning to occur around pH 5.9 in postmortem muscle attaining an ultimate pH of about 5.4-5.5. Thus, the sharp drop in the tensile response (Figure III.19) and extensibility (Figure III.20) and the appearance of the muscle fibres in Figures III.28-III.31 is probably the result of the formation of rigor bonds.

Finally, postrigor samples stretched to initial yield had two different appearances. The first is seen in Figure III.32, where extension results in the totally disrupted fibre shown in the photograph, and the second is shown in Figure III.33 where extension produced breaks and regions of extension at initial yield. These breaks in the fibre will continue to expand as the muscle is stretched.

Locker and Wild (1982) have confirmed the above histological responses to extension at rigor. However, from electron micrographs of muscle at the yield point they have concluded that the mechanism of yielding at rigor is a failure of actin filaments, or their attachments, followed by elastic extension of gap filaments within the I band. This observation (for rigor and early postrigor muscle) is supported by the size of the majority of A-bands in the light microscope photographs reported here. The A-bands appear narrow, with the I-bands showing extension.



The appearance of the stretched regions of sarcomeres near the time rigor bonds are beginning to form (e.g. Figure III.27) indicates A-bands that have broadened, which may support the proposal that weaknesses in the actin-myosin interactions (fewer crossbridges) and weaknesses in the region of the M-line allow certain regions to extend, and this extension involves the whole sarcomere.

### Conclusion

The results reported in this section lead to two major conclusions.

The first is that rigor development leads to major changes in the muscle. This is most evident in the mechanical properties of the muscle. The once pliable muscle becomes rigid due to conditions that favor the formation of rigor bonds. It is essential that the rate at which these transitions are occurring and the extent of the postmortem changes be measured, so that their influence on the water mobility in the muscle may be assessed.

The second conclusion is that the changes in the biochemical and physiological properties of the muscle are different in each carcass. This observation is an important consideration in this study. The factors contributing to the diversity in these properties may also be reflected in the results of the measurements used to examine the state of water in muscle.



### C. State of Water in Muscle

NMR T,

Figures III.34-III.36 contain the data obtained from eighteen carcasses where T<sub>1</sub> is plotted versus time postmortem (hr). Most of the curves demonstrate an initial rise in T<sub>1</sub> to a peak followed by a decline. The peak T<sub>1</sub> for a given carcass is near rigor (assessed by isometric tension development) but not always coincident with it. The temperature of the muscle in the NMR (24°C) was slightly higher than the temperature of the muscle (22°C) in other measurements. This may have slightly accelerated rigor development in the NMR. The result of this could be some displacement of the peak T<sub>1</sub> toward shorter times postmortem. Table III.6 presents the pH at the NMR T<sub>1</sub> peak. With the exception of sample 15, the pH was low and nearing the ultimate pH. (Sample 15 may be expected to be inconsistent since the fibre typing data [Table III.1] showed a high percentage of red fibres in this sample. The pH profiles and other measurements made in this study for carcass 15 were from samples removed normally from the ST.) Based on the studies of isotonic contraction and the mechanical properties of muscle entering rigor, the NMR T<sub>1</sub> peak occurs when the actin-myosin interactions are nearly maximal and rigor contraction is nearing completion. The size of the initial rise and the slope postpeak are observed to vary between carcasses. Currie *et al.* (1981) reported a



Table III.6 pH at peak T<sub>1</sub> compared to ultimate pH

Carcass Number	pH at Peak	Ultimate pH
1	---	5.65
2	---	5.55
3	5.51	5.50
4	5.46	5.42
5	5.46	5.46
6	5.64	5.42
7	5.52	5.52
8	5.68	5.67
9	5.50	<5.38
10	5.22	<5.20
11	5.18	5.12
12	5.48	5.46
13	5.58	5.42
14	5.50	5.38
15	6.10	5.52
16	5.42	5.42
17	5.27	5.27
18	5.68	5.65

Figure III.34. NMR T<sub>1</sub> profile for carcass 1 (●-●-●), carcass 2 (▼-▼-▼), carcass 3 (▲-▲-▲), carcass 4 (◆-◆-◆), carcass 5 (■-■-■) and carcass 6 (♦-♦-♦) vs time postmortem.

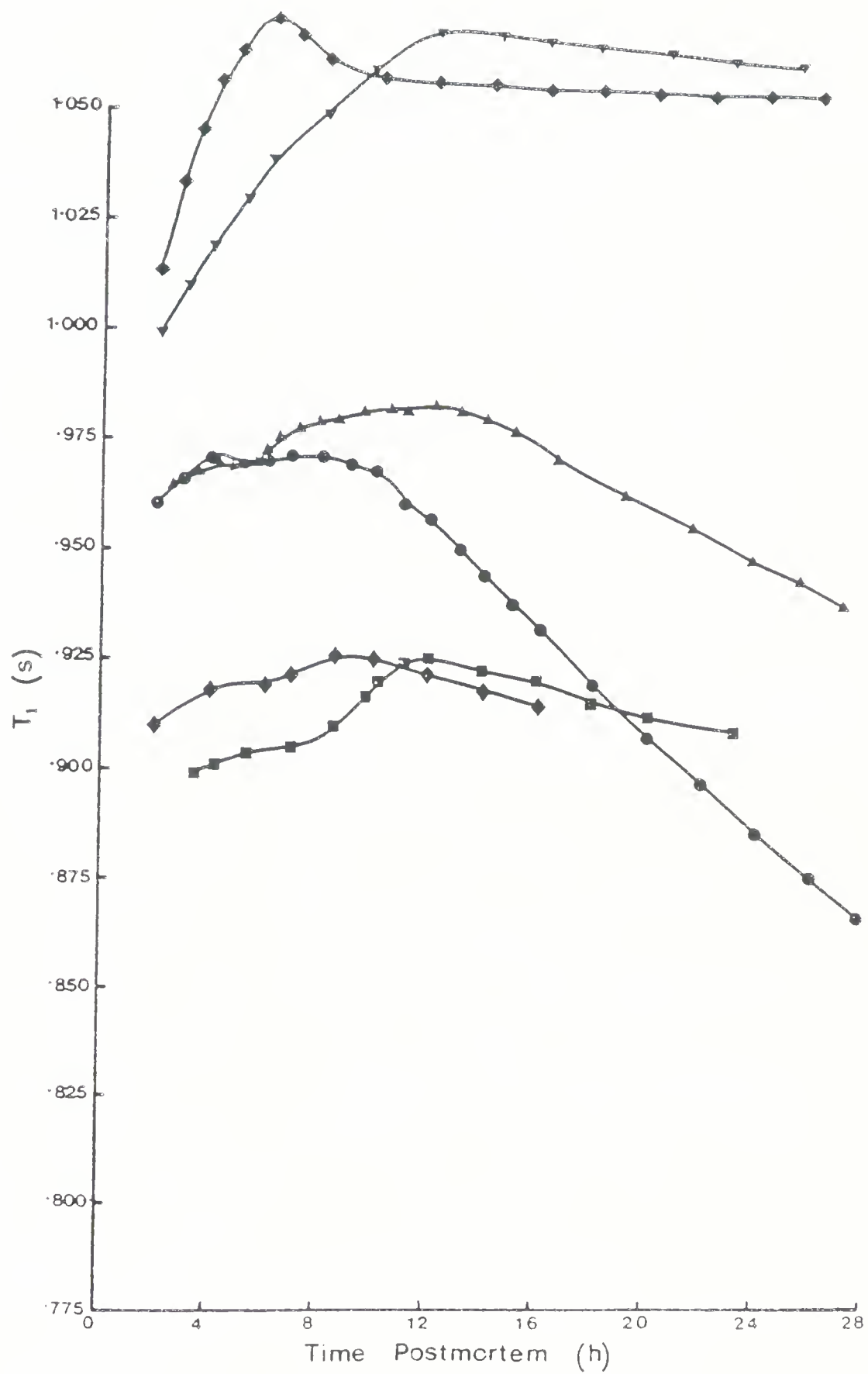


Figure III.35. NMR T<sub>1</sub> profile for carcass 7 (•-•-•), carcass 8 (▼-▼-▼), carcass 9 (▲-▲-▲), carcass 10 (◆-◆-◆), carcass 11 (■-■-■) and carcass 12 (♦-♦-♦) vs time postmortem.

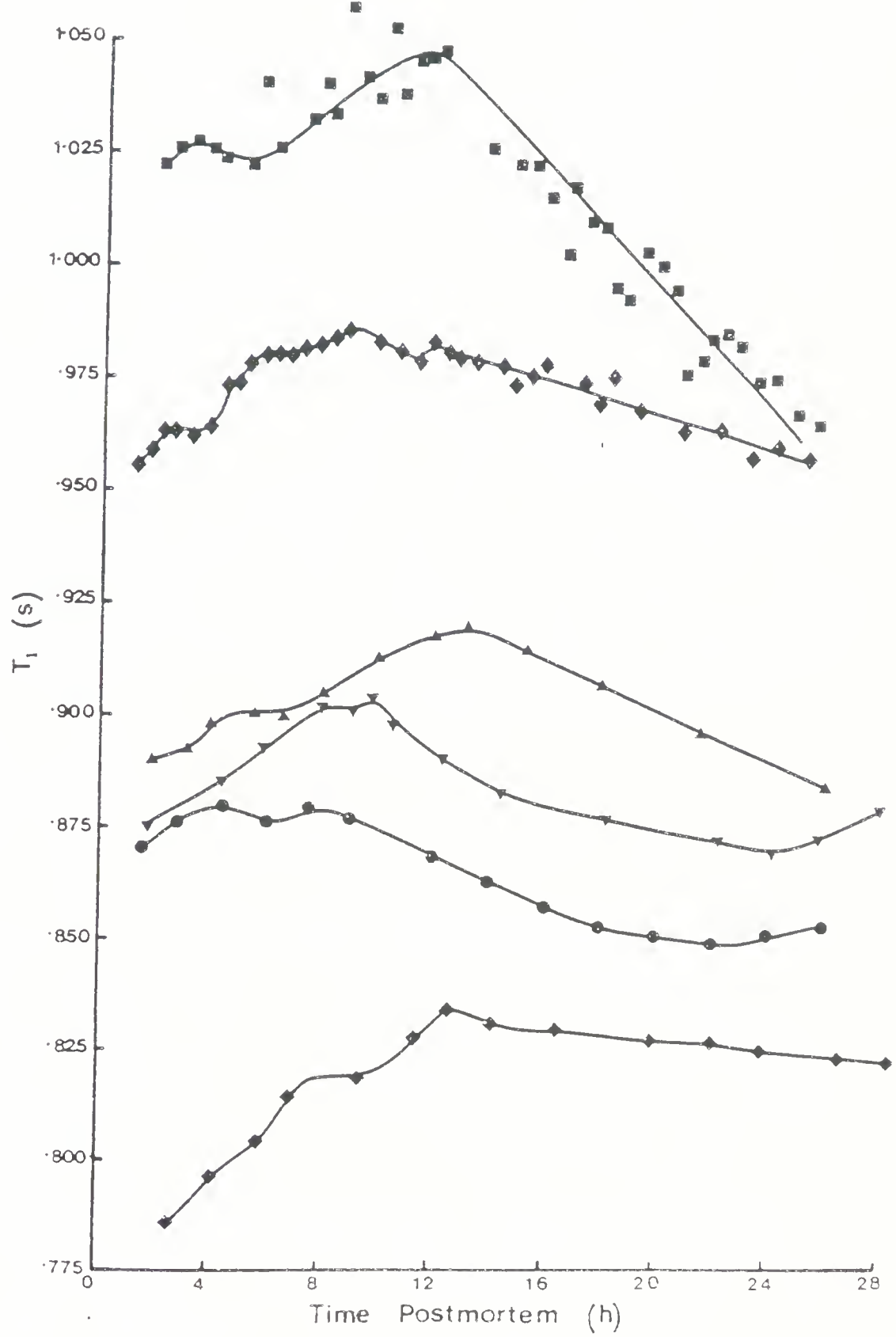
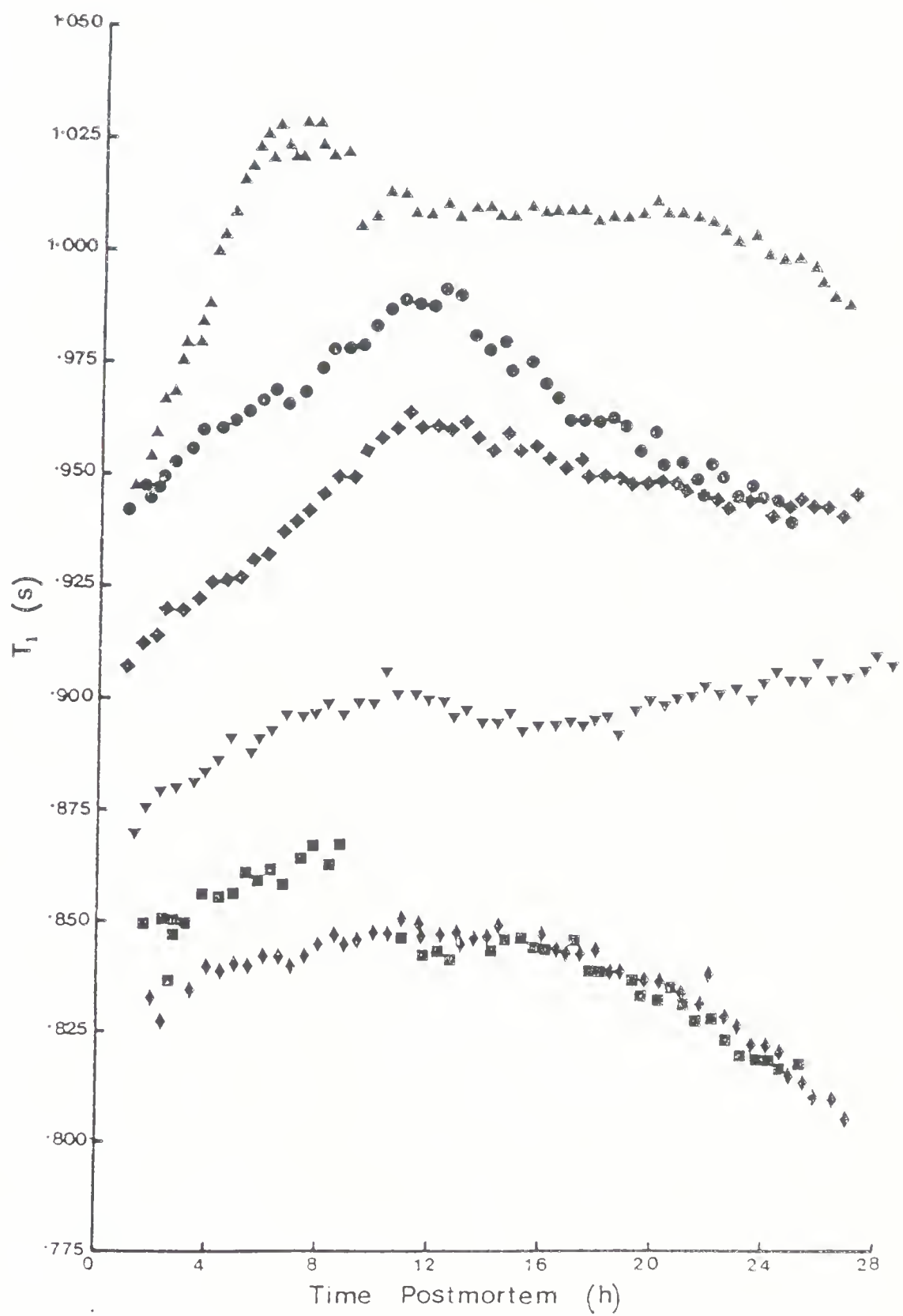


Figure III.36. NMR T<sub>1</sub> profile for carcass 13 (•-•-•), carcass 14 (▼-▼-▼), carcass 15 (▲-▲-▲), carcass 16 (◆-◆-◆), carcass 17 (■-■-■) and carcass 18 (♦-♦-♦) vs time postmortem.





significant negative correlation between the initial rise in  $T_1$ , (the difference between the peak  $T_1$  value and the  $T_1$  value upon extrapolation to zero time;  $\Delta T_1$ ) and the slope immediately following the peak. These results have been confirmed from the data plotted in Figures III.34-III.36 ( $r=-0.564$ ; d.f.=16). It was generally observed that, if  $\Delta T_1$  was large, the slope was minimal or little reduction in  $T_1$  postpeak occurred.

This correlation may relate to the state of water in prerigor and postrigor muscle as follows: An increase in  $T_1$  represents an increase in water mobility. Thus a large  $\Delta T_1$  relates to a large increase in water mobility, which is a result of an increase in the "free" compared to "bound" water fraction in the muscle. The significant negative correlation between  $\Delta T_1$  and the slope postpeak indicates that prerigor events affect the ability of the muscle to restructure the water following the extremes of rigor. If the events during rigor development contribute to a large increase in water mobility in the prerigor muscle, there is little increase in the "bound" water fraction associated with the muscle macromolecules postrigor. This explanation of the  $T_1$  data is a broad interpretation and is simplistic. In section D further evidence will be presented which suggests that  $T_1$  reflects alterations in the intrafibre water affinity. These changes in the intrafibre water affinity prerigor, postpeak and postrigor may influence changes in the  $T_1$  profile.



The rate of postmortem rigor development measured by pH fall does not correlate with  $\Delta T_1$ . The correlation coefficient relating the initial rate of pH fall to  $\Delta T_1$  is small ( $r=0.399$ ; d.f.=14). These results imply that a pH fall cannot be used to predict alterations in the state of the water of a carcass. Additional factors must be involved leading to an alteration in the water holding capacity of the myofibrillar proteins or to a physical compartmentalization of the water lost by the muscle proteins during rigor development. Mathur-De Vré (1979) in her review cited references which suggested that both compartmentalization and differences in hydration of the proteins were considered to contribute to the  $T_1$ .

Another obvious characteristic of the data is the variation in initial  $T_1$ . The initial  $T_1$  seems to have no relationship to the type of profile which follows. For example, carcasses 2 and 10 are similar in change in the  $T_1$  prerigor and the slope postpeak, but the initial  $T_1$ 's are very different. There was no significant correlation found between the initial  $T_1$  and initial pH ( $r=0.229$ ; d.f.=14) or the initial ATP concentration ( $r=-0.528$ ; d.f.=10) [Carcass number 10 was omitted from the calculation of correlation coefficient between initial  $T_1$  and the initial ATP concentration since the first ATP sample was not measured until 2.5 hr in a carcass where the initial ATP levels were falling.] Since the early postmortem pH and ATP are not major factors contributing to the initial  $T_1$ , other factors



must be involved.

The moisture contents of carcasses 6-18 are presented in Table III.7. The correlation between the initial  $T_1$  and the percent moisture was significant ( $r=0.576$ ; d.f.=11). Thus the position of the  $T_1$  profile for a given carcass is determined primarily by the water content of the fibre. The positive correlation is understandable since a higher moisture content in the muscle would lead to a higher free water content and thus a higher measured  $T_1$ .

The initial ATP concentration may influence the initial  $T_1$  value. This supposition is supported by several observations. First, the correlation between the initial ATP concentration and the initial  $T_1$  is nearly significant ( $r=-0.528$ ; d.f.=10). The negative sign of the correlation coefficient is expected in the light of the report by Hamm (1960) that ATP is a major factor contributing to the water holding capacity of the muscle proteins. Thus, when ATP concentrations are high, the "free" water content of the muscle could be less, resulting in a lower  $T_1$ . A second consideration is the significant correlation between the peak  $T_1$  and the moisture content. The correlation coefficient ( $r=0.680$ ; d.f.=11) is nearly significant at the 0.01 probability level. At this time the ATP is very low and thus the moisture content may contribute more to the  $T_1$  value than in the early postmortem muscle. Although factors such as ATP concentrations and the state of myofibrillar proteins may modify the  $T_1$  values, the major factor



Table III.7 Percent moisture and initial and peak T<sub>i</sub>

Carcass Number	Initial T <sub>i</sub>	Peak T <sub>i</sub>	% Moisture
6	.908	.927	79.0±.6
7	.863	.880	79.6±.1
8	.866	.904	79.5±.2
9	.885	.920	76.8±.4
10	.770	.834	77.2±.8
11	1.01	1.05	79.5±.6
12	.950	.986	78.0±.6
13	.940	.992	79.6±.6
14	.867	.900	77.8±.5
15	.925	1.03	80.8±.9
16	.902	.964	78.8±.7
17	.842	.868	76.2±.1
18	.830	.850	75.2±.5



contributing to  $T_1$  in the muscle is the moisture content. This observation (that  $T_1$  is primarily a measure of the muscle water content) has been supported from the measurement of  $T_1$  in the ST from 32 carcasses (obtained from the Department of Animal Science) aged 7 days. The correlation coefficient ( $r=0.514$ ; d.f.=30) relating  $T_1$  and moisture was highly significant. A measure of the  $T_1$  of the ST from 10 carcasses (obtained from a supermarket) aged 14 days was significant ( $r=0.735$ ; d.f.=8). Inch *et al.* (1974), in their examination of neoplastic and nonneoplastic tissues from mice and humans, also found that  $T_1$  values are related directly to the water content.

The importance of the  $T_1$  measurements in this study is not the determination of the initial  $T_1$ , or peak  $T_1$ , for a carcass. The major useful function of the  $T_1$  determinations is to provide a sensitive measure of the effects of the biochemical and physiological changes occurring in the muscle during rigor development on the muscle water. Thus an interpretation of the small changes in the  $T_1$  values prerigor and postrigor may provide an insight into the factors immobilizing water in meat.

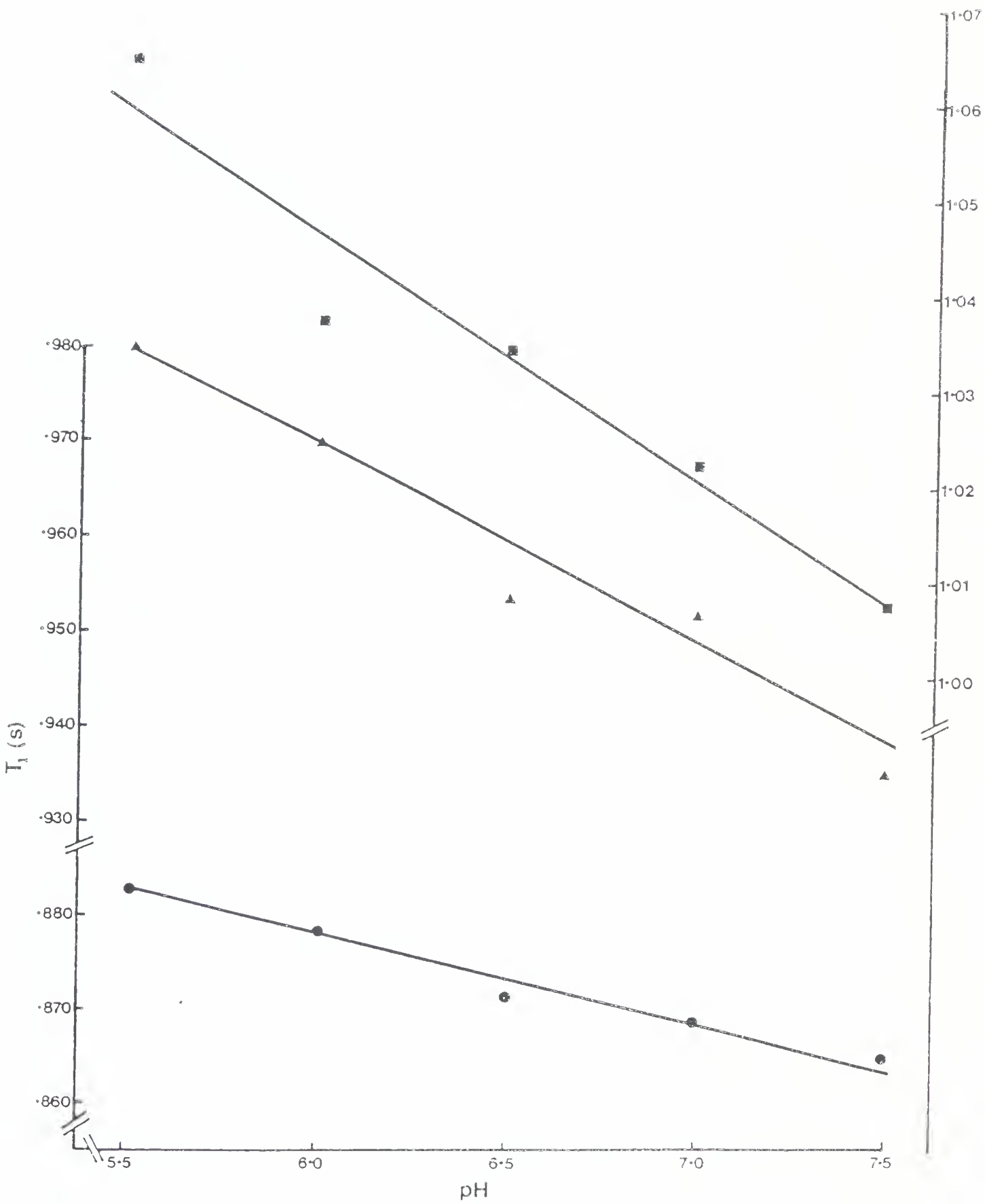
During the development of rigor several changes influencing the water holding properties of the muscle are occurring simultaneously. The pH falls, resulting in a reduction in the charge on the proteins due to the approach of their isoelectric points. Hamm (1974) has shown that near the isoelectric point a greater number of intermolecular



salt bridges develop which tighten the interfilamental structure of the muscle. This can occur because the like-charges causing repulsion between the thick and thin filaments have been lost. These factors (tightening of the muscle structure and reduction in total charge) reduce the number of sites available to order the water in the muscle. A second factor that is changing is the ATP concentration. Hamm (1960) considered two-thirds of the loss in water holding capacity to be due to the disappearance of ATP and one-third of the postmortem loss to be due to the fall in pH. A third factor is changes in the ion distribution in the muscle. Arnold *et al.* (1956) were the first to discuss the affects of ions on the properties of postmortem muscle. They observed an improvement in water holding capacity and tenderness when there was an increase in the extractable  $\text{Ca}^{2+}$  ions bound to the muscle proteins. They interpreted their results as  $\text{Ca}^{2+}$  being gradually replaced by monovalent cations which increased the charge on the muscle proteins and increased their hydration. Changes in the ion distribution have been confirmed by many authors (Asghar and Yeates, 1978; Webb *et al.*, 1967; El Badawi *et al.*, 1964; Swift and Berman, 1959).

In order to separate the contribution of each of these factors on water in the muscle, model systems of myofibrils were prepared in which each of the factors could be varied. Figure III.37 illustrates the affect of pH on  $T_1$  of myofibrils at different moisture contents. When the pH is

Figure III.37. Plot of NMR  $T_1$  vs pH of myofibrils at 82% moisture (■-■-■), 80% moisture (▲-▲-▲) and 78% moisture (●-●-●).



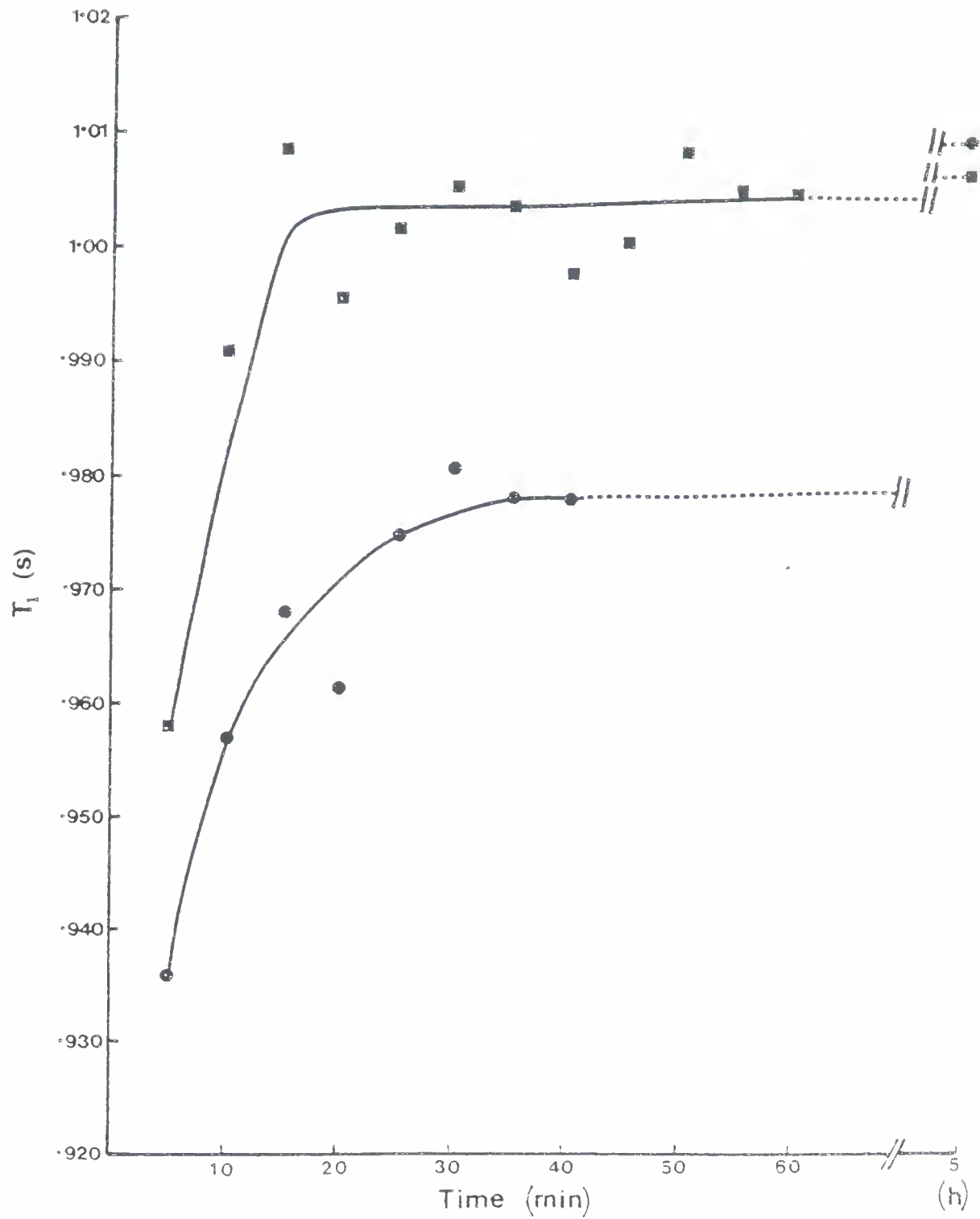


lowered, the  $T_1$  increases. This is to be expected since the reduction of the charge on the myofibrillar proteins would increase the "free" water and thus increase  $T_1$ . Clearly, pH fall would contribute to  $\Delta T_1$  in the  $T_1$  profiles for the muscle samples in Figures III.34-III.36. The moisture content of the muscle will influence the effect pH has on the "free" water content. If the percent water is high, the pH effect is greater on  $T_1$  than at lower water contents. For example, the slope for 82% moisture myofibrils is -0.02 sec ( $T_1$ )/pH unit compared to -0.0075 sec ( $T_1$ )/pH unit for 78% moisture myofibrils. Thus differences in the moisture content between muscle samples could affect  $\Delta T_1$  for the carcasses studied. It must not be a major factor since the correlation coefficient between the percentage of water and  $\Delta T_1$  was nonsignificant ( $r=0.500$ ; d.f.=11).

The affect of ATP on  $T_1$  is illustrated in Figure III.38. When the ATP was first added to the buffered myofibrils, there was a dramatic drop in the  $T_1$  measured. The myofibrils in the presence of EGTA (ethyleneglycol bis[ $\beta$ -amino-ethylether]-N,N'-tetraacetic acid) and ATP rapidly regained  $T_1$  values near that of the control. The myofibrils in the presence of  $Ca^{2+}$  maintained a suppressed  $T_1$  for a prolonged period. This affect was reversed within 5 hr of the ATP addition since the  $T_1$  measured then had regained values near the  $Ca^{2+}$  control without ATP.

An explanation for the above results involves several factors. As the dry ATP is added to the myofibril there is

Figure III.38. Profile of NMR T<sub>1</sub> vs incubation time of myofibrils in the presence of ATP and 500  $\mu\text{M}$  EGTA (■-■-■) or 500  $\mu\text{M}$  Ca<sup>2+</sup> (●-●-●). The T<sub>1</sub> value for 500  $\mu\text{M}$  EGTA without ATP added was 1.025 s and for 500  $\mu\text{M}$  Ca<sup>2+</sup> without ATP was 1.029 s.





time (reflected by the EGTA/ATP curve) needed for the contents of the NMR tube to come to equilibrium. At this time of equilibrium the EGTA/ATP containing tube has values near that of the control. ATP is unable to remove EGTA from positively charged protein binding sites, and for this reason charges on the myofibrillar proteins may not be exposed. In the presence of EGTA the myofibrillar ATPase would also be blocked (McCubbin and Kay, 1980). This would keep the  $T_1$  values high. The combination of  $\text{Ca}^{2+}$  and ATP, resulting in a low  $T_1$ , may be due to the activation of the myofibrillar ATPase. Once the  $\text{Ca}^{2+}$  binds with the troponin complex the ATPase would be activated and more of the "free water" could be bound and the  $T_1$  would fall. A second reason was proposed by Hamm (1960) when he showed that ATP has the ability to complex  $\text{Ca}^{2+}$ . If the ATP could remove the  $\text{Ca}^{2+}$  associated with the charges on the proteins, more charges would be exposed, allowing more water to be "bound" and lead to a lower measured  $T_1$ . After a period of time the ATP will be totally hydrolysed and will no longer be able to either bind the  $\text{Ca}^{2+}$  or dissociate the actin-myosin bonds. The  $\text{Ca}^{2+}$  that had been bound by ATP would be free to bind to the protein and the rigor bonds would be irreversibly reformed. This would lead to an increase in the mole fraction of "free water" and a return of the  $T_1$  values to near the control values.

The implication of ATP binding  $\text{Ca}^{2+}$  and thus affecting water holding capacity has now been questioned by Hamm's

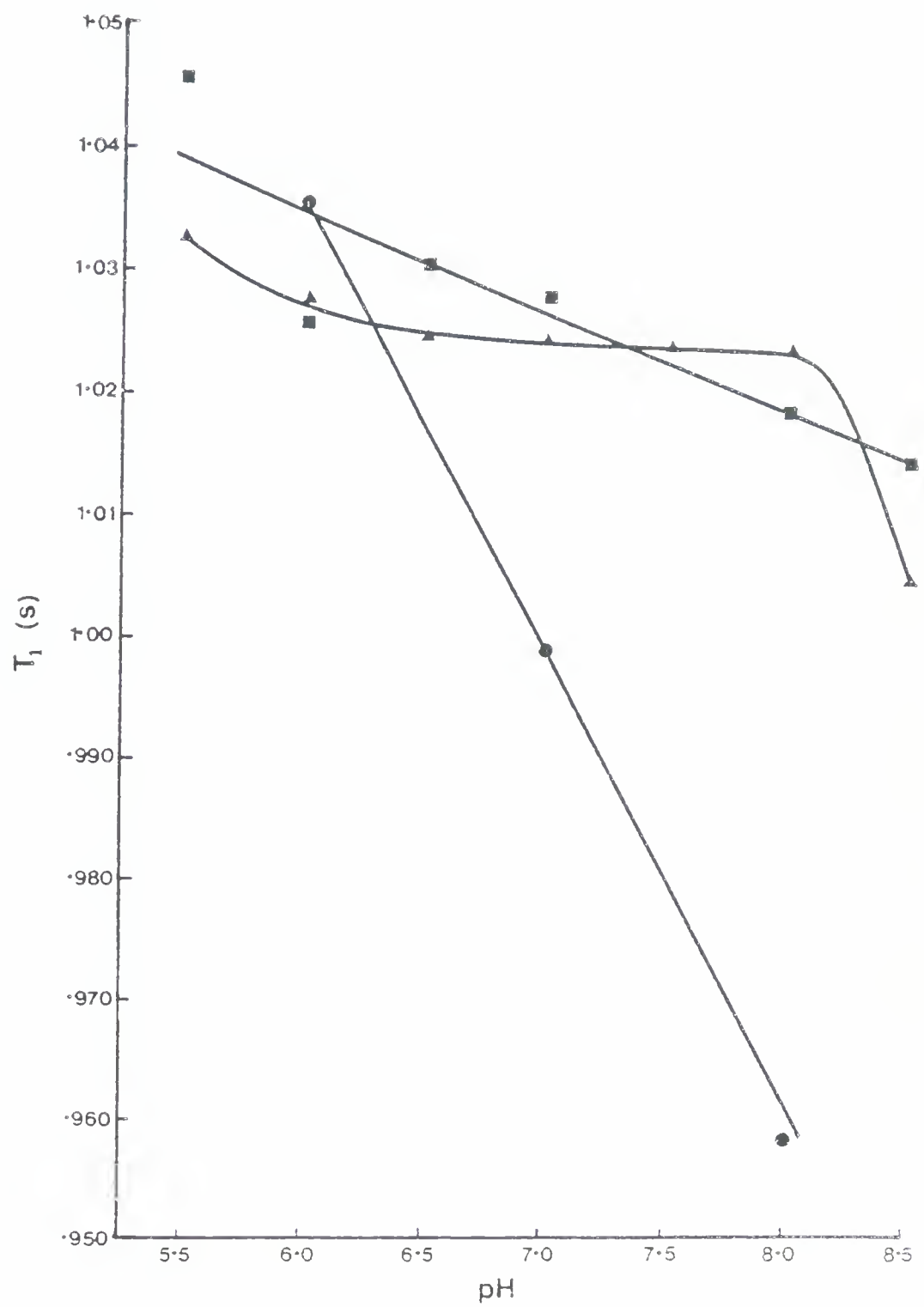


group. Honikel *et al.* (1981) have examined the affect of pH and ATP concentration on the water holding capacity of beef entering rigor and have suggested that the strong fall is due to the development of rigor mortis initiated by the depletion of ATP and not the postmortem hydrolysis of ATP itself.

In this study it is not known whether it is the myofibrillar ATPase or the binding of the  $\text{Ca}^{2+}$  by ATP that results in the lowered  $T_1$ . Nor is it known which mechanism is the more important in contributing to these results. The addition of ATP alone has contributed to a drop in the  $T_1$  of about 0.020 sec. The myofibrils in the absence of EGTA or  $\text{Ca}^{2+}$  have a  $T_1$  of nearly 1 sec at pH 7.0 (the pH of this assay). If the addition of the ATP was considered to lower the  $T_1$  by 0.020 sec, the  $T_1$  in the absence of  $\text{Ca}^{2+}$  would be about 0.980, which is about the same value obtained when the tube containing  $\text{Ca}^{2+}$  and ATP had equilibrated. Thus it would appear that binding of  $\text{Ca}^{2+}$  by ATP contributing to a reduced  $T_1$ , cannot be ruled out.

Figure III.39 presents the results obtained when Ca and EGTA are added to the myofibrils without ATP. In both instances  $\text{Ca}^{2+}$  and EGTA interfere with the immobilization of water by the myofibrillar proteins, particularly at high pH. At pH 6.0 the differences between the  $\text{Ca}^{2+}$  or EGTA and pH effects upon  $T_1$  of the hydrated myofibrils become minimal. This may be due to the protonation of some of the carboxyl groups. McCubbin and Kay (1980) have reported that pK values

Figure III.39. Plot of NMR T<sub>1</sub> vs pH for myofibrils in buffer (●-●-●), buffer plus EGTA (▲-▲-▲) and buffer plus Ca<sup>2+</sup> (■-■-■).





as high as 6 are not unusual, especially if the carboxyl groups are adjacent to other carboxylates and if the environment is somewhat hydrophobic. The protonation of these carboxyl groups may interfere with  $\text{Ca}^{2+}$  binding and also that of water, resulting in similar  $T_1$  values. The affect of EGTA on  $T_1$  is surprising but may also be explained by an alteration of the charge on the proteins. The ionized carboxyls of EGTA may be attracted to the charged amino groups of the myofibrillar proteins thus interfering with the ability of the myofibrils to bind water at these sites. The major implication of these results is that any substance which interferes with the charge on the myofibrillar proteins reduces the hydration of the myofibrillar proteins and thus increases  $T_1$ . This appears most evident when the pH is high since the addition of ions will associate with the charge, reduce the water that can bind and increase the  $T_1$  values. These results would imply that, as the muscle nears a low ultimate pH, the ion effects would become less important in determining the  $T_1$  values measured.

One of the conclusions reached by Currie and Wolfe (1980) is that the intrafibre water may be an important factor involved in some of the mechanical properties of muscle and thus tenderness. Since  $T_1$  is a measure of the water in the carcass, the relationship between  $T_1$  and tenderness was assessed. Tables III.8 and III.9 present the data obtained from the analysis of 32 carcasses (ultimate pH range 5.60-6.85) and the correlation coefficients of all the



Table III.8 Data obtained for parameters tested for 32 carcasses

Carcass Number	T <sub>1</sub> Raw	T <sub>1</sub> Cooked	H <sub>2</sub> O Raw	H <sub>2</sub> O Cooked	Juici- ness	Tender- ness	OTMS	pH
1	.912	.617	76.6	73.5	4.2	5.0	.131	6.50
2	.952	.693	76.0	70.9	4.1	5.4	.126	6.74
3	.970	.670	76.7	73.9	4.1	4.7	.107	6.50
4	.992	.718	74.3	75.0	4.0	6.0	.092	6.78
5	.982	.699	76.4	71.0	4.3	5.9	.111	6.78
6	.946	.750	76.5	73.5	4.2	6.3	.116	6.85
7	.982	.676	75.8	75.0	4.6	5.6	.103	6.80
8	.969	.727	75.9	69.2	4.2	5.3	.105	6.35
9	.947	.698	76.3	70.4	4.2	4.6	.150	6.49
10	.973	.700	76.0	73.8	4.3	4.8	.138	6.36
11	.902	.716	76.2	73.9	4.4	5.1	.128	6.46
12	.889	.730	74.6	74.4	4.1	5.2	.120	6.46
13	.914	.716	75.6	72.6	4.2	5.1	.121	6.23
14	.906	.796	76.8	71.7	4.2	5.3	.172	6.36
15	.839	.722	73.6	68.3	4.6	5.6	.120	6.38
16	.975	.712	77.0	74.9	4.4	6.1	.108	6.58
17	.838	.626	73.6	72.3	4.7	5.3	.132	5.74
18	.903	.738	74.0	71.8	3.4	4.1	.152	5.75
19	.696	.633	73.7	69.6	4.3	5.0	.138	5.76
20	.937	.682	75.7	70.3	4.1	4.8	.139	6.36
21	.866	.656	74.5	70.5	4.3	4.6	.162	5.73
22	.813	.661	75.0	66.8	4.4	4.6	.182	5.68
23	.836	.601	74.3	67.4	4.3	4.3	.189	5.74
24	.907	.718	75.3	69.2	4.1	5.2	.144	6.20
25	.832	.630	77.4	71.8	4.2	4.7	.155	6.08
26	.858	.631	76.0	69.9	3.8	4.3	.140	5.60
27	.877	.621	76.6	70.9	4.6	4.4	.160	5.91
28	.874	.657	74.5	69.8	4.7	5.1	.132	5.82
29	.866	.694	75.0	71.9	4.4	4.2	.192	6.00
30	.720	.638	73.7	63.9	4.1	4.4	.146	5.62
31	.827	.606	74.5	70.7	4.0	3.9	.187	5.67
32	.809	.607	74.9	67.9	3.8	4.7	.182	5.69



Table III.9 Correlation coefficients for the parameters tested in Table III.8

	T <sub>1</sub> Raw	T <sub>1</sub> Cooked	H <sub>2</sub> O Raw	H <sub>2</sub> O Cooked	Juici- ness	Tender- ness	OTMS	pH
T <sub>1</sub> Raw	1.00	.547	.514	.654	-.017	.499	-.565	.795
T <sub>1</sub> Cooked	.547	1.00	.246	.366	-.098	.543	-.399	.601
H <sub>2</sub> O Raw	.514	.246	1.00	.312	-.105	.153	-.132	.504
H <sub>2</sub> O Cooked	.654	.366	.312	1.00	.072	.440	-.502	.616
Juici- ness	-.017	-.098	-.105	.072	1.00	.303	-.128	.126
Tender- ness	.499	.543	.153	.440	.303	1.00	-.760	.754
OTMS	-.565	-.399	-.132	-.502	-.128	-.760	1.00	-.700
pH	.795	.601	.504	.616	.126	.754	-.700	1.00



parameters tested, respectively. The  $T_1$  and the water content of both raw and cooked samples, the juiciness and tenderness of all samples as assessed by a trained taste panel, OTMS-Warner Bratzler shear data and pH were examined for each of the carcasses. Two of the most significant correlations were between pH and  $T_1$ , raw ( $r=0.795$ ; d.f.=30) and tenderness ( $r=0.754$ ; d.f.=30). These significant correlations involving pH appear to be due to the nature of the samples used in this portion of the study. Several of the high pH carcasses were dark cutters. Martin and Fredeen (1974) found a significant correlation between pH and tenderness if stressed animals were included in their study. Their recommendation for a better understanding of pH/tenderness relationships is to separate the populations. Under these circumstances, when data were not pooled over the entire pH range, they observed no significant correlations between pH and tenderness. This observation is confirmed in this study. When only ten carcasses ( $pH<5.8$ ) from the 32 carcasses sampled were tested for correlations, no significant correlations between pH and tenderness ( $r=0.300$ ; d.f.=8) and  $T_1$  ( $r=0.113$ ; d.f.=8) were observed. Thus the significant relationship between  $T_1$ , (both raw and cooked) and tenderness ( $r=0.499$  and  $0.543$ , respectively; d.f.=30) in Table III.9 is a result of the extremes in the type of samples examined. A comparison of the 10 carcasses ( $pH<5.8$ ) with respect to  $T_1$ , (both raw and cooked) and tenderness did not reveal a significant correlation.



( $r=-0.351$  and  $-0.094$ , respectively; d.f.=8). A surprising result of the work is seen in Table III.9 where there is no correlation found between juiciness and  $T_r$  (raw or cooked) or water content (raw or cooked). This was also found when just the ten carcasses were compared. The correlations between juiciness and  $T_r$  raw ( $r=-0.329$ ; d.f.=8) and  $T_c$  cooked ( $r=-0.452$ ; d.f.=8) and water content raw ( $r=-0.468$ ; d.f.=8) and water content cooked ( $r=-0.076$ ; d.f.=8) were not significant. This may be due to the narrow range in the juiciness scores (Table III.8) assigned these samples by the taste panel.

In order to confirm these observations an additional 10 samples (aged 14 days) from a local supermarket were examined. The results obtained are included in Table III.9. Both the OTMS-Warner Bratzler shear and tensile measurements were used to assess tenderness of the samples obtained. The final yield was measured in the tensile test since the initial yield is not well defined for samples of this aging period. As was discussed earlier, rupture of the fibre occurs without any deflection of the recorder pen. The initial yield is measured at a tension that is within the range of 80-90% of the final yield -- well beyond the point at which the fibre yields. The agreement between the two methods (OTMS-Warner Bratzler versus tensile measurements) of assessing tenderness was significant ( $r=0.758$ ; d.f.=8). The lack of a correlation between  $T_r$  and tenderness as measured by OTMS-Warner Bratzler ( $r=0.062$ ; d.f.=8) and



tensile final yield ( $r=0.132$ ; d.f.=8) supports the results obtained from the 10 carcasses sampled with a pH<5.8. The  $T_1$  of meat reflects the properties of the water in the whole muscle sample and it is probable that this is the reason no correlation is found. If tenderness is related to the amount of water associated with myofibrils (thus affecting their interfilamentary and intermyofibrillar distances) the water in other regions of the cell (in extracellular spaces, organelles, etc.) will not be as important to the measure of tenderness. However, the water in these locations will affect the measured  $T_1$ . From these results it appears that the comparison of  $T_1$  values from carcass to carcass reveals very little about differences in the state of the water in the carcasses, except for perhaps a prediction of water content.

### Expressed juice

The expressed juice is a measure of WHC. Offer and Trinick (1983) have indicated that the amount of water measured in WHC determinations depends upon the pressure applied. Excessive pressure ( $\approx 4 \times 10^6$  Pa) will remove most of the water of the meat, including much of the myofibrillar water. At a lower pressure ( $\approx 10^5$  Pa) the water expressed includes most of the extracellular water and part of the intracellular water situated between myofibrils. The pressure exerted on the muscle in this study using the centrifugation technique was  $4.2 \times 10^6$  Pa. This would



contribute to an excessive pressure on the muscle and may explain why the range in WHC of the postrigor meat from the 12 carcasses measured was so narrow (mean  $28.8 \pm 2.1\%$ ; Figures III.2-III.12).

Carcasses 7-10 were the only ones for which expressed juice data were measured beyond 30 hr postmortem. Carcasses 7 and 8 showed no improvement in WHC over the four day postmortem period. Carcasses 9 and 10 showed a slight improvement in WHC following the peak in the expressed juice values. The high centrifugal pressures used in this study may make it difficult to measure any improvement in WHC with aging. However, the reduction in the expressed juice values of carcasses 9 and 10 under the same experimental conditions as carcasses 7 and 8 implies a difference between carcasses in their postrigor water holding capacities. The fact that carcasses 7 and 8 were not as effective in reordering the water in the muscles and thus improving the WHC as other carcasses examined in this study is supported by the NMR T<sub>1</sub> data in Figure III.35. Carcasses 7 and 8 were two of only 3 carcasses wherein the T<sub>1</sub> values increased in the postrigor period. An increase in T<sub>1</sub> reveals a greater mobility of the water in the muscle. Thus the factors which normally lead to a restriction of water mobility must not be occurring in these carcasses. An improvement in WHC with postmortem aging has been observed by many researchers (Asghar and Yeates, 1978; Lawrie, 1979). Hamm (1960) suggested that the major reason for an improvement in the WHC with aging is due to



proteolytic processes. He stated that the splitting of only a few bonds may be all that is needed to contribute to a considerable loosening of protein structure and an increase in hydration. Lawrie (1979) indicated that changes in the ion-protein relationships (Arnold *et al.*, 1956), there being a net increase in charge through absorption of  $K^+$  and release of  $Ca^{2+}$  ions, may also contribute to an increase in WHC.

Although the centrifugal pressure used in this study was high, it was not sufficient to remove intermyofibrillar and interfilamental water from the early prerigor muscle. The expressed juice values in the carcasses studied were low for several hours before they increased to the high values measured near rigor. Almost all carcasses were found to have initial expressed juice values of 5% or less, although some carcasses rapidly lost their WHC (carcasses 7 and 8, Figure III.2). Thus the view of Offer and Trinick (1983) regarding the removal of extracellular water as well as myofibrillar water at high pressure, may well apply only to postrigor muscle. Water retention in spite of the excessive pressures used in this study reaffirms the strong water retentive properties of prerigor muscle.

The postmortem biochemical events associated with the fall in pH are related to the loss of WHC. The correlation coefficient between the time to the ultimate pH and the time when the expressed juice is maximal or near maximal is highly significant ( $r=0.796$ ;  $d.f.=10$ ).



The fact the pH fall itself contributes to the percentage of expressed juice is evident from Figures III.40-III.43. The figures contain pH hydration curves in which the area of the water pressed from the muscle vs the pH of the muscle homogenate is plotted. The larger the area of the spot, the lower the WHC of the muscle. It is seen from all the plots that the minimum hydration or the lowest WHC was between pH 5.0-5.5. These results confirm those of Hamm (1960). As the pH falls in the postmortem muscle and approaches 5.5, the WHC is reduced since the isoelectric points of the proteins are reached. These data reinforce the concept that charged sites are needed to retain the muscle water. The proteins do not have to be negatively charged, as they are above pH 5.0, to retain water. As the pH is reduced below 5.0, the hydration of the muscle proteins increases. This would be a result of the positive charge on the proteins increasing as the isoelectric point is passed.

The pH hydration curves at different times postmortem for a given carcass do not seem to show a significant shift in their position or slope. If the method would have been sensitive enough (Hamm, 1960), this may have indicated alterations in the ion relationships in the carcass. Since the method was not sensitive enough, the determination of hydration curves was abandoned.

The vertical position of the curves between carcasses does seem to reflect differences in the WHC of these carcasses. In Figure III.40 the peaks of the hydration

Figure III.40. Plot of planimeter area vs pH of meat homogenate at 90 min ( $\blacktriangle-\blacktriangle-\blacktriangle$ ), 160 min ( $\blacktriangledown-\blacktriangledown-\blacktriangledown$ ), 415 min ( $\blacksquare-\blacksquare-\blacksquare$ ) and 485 min ( $\bullet-\bullet-\bullet$ ) postmortem for carcass 7.

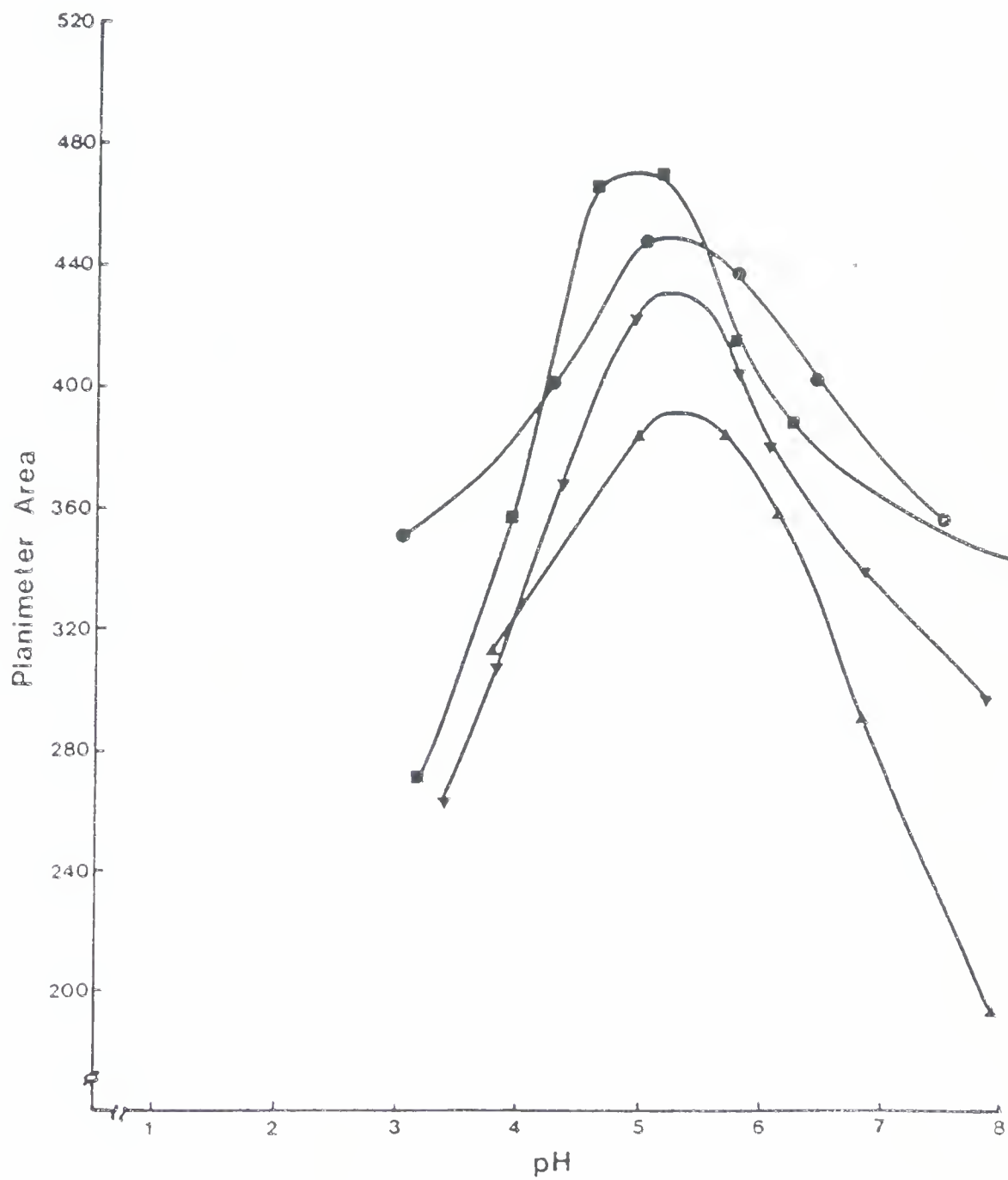


Figure III.41. Plot of planimeter area vs pH of meat homogenate at 18 min (●-●-●), 101 min (■-■-■), 195 min (▲-▲-▲) and 320 min (▼-▼-▼) postmortem for carcass 8.

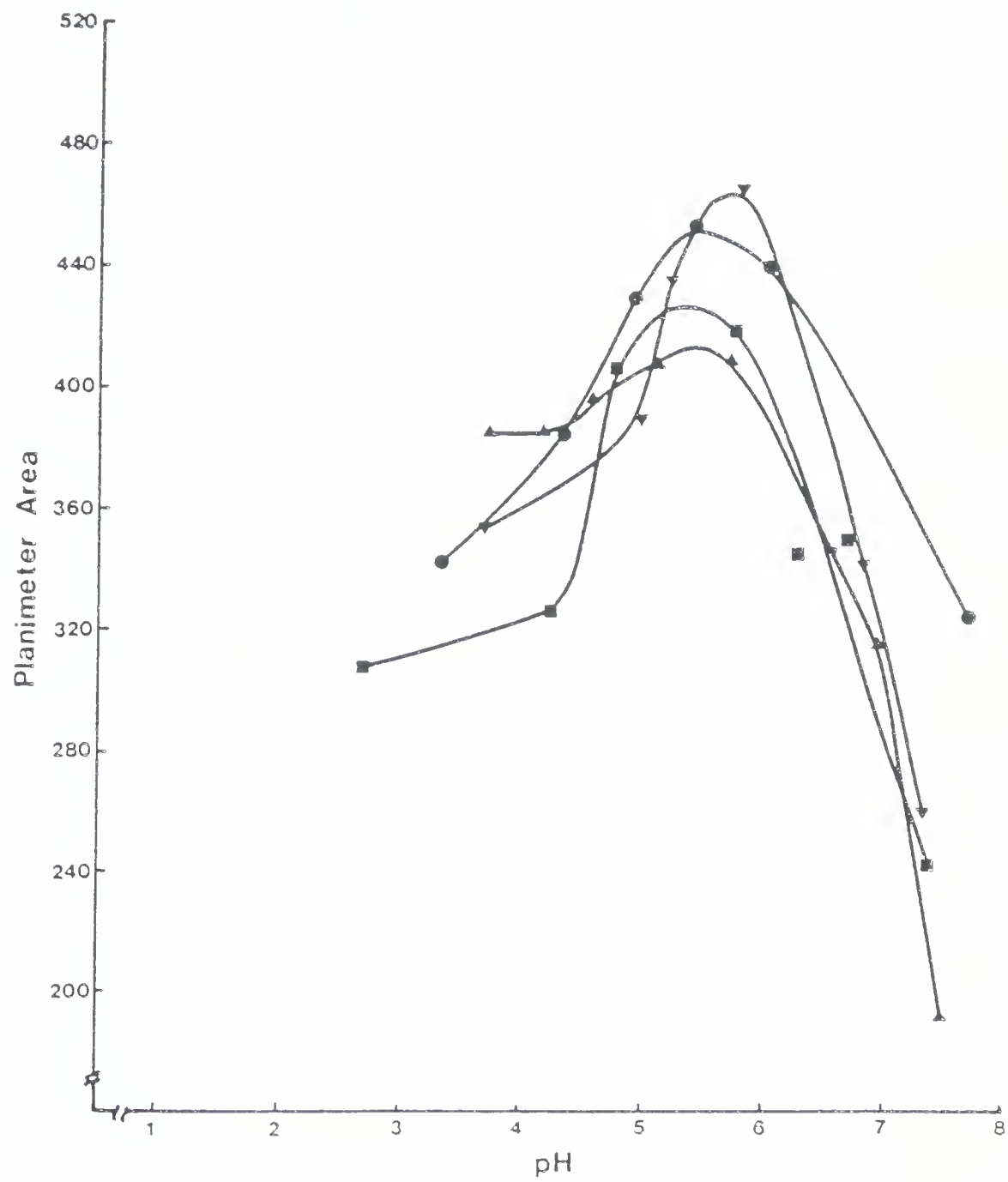


Figure III.42. Plot of planimeter area vs pH of meat homogenate at 222 min (■-■-■), 590 min (●-●-●) and 740 min (▲-▲-▲) postmortem for carcass 9.

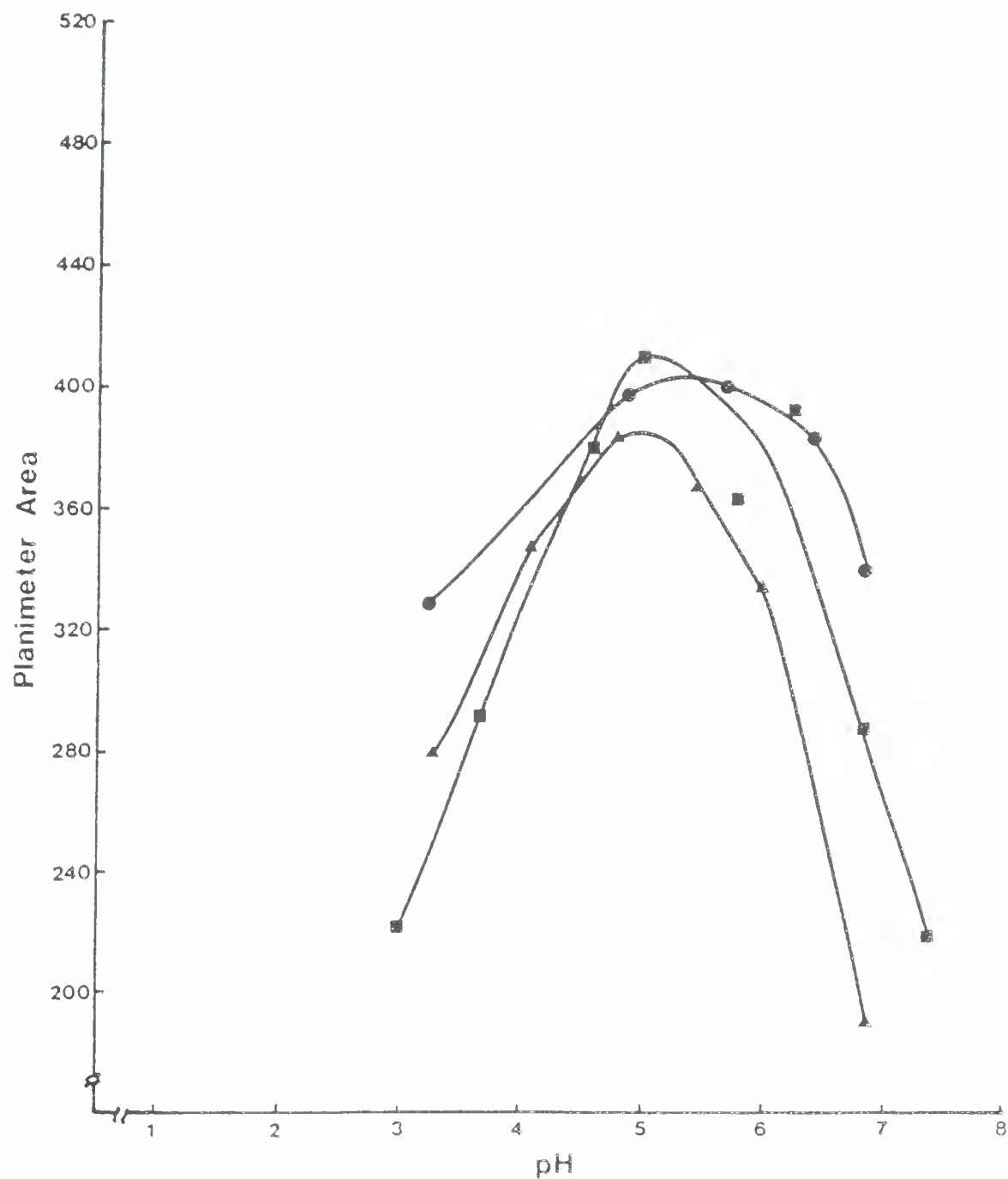
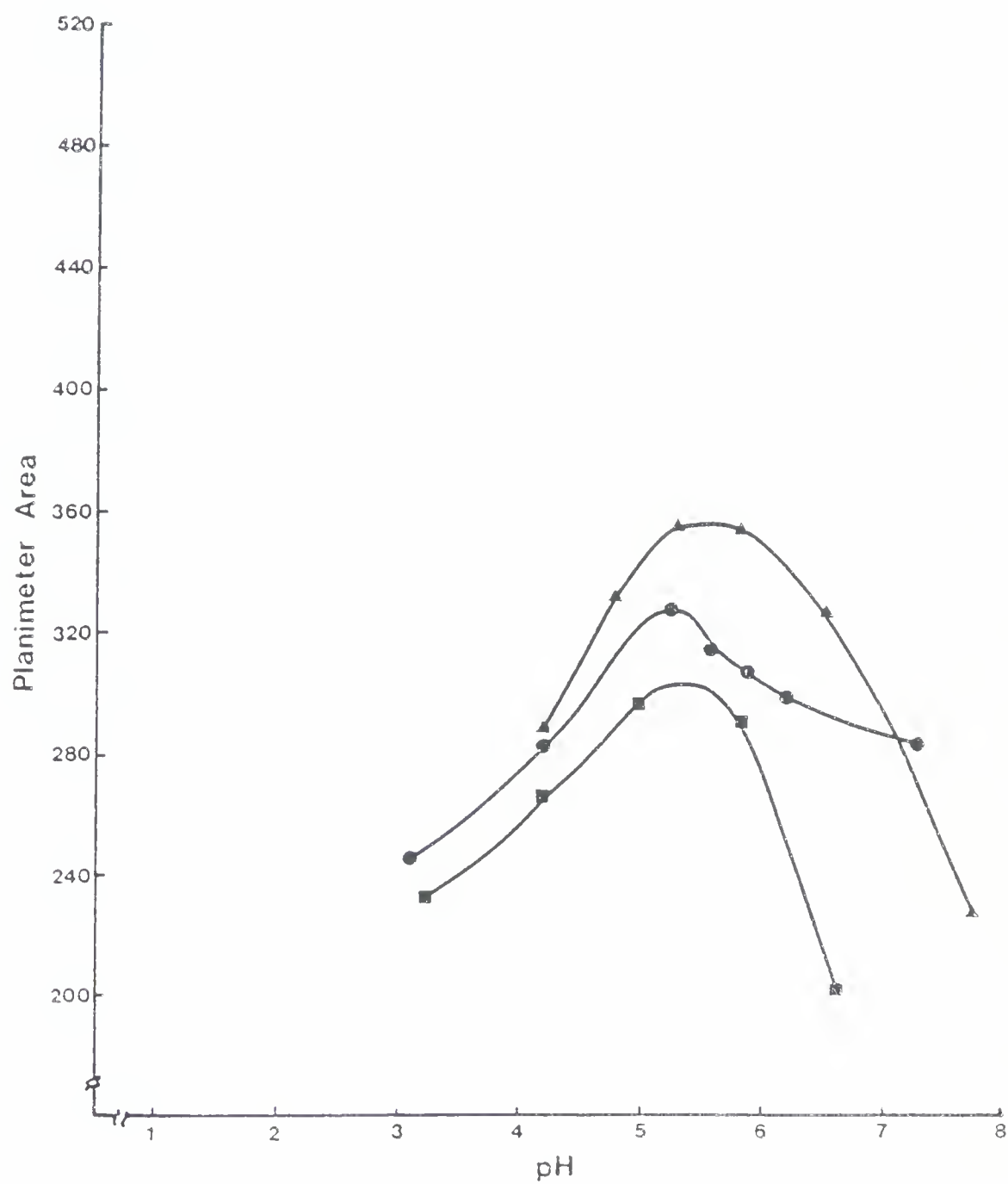


Figure III.43. Plot of planimeter area vs pH of meat homogenate at 350 min ( $\blacktriangle-\blacktriangle-\blacktriangle$ ), 690 min ( $\bullet-\bullet-\bullet$ ) and 875 min ( $\blacksquare-\blacksquare-\blacksquare$ ) postmortem for carcass 10.





curves for carcass 7 average about 420. This position is very similar for carcass 8 (Figure III.41). The expressed juice values for these same carcasses rapidly increase postmortem (Figure III.2). The relatively large areas from the pH hydration curves and the rapid increase in the expressed juice values both demonstrate a reduced WHC in the muscles of these carcasses. The results in Figures III.42 and III.43 show a lower average peak in the hydration curves at about 390 and 320, respectively. The greater prerigor WHC of these carcasses (9 and 10) is seen in Figures III.3 and III.4. The expressed juice of carcass 9 in Figure III.3 is low (about 1%) for the first 6 h. The expressed juice of carcass 10 in Figure III.4 is even lower (about 0.5%) for an even longer period of time. These observations clearly demonstrate that carcasses differ in their WHC and that the development of rigor dramatically reduces WHC.

### Swelling capacity

The swelling capacities of carcasses 8 through 18 have been plotted at various times postmortem and are presented in Figures III.44-III.54. In carcasses 9 through 18 the prerigor swelling capacity was large and then decreased as rigor maximum neared. There is an apparent correlation between the maximum isometric tension and the point at which the swelling capacity is low. The only clear exception to this observation was carcass 18 where the swelling capacity was in the vicinity of 35% when the maximum isometric

Figure III.44. Carcass 15. Plot of swelling capacity (●-●-●) vs time postmortem; the standard deviation is 7-16% (ave. 11%) of the mean. Plot of ECS dw (■-■-■) vs time postmortem; the standard deviation is 9-24% (ave. 15%) of the mean. Plot of ECS app (▲-▲-▲) vs time postmortem; the standard deviation is 11-40% (ave. 30%) of the mean. The symbol (▽) represents the time postmortem of maximum isometric tension.

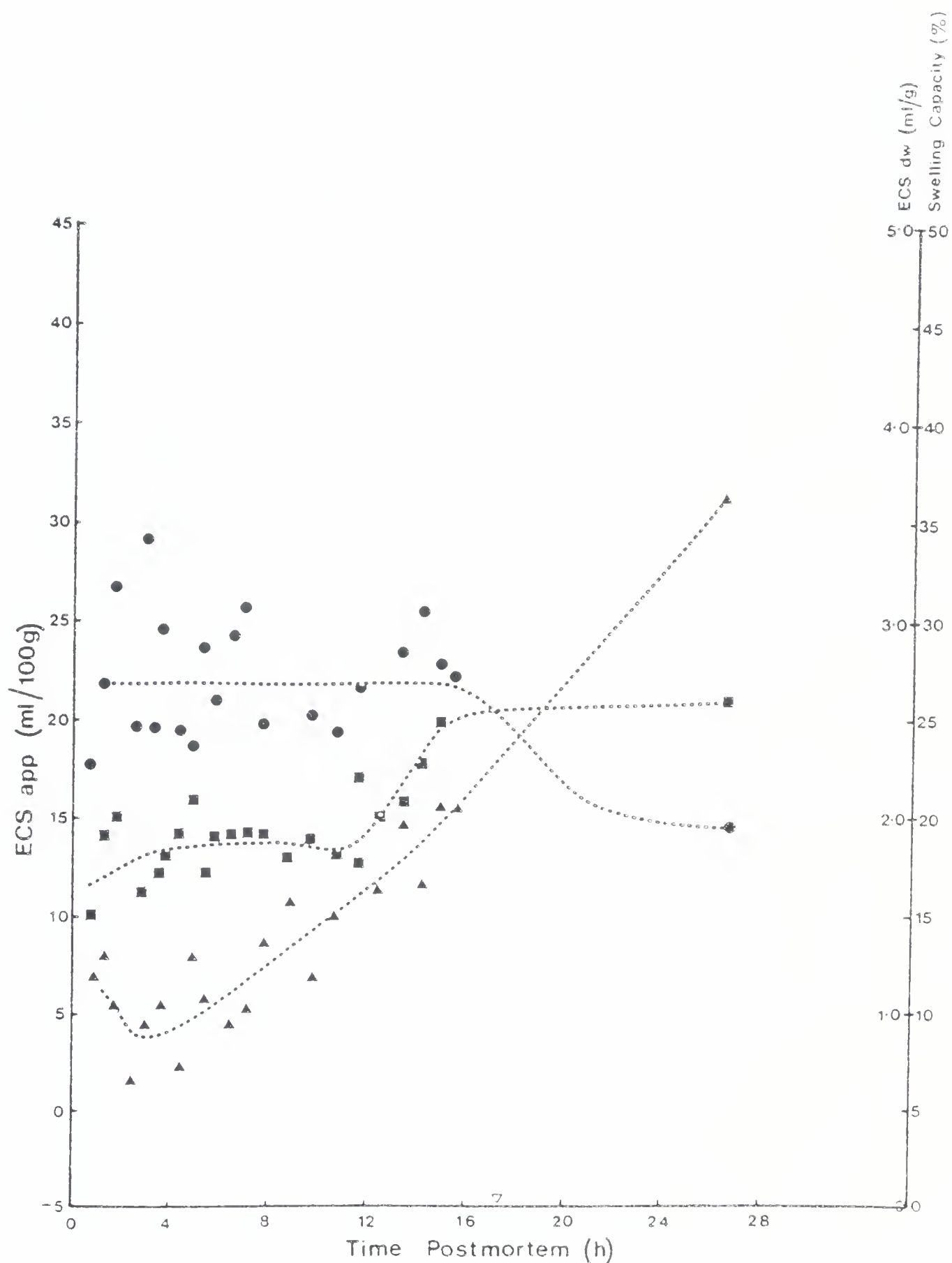


Figure III.45. Carcass 10. Plot of swelling capacity (●-●-●) vs time postmortem; the standard deviation is 5-15% (ave. 10%) of the mean. Plot of ECS dw (■-■-■) vs time postmortem; the standard deviation is 2-20% (ave. 10%) of the mean. Plot of ECS app (▲-▲-▲) vs time postmortem; the standard deviation is 8-25% (ave. 18%) of the mean. The symbol (▽) represents the time postmortem of maximum isometric tension.

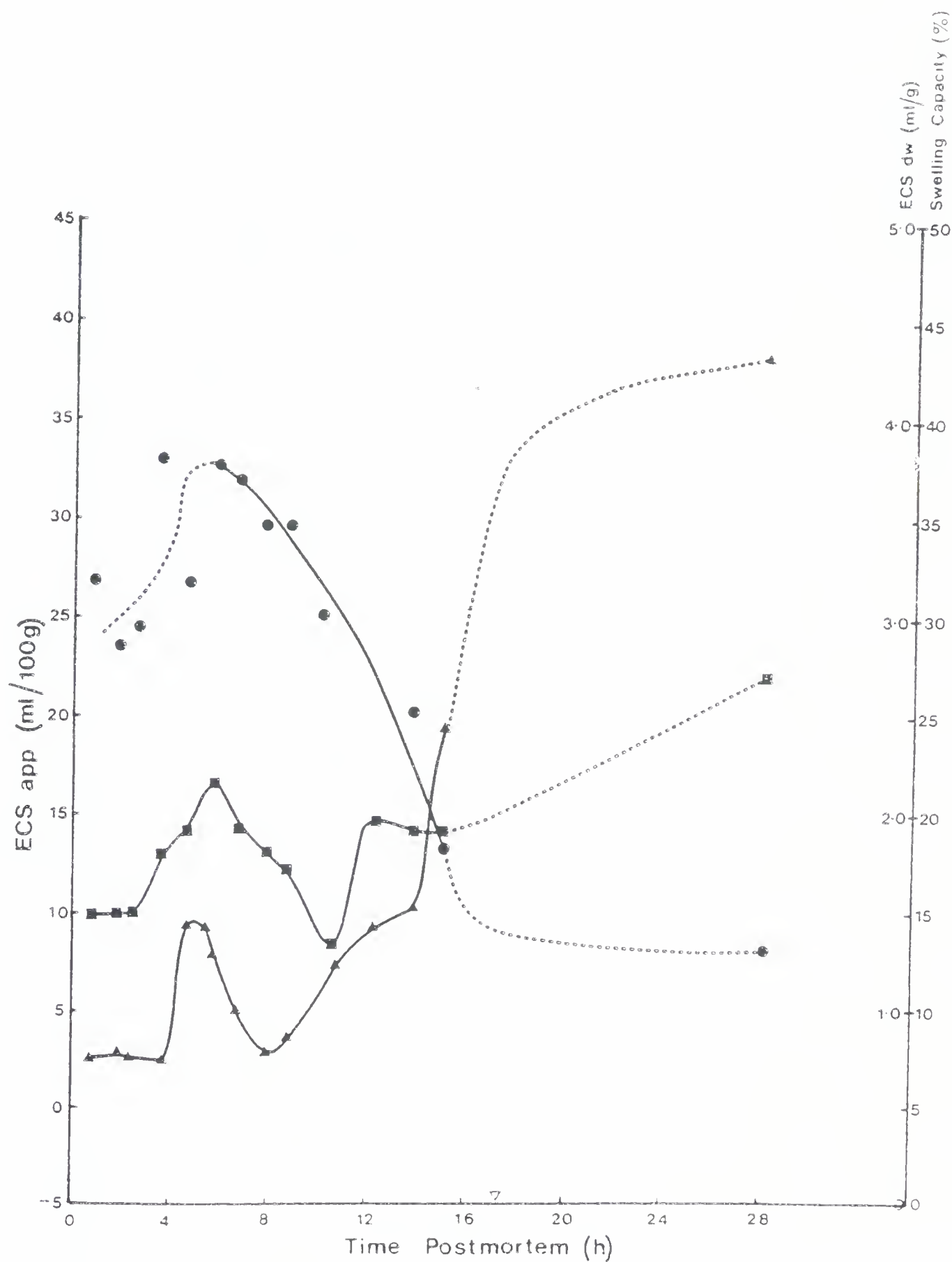


Figure III.46. Carcass 16. Plot of swelling capacity (•-•-•) vs time postmortem; the standard deviation is 3-25% (ave. 12%) of the mean. Plot of ECS dw (■-■-■) vs time postmortem; the standard deviation is 2-22% (ave. 11%) of the mean. Plot of ECS app (▲-▲-▲) vs time postmortem; the standard deviation is 13-45% (ave. 26%) of the mean. The symbol ( $\nabla$ ) represents the time postmortem of maximum isometric tension.

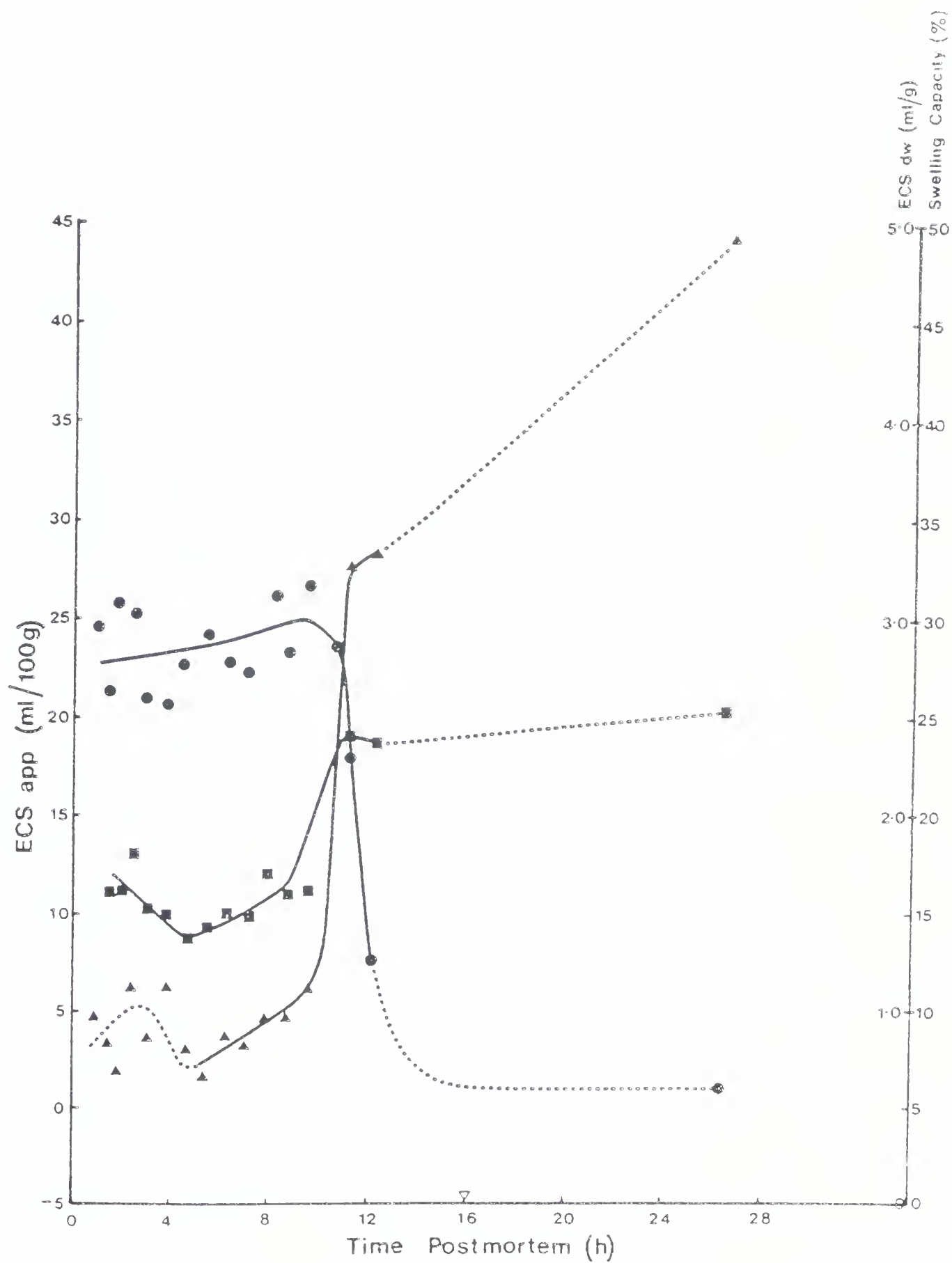


Figure III.47. Carcass 13. Plot of swelling capacity (•-•-•) vs time postmortem; the standard deviation is 2-25% (ave. 12%) of the mean. Plot of ECS dw (■-■-■) vs time postmortem; the standard deviation is 4-20% (ave. 10%) of the mean. Plot of ECS app (▲-▲-▲) vs time postmortem; the standard deviation is 15-60% (ave. 38%) of the mean. The symbol ( $\nabla$ ) represents the time postmortem of maximum isometric tension.

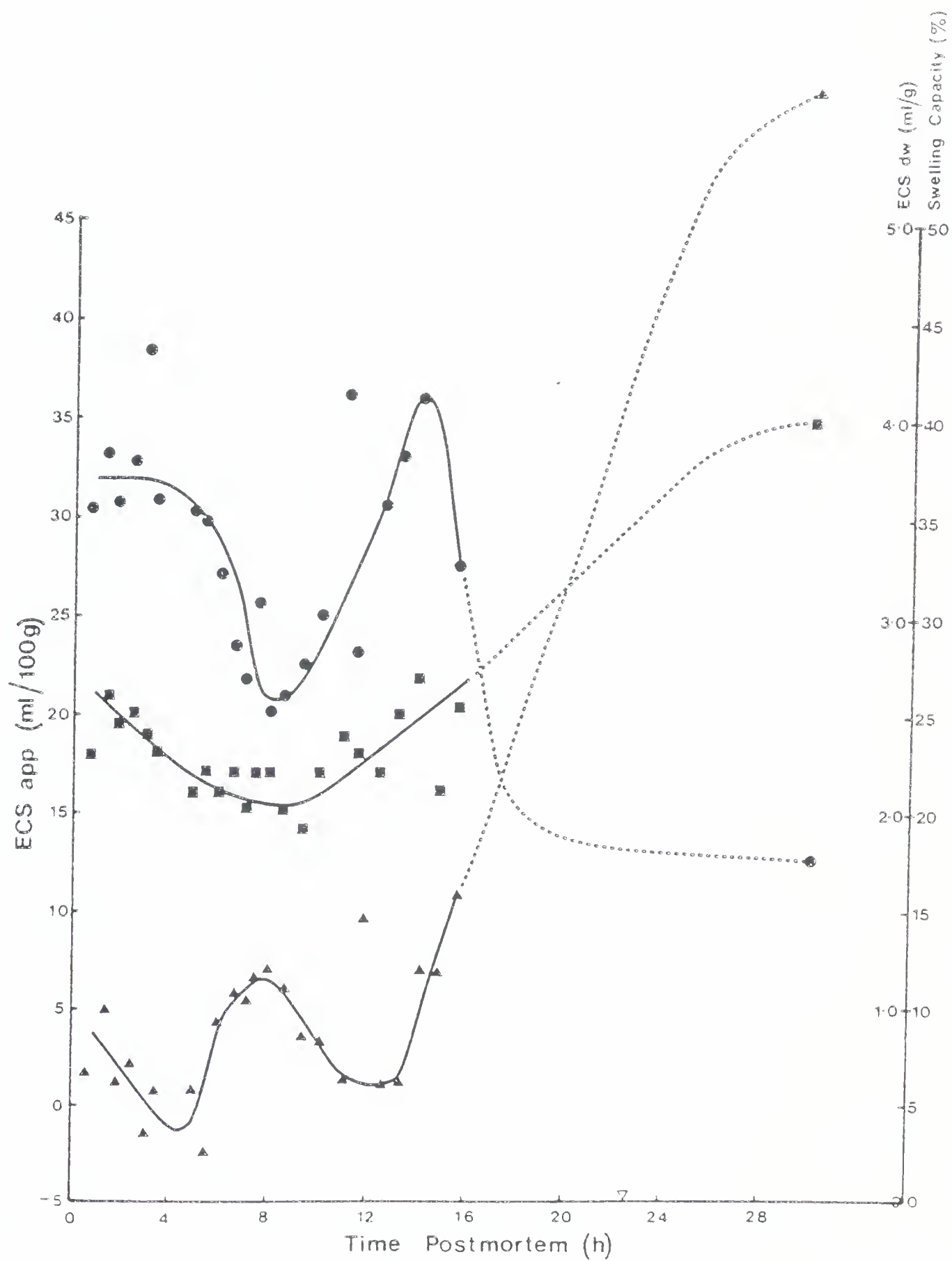


Figure III.48. Carcass 11. Plot of swelling capacity (•-•-•) vs time postmortem; the standard deviation is 2-19% (ave. 10%) of the mean. Plot of ECS dw (■-■-■) vs time postmortem; the standard deviation is 1-20% (ave. 10%) of the mean. Plot of ECS app (▲-▲-▲) vs time postmortem; the standard deviation is 1-42% (ave. 22%) of the mean. The symbol (▽) represents the time postmortem of maximum isometric tension.

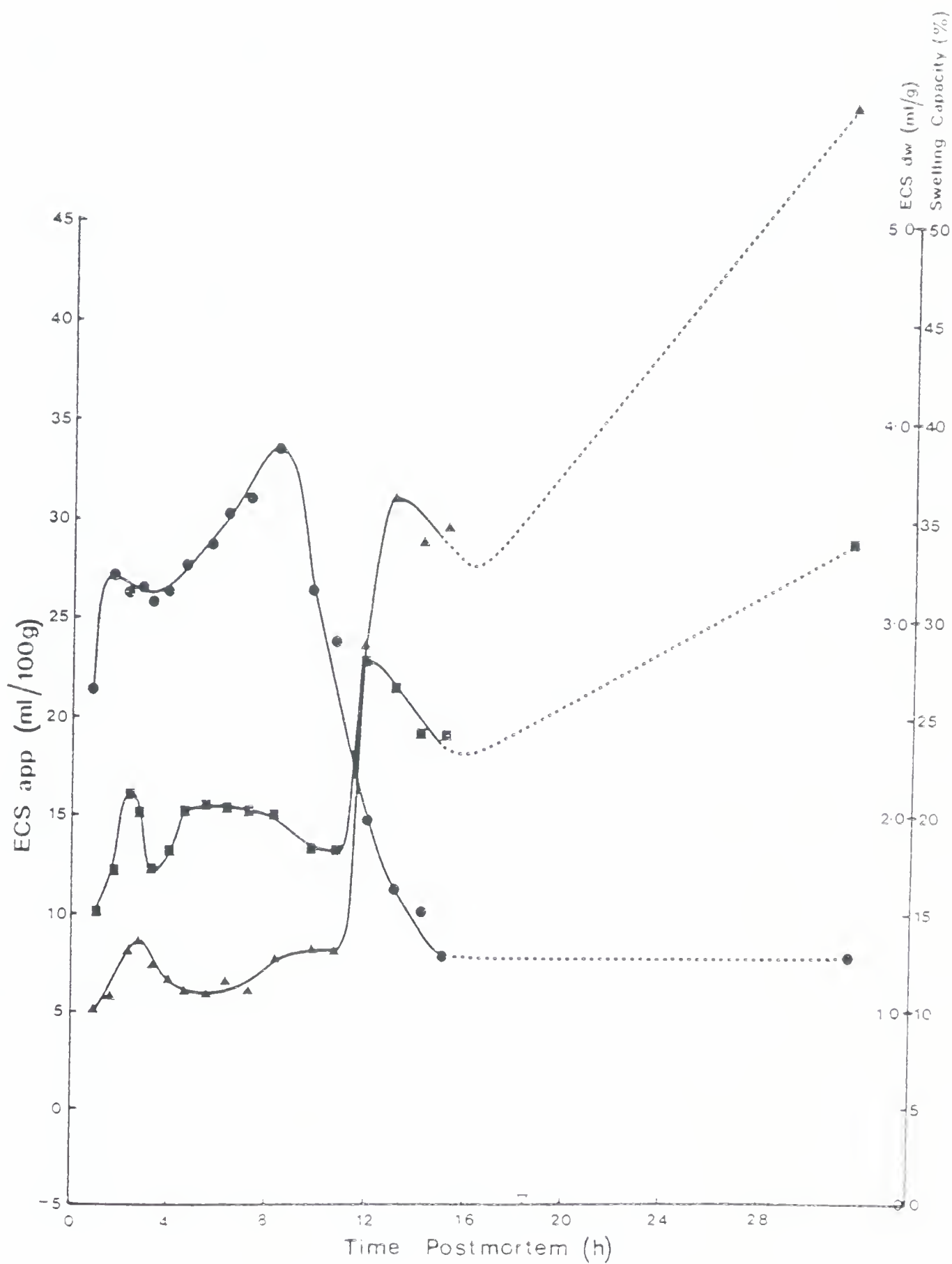


Figure III.49. Carcass 14. Plot of swelling capacity (•-•-•) vs time postmortem; the standard deviation is 3-16% (ave. 9%) of the mean. Plot of ECS dw (■-■-■) vs time postmortem; the standard deviation is 3-16% (ave. 11%) of the mean. Plot of ECS app (▲-▲-▲) vs time postmortem; the standard deviation is 3-40% (ave. 14%) of the mean. The symbol ( $\nabla$ ) represents the time postmortem of maximum isometric tension.

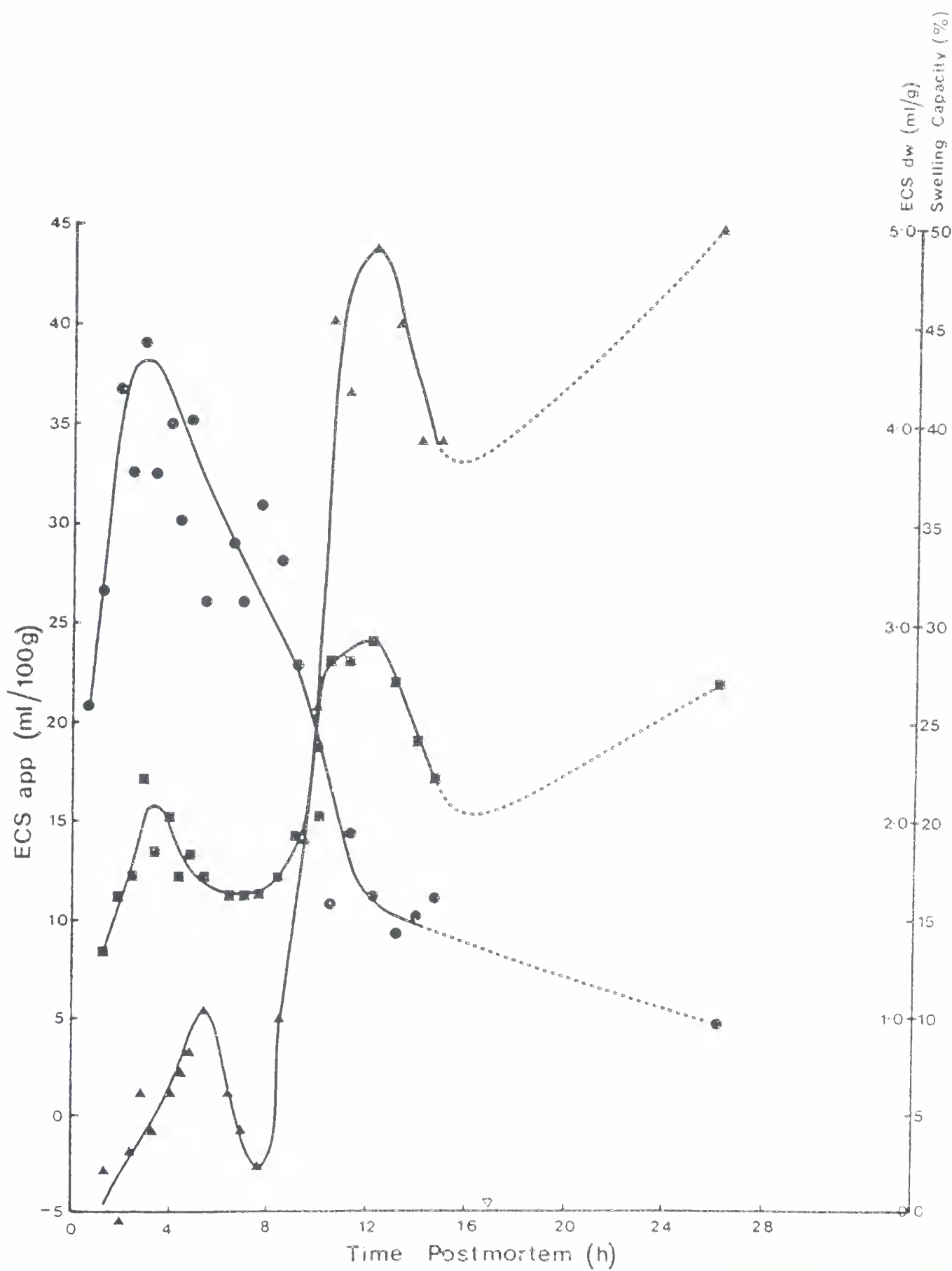


Figure III.50. Carcass 12. Plot of swelling capacity (•-•-•) vs time postmortem; the standard deviation is 2-20% (ave. 12%) of the mean. Plot of ECS dw (■-■-■) vs time postmortem; the standard deviation is 6-27% (ave. 15%) of the mean. Plot of ECS app (▲-▲-▲) vs time postmortem; the standard deviation is 6-42% (ave. 25%) of the mean. The symbol (▽) represents the time postmortem of maximum isometric tension.

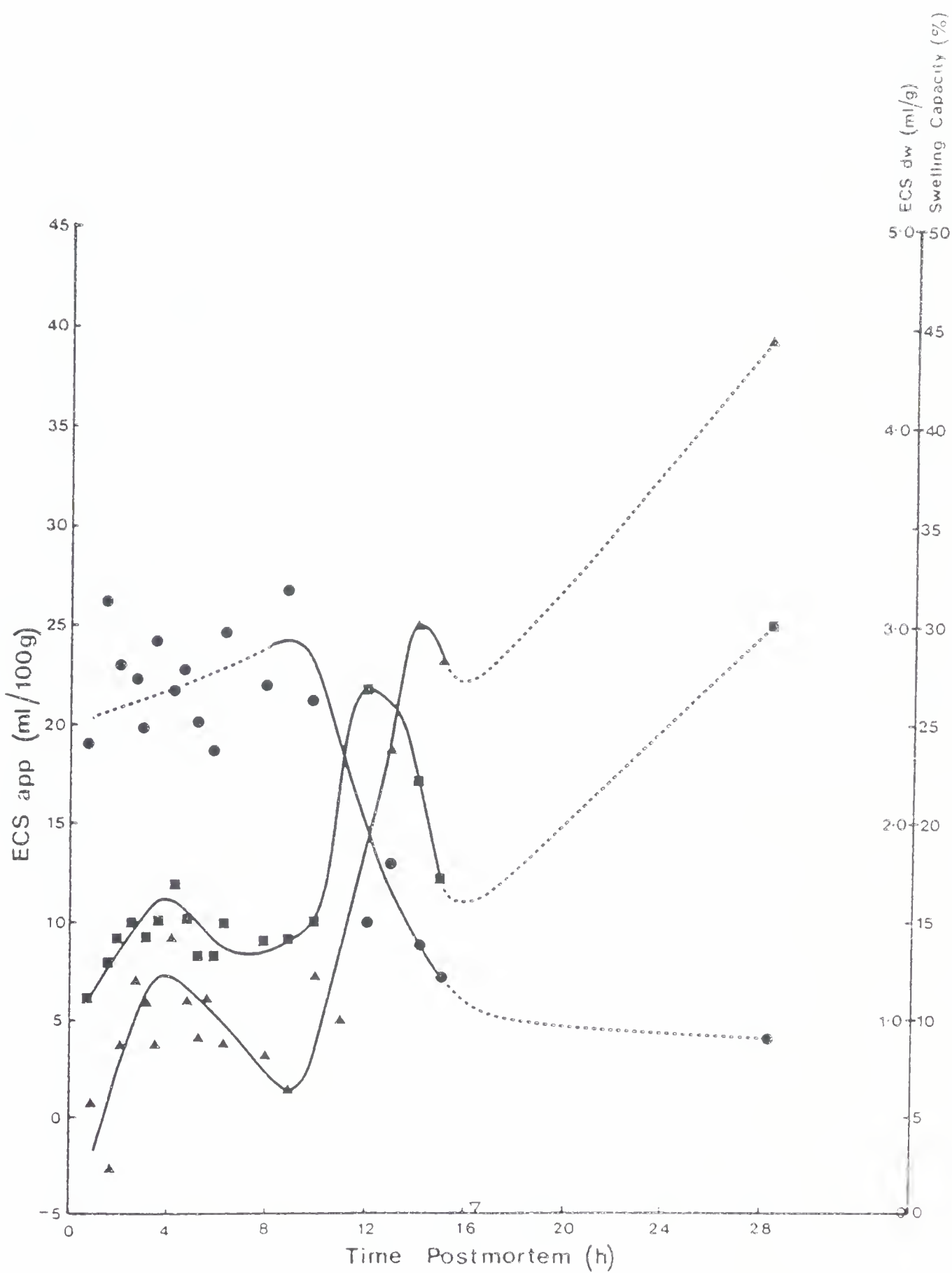


Figure III.51. Carcass 8. Plot of swelling capacity (•-•-•) vs time postmortem; the standard deviation is 4-20% (ave. 10%) of the mean. Plot of ECS dw (■-■-■) vs time postmortem; the standard deviation is 5-22% (ave. 11%) of the mean. Plot of ECS app (▲-▲-▲) vs time postmortem; the standard deviation is 8-25% (ave. 14%) of the mean.

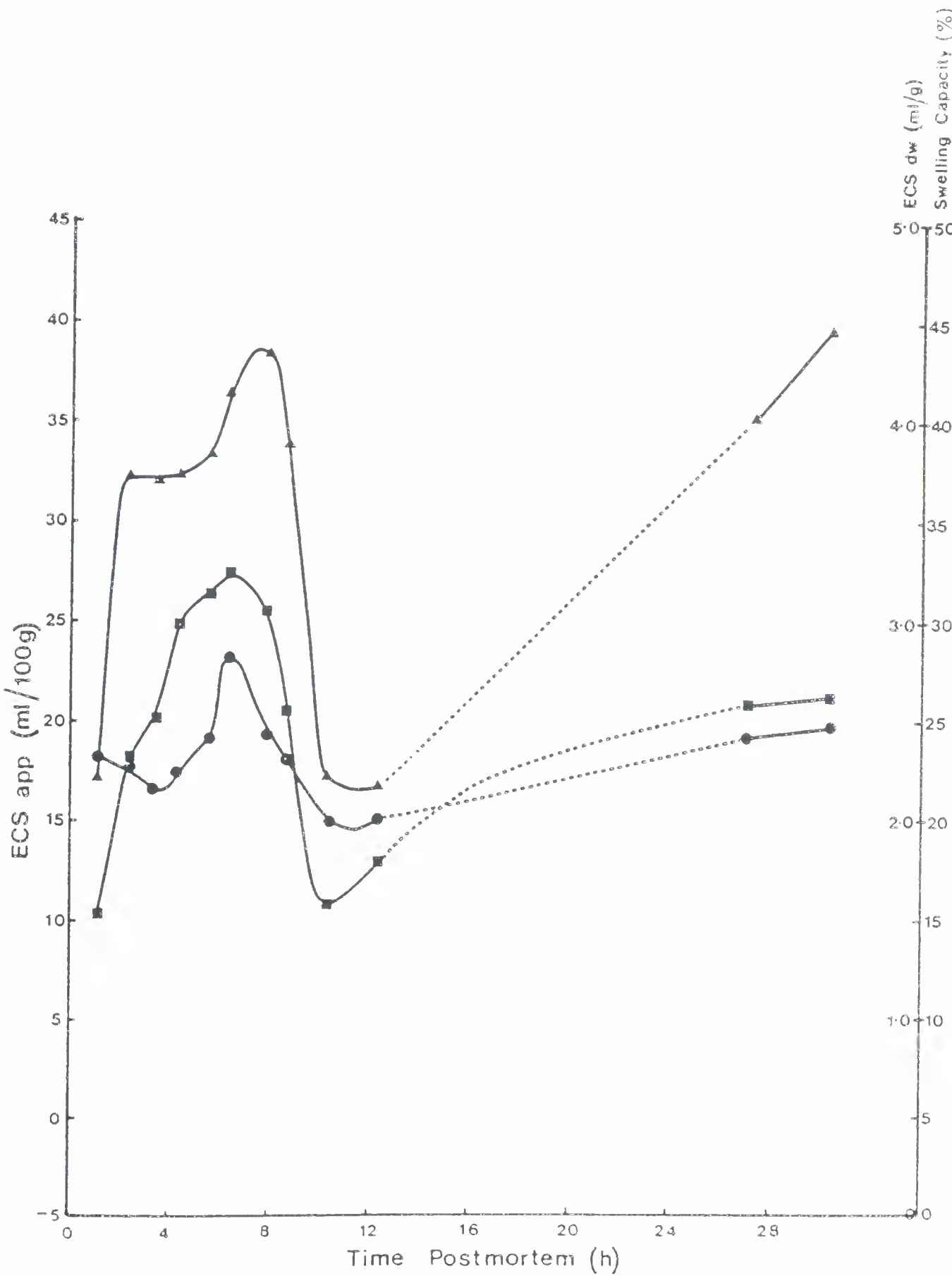


Figure III.52. Carcass 9. Plot of swelling capacity (•-•-•) vs time postmortem; the standard deviation is 4-26% (ave. 16%) of the mean. Plot of ECS dw (■-■-■) vs time postmortem; the standard deviation is 2-12% (ave. 8%) of the mean. Plot of ECS app (▲-▲-▲) vs time postmortem; the standard deviation is 2-22% (ave. 10%) of the mean. The symbol ( $\nabla$ ) represents the time postmortem of maximum isometric tension.

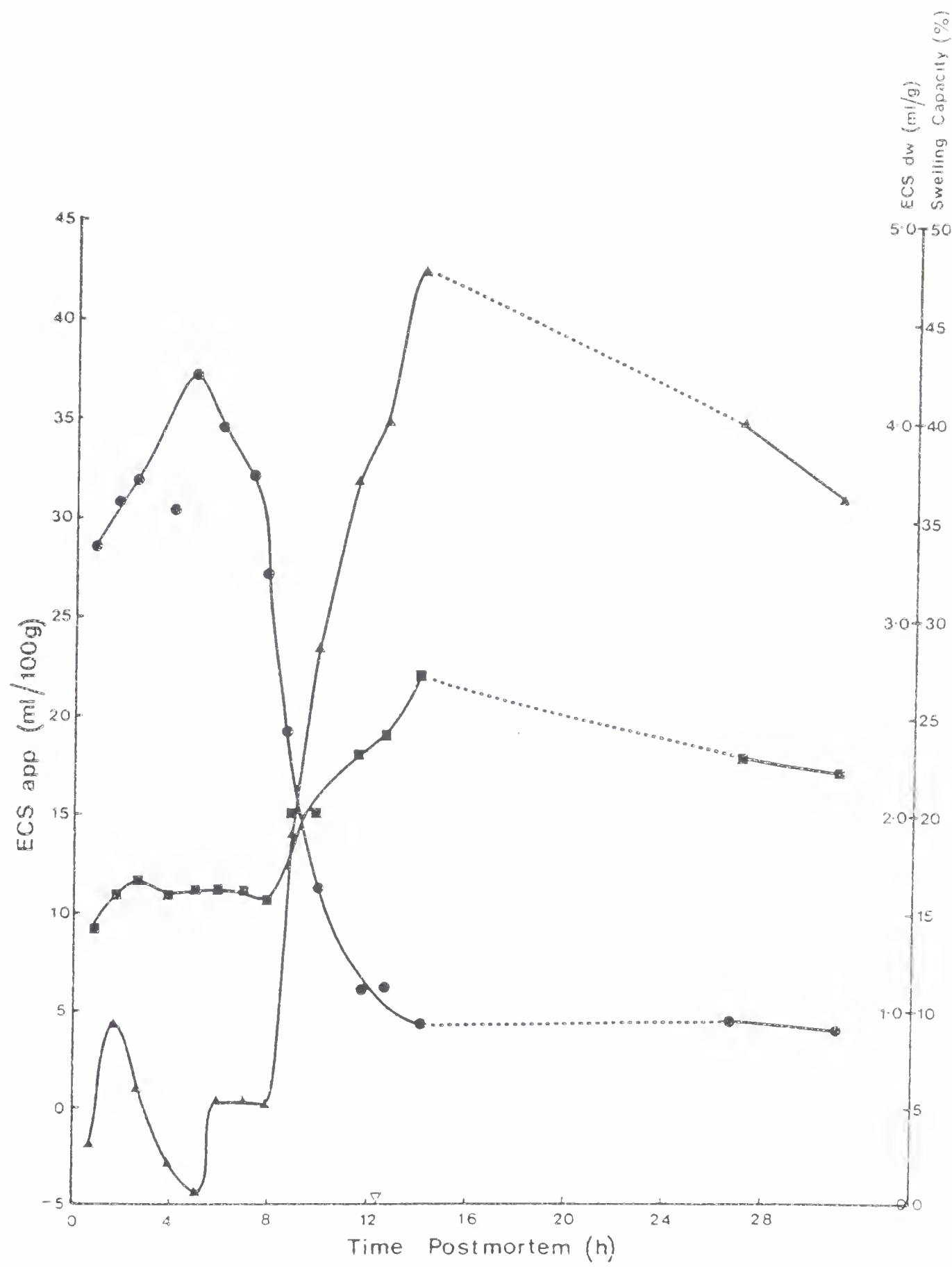


Figure III.53. Carcass 17. Plot of swelling capacity (•-•-•) vs time postmortem; the standard deviation is 1-18% (ave. 10%) of the mean. Plot of ECS dw (■-■-■) vs time postmortem; the standard deviation is 7-12% (ave. 9%) of the mean. Plot of ECS app (▲-▲-▲) vs time postmortem; the standard deviation is 2-28% (ave. 18%) of the mean. The symbol (▽) represents the time postmortem of maximum isometric tension.

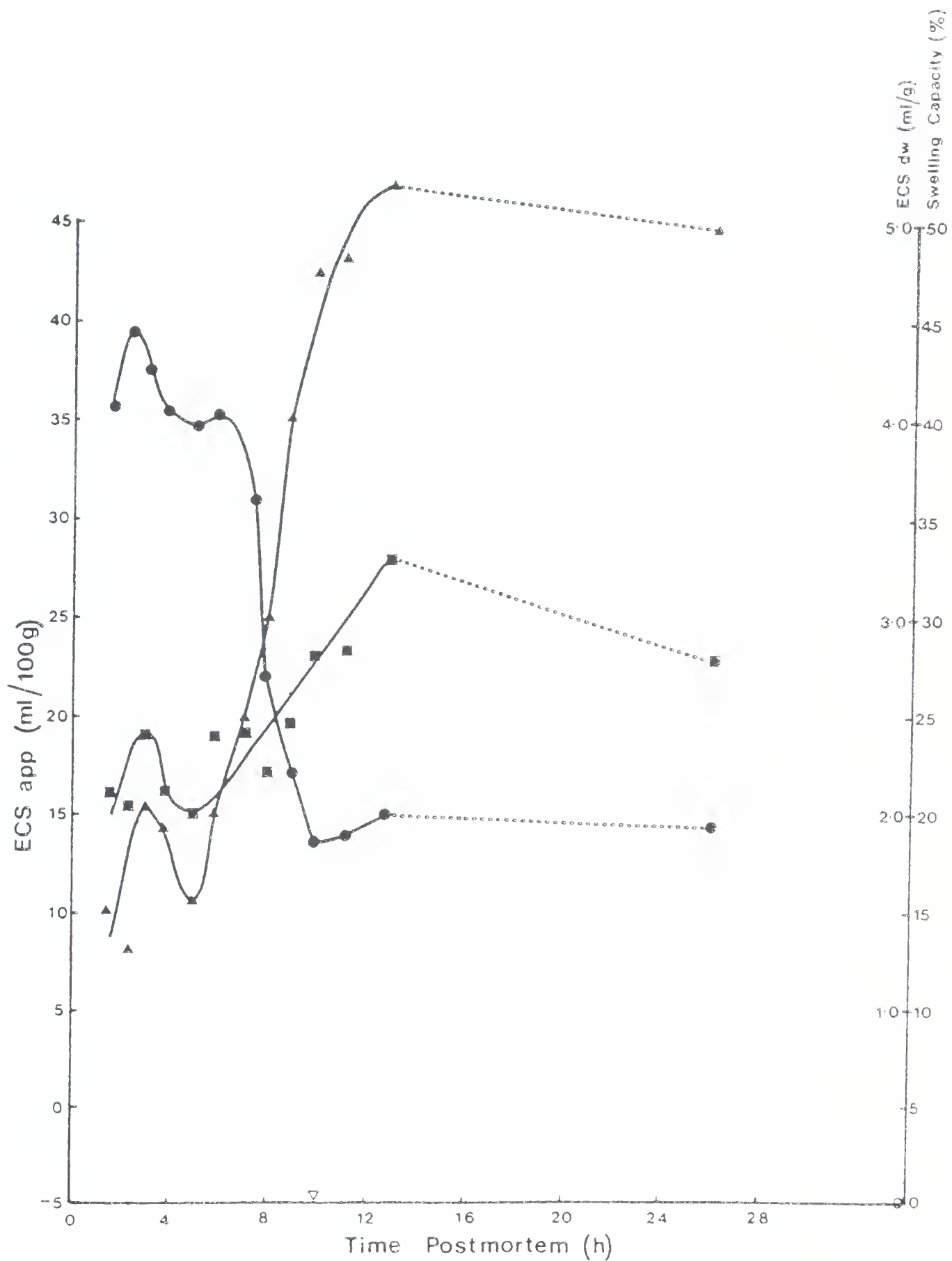
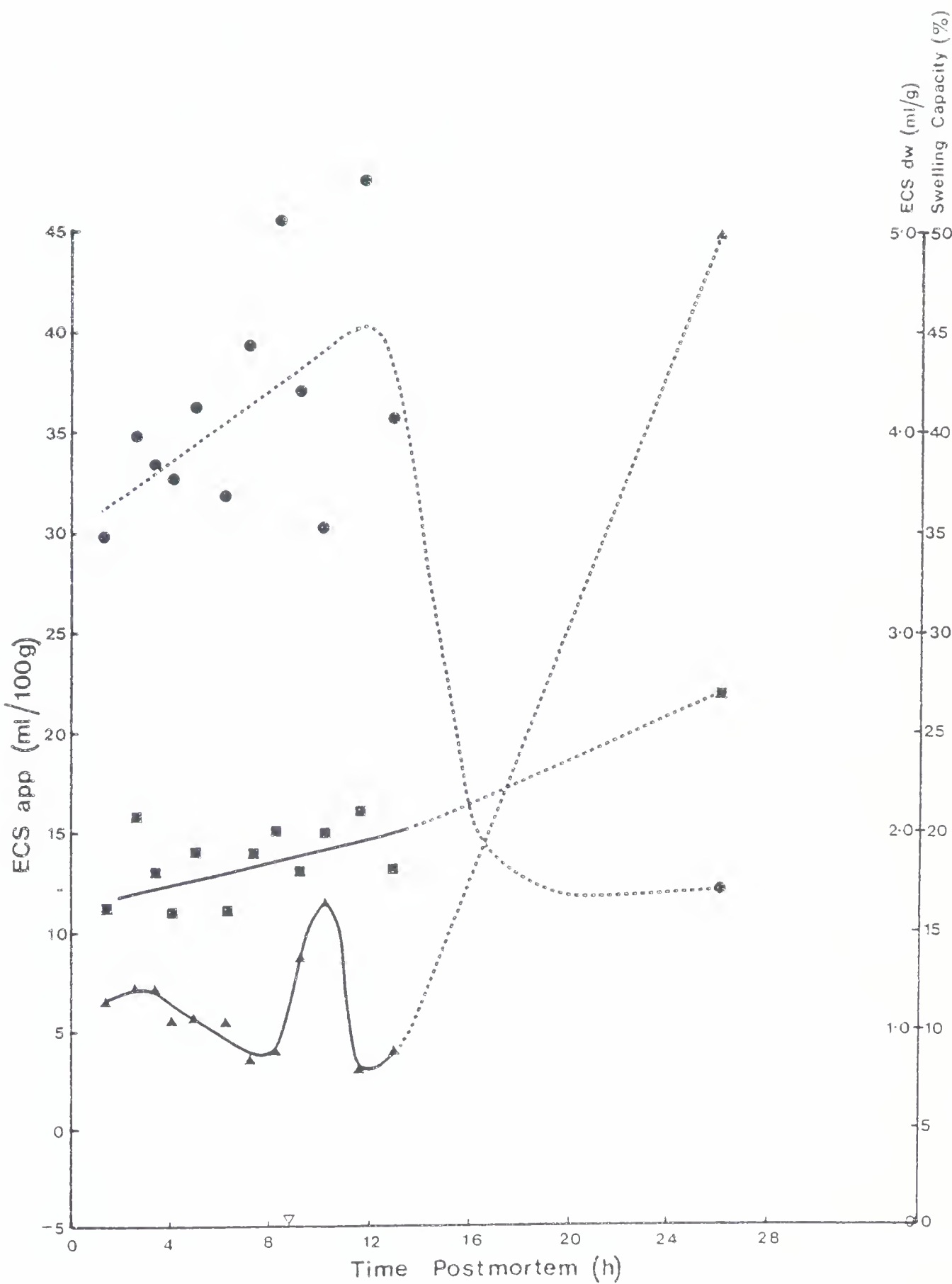


Figure III.54. Carcass 18. Plot of swelling capacity (●-●-●) vs time postmortem; the standard deviation is 1-18% (ave. 10%) of the mean. Plot of ECS dw (■-■-■) vs time postmortem; the standard deviation is 7-12% (ave. 9%) of the mean. Plot of ECS app (▲-▲-▲) vs time postmortem; the standard deviation is 2-28% (ave. 18%) of the mean. The symbol ( $\nabla$ ) represents the time postmortem of maximum isometric tension.





tension was attained. The correlation coefficient could not be calculated since the time to the maximum isometric tension was often not reached until after the extracellular space (ECS) measurements were stopped. The swelling capacity was calculated from data collected during the ECS determinations. The time to the maximum isometric tension is indicated in the figures so that a comparison between the swelling capacity and the maximum isometric tension can be made.

If at the time of the peak in isometric tension the rigor bonds generating the tension are maximal, the crossbridges between the thick and thin filaments could be implicated as the factor restricting the swelling. Offer and Trinick (1983) indicated that the structural constraints in the postrigor myofibril which restrict swelling are the crossbridges between the thick and thin filaments and the M and Z-lines. In prerigor muscle when the ATP concentrations are high the crossbridges will be dissociated. The only constraint to swelling will be the M and Z-lines and the sarcolemma. This constraint will not be as significant as the crossbridges and the swelling capacity of the tissue will be large. When rigor bonds form, the crossbridges restrict the swelling and the swelling capacity is low. This interpretation could explain the close correlation between the peak in the isometric tension profile and the minimal swelling capacity in Figures III.44-III.54.



These observations agree with the findings of Godt and Maughan (1977). They examined whether the swelling of the skinned muscle fibres of the frog was due to (a) swelling of the sarcoplasmic reticulum [SR] (observed in electron micrographs) or (b) forces arising from the charged nature of the myofilaments, either electrostatic repulsion between similarly charged filaments or a Donnan-osmotic mechanism. They concluded that the latter mechanism of swelling (b) was the major factor. They found that in the presence of 200 mM sucrose, which would shrink the dilated sarcoplasmic reticulum, no affect on the skinned fibre cross sectional area (the method they used to measure swelling) was found. For this reason they rejected the swelling of the SR as a dominant factor.

The two mechanisms contributing to the swelling capacity of muscle fibres which are based on the charged nature of the myofilaments may require some explanation. At a pH greater than the isoelectric point the myofilaments are negatively charged. As a result, the first mechanism may be viewed as a mutual repulsive force arising between the two negatively charged filaments. This separates the filaments, allowing water to enter and associate with them. The second mechanism is the Donnan-osmotic force. This force is a result of water entering the filament lattice to dilute the excess concentration of counter ions surrounding the charged filaments. If this force is great enough, the muscle will swell. This latter postulate is interesting in the light of



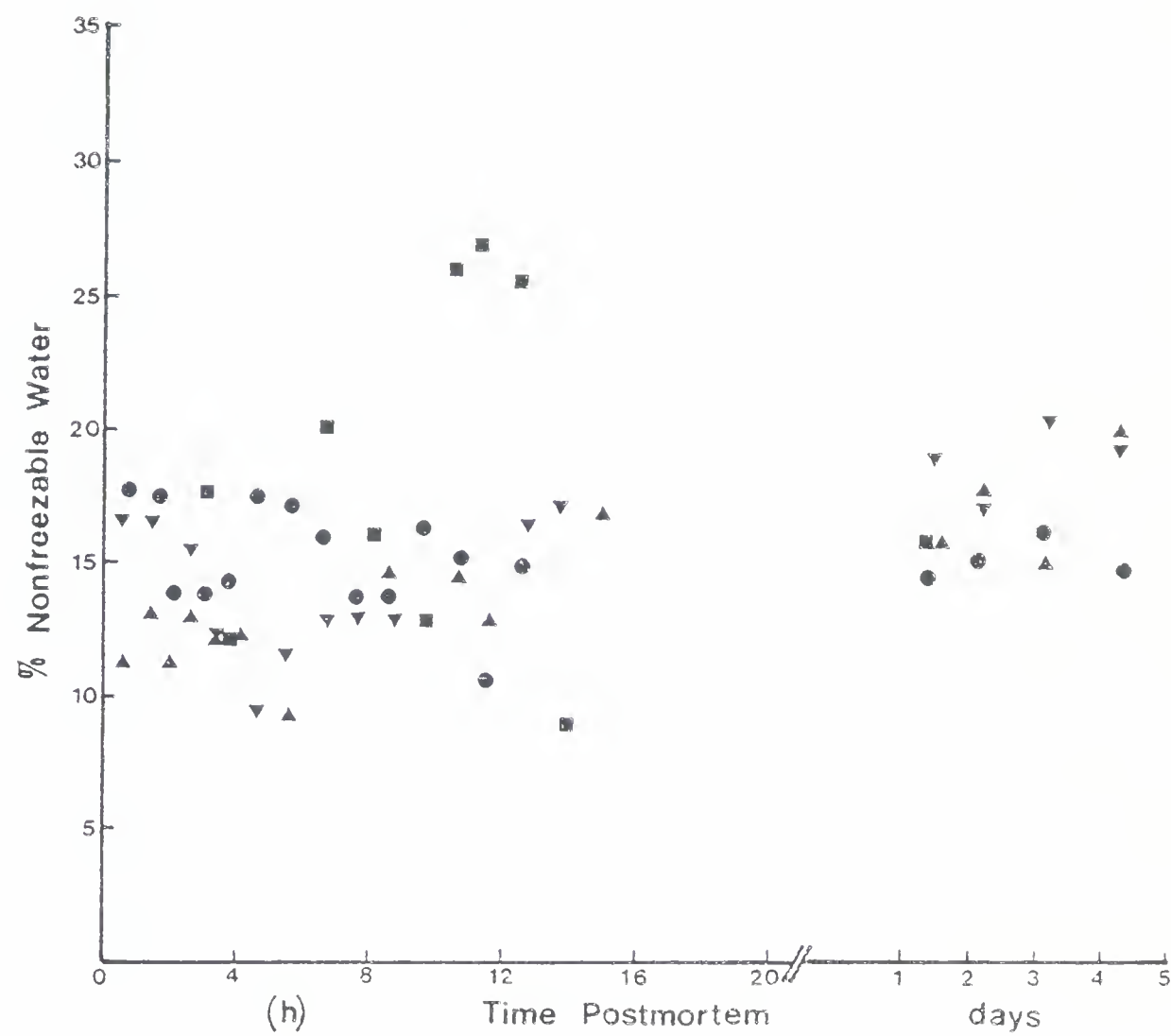
the findings of Winger and Pope (1980-81). They found the osmotic pressure of prerigor muscle to be about 200 mOs. The postrigor osmotic pressure (480-544 mOs) was almost twice the prerigor osmotic pressure. They considered the increase in the osmotic pressure to be due to low molecular weight components that are tightly bound to various macromolecules in the prerigor muscle coming free in the postrigor muscle. For this reason the Donnan-osmotic force would be expected to be the greatest postrigor. This is not observed to affect the swelling capacity of the muscle since it is the lowest postrigor. There is no doubt that the constraint of the crossbridges between the thick and thin filaments is preventing the swelling although the Donnan-osmotic forces would be the greatest.

In most of the carcasses tested an increase in the swelling capacity of the early prerigor samples was observed. An explanation for this increase, in some carcasses, may be an increase in the Donnan-osmotic force due to the release of some low molecular weight components at this time (e.g., nucleotides, ions, glucose, sugar phosphates and glycolytic intermediates). This would increase the swelling capacity since the constraint of the crossbridges would be lacking.

#### Differential scanning calorimetry (DSC)

The percentage of nonfreezable water is plotted vs time postmortem in Figure III.55 for carcasses 8, 9, 10 and 18.

Figure III.55. Plot of % nonfreezable water vs time postmortem for carcass 8 (●-●-●), carcass 9 (▲-▲-▲), carcass 10 (▼-▼-▼) and carcass 18 (■-■-■).





Although the data are very scattered it is generally observed that the prerigor data points are within the experimental error of the postrigor data points. These results may seem rather surprising. For example, one may expect the reduction in pH to reduce the protein charge and thus reduce the amount of water hydrating the proteins (reduction in the percentage of nonfreezable water). But this was not the case. These results confirm the proposal of Hamm (1974). He stated that the remarkable changes in WHC of meat caused by changes of protein charge (pH), by rigor mortis, by heating, etc., cannot be due to any changes in the hydration water. Clearly then, in this study, we are interested in the factors affecting the free water immobilized within the microstructure of the muscle.

The scatter in the datum points of this study seems to be a result of difficulties in determining the exact water content of the muscle strips. The water contents of the individual strips used in the DSC study were not determined. The moisture content value determined for the carcass was used to calculate the total amount of water in the muscle strip. Evaporation of the moisture from the strip, slight differences in the water content of the muscle from one region to the next and errors in the weighing of the muscle strip due to the small sample size could contribute to errors in the calculation of the total water content.

Stabursvik and Martens (1980) studied the thermal denaturation of proteins in postrigor muscle using DSC. They



removed the connective tissue and sarcoplasmic proteins which had previously caused interferences in DSC thermograms. They observed that the first two peaks in the 50-70°C region were due to myosin denaturation and that these were pH dependent. At pH 5.4 two peaks exist, but in the pH range of 6.0-7.0 the two peaks merge into one single peak, which again splits into two separate peaks above pH 7.0. These transitions are difficult to see in the intact muscle since the sarcoplasmic proteins also exhibit transitions in the same region. The third peak, at about 77°C, is considered to be due to actin and is not influenced by pH change.

The thermograms obtained in this study did not reveal transitions in the three peaks that could be clearly related to pH drop. This is likely due to the transitions attributed to the sarcoplasmic proteins interfering with the myosin denaturation peaks.

#### **Extracellular space (ECS) measurements**

From the equations developed for ECS app and ECS dw in the Materials and Methods section, two different parameters can be followed by the ECS measurements. Neither method measures the true ECS. The source of error in the ECS app measurements in early prerigor muscle is the size of the change in the intracellular space. The swelling of the tissue during its incubation can include the intracellular space. Thus differences in the amount of the intracellular



water uptake between carcasses can be detected. A low ECS app reflects a greater uptake of water by the intracellular spaces and would suggest that the intrafibre water affinity is high. ECS dw is a measure of the total amount of inulin entering the muscle strip after swelling. As long as the membrane remains intact the inulin is confined to the ECS. ECS dw under these circumstances reflects the size of the ECS after swelling.

The interpretation of the ECS profile becomes very complex in view of the fact there is a change in the swelling capacities during postmortem rigor development. When the swelling capacities are the same between samplings, interpretation of the data is simplified. For example, if the ECS was the major site of swelling, the ICS would have to fall to maintain the same swelling capacity and, as a result, the ECS dw and ECS app would increase. If the ICS were the major site of the swelling and the swelling capacity was the same as the previous sample, the reverse of the above situation would exist and both ECS dw and ECS app would decrease.

The complexity of the problem can be illustrated with a second possibility. If the swelling of a sample increased in comparison to a previous sample, the following situations could result. If the swelling were confined to the ECS, the ECS dw would increase, but if the ICS swelling were exactly the same as the previous sample, the ECS app would remain the same. Conversely, if the swelling were confined to the



ICS, the ECS dw would remain the same and the ECS app would decrease if the ECS had remained the same as the previous sample. If both the ECS and ICS were to swell, contributing to an increased swelling capacity, then the ECS dw would increase but the ECS app would decrease in comparison to a previous sample. A third consideration is when the swelling capacity of a sample decreases. If the ECS were the site of reduced uptake and the change in ICS remained the same as the previous sample, then the ECS dw would decrease but ECS app would remain the same as the previous sample. If the ICS were the site of reduced uptake and the change in the ECS remained the same as the previous samples, the ECS dw would be the same and ECS app would increase. A reduction in both the ECS and ICS would result in the ECS dw decreasing and ECS app increasing in comparison to a previous sample.

The above interpretation of the ECS measurements will only hold true during the early prerigor period when the cell membrane is intact. A comparison of the incubation profiles (Materials and Methods section, Figures II.13 and II.14) of the prerigor and postrigor muscle shows that only the prerigor muscle is capable of excluding inulin from the intracellular spaces. In Figure II.13 the ECS dw rose to a constant value within 1 hr, while the ECS app remained small for nearly a 3 hr incubation period. However, Figure II.14 presents a different profile in which both expressions of ECS show a rise to high values within 1 hr. The results in Figure II.13 can be explained by the inulin permeating the



ECS within 1 hr but being excluded from the ICS by a still intact membrane. In the postrigor muscle (Figure II.14) the membrane is no longer capable of excluding inulin and the intracellular spaces also become permeated. The loss of membrane selectivity is also supported by the size of the ECS dw in the late prerigor and early postrigor periods. Although the tissue does not swell as much in the postrigor period, the water content of the tissues is still in the region of 80%. From measurements of the nonfreezable water in this study (DSC) and NMR (Belton *et al.*, 1972), the bound water which would not partake in any water translocation occurring within the muscle is about 15-20%. If 15% of the water is considered to be strongly bound, then the water available for translocation is about 3.4 mL/g dry weight. For most carcasses, greater than 75% of the available water (postrigor) would have to be confined to the ECS. This figure is ridiculously high and can only be explained by inulin uptake into the ICS. Therefore, the time at which a rise to these high values occurs probably marks a time of membrane failure and thus increased permeability to inulin. It should be remembered in examining the results to follow that although some of the early prerigor ECS dw values are quite high, the water content of the muscle following incubation is much higher and thus the percentage of the water in the ECS is reduced to more reasonable values if this increase in the water content of the prerigor muscle cell is considered.



Because of the complexities described here in interpreting the ECS data, the ECS results can best be understood by looking at the trends indicated in the plots, rather than comparing individual data points. However, when the changes in the swelling capacities are very different, some understanding of the above complexities in the ECS data can help in its interpretation. Each of the carcasses examined in this study responded differently during rigor development. The application of the ECS data to the understanding of the state of the water in the muscle will be included in section D.

### Conclusion

The methods used in this section to assess the state of water in muscle have included NMR T<sub>1</sub> determinations of water in muscle and model systems, expressed juice as a measure of WHC, differential scanning calorimetry (DSC) and extracellular space measurements. The NMR T<sub>1</sub> data obtained from each of the carcasses reflect the diversity between carcasses observed in the data presented in section B. This implies that the state of the water in the muscle is affected by the rate and type of rigor development and that NMR T<sub>1</sub> measurement is sensitive to these changes. The NMR of the model systems has indicated that pH, ATP and ions have an affect on the water associated with the myofibrils in the muscle. The DSC results confirm the findings of others that the water of hydration (a fraction of the nonfreezable



water) does not seem to be dramatically affected by rigor development. This suggests that it is the factors immobilizing the freer water in the muscle that are of prime concern in this study. The ECS measurements are seen as a means of measuring the intrafibre water affinity as well as the size of the ECS after incubation. The opportunity of assessing differences in intrafibre water affinities is a unique approach to the study of water in meat.

#### D. Interrelation of the Biochemical and Physiological Events in the Carcass and the State of Water in the Muscle

This section will be approached with a carcass by carcass discussion of the results obtained. NMR  $T_1$  is the principal method used to assess the state of the water in the muscle. Thus the results of the other methods used to measure the rate of rigor onset and the water properties in the muscle will be considered in the interpretation of the  $T_1$  profiles. The carcasses to be discussed for which the data are most complete will be carcasses 8 through 18. Information obtained from carcasses 4 through 7 will be included in the Appendices. The approach will not be chronological, but in the order of decreasing  $\Delta T_1$ . Some of the interpretations of these data are speculative. This is particularly true where the data interpretation includes references to the nature and the number of rigor bonds and dimensions of the interfilamentous spacings.



**Carcass 15 ( $\Delta T_1=0.105$  sec)**

As mentioned earlier, this sample was purposely taken to be high in its red fibre content. For this reason some discrepancies were observed between the time to the peak  $T_1$  and pH. However, an examination of the results obtained on this carcass may suggest that the overall water properties of this carcass could be considered independent of fibre type. That is, the NMR  $T_1$  profile for a sample with a greater white fibre content would have had a similar  $\Delta T_1$ , although the time of the various events of the  $T_1$  profile may have differed. The reason for this viewpoint is based on the ECS data in Figure III.44 which were from muscle strips sampled from the center of the muscle (higher white fibre content). Although the datum points were quite scattered, both the ECS dw and ECS app steadily increased. The intrafibre water affinity was reasonably high initially (low ECS app), but any affinity for the water was steadily lost (rising ECS dw and ECS app). This observation is supported by the expressed juice data for carcass 15 in Figure III.9. Here again the values were very scattered, but the initial expressed juice values over the first 12 h were the highest of all the carcasses (average  $\approx 10\%$ ).

Edzes and Samulski (1978) consider the water in the ECS to have a larger  $T_1$  than the water associated with the myofibrils. If this is true, the extraordinarily large increase in  $T_1$  (Figure III.36) could be due to the fibres initially having a relatively high affinity for the muscle



water (low ECS app and low  $T_1$ ), but as rigor developed the loss of intrafibre water affinity was very great. The intrafibre water would be lost to the ECS and the  $T_1$  would increase dramatically.

It is interesting that the swelling capacity remained relatively high in this carcass. In fact it had the highest swelling capacity at 27 h (19.5%) of all the carcasses examined. This may not be a totally surprising observation since the  $T_1$  values, although nearly constant postpeak for 10 hr (slope = -.000125 sec/hr), began to fall quite steeply postrigor (slope = -0.00335 sec/hr). The reason for the larger slope postrigor observation can be explained in terms of the interfilamentous spacings. It has been shown by many (Offer and Trinick, 1983; Matsubara and Elliot, 1972; Goldman *et al.*, 1979; Millman and Nickel, 1980; Millman *et al.*, 1981; Millman, 1981) that an increase in the interfilamentous spacing increases the amount of water that can be retained within a muscle. The question is how can the interfilamentous spacing in this study be assessed? The answer may rest with the magnitude of the isometric tension developed in the prerigor muscle. Godt and Maughan (1977), in their studies on skinned frog muscles, observed that, when the  $\text{Ca}^{2+}$ -activated tension was measured in solutions containing polyvinylpyrrolidone and dextran T fractions, the maximal calcium activated tension was reduced compared to the control. When the muscle was returned to a polymer-free solution, maximal tension increased to the control value.



These findings indicate that, when the interfilamental spacing is small (such as in the polymer solutions which shrink the fibre), the tension is small. When the fibre has swollen and the interfilamental spacing is larger then tension generated is greater. The potentiation of tetanic tension of intact muscle by hypotonic solutions (Edman and Andersson, 1968; April and Brandt, 1973) supports the above results. The incubation of a fibre in a hypotonic solution would tend to swell the fibre, increasing the interfilamental spacing. For this reason a high isometric tension in this study will be viewed as indicating a large interfilamental spacing. Conversely, a low isometric tension would suggest a small interfilamental spacing.

The isometric tension generated by this carcass was the fourth highest of all the carcasses examined ( $80.5 \text{ g/cm}^2$ ). This would suggest that the interfilamental spacing was quite large and is the reason the slope in the  $T_i$  values postrigor was so great. The factors contributing to the interfilamental spacing would allow for the muscle water lost by the fibre to more rapidly and more freely return to the fibre. The high swelling capacity postrigor (19.5%) indicates few constraints to swelling. This may be due to weaknesses in the M- and Z-lines or a reduced number of crossbridges (Offer and Trinick, 1983). If this is true, the number of charged sites for water interaction may be greater and the muscle water will relocate within the fibre. The ATP concentrations remained low postrigor (16 to 26 hr) and did



not increase as observed in some other carcasses. For this reason ATP could have had no effect on the reordering of the water in the muscle.

The reason for the rapid loss of intrafibre water in the early prerigor period may be related to the loss of ATP. The initial ATP concentration was quite low ( $\approx 5.1 \mu\text{mole/g}$ ) and declined steadily until rigor was attained (18 hr). The fall in ATP may have contributed to crossbridge formation as a result of the release of  $\text{Ca}^{2+}$  from the sarcoplasmic reticulum. The isometric tension was initiated at about 4 hr. The formation of the crossbridges would result in a reduction in the number of water interactive sites as well as the tightening of the interfilamentous spacings. Therefore, the once high intrafibre water affinity would rapidly be lost and a large  $\Delta T_1$  and increase in the ECS measurements would result.

The rapid increase in the intrafibre water affinity postpeak (fall in  $T_1$  at 7 hr) occurs during the time the isometric tension is beginning to rise more steeply, but it is short lived. The period between 9 and 19 hr shows little change in the  $T_1$  values. It would appear that, although the interfilamentous spacing is quite large, the drop in pH and the nearing of the ultimate pH may reduce the repulsive force and increase the number of salt bridges tightening the myofibrillar structure (Hamm, 1974). When the salt bridges begin to break postrigor [after 19 hr due to  $\text{K}^+$  incorporation (Arnold *et al.*, 1956)], the large



interfilamental spacing contributes to a rapid uptake of water.

It is interesting that nothing about the pH fall itself may have suggested that a large loss of intrafibre water would have ensued during the first 7 hr postmortem. The initial rate of pH fall was low (0.29 pH units/hr), the initial pH was very high (6.82 at 1 hr) and the ultimate pH at rigor was normal (5.52). For this reason pH cannot be used as an accurate predictor of changes in WHC during the development of rigor. The slight increase in pH is not significant enough on its own to improve the WHC (Hamm, 1960) and thus contribute to the high swelling capacity measured post rigor.

#### Carcass 10 ( $\Delta T_1=0.065$ sec)

The NMR  $T_1$  profile initially showed a relatively rapid increase in  $T_1$  with time postmortem (Figure III.35). If the same rate of  $T_1$  increase had continued until the peak at 12.7 hr, the  $\Delta T_1$  would have been considerably greater. The  $T_1$  profile obtained for this carcass shows a plateau in the rate of  $T_1$  increase near 7 hr. A change in the intrafibre water affinity may explain this alteration in the  $T_1$  data. The ECS data for carcass 10 are in Figure III.45. The initial ECS app was quite low (2.5 mL/100 g), indicating an intermediate intrafibre water affinity. As rigor development progressed, both ECS app and ECS dw showed a large increase in their values. This would correspond to the relatively



rapid increase in  $T_1$ . A continued loss of intrafibre water affinity does not occur as observed in carcass 15 (also carcasses 4 and 7 as discussed in Appendices D and G). Rather, a reduction in ECS dw and ECS app occurs, indicating a temporary increase in the intrafibre water affinity at about the same time as a plateau in the  $T_1$  data was observed. Soon the factor(s) contributing to the increased intrafibre water affinity are lost and the ECS dw and ECS app increase, as does the  $T_1$  data. However, the  $T_1$ , ECS dw and ECS app increases (Figures III.35 and III.45) are minimal, suggesting a relatively high intrafibre water affinity remains. This interpretation is supported by the expressed juice data ( $\approx 0.5\%$ , prerigor) in Figure III.4, which demonstrate a high water holding capacity in this muscle.

The initial rate of pH fall (1.33 units/hr) is one of the most rapid rates recorded (same as carcass 4). This and the decline in ATP (Figure V.7) likely contribute to  $\text{Ca}^{2+}$  release and the early development of isometric tension recorded in Figure III.4. The early rapid rise in the isometric tension ( $\approx 3.5$  hr) indicates that rigor bonds were forming, which would rapidly reduce the intrafibre water affinity.

All the initial evidence would lead one to predict a carcass having a very low intrafibre water affinity and thus an expected low WHC. The initial rise in the ECS measurements and  $T_1$  all confirm these initial trends.



However, the expressed juice values (Figure III.4) are the lowest of all the carcasses examined. How can these results be explained?

The clue seems to rest with the extraordinary glycolytic activity associated with this carcass. Although the ATP initially declined, which likely contributed to the early prerigor results, the ATP levels did not reach a point at which they fell rapidly to low postrigor values. In fact the ATP concentrations were 0.5  $\mu\text{mole/g}$  and 0.2  $\mu\text{mole/g}$  at 16 hr and 28 hr, respectively. It was not until day 2 that the ATP levels were at the more normal postrigor values ( $\approx 0.05 \mu\text{mole/g}$ ) and the expressed juice increased to the expected values. In Part B it was observed that the ATP levels were maintained by an extended glycolytic activity (pH still dropping at 36 hr).

The ATP concentration maintained during the prerigor period appears to have enhanced the swelling capacity (Figure III.45). The ATP in this carcass may have been able to reduce the number of crossbridges leading to a greater interfilamental spacing and thus an enhanced WHC. A fairly large interfilamental spacing may be expected since the isometric tension for this carcass was quite high (70 g/cm<sup>2</sup>).

The reason why the isometric tension (Figure III.4) was lost when the ATP concentration was so high is not definitely known. For most carcasses the isometric tension did not cease until the ATP concentration was much lower. An



explanation for this observation was discussed in Part B, where it was proposed that the myofibrillar ATPase was inhibited for some reason.

The reason for the reduced  $T_1$  slope postpeak (slope = -0.00062 sec/hr) is not entirely clear. This is especially true in view of the fairly large interfilamentous spacing. The most likely reason for this observation is the formation of salt bridges due to extensive glycolysis (>36 hr) and the loss of repulsive forces near the isoelectric point of the myofibrillar proteins. Perhaps once glycolysis ceased and the number of salt bridges was reduced by the uptake of  $K^+$  the fall in  $T_1$  would have been even more rapid than carcass 15.

The rapid pH fall and the low ultimate pH (<5.2) recorded for this carcass emphasize the fact that pH alone does not in itself explain the reason for a muscle possessing a certain WHC. It may have been expected with the very low pH that the WHC would also have been low (Bouton *et al.*, 1971). The recorded pH does provide a simple means of measuring the glycolytic activity within a carcass

#### Carcass 16 ( $\Delta T_1=0.060$ sec)

The NMR  $T_1$  data (Figure III.36) for carcass 16 consists of a rapid initial increase in  $T_1$ , a small plateau near 4 hr, and then an increase again to peak at 11 hr postmortem. The postpeak period reveals a rapid and then a slow fall in the  $T_1$  values. The initial ECS app in Figure



III.46 is 2.5 mL/100 g. This value is similar to carcass 10 and represents in this study an intermediate intrafibre water affinity. The initial ECS data are quite scattered in the early prerigor period. It appears from the NMR T<sub>1</sub> response that, if the ECS were more accurately determined, a peak would have more clearly been detected at this time. A rapid increase in the ECS data would have represented a rapid loss of the intrafibre water affinity and thus the initially rapid increase in T<sub>1</sub>. In the region of 4 h postmortem the plateau in the NMR T<sub>1</sub> data is accompanied by a fall in ECS app and ECS dw. It is at 5 hr that the smallest ECS app value was measured, indicating an increase in the intrafibre water affinity. It is about this time that the plateau in the T<sub>1</sub> data is about to give way to a more rapid increase in the T<sub>1</sub> values. The ECS data also increases from this point. Thus the T<sub>1</sub> and ECS data are supportive in predicting that the intrafibre water affinity is quite low. The expressed juice results (Figure III.10) also support a loss in the intrafibre water affinity, contributing to a low WHC. The expressed juice values were initially quite high ( $\approx 3\%$ ) and were seen to rise quite rapidly after about 4 hr postmortem.

The ATP data (Figure V.19) obtained from this carcass infer that ATP concentration alone is incapable of maintaining a high WHC and a high intrafibre water affinity. The reason for this conclusion is the surprisingly high ATP concentrations which were maintained in this carcass for a



period of 7 hr. Within this same period (particularly from 5 hr postmortem on) the intrafibre water affinity was rapidly being lost (ECS data, T<sub>i</sub> and WHC). The isometric tension data in Figure III.10 reveal crossbridge formation within 4 hr postmortem. It is possible that the early formation of the crossbridges contributed to the loss of the intrafibre water affinity similar to that suggested for carcass 15. These results would imply that the interfilamentary crossbridges and the inability of ATP to dissociate or alter the configuration of the crossbridges may be the major factor contributing to the loss of WHC. In carcass 10 the ATP levels enhanced water retention. The variability in the response of the muscles to ATP is one of the most surprising results observed in this study. However, these variations may lend support to the finding of Izumi *et al.* (1981). In the present study the view has been taken that Ca<sup>2+</sup> release is necessary in postmortem muscle before crossbridge formation can occur. However, this release of Ca<sup>2+</sup> to alter the Tn complex is not always necessary for crossbridge formation to occur. It has been observed that crossbridge formation and the initiation of isometric tension can occur in the absence of Ca<sup>2+</sup> if the ATP levels are low. It is this type of "rigor tension" that Izumi *et al.* (1981) were examining. This approach can provide some information about the nature of the rigor complex relative to ATP concentration. Firstly, it was observed that the "critical ATP concentration" necessary for inducing rigor



contraction from the relaxed state and for inducing dissociation of the rigor complex is decreased with decreasing pH. Secondly, the critical ATP concentration effecting rigor contraction or dissociating rigor complexes is related to a threshold level in the amount of rigor complexes formed in the fibres. If the number of rigor complexes rises above this threshold level, the fibres suddenly and completely go into rigor and rigor contraction may ensue. However, if the number of rigor complexes falls below the threshold value, the fibre will remain in a relaxed state. Thirdly, after a relaxation has been induced (by increasing the ATP concentration), after a rigor contraction has first been initiated, the crossbridges that remain undissociated will enhance the isometric rigor contraction when the ATP levels are reduced, but the critical ATP concentration has now risen.

Based on the above results, Izumi *et al.* (1981) stated a most interesting point relative to this study: "This suggests that the configuration of the rigor complex may be variable with ATP, and ATP concentration is one of the factors in determining the configuration of the rigor complex". This observation may help to explain some of the variability we have observed in the response of different carcasses to ATP concentration. If the configuration of the rigor complex is different, it may also affect the intrafibre water affinity detected by T<sub>1</sub> and ECS measurements.



Although the isometric tension data suggest a high interfilamentous spacing (max. tension 82 g/cm<sup>2</sup> at 16 hr), the swelling capacity did not respond in the same manner as carcass 10 (an increase in the swelling capacity in the presence of ATP). Perhaps the number of crossbridges was greater in this carcass (16), due to the inability of ATP to rapidly dissociate the crossbridges and thus restrict the swelling, or perhaps the structural properties of the M- and Z-lines were different in this carcass. Both of these factors may contribute to a higher expressed juice value measured in this carcass (lower WHC). Offer and Trinick (1983) observed considerable variation between preparations in the swelling of myofibrils as a result of salt treatment. They observed variation in the appearance of the Z-line (whether it would swell or not) and variation in the salt concentration at which the A band was extracted. They suggested that swelling is partly due to the disruption of structural constraints such as the attached crossbridges, the M and Z-lines and perhaps others as yet unknown. If there is a variation between myofibrillar preparations in the appearance of the myofibril upon swelling and in the salt concentrations at which the A band is affected, then certainly there must be variation in the nature of the crossbridges and the M and Z lines from one carcass to the next. Thus inconsistencies in the maximum isometric tension may be expected, which may cloud some of the interpretations of the interfilamentous spacings. Carcass to carcass



variation may also affect the response of the myofibril to the ATP concentration. ATP may enhance the intrafibre water affinity in some carcasses but not others. For example, the rapid ATP production of carcass 10 (high glycolytic rate) was utilized in some way (perhaps the dissociation of crossbridges) in the early prerigor muscle to maintain a high WHC. The glycolytic rate of this carcass (16) was also quite rapid, but the ATP was not utilized to maintain a high WHC. In fact the ATP concentration remained high (about 7  $\mu$ mole/g) for 8 hr. After 8 hr a more rapid rate of isometric tension development was observed which may have been promoted by these high ATP levels. It may be possible that this utilization of ATP contributed to a higher isometric tension than that predicted by the interfilamental spacing alone. Izumi *et al.* (1981) observed that higher ATP concentrations could increase the tension developed.

The slope of the  $T_1$  data postpeak reveals two aspects. The slope from immediately postpeak to the point of rigor at 16 hr (slope = -0.00194 sec/hr) is greater than the slope beyond 16 hr (slope = -0.000769 sec/hr). This seems to suggest that factors contributing to the increase in the intrafibre water are more favorable during the time the myofibrillar ATPase is active than when it ceases. During the ATPase activity, part of the contraction cycle consists of dissociation of the crossbridges when the myosin-ATP complex is formed. Perhaps this enhances the water affinity of the fibre during this activity. For this reason the slope



until isometric tension ceased (rigor) would be greater than the postrigor period. In the postrigor period the crossbridges are permanently formed in the absence of the ATPase and the intrafibre water uptake would be reduced as would the slope of the  $T_1$  values. The low ATP concentration (postrigor) implies that ATP played no role in the intrafibre water uptake in this carcass.

#### Carcass 13 ( $\Delta T_1 = 0.052$ sec)

The initial ECS data (Figure III.47) indicate a fairly high intrafibre water affinity (low ECS app, 2.5 mL/100 g) which increases initially (ECS app falls). This is mirrored by the  $T_1$  data (Figure III.36), where the initial readings were quite constant. At approximately 5 hr the swelling capacity fell rapidly. The ECS dw remained relatively constant throughout this time, but the ECS app rose. This indicates a reduction in the swelling capacity of the ICS only and may be interpreted as a reduction in the intrafibre water affinity. This is mirrored by a rise in the  $T_1$ . Following this an increase in the intrafibre water affinity (reduction in ECS app) occurs. This is reflected by plateaus in the  $T_1$  profile at 6 and 8 hr. After this period the ECS increased slowly, with a comparable rise in  $T_1$ .

The reduction in the swelling capacity during the period from 5 hr to 12 hr, followed by a rapid rise is a surprising observation. The ATP data (Figure V.13) provide some insight into the factors contributing to these



observations. The ATP concentration fell until it was about 0.78  $\mu\text{mole/g}$  at 12 hr. This was quickly followed by a rapid rise in ATP to reach a concentration of 1.3  $\mu\text{mole/g}$  near 13 hr. The ATP then fell to reach about 0.2  $\mu\text{mole/g}$  at 16 hr and then rose again to 0.65  $\mu\text{mole/g}$  at 28 hr.

During the first 12 hr the general trend was a reduction in the intrafibre water affinity. The  $T_1$  profile was observed to rise and then peak at this time (12 hr, when the swelling capacity and ATP concentration were low). Immediately after the ATP was produced, the  $T_1$  values dropped quite quickly until 17 hr. During the period from approximately 7 hr to 17 hr the isometric tension development (Figure III.7) was increasing quite rapidly, indicating a high myofibrillar ATPase activity. Thus the reduction in  $T_1$  (12 hr-17 hr, slope = -.00572 sec/hr, showing an increase in intrafibre water affinity) was associated with a high ATPase activity. The sudden production of ATP did not increase the rate of isometric tension development but it did contribute to an increase in the swelling capacity and intrafibre water affinity. Perhaps the ATP was highly effective in dissociating the crossbridges. Between 17 and 23 hr the isometric tension increased slightly ( $59 \text{ g/cm}^2$  to  $61.5 \text{ g/cm}^2$ ). During this same period the pH was falling and producing ATP. In fact the ATP levels rose even though isometric tension was being generated. These results reveal a reduced myofibrillar ATPase. During this same period the  $T_1$  data was not falling



as rapidly (slope = -.00276 sec/hr), suggesting a reduced intrafibre water affinity. The observations may be due to the ATP (at the lower concentrations) taking longer to diffuse to the binding sites on myosin. As a result, the period of time during which the myosin-ATP complex is formed is reduced. This may contribute to an increase in the overall number of crossbridges as compared to the situation when the ATPase activity is high. This may reduce the interfilamental spacing and thus the intrafibre water affinity is reduced.

The postrigor  $T_1$  data were not collected in this carcass since rigor maximum was not reached until about 24 hr, at which time the collection of data was stopped. Therefore, it is not known what the postrigor  $T_1$  slope was.

The isometric tension was quite high ( $62.5 \text{ g/cm}^2$ ), which would suggest a fairly high interfilamental spacing which may also explain in part the relatively rapid reduction in  $T_1$ . The expressed juice values in this carcass, although quite high initially ( $\approx 5\%$ ), did not increase rapidly. This suggests a carcass having a reasonably high WHC.

#### Carcass 11 ( $\Delta T_1=0.040 \text{ sec}$ )

The  $T_1$  data in Figure III.35 result in a plot having a bimodal appearance, with peaks at 3.2 and 12 hr. The slope postpeak was very steep.



The initial ECS app values (Figure III.48) are quite high in this carcass, revealing a low initial intrafibre water affinity. This would have resulted in an initial  $T_1$ , that would be slightly higher. This observation may be part of the explanation as to why the  $\Delta T_1$  was not as great in this carcass. If the initial  $T_1$  was high, even though similar water retentive properties between carcasses would exist at the peak, the  $\Delta T_1$  values would be smaller. The reduction in ECS app after 3 hr is related to the reduction in the  $T_1$ , during the same time period. These observations support an increase in the intrafibre water affinity at this time.

The increase in the swelling capacity and ECS dw and a fairly constant ECS app after 4 hr reflect a decrease in the intrafibre water affinity, leading to the rise in  $T_1$ . These results reveal a generally low initial intrafibre water affinity. The expressed juice is also quite high in this carcass, supporting the above conclusions.

The reduction in the  $T_1$  data when the intrafibre water affinity increases at 3 hr is the most pronounced of all the carcasses examined. The reason for this may be indicated in the isometric tension profile (Figure III.5). The tension did not begin to increase until 7 hr postmortem. This suggests the crossbridges did not begin forming until that time. Thus factors (perhaps an increase in osmotic pressure) that contribute to an increase in the intrafibre water affinity, often seen during this early prerigor period, may have been enhanced by the absence of rigor bonds. The



initial ATP concentration was relatively low and constant for the first 5 hr ( $\approx 5.3 \mu\text{mole/g}$ ). Perhaps the lower ATP levels were due to the maintenance of a high SR ATPase maintaining  $\text{Ca}^{2+}$  levels within the SR and thus preventing rigor bond formation.

Another reason for the absence of rigor bonds may be the following: The tension generated for this carcass was very high ( $98 \text{ g/cm}^2$ ), which would lead one to predict a large interfilamentous spacing. It is proposed that the absence of tension development early prerigor may also indicate a large interfilamentous distance. The conditions just after 4 hr (pH below 5.9, ATP falling) seem to be ideal from the interpretation of isotonic contraction and mechanical measurement data (discussed earlier in Part B) for crossbridges to be forming. But, as described above, no evidence of rigor bonds was detected until 7 hr, when the isometric tension development begins. Is it possible that at lower  $\text{Ca}^{2+}$  levels (such as may exist near pH 5.9) the inhibitory action of the Tn complex is only partially removed? For muscles where the thick and thin filaments have a close proximity perhaps crossbridges may be able to form when the  $\text{Ca}^{2+}$  concentration is low, but in carcasses with a large interfilamentous spacing crossbridges could not form. In support of this concept, Maughan and Godt (1981) suggested that, if the interfilamentous spacings are very small, crossbridges may form even in a relaxing solution. But in muscles where the filament spacing is large (perhaps



this carcass) the  $\text{Ca}^{2+}$  levels would have to become much higher before the inhibitory action of the Tn complex is totally removed and rigor bonds are formed. These levels would not have been reached until 7 hr postmortem, when isometric tension was generated. The rapid reduction in the  $T_1$  values postpeak (slope = -0.00663 sec/hr) may be due to the water having initially been lost by the fibre rapidly coming back from the ECS to fill the large interfilamental spaces as the concentration of the small molecules within the fibre increased.

#### Carcass 14 ( $\Delta T_1=0.038$ sec)

The  $T_1$  profile for this carcass (Figure III.36) consisted of an increase in  $T_1$  to peak at 10 hr, a slight decrease and then a rise in  $T_1$  postrigor. The ECS app data (Figure III.49) show an initially high intrafibre water affinity. This is rapidly lost until about 5 hr after which the intrafibre water affinity increases, as supported by both a drop in ECS app and  $T_1$  for a short while, and then the  $T_1$  increases to peak at 10 h. The ECS data suggest this increase in  $T_1$  was due to a decrease in the intrafibre water affinity since the ECS app also rose. The expressed juice rose quite quickly in this carcass, reaching a constant value within 12 hr even though rigor was not attained, as judged by isometric tension, until 17 hr. This loss of expressed juice and the rise in  $T_1$  parallel the fall in ATP (Figure V.15). The ATP concentration was 0.1  $\mu\text{mole/g}$  by



12 hr and by 15 hr was 0.05  $\mu$ mole/g, remaining at that level until 17.5 hr when the ATP measurements were completed. The 27 hr ATP concentration was 0.15  $\mu$ mole/g. The slight increase in ATP may have been due to glycolysis continuing after the isometric tension peak at 17 hr. The pH continued to fall until almost 23 hr, but the ATP produced may not have been utilized.

The decrease in the  $T_1$ , after 12 hr (slope = -0.00169 sec/hr) and the increase in  $T_1$ , after the isometric tension ceased ( $\approx$ 17 hr; slope = +.00116 sec/hr) may be interpreted as a greater intrafibre water affinity during isometric tension than when ATP levels are increasing slightly. The fact that ATP may not in itself always contribute to an enhanced intrafibre water affinity may be emphasized through an examination of the data obtained in the model systems. In Figure III.38 data are presented where ATP was added to myofibrils in the presence of EGTA and  $\text{Ca}^{2+}$ . The  $T_1$ , of the EGTA/ATP tube rapidly increased to a slightly reduced but fairly constant value ( $T_1 \approx 1.005$ ) compared to the control tube ( $T_1 = 1.025$ ). Certainly the ATP concentration in the EGTA/ATP tube would have been high for a considerable portion of the first 60 min of  $T_1$  measurements, but this did not lower the  $T_1$ , as seen by a similar  $T_1$  value after 5 hr ( $T_1 = 1.007$ ). In the Ca/ATP tube the  $T_1$  was very much reduced (constant  $T_1$  value at about 0.978). It appears that once the myofibrillar ATPase is activated by  $\text{Ca}^{2+}$  the  $T_1$  will drop. Thus the decrease in  $T_1$ , after 12 hr occurred when the



isometric tension was being generated and the myofibrillar ATPase would have been active. When this activity ceased, even though ATP was being synthesized, the high intrafibre water affinity was lost and the  $T_c$  increased.

The loss of intrafibre water (rising  $T_c$ ) after 17 hr is not surprising when the maximum isometric tension data are examined. The maximum isometric tension was only 24.5 g/cm<sup>2</sup>, which would equate with a very small interfilamental spacing.

#### Carcass 12 ( $\Delta T_c = 0.037$ sec)

The  $T_c$  data (Figure III.35) collected for this carcass showed an initially rapid rise, a plateau at 2-4 hr and then a varied rate of  $T_c$  rise (rapid then slow) to a peak at 9 hr. The postpeak  $T_c$  data consist of a reduced slope until 16 hr (slope = -0.00107 sec/hr) and then a slightly more rapid decline (slope = -0.00182 sec/hr).

The intrafibre water affinity is initially high (low ECS app; Figure III.50) but is lost quite rapidly (ECS app increases). The reduction in the ECS data at  $\approx$ 3-4 hr (data are quite scattered) reveals an increase in intrafibre water affinity, which is then lost (rising ECS app). Therefore, the ECS data agree with the  $T_c$  profile obtained.

The isometric tension profile (Figure III.6) shows rigor bond formation at about 4 hr, at which time the  $T_c$  profile was observed to rise. The maximum isometric tension was obtained at 16.5 hr. Thus the reduced rate of  $T_c$  decline



(9 hr to 16 hr; slope = -0.00107 sec/hr) was during the time of rapid isometric tension development (an active myofibrillar ATPase). This result is different from that observed with carcass 13 and 16. The ATP profile shows an enhanced level of ATP (Figure V.11) during this same period, but it did not seem to be utilized to enhance crossbridge dissociation. It is about 2.1  $\mu\text{mole/g}$  near 10 hr but increases to about 3.8  $\mu\text{mole/g}$  near 12 hr and then falls to 0.05  $\mu\text{mole/g}$  at 15 hr. The ATP level in carcass 13 also increased but it was after the ATP had dropped much lower (0.78  $\mu\text{mole/g}$ ). Under these conditions the swelling capacity increased as the ATP concentration increased. In this carcass (12) the increase in ATP did not improve the swelling capacity nor increase the slope of the  $T_1$  profile. It would seem that in this carcass (12) the rise in ATP levels in the prerigor muscle could not enhance the swelling capacity, illustrating the carcass to carcass variation in response to ATP levels. The glycolytic activity (pH fall continued until 18 hr postmortem) following the cessation of isometric tension produced a small amount of ATP (0.15  $\mu\text{mole/g}$  at 28 hr). This increase in ATP concentration postrigor is similar to that of carcass 14, where the  $T_1$  actually increased postrigor.

A logical question is: "Why is the  $T_1$  slope enhanced postrigor in this muscle while similar circumstances contributed to a rise in the  $T_1$  data for carcass 14?" The answer may be two-fold. Firstly, although the ATP levels



increased to the same values, the muscles may differ in their response to ATP. Secondly, and the most likely, are differences in the dimensions of the lattice. The isometric tension generated is far greater in this carcass compared to carcass 14 ( $24.5 \text{ g/cm}^2$ ). Those results suggest that the interfilamentous distances for carcass 12 are greater than those of carcass 14. As a result the water more easily enters the interfilamentous spaces and the  $T_1$  falls.

The initial expressed juice (Figure III.6) was relatively high ( $\approx 4\%$ ) in this carcass and rose quickly when the isometric tension rate increased at 9 hr. The loss of WHC under high pressure where the isometric tension rapidly develops is common in almost all the carcasses examined. However, the  $T_1$  response in this carcass is actually declining. These results support the concept that the  $T_1$  is measuring factors affecting the weakly immobilized water in the carcass, whereas WHC measurements, especially at high pressure, are not.

#### Carcass 8 ( $\Delta T_1 = 0.035 \text{ sec}$ )

Carcass 8 was the only animal in this study for which the muscle was soft and exudative. Isometric tension data were not obtained for this carcass, but the unique properties of this carcass in this study warrant placing it in this section.

This animal was viewed as stress-susceptible, as evidenced by preslaughter hyperventilation and an extremely



rapid postmortem pH fall (Figure III.2). These observations were supported by rapid drop in ATP (Figure V.3; 0.05  $\mu\text{mole/g}$  at 4.5 hr).

During the postmortem period the ECS app (Figure III.51) was immediately high (17 mL/100 g at 1 hr; 32 mL/100 g at 2 hr) and continued to rise to peak at 36 mL/100 g at 7.5 hr. This was followed by a period in which the ECS app fell to 16 mL/100 g at 12 hr, but then rose to 39 mL/100 g at 30 hr. The ECS data may be interpreted as an immediate loss of membrane functionality, which may later regain some partial functionality, only to lose it again as rigor developed. The loss of membrane functionality may lend support to the concept of a generalized membrane defect being associated with stress-susceptible animals (Basarab *et al.*, 1980; King *et al.*, 1976).

Although the pH did not fall very much after 7.5 hr, the ultimate pH (5.68) was reached by 20 hr postmortem. This continuing glycolytic activity contributed to an increase in ATP. At 7.5 hr the ATP concentration was 0.05  $\mu\text{mole/g}$ , but by 9 hr it had risen to 0.15  $\mu\text{mole/g}$ . Although the  $T_1$  values rose quite rapidly (Figure III.35) during the prerigor period, they began to fall when the ATP levels increased at 9 hr. The slope showed varying rates of decline until 24 hr, when the  $T_1$  values again began to rise. Without the isometric tension profile it is difficult to interpret the  $T_1$  data with respect to interfilamental spacings. The reduction in ECS app may have indicated an increase in the



intrafibre water affinity, but the loss of membrane impermeability to inulin makes the interpretation difficult.

#### Carcass 9 ( $\Delta T_1 = 0.035$ sec)

The ECS data (Figure III.52) show an initial increase in ECS app and ECS dw which leads to a rise in the  $T_1$  profile (Figure III.35). In the region of 4-7 hr the  $T_1$  plateaus and at the same time ECS app falls to some of the lowest ECS app (-4.5 mL/100 g) values determined. Thus the intrafibre water affinity can be viewed as particularly high. However, the  $T_1$  values do not fall (compare with carcass 11) since isometric tension development had begun by 2.5 hr postmortem (Figure III.3). After 7 hr the  $T_1$  values rise to peak at 13 hr postmortem. The ECS data are also rising rapidly during this period, confirming a loss in the intrafibre water affinity.

The maximum isometric tension (62.5 g/cm<sup>2</sup>) was reached at 12.5 hr, but the pH continued to fall. The rate of pH fall actually increased after 13 hr and, as a result, the ATP levels quickly rose (in the absence of the myofibrillar ATPase) to be greater than 0.5  $\mu$ mole/g at 15 hr. The combination of a large interfilamentous space and high ATP levels contributes to a rapid increase in the intrafibre water (fall in  $T_1$ ; slope = -0.00268 sec/hr). Perhaps the ATP may actually have dissociated some of the rigor bonds.



### Carcass 17 ( $\Delta T_1=0.031$ sec)

Although the initial ECS app (Figure III.53) is very high, the intrafibre water affinity increased or at least remained the same between 1.5-3 hr postmortem. Both the ECS data and the  $T_1$  data (Figure III.36) revealed a strange pattern of change in intrafibre water affinity. The intrafibre water affinity would be rapidly lost and regained or remain constant, this cycle being repeated. The initial rapid rise in  $T_1$  near 4 hr was evidently due to the formation of crossbridges since the isometric tension (Figure III.11) was initiated at that time. Problems with the NMR unit interrupted the collection of data between 9 and 11 hr. It is not known if the reduction in  $T_1$  observed here is actual or due to the readjustment of the frequency of the NMR. (Because of the apparent similarities in the ATP concentrations, isometric tension, pH and  $T_1$  profiles between carcasses 17 and 18 near rigor, the following section on carcass 18 can be examined for discussion of similar results.)

### Carcass 18 ( $\Delta T_1=0.020$ sec)

The ECS data (Figure III.54) for this carcass show very little change in the intrafibre water affinity with time postmortem. In fact the initial  $T_1$  value (Figure III.36) declined until the crossbridge formation at 3 hr caused a sharp rise in the  $T_1$ . The overall swelling capacity tended to increase during this time. The approximately uniform



divergence in ECS dw and ECS app with swelling may be interpreted as a nearly uniform increase in both the ECS dw and ECS app. This would be expected if little change in intrafibre water affinity were occurring. The loss of intrafibre water affinity between 8 and 10 hr followed by an increase in the intrafibre water affinity at 12 hr, as judged by the ECS data, was not observed in the T<sub>1</sub> data.

The isometric tension peaks (79 g/cm<sup>2</sup>; Figure III.12) near 8.5 h and a second peak at 12 hr (65 g/cm<sup>2</sup>) correspond to an ATP concentration of 2.4 μmole/g at 8.5 hr and 0.35 μmole/g at 12 hr. However, the ATP concentration (Figure V.23) at 27 hr was 0.05 μmole/g. These observations suggest ATP levels were falling when isometric tension was not being generated. The source of ATP utilization in the absence of isometric tension is not known. The ultimate pH at 8 hr confirms the presence of rigor near 8 hr but, except for the isometric tension peak at 12 hr, no clear source of ATP utilization is evident.

The pH profile is surprising and unique (Figure III.12). The most interesting aspect of these data may be related to the T<sub>1</sub> data. The T<sub>1</sub> values remained nearly constant between 8.5 and 16 hr. During the period between 8 and 14 h postmortem pH rapidly rose from an ultimate pH of 5.65 to 5.77 and then slowly increased at a uniform rate. Thus a correlation between pH rise and a constant T<sub>1</sub> seems to exist. An explanation for this observation is not known.



The high isometric tension would denote a large interfilamental spacing. This would contribute to the rapid reduction in the  $T_1$  data after 16 hr. The  $T_1$  slope gradually increased with time postmortem. The rate may actually be increasing with a fall in ATP concentration. Little change in the  $T_1$  profile between 11 and 17 hr may reflect the tightening of the myofibrillar structure due to salt bridge formation. When the salt bridges are removed, the reduction in  $T_1$  associated with a large interfilamental spacing may be quite rapid.

#### Statistical Correlations

From the above discussion of carcasses 9 to 18 it would be expected that some of the measurements would reveal significant correlation coefficients relevant to this study. Several of the correlation coefficients that are related to the interpretation of the  $T_1$  data are presented in Table III.10. The information presented has been obtained from the more extensive table of Pearson's correlation coefficients found in Appendix H (Table V.2).

One of the measurements used to interpret the plot of  $T_1$  vs time postmortem has been ECS app. The rise and fall in the prerigor ECS app profile, for many of the carcasses, has been interpreted as an initial loss of intrafibre water followed by a regaining of this water. The significant correlations between the time to the  $T_1$  plateau and the time to the initial ECS app peak ( $r=.7451$ ,  $p=.020$ ), the time to



Table III.10 Pearson's correlation coefficients of selected variables from carcasses 9-18

	r	p
Time to $T_1$ , plateau and time to initial ECS app peak	0.7451	0.020
initial ECS app postpeak minimum	0.6721	0.038
ECS app of 15 mL/100 g	0.6641	0.029
$\Delta T_1$ , and		
initial expressed juice (%)	0.6639	0.029
moisture content	0.6793	0.025
time to ECS app of 15 mL/100 g	0.7320	0.014
time to 10% expressed juice	0.6061	0.046
time to 20% swelling capacity	0.6810	0.025
postrigor expressed juice (%)	0.8067	0.005
First postpeak $T_1$ , slope and		
prepeak isometric slope	-0.6566	0.031
time to maximum isometric tension	-0.6075	0.046
Second postpeak $T_1$ , slope and		
maximum isometric tension	-0.7687	0.009
time of isometric tension initiation	-0.6220	0.041
Initial $T_1$ , and		
first postpeak $T_1$ , slope	-0.7042	0.016
second postpeak $T_1$ , slope	-0.6198	0.042
Peak $T_1$ , and		
first postpeak $T_1$ , slope	-0.6288	0.039
second postpeak $T_1$ , slope	-0.5892	0.052
Maximum isometric tension and		
initial ECS app	0.8650	0.002
initial ECS app postpeak minimum	0.6729	0.038
Initial expressed juice and		
postrigor swelling capacity	0.6101	0.045
Time to 5 $\mu$ mole ATP/g and		
postrigor swelling capacity	-0.6744	0.026
Time to 1 $\mu$ mole ATP/g and		
time to ECS app of 15 mL/100 g	0.7138	0.027
Postrigor ATP concentration and		
time to peak $T_1$	0.6478	0.033
time to $T_1$ , plateau	0.7542	0.011
time to initial ECS app peak	0.6511	0.045
time to initial ECS app postpeak minimum	0.7480	0.019
prepeak isometric tension slope	-0.7744	0.008

All times in hours.



the ECS app minimum after the ECS app peak ( $r=.6721$ ,  $p=.038$ ) and the time to an ECS app value of 15 mL/100 g ( $r=.6641$ ,  $p=.029$ ) all support the view that  $T_1$  is reflecting the changing intrafibre water affinity of the muscle as it enters rigor. Thus the  $T_1$  and ECS measurements are a measure of a similar muscle property.

The difference between the initial  $T_1$  and the peak  $T_1$  is termed  $\Delta T_1$ . The significant correlations presented in Table III.10 indicate that  $\Delta T_1$  is large if the initial expressed juice is high (low water holding capacity;  $r=.6639$ ,  $p=0.29$ ) or the moisture content is high ( $r=.6793$ ,  $p=.025$ ). The  $\Delta T_1$  is also large if the time to the ECS app value of 15 mL/100 g ( $r=.7320$ ,  $p=.014$ ), time to 10% expressed juice ( $r=.6061$ ,  $p=.046$ ) and the time for the swelling capacity to reach 20% swelling capacity ( $r=.6810$ ,  $p=.025$ ) are long. A muscle with a large postrigor expressed juice value would also correlate with a large  $\Delta T_1$  ( $r=.8067$ ,  $p=.005$ ). It is interesting that the above factors that were showing significant correlations with  $\Delta T_1$  are also measurements of water properties. For this reason the correlations do not indicate a cause for the size of the  $\Delta T_1$ , but are a response to a similar causative factor.

Several of the carcasses studied had, for the same carcass, different postpeak  $T_1$  slopes. The first postpeak  $T_1$  slope showed a significant correlation with the prepeak isometric slope ( $r=-.6566$ ,  $p=0.031$ ). This means that a greater negative  $T_1$  slope would correlate with a rapid



isometric tension development. This correlation would support the view discussed earlier in this thesis that the ordering of the water (reduction of  $T_1$ ) was enhanced during isometric tension development (a rapid ATPase). The initial postpeak  $T_1$  slope and the time to the maximum isometric tension were also significantly correlated ( $r=-.6075$ ,  $p=.046$ ). Thus a greater negative  $T_1$  slope (an increase in the rate of ordering the muscle water) correlated with a more lengthy rigor development.

The second postpeak slope, usually postrigor, showed a significant correlation with the remaining two isometric tension related measurements made. Here the second postpeak  $T_1$  slope showed a significant correlation with both the maximum isometric tension ( $\text{g/cm}^2$ ;  $r=-.7687$ ,  $p=.009$ ) and the time of the isometric tension initiation ( $r=-.6220$ ,  $p=.041$ ). A large isometric tension has been interpreted as indicating a large interfilamentous space. The above significant correlation ( $r=-.7687$ ,  $p=.009$ ) would suggest that a large interfilamentous spacing (high maximum isometric tension) would enhance the reordering of the water in the postrigor muscle (second  $T_1$  slope was generally postrigor) as revealed by a large negative  $T_1$  slope. It was also suggested in the current study that a delayed isometric tension initiation may be due to a large interfilamentous space. The significant correlation between the second  $T_1$  slope and the time of isometric tension initiation ( $r=-.6220$ ,  $p=.041$ ) supports this proposal. Thus both of the  $T_1$  postpeak slopes show



significant correlations with different aspects of the isometric tension profile. Common factors associated with both the initial and second postpeak  $T_1$  slopes were the initial and peak  $T_1$  values. Thus the correlations between initial  $T_1$  values and the initial and second postpeak slopes were ( $r=-.7042$ ,  $p=.016$ ) and ( $r=-.6198$ ,  $p=.042$ ), respectively. These correlations suggest that a high initial or peak  $T_1$  would correspond to a rapid fall in the  $T_1$  values measured postpeak. It appears that the greater the content of free water in prerigor muscle, the greater the rate of reordering in the postrigor muscle. The moisture content of the muscle did not show a significant correlation with postpeak  $T_1$  slopes as one may expect from the above correlation.

The ECS app and  $T_1$  data are considered to reveal changes in the intrafibre water affinity. However, a puzzling correlation has been found between the maximum isometric tension and initial ECS app ( $r=.8650$ ,  $p=.002$ ) and the initial postpeak ECS app minimum ( $r=.6729$ ,  $p=.038$ ). These significant correlations imply that a large isometric tension relates to a high ECS app. However, high ECS app has been interpreted as indicating a low intrafibre water affinity. On the other hand, a high isometric tension is considered to equate with a large interfilamental space which contributes to an enhanced rate of postpeak  $T_1$  reduction (ordering of the muscle water).



It would seem logical that a large interfilamental space would lead to a fibre having a high intrafibre water affinity. Thus a low ECS app may be expected to correlate with a large isometric tension. The opposite is found. An explanation for the above seeming discrepancy may be the following. The ECS app measurement is only reliable when the membrane of the muscle fibre is functional (excludes inulin). At the time of maximum isometric tension the evidence exists that the membrane is no longer excluding inulin and thus a comparison of the intrafibre water affinity, at that point in time, on the basis of ECS app data can not be made. It does force one to conclude that the intrafibre water affinity is not consistent throughout rigor development. It is interesting that a high  $T_1$  (high free water content, perhaps as a result of a low intrafibre water affinity) correlates with more rapid postpeak  $T_1$  slopes (see above). This is in agreement with the observation that a high ECS app (low intrafibre water affinity) shows a significant correlation with maximum isometric tension (large interfilamental space). An additional relationship supporting the above correlations is the significant correlation between the initial expressed juice and the postrigor swelling capacity ( $r=.6101$ ,  $p=.045$ ). This positive correlation indicates that a high initial expressed juice (low WHC) prerigor correlates with a high postrigor swelling capacity. Hamm (1974) indicated that meat with a high swelling capacity also has good water retentive



properties. Thus all these correlations seem to suggest that a low water holding capacity prerigor relates to improved water retention properties postrigor.

In the discussion of the individual carcasses it has been found that the response to ATP levels in the muscle is variable. For some carcasses ATP would appear to enhance the water holding properties of the meat but again in others the ATP had no affect. This variability in response has meant that very few significant correlations between ATP and other factors have been found.

One of the significant correlations is between the time postmortem to 5  $\mu$ mole ATP/g of muscle and the postrigor swelling capacity ( $r=-.6744$ ,  $p=.026$ ). This negative correlation suggests that the more rapidly the ATP concentration is depleted prerigor, the greater is the swelling capacity postrigor. It may be that this loss of ATP is related to the reduced water holding capacity prerigor, which in turn could be associated with an improved water holding capacity postrigor. The nature of the relationship, however, is unclear.

Another significant correlation involving ATP is the time postmortem to 1  $\mu$ mole/g ATP and the time to an ECS app of 15 mL/100 g ( $r=.7138$ ,  $p=.027$ ). The longer it takes to reach 1  $\mu$ mole ATP/g, the longer it takes for the ECS app to rise to 15 mL/100 g. Perhaps this indicates that ATP is needed to maintain the functionality of the cell membrane so that inulin can be excluded from the membrane.



The only measurement of ATP that had any relation to  $T_1$ , was the postrigor ATP concentration. Postrigor ATP concentration showed a significant correlation between the time to peak  $T_1$  ( $r=.6748$ ,  $p=.033$ ) and the time to the  $T_1$  plateau ( $r=.7542$ ,  $p=.011$ ). This positive correlation indicates that if the time to these  $T_1$  points is long the ATP concentration postrigor is high. In agreement with this correlation, the postrigor ATP concentration and the time to the initial ECS app peak ( $r=.6511$ ,  $p=.045$ ) and the time to the ECS app postpeak minimum ( $r=.7480$ ,  $p=.019$ ) also showed significant correlations. Since both  $T_1$  and ECS app are viewed as measuring a similar muscle property, the fact that both of these parameters are significantly correlated is not surprising. The only other significant correlation involving ATP was the correlation between the postrigor ATP concentration and the prepeak isometric tension slope ( $r=-.7744$ ,  $p=.008$ ). This negative correlation indicates that a high postrigor ATP concentration relates to a low prepeak isometric slope. A reason for the low prepeak isometric slope may be a reduced ATPase activity. For this reason the glycolytic activity of the carcass may lead to a production of ATP without it being fully utilized by the contractile mechanism of the muscle and thus the postrigor ATP levels will be high.



## Conclusion

The major contribution of this study has been the development of several techniques which may provide a fresh approach to the study of muscle water.

The NMR T<sub>1</sub> determination of water in muscle is not a new technique, but the measurement of T<sub>1</sub> during the course of rigor development on several beef carcasses is a new application of the technique. The T<sub>1</sub> profile generated in this approach has revealed a very sensitive method of measuring changes in the intrafibre water. A reduction in T<sub>1</sub> has been interpreted as an immobilization of the muscle water. A major factor leading to the immobilization of the muscle water is the association of the water with the myofibrils within the muscle fibre. The amount of water associated with the myofibrils is primarily a result of the interfilamentous spacing between the thick and thin filaments. This water cannot be viewed as "bound" water, but may, as Offer and Trinick (1983) stated, be water maintained by capillarity and be similar to "bulk" water. This perhaps explains why the changes in T<sub>1</sub>, although detectable, are small. A comparison of expressed juice measurements and T<sub>1</sub> demonstrates that the T<sub>1</sub> measurement is sensitive to this "free" water. The WHC measurements show the water in the postrigor muscle is not firmly held, since the expressed juice values are high. However, the T<sub>1</sub> values may actually be falling when the expressed juice values are rising or remaining constant. Clearly the T<sub>1</sub> is measuring a reordering



of this weakly immobilized water.

An explanation for the general shape of the T<sub>1</sub> profile may include the following: Initially the T<sub>1</sub> rises rapidly, likely due to the hyperosmotic environment of the extracellular space. Shortly after this initial rise, conditions within the cell are altered such that the intrafibre water affinity increases. In view of the observations of Winger and Pope (1980-81), this is likely due to an increase in the concentration of the small molecules within the cell. This increase in intrafibre water affinity is short lived since numerous crossbridges are formed during the rapid development of isometric tension, which tighten the interfilamentary spacing and water is lost from the cell. Another factor contributing to an increase in T<sub>1</sub>, may be an increase in the number of salt bridges. Hamm (1974) suggested that, as the pH drops and the isoelectric points of the myofibrillar proteins are reached, the repulsive forces decrease and the number of salt bridges increases. Salt bridges between the fixed anions in the cell ( $\beta$ - and  $\gamma$ -carboxyl groups) and the fixed cationic groups ( $\epsilon$ -amino, quanidyl and imadazole groups) can occur, tightening the muscle structure and forcing water into the extracellular space.

As the small molecule concentration increases and the effect of an increased number of crossbridges equilibrates, a peak in the T<sub>1</sub> profile is obtained. The isometric tension may or may not be complete at the time of this peak. In



fact, it has generally been observed in this study that the intrafibre water affinity is enhanced postpeak if the isometric tension was still being generated. Since the myofibrillar ATPase is active during this period of isometric tension, it was suggested that a greater intrafibre affinity exists when the ATPase is active than when it is absent. During ATPase activity more of the crossbridges are dissociated when the myosin-ATP complex is formed than when the isometric tension is not generated. This may increase the interfilamental spacing and enhance the intrafibre water affinity.

In all but three carcasses the  $T_1$  continued to fall during the postrigor period. It is difficult to envisage this increase in intrafibre water affinity to be due to a reduction in the number of crossbridges. The increase in the ATP concentration of some carcasses after the isometric tension peaked might be considered to reduce the number of crossbridges. However, the presence or absence of ATP seemed to have little bearing on the size of the slope postrigor. Rather than ATP influencing the size of the slope postrigor, it is more likely a result of the size of the interfilamental spacing and a reduction in the number of salt bridges which increases the intrafibre water affinity.

Ling and Peterson (1977) examined cell swelling in high concentrations of KCl. Normally, cells in a hypertonic environment shrink. However, in the presence of high KCl concentrations cells swell. Previously this had been thought



to be due to a high permeability of the cell membrane to KCl. But Ling and Walton (1976) showed that swelling in concentrated KCl was indifferent to the presence of an intact cell membrane. Ling and Peterson (1977) concluded that for the fixed anions in the cells ( $\beta$ - and  $\gamma$ -carboxyl groups)  $K^+$  is preferred to  $Na^+$ . For this reason, although high  $Na^+$  concentrations will cause the cell to shrink,  $K^+$  will cause the cell to swell since the salt bridges will be disrupted by  $K^+$ . Perhaps the breakage of the salt bridges (formed during rigor development) by  $K^+$  increases the intrafibre water affinity. It may be possible that there are fewer salt bridges in carcasses where the interfilamental spacing is large and for each salt bridge disrupted the intrafibre water affinity is enhanced to a greater degree than for carcasses where the interfilamental spacing is small. The early observations of Arnold *et al.* (1956), wherein the WHC improved with an increase in the extractable  $Ca^{2+}$ , may also contribute to the fall in  $T_1$ . It may be that  $Ca^{2+}$  could bridge two carboxyls, tightening the myofibrillar structure. The displacement of  $Ca^{2+}$  by a monovalent ion, such as  $K^+$ , would open up the structure and increase the intrafibre water affinity.

The sensitivity of the  $T_1$  measurement to intrafibre water affinity should be invaluable in further studies of muscle water. A measure of the changes in  $T_1$  of the muscle will provide a history of changes in the muscle water that should help in the interpretation of postrigor water holding



properties.

A second technique that has been developed in this study is the ECS measurement. This is a unique approach to the measure of the intrafibre water affinity. Although the  $T_1$  profile reflects changes in the intrafibre water affinity, it does not allow the researcher to classify the early prerigor muscles as having a high, intermediate or low intrafibre water affinity. The ECS measurement does provide a means to achieve this classification. The importance of this measurement in establishing the initial intrafibre water affinity is supported by the results obtained for carcass 6 (Appendix F). Although the  $\Delta T_1$  was very small, the ECS data revealed a very low intrafibre water affinity in the early prerigor muscle. Unfortunately, the technique is only applicable to the early prerigor muscle since the membrane becomes permeable to the inulin near rigor. The results obtained from the stressed animal (carcass 8) confirm the concept of membrane failure in the early postmortem period of stressed animals. The return of the ECS values to more reasonable ones as rigor progressed implies that the membrane may regain functionality after the initial failure. It remains to be seen whether the increase in ATP concentration, after initially being lost, may be the source of the regaining of membrane functionality. The ECS measurement developed in this study may serve as an additional tool to examine membrane functionality.



For the majority of the carcasses, the ECS app rose and then fell in the early prerigor muscle. This has been interpreted as a loss of intrafibre water affinity which gave way to an increase in intrafibre water affinity. This observation is supported by a comparable rise and then a plateau in the  $T_1$  profile before rising again. Heffron and Hegarty (1974) were the first to demonstrate the loss of water from the fibre into the ECS. This was shown by both ECS measurements and the shrinkage of the fibres observed in photographs of transverse sections of muscle fibres entering rigor. They did not report the reduction in ECS near 4 to 5 hr postmortem that was observed in this study. The reason for this may be the fact that mouse muscle rapidly enters rigor ( $\approx 3$  hr) and the incubation period would interfere with the measurement of these more rapid transitions.  $T_1$  profiles of some rat muscle samples (personal observation at the beginning of this study) did reveal plateaus, suggesting similar changes to those with beef are occurring in the muscle water of the rat. A second factor may be differences in the incubation procedure. In Heffron and Hegarty's (1974) study the muscle was incubated in the presence of 95%  $O_2$ , 5%  $CO_2$ , whereas in this study the gases were omitted. The  $O_2$  introduced into the study may have helped the muscle regain some of the functionality lost during rigor development and would have made detection of the fall in ECS impossible. The initial increase in ECS observed in this study does show that water is moving into the ECS, supporting the results of



Heffron and Hegarty (1974), Pearson *et al.* (1974) and Penny (1977).

The translocation of water observed in this study may influence the mechanical properties of meat. It has been observed that during the development of rigor the initial and final yield tensions rise until crossbridges begin to form about pH 5.9. The phase contrast micrographs presented in this study reveal that this rise in tension is accompanied by an extensive stretching of the muscle fibre without myofibrillar units slipping past one another. This observation could be explained by a reduction in the intrafibre water, due to the movement of the water out of the fibre, which increases the adhesive forces between myofibrillar units. The adhesive tension profiles support the above observations in that a rise in tension was observed until rigor bonds formed. However, the response near rigor showed a variability between carcasses which reflected differences in the rate of rigor development. These observations support the conclusion that differences in the intrafibre water affinity are reflected in the mechanical properties of meat.

A third method developed was the HPLC determination of ATP and its metabolites. The role of ATP and its affect on intrafibre water affinity has been variable. In some carcasses high ATP levels enhanced the WHC and increased the intrafibre water affinity, whereas in others the affect was negligible. Perhaps the observations of Izumi *et al.* (1981),



discussed earlier, may be relevant to these observations.

As an overview of the role of ATP in affecting the WHC in the muscle, the results in this study support the conclusions of Honikel *et al.* (1981) who consider that the hydrolysis of ATP itself is not the main reason for postmortem alteration in WHC. Rather, it is the development of rigor mortis initiated by the depletion of ATP that alters the postmortem WHC. This would lead to a reduction in the interfilamentous spacing due to crossbridge formation (Goldman *et al.*, 1979). Offer and Trinick (1983), although discussing primarily the effect of salt concentration on WHC, have re-emphasized the repulsive forces between the filaments as the major factor affecting WHC. Any substance which can disrupt the constraints to swelling (Z- and M-lines and crossbridges), leading to a widening of the interfilamentous spacing, will enhance WHC. Thus the variability in the swelling and intrafibre water affinity of the postrigor muscle strips in the presence of ATP may be reflected in a variability in the concentration at which ATP can effect dissociation of the crossbridges, as suggested by Izumi *et al.* (1981). A variability in the extent of crossbridge formation may be supported by Offer and Trinick (1983), who found differences in the concentration of NaCl required to remove the above-mentioned constraints to swelling.

Many of the interpretations of the data in this study require further examination to substantiate them. It will be



necessary to include measurements of the lattice spacing, ion distribution and the nature and number of crossbridges to provide a more definitive explanation of the observations contained in this study. An examination of myofibrils from the respective muscles using the procedure of Offer and Trinick (1983) may provide information about the carcass to carcass variability in the constraints to swelling (Z- and M-lines and the strength of the crossbridges). This, in conjunction with the methods developed in this study, should allow meat researchers to classify muscle into different categories of water retention properties and then carefully examine why these differences exist.



#### IV. REFERENCES

- April, E.W. and Brandt, P.W. 1973. The myofilament lattice: studies on isolated fibres. III. The effect of myofilament spacing upon tension. *J. Gen. Physiol.* 61:490.
- Arnold, N., Wierbicki, E. and Deatherage, F.E. 1956. Post mortem changes in the interactions of cations and proteins of beef and their relation to sex and diethyl-stilbestrol treatment. *Food Technol.* 10:245.
- Asghar, A. and Yeates, N.T.M. 1978. The mechanism for the promotion of tenderness in meat during post-mortem aging process. *Crit. Rev. Food Sci.* 10:115.
- Attrey, D.P., Radhakrishna, K. and Sharma, T.R. 1981. A reappraisal of methods of determination of total nucleotides in sheep postmortem muscle. *J. Food Sci. Technol.* 18:18.
- Aubin, M., Prud'homme, R.E., Pezolet, M. and Caille, J.-P. 1980. Calorimetric study of water in muscle tissue. *Biochim. Biophys. Acta.* 631:90.
- Basarab, R.T., Berg, R.T. and Thompson, J.R. 1980. Erythrocyte fragility in "double-muscled" cattle. *Can. J. Anim. Sci.* 60:869.
- Behnke, J.R., Fennema, O. and Haller, R.W. 1973. Quality changes in prerigor poultry at -3°C. *J. Food Sci.* 38:275.



- Belton, P.S., Jackson, R.R. and Packer, K.J. 1972. Pulsed NMR studies of water in striated muscle. I. Transverse nuclear spin relaxation times and freezing effects. *Biochim. Biophys. Acta* 286:16.
- Belton, P.S., Packer, K.J. and Sellwood, T.C. 1973. Pulsed NMR studies of water in striated muscle. II. Spin-lattice relaxation times and the dynamics of the non-freezing fraction of water. *Biochim. Biophys. Acta* 304:56.
- Bendall, J.R. 1961. In: "The Structure and Function of Muscle"; Bourne, G.H. (ed.); Vol. III, p. 264; Academic Press, NY.
- Bendall, J.R. 1973. Postmortem changes in muscle. In: "The Structure and Function of Muscle"; Bourne, G.H. (ed.); Vol. II, 2nd ed., p. 243; Academic Press, NY.
- Bendall, J.R. 1975. Cold contracture and ATP turnover in the red and white musculature of the pig postmortem. *J. Sci. Food Agric.* 26:55.
- Bendall, J.R. and Davey, C.L. 1957. Ammonia liberation during rigor mortis and its relation to changes in the adenine and inosine nucleotides of rabbit muscle. *Biochim. Biophys. Acta* 26:93.
- Berman, M.C. and Kinch, J.E. 1973. Biochemical features of malignant hyperthermia in Landrall pigs. In: "International Symposium on Malignant Hyperthermia"; Gordon, R.A., Brett, B.A. and Kalon, W. (eds.); p. 287; Thomas, Springfield, IL.



Bouton, P.E., Harris, R.V. and Shorthose, W.R. 1971. Effect of ultimate pH upon the water holding capacity and tenderness of mutton. *J. Food Sci.* 36:435.

Bouton, P.E. and Harris, P.V. 1972a. The effects of cooking temperature and time on some mechanical properties of meat. *J. Food Sci.* 37:140.

Bouton, P.E. and Harris, P.V. 1972b. A comparison of some objective methods used to assess meat tenderness. *J. Food Sci.* 37:218.

Bouton, P.E., Harris, P.V. and Shorthose, W.R. 1972. Effect of ultimate pH on ovine muscle water holding capacity. *J. Food Sci.* 37:351.

Bouton, P.E., Harris, P.V. and Shorthose, W.R. 1975. Possible relationships between shear, tensile and adhesion properties of meat and meat structure. *J. Texture Studies* 6:297.

Calkins, C.R., Dutson, T.R., Smith, G.C. and Carpenter, Z.L. 1982. Concentration of creatine phosphate, adenine nucleotides and their derivatives in electrically stimulated and nonstimulated beef muscle. *J. Food Sci.* 47:1350.

Carroll, R.J., Rorer, F.P., Jones, S.B. and Cavanaugh, J.R. 1978. Effect of tensile stress on the ultrastructure of bovine muscle. *J. Food Sci.* 43:1181.

Cassens, R.G., Marple, D.N. and Eikelenboom, G. 1975. Animal physiology and meat quality. *Adv. Food Res.* 21:71.



- Chang, D.C., Hazlewood, C.F. and Woessner, D.E. 1976. The spin lattice relaxation times of water associated with early postmortem changes in skeletal muscle. *Biochim. Biophys. Acta.* 437:253.
- Chen, S.C., Brown, P.R. and Rosie, D.M. 1977. Extraction procedures for use prior to HPLC nucleotide analysis using microparticle chemically bonded packings. *J. Chrom. Sci.* 15:218.
- Chou, D.H. and Morr, C.V. 1979. Protein-water interaction and functional properties. *J. Am. Oil Chem. Soc.* 56:53A.
- Currie, R.W., and Wolfe, F.H. 1979. Relationship between pH fall and initiation of isotonic contraction in postmortem beef muscle. *Can. J. Anim. Sci.* 59:639.
- Currie, R.W. and Wolfe, F.H. 1980. Rigor related changes in mechanical properties (tensile and adhesive) and extracellular space in beef muscle. *Meat Sci.* 4:123.
- Currie, R.W., Jordan, R. and Wolfe, F.H. 1981. Changes in water structure in postmortem muscle, as determined by NMR T<sub>1</sub> values. *J. Food Sci.* 46:822.
- Currie, R.W., Sporns, P. and Wolfe, F.H. 1982. A method for the analysis of ATP metabolites in beef skeletal muscle by HPLC. *J. Food Sci.* 47:1226.
- Davey, C.L. 1961. The amination of inosine monophosphate in skeletal muscle. *Archiv. Biochem. Biophys.* 95:296.



Edman, K.A.P. and Andersson, K.E. 1968. The variation in active tension with sarcomere length in vertebrate skeletal muscle and its relation to fibre width. *Experientia* 24:134.

Edzes, H.T. and Samulski, E.T. 1978. The measurement of cross relaxation effects in the proton NMR spin lattice relaxation of water in biological systems: Hydrated collagen and muscle. *J. Magnetic Res.* 31:207.

Eino, M.F. and Stanley, D.W. 1973. Catheptic activity, textural properties and surface ultrastructure of post-mortem beef muscle. *J. Food Sci.* 38:45.

El-Badawi, A.A., Anglemier, A.F. and Cain, R.F. 1964. Effects of soaking in water, thermal enzyme inactivation and irradiation on the textural factors of beef. *Food Technol.* 18:1807.

Fischer, C. and Honikel, K. 1978. Biochemische Unterschude von blassen, wäbrigem und dunklem, leimigem Rindfleisch kurz nach der Schlachtung. *Die Fleischwirtschaft* 58:1348.

Franzini-Armstrong, C. 1973. The stucture of a simple Z line. *J. Cell Biol.* 58:630.

Fung, B.M. and Puon, P.S. 1981. Nuclear magnetic resonance transverse relaxation in muscle water. *Biophys. J.* 33:27.

Gard, D.L. and Lazarides, E. 1979. Specific fluorescent labeling of chicken myofibril z-line proteins catalysed by guinea pig transglutaminase. *J. Cell Biol.* 81:336.



- Godt, R.E. and Maughan, D.W. 1977. Swelling of skinned muscle fibres of the frog: experimental observations. *Biophys. J.* 19:103.
- Goldman, Y.E., Matsubara, I. and Simmons, R.M. 1979. Lateral filamentary spacing in frog skinned muscle fibers in the relaxed and rigor states. *J. Physiol.* 295:80P.
- Goll, D.E., Arakawa, N., Stromer, M.H., Busch, W.A. and Robson, R.M. 1970. Chemistry of muscle proteins as food. In: "The Physiology and Biochemistry of Muscle as Food. II."; Briskey, E.J., Cassens, R.G. and Marsh, B.B. (eds.); Ch. 36, p. 755; Univ. Wisconsin Press, Madison, WI.
- Grau, R. and Hamm, K. 1957. Über das Wasserbindungvermögen des Sägetiermuskels. II. M.H. Über die Bestimmung der Wasserbindung des Muskels. *Z. Lebensm. Untersuch. u. Forsch.* 105:446.
- Guth, L. and Samaha, F.J. 1969. Qualitative differences between actomyosin ATPase of slow and fast mammalian muscle. *Exp. Neurol.* 25:138.
- Hamm, R. 1960. Biochemistry of meat hydration. *Adv. Food Res.* 10:355.
- Hamm, R. 1974. Water holding capacity of meat. *Proc. East. Sch. Agric. Sci. Univ. Nottingham.* p. 321.
- Hamm, R., Honikel, K.O., Fischer, C. and Hamid, A. 1980. Veränderungen des Rindfleisches nach dem Schlachten und ihre Auswirkungen auf das Wasserbindungsvermögen. *Fleischwirtschaft* 60(9):1567.



- Harris, P.V. 1976. Structural and other aspects of meat tenderness. *J. Texture Stud.* 7:49.
- Hawrysh, A.J., Price, M.A. and Berg, R.T. 1979. The influence of cooking temperature on the eating quality of beef from bulls and steers fed 3 levels of dietary roughage. *Can. Inst. Food Sci. Technol. J.* 12:72.
- Hay, J.D., Currie, R.W. and Wolfe, F.H. 1973a. Effect of postmortem aging on chicken breast muscle sarcoplasmic reticulum. *J. Food Sci.* 38:700.
- Hay, J.D., Currie, R.W. and Wolfe, F.H. 1973b. Polyacrylamide disc gel electrophoresis of fresh and aged chicken muscle proteins in sodium dodecylsulfate. *J. Food Sci.* 38:987.
- Hay, J.D., Currie, R.W., Wolfe, F.H. and Saunders, E.S. 1973. The effects of postmortem aging on chicken muscle fibrils. *J. Food Sci.* 38:981.
- Hazlewood, C.F., Chang, D.C., Nichols, B.L. and Woessner, D.E. 1974. Nuclear magnetic resonance transverse relaxation times of water protons in skeletal muscle. *Biophys. J.* 14:583.
- Heffron, J.J.A. and Hegarty, P.V.J. 1974. Evidence for a relationship between ATP hydrolysis and changes in extracellular space and fibre diameter during rigor development in skeletal muscle. *Comp. Biochem. Physiol.* 49A:43.



- Hegarty, P.V.J. 1972. Molecular and macroscopic extensibility of rigor skeletal muscle due to stretch tension. *Life Sci.* 11:155.
- Honikel, K.O., Fischer, C., Hamid, A. and Hamm, R. 1981. Influence of postmortem changes in bovine muscle on the water-holding capacity of beef. Postmortem storage of muscle at 20°C. *J. Food Sci.* 46:1.
- Hostetler, R.L., Link, B.A., Landmann, W.A. and Fitzhugh, H.A. 1972. Effect of carcass suspension on sarcomere length and shear force of some major bovine muscles. *J. Food Sci.* 37:132.
- Hunt, M.C. and Hedrick, H.B. 1977a. Profile of fibre types and related properties of five bovine muscles. *J. Food Sci.* 42:513.
- Hunt, M.C. and Hedrick, H.B. 1977b. Histochemical and histological characteristics of bovine muscles from four quality groups. *J. Food Sci.* 42:578.
- Hunt, M.C. and Hedrick, H.B. 1977c. Chemical, physical and sensory characteristics of bovine muscle from four quality groups. *J. Food Sci.* 42:716.
- Inch, W.R., McCredie, J.A., Knispel, R.R., Thompson, R.T. and Pintar, M.M. 1974. Water content and proton spin relaxation time for neoplastic and non-neoplastic tissues from mice and humans. *J. National Cancer Inst.* 52:353.



- Izumi, K., Ito, T. and Fukazawa, T. 1981. Effect of ATP concentration and pH on rigor tension development and dissociation of rigor complex in glycerinated rabbit psoas muscle fibre. *Biochim. Biophys. Acta* 678:364.
- Khan, A.W. and Frey, A.R. 1971. A simple method for following rigor mortis development in beef and poultry meat. *Can. Inst. Food Technol. J.* 4:139.
- Khan, A.W. and Lentz, C.P. 1973. Influence of ante-mortem glycolysis and dephosphorylation of high-energy phosphates on beef aging and tenderness. *J. Food Sci.* 38:56.
- Khym, J.X. 1975. An analytical system for rapid separation of tissue nucleotides at low pressures on conventional anion exchangers. *Clin. Chem.* 21:1245.
- King, W.A., Ollivier, L. and Basrur, P.K. 1976. Erythrocyte osmotic response test on malignant hyperthermia - susceptible pigs. *Ann. Gént. Sél. Anim.* 8:537.
- Lawrie, R.A. 1979. *Meat Science*; 3rd ed.; Pergamon Press, NY.
- Ling, G.N. and Walton, C.L. 1976. What retains water in living cells? *Science* 191:293.
- Ling, G.N. and Peterson, K. 1977. A theory of cell swelling in high concentrations of KCl and other chloride salts. *Bull. Math. Biol.* 39:721.
- Locker, R.H. 1960. Degree of muscular contraction as a factor in tenderness of beef. *Food Res.* 25:304.



- Locker, R.H. and Wild, D.J.C. 1982. Yield point in raw beef muscle. The effects of ageing, rigor temperature and stretch. *Meat Sci.* 7:93.
- Martin, A.H. and Fredeen, H.T. 1974. Postmortem pH change as related to tenderness and water holding capacity of muscle from steer, bull and heifer carcasses. *Can. J. Animal Sci.* 54:127.
- Mathur-De Vré, R. 1979. The NMR studies of water in biological systems. *Prog. Biophys. Molec. Biol.* 35:103.
- Matsubara, I. and Elliott, G.F. 1972. X-ray diffraction studies on skinned single fibres of frog skeletal muscles. *J. Molec. Biol.* 72:657.
- Maughan, D.W. and Godt, R.E. 1981. Radial forces within muscle fibres in rigor. *J. Gen. Physiol.* 77:49.
- McCubbin, W.D. and Kay, C.M. 1980. Calcium-induced conformational changes in the troponin-tropomyosin complexes of skeletal and cardiac muscle and their roles in the regulation of contraction-relaxation. *Accounts Chem. Res.* 13:185.
- Millman, B.M. and Nickel, B.G. 1980. Electrostatic forces in muscle and cylindrical gel system. *Biophys J.* 32:49.
- Millman, B.M. 1981. Filament lattice forces in vertebrate striated muscle: relaxed and in rigor. *J. Physiol.* 320:118P.
- Millman, B.M., Racey, T.J. and Matsubara, I. 1981. Effects of hyperosmotic solutions on the filament lattice of intact frog skeletal muscle. *Biophys. J.* 33:189.



- Moller, A.J., Vestergaard, T. and Wismer-Pederson, J. 1973. Myofibril fragmentation in bovine longissimus dorsi as an index of tenderness. *J. Food Sci.* 38:824.
- Nagainis, P. and Wolfe, F.H. 1982. Calcium activated neutral protease hydrolyzes Z-disc actin. *J. Food Sci.* 47:1358.
- Naguno, Y. and Matsuo, H. 1979. Fish and meat gel strength and water binding increase with guanylate. *Jpn. Kohai Tokhyo Koho 79 19454 (C1 A23L 1/31) 16 July 1979, Appl. 70/68, 650 07 Aug 1970.*
- Nakamura, R. 1973. Factors associated with postmortem increase of extractable Ca in chicken breast muscle. *J. Food Sci.* 38:1113.
- Newbold, R.P. and Scopes, R.K. 1967. Post-mortem glycolysis in ox skeletal muscle. *Biochem. J.* 105:127.
- Nuss, J.I. and Wolfe, F.H. 1980-81. Effect of post-mortem storage temperatures on isometric tension, pH, ATP, glycogen and glucose-6-phosphate for selected bovine muscles. *Meat Sci.* 5:201.
- Offer, G. and Trinick, J. 1983. On the mechanism of water holding in meat: the swelling and shrinking of myofibrils. *Meat Sci.* 8:245.
- Pappius, H.M. and Elliot, K.A.C. 1956. Water distribution in incubated slices of brain and other tissues. *Can. J. Biochem. Physiol.* 34:1007.
- Pearson, R.T., Duff, I.D., Derbyshire, W. and Blanshard, J.M.V. 1974. An NMR investigation of rigor in porcine muscle. *Biochim. Biophys. Acta* 362:188.



- Peemoeller, H. and Pintar, M.M. 1979. Nuclear magnetic resonance multiwindow analysis of proton local fields and magnetization distribution in natural and deuterated mouse muscle. *Biophys. J.* 28:339.
- Peemoeller, H., Pintar, M.M. and Kydon, D.W. 1980. Nuclear magnetic resonance analysis of water in natural and deuterated mouse muscle above and below freezing. *Biophys. J.* 29:427.
- Penny, I.F. 1977. The effect of temperature on the drip, denaturation and extracellular space of pork *longissimus dorsi* muscle. *J. Sci. Food Agric.* 28:329.
- Pezolet, M, Pigeon-gosselin, M., Savoie, R. and Caillé, J.P. 1978. Laser Raman investigation of intact single muscle fibres. On the state of water in muscle tissues. *Biochim. Biophys. Acta* 544:394.
- Ranken, M.D. 1976. The water holding capacity of meat and its control. *Chem. and Ind.* 24:1052.
- Riss, T.L., Zorich, N.L., Williams, M.D. and Richardson, A. 1980. A comparison of the efficiency of nucleotide extraction by several procedures and the analysis of nucleotides from extracts of liver and isolated hepatocytes by HPLC. *J. Liquid Chrom.* 3:133.
- Rowe, R.W.D. 1974. Collagen fibre arrangement in intramuscular connective tissue. Changes associated with muscle shortening and their possible relevance to raw meat toughness measurements. *J. Food Technol.* 9:501.



- Rowe, R.W.D. 1977a. The influence of the collagen fibre network of muscle on the compliance and tensile strength of muscles subjected to loads at right angles to the muscle fibre axis. *Meat Sci.* 1:135.
- Rowe, R.W.D. 1977b. The effect of prerigor stretch and contraction on the post-rigor geometry of meat samples in relation to meat toughness. *Meat Sci.* 1:205.
- Scopes, R.K. 1964. The influence of post-mortem conditions on the solubilities of muscle proteins. *Biochem. J.* 91:201.
- Shmukler, H.W. 1970. The purification of  $\text{KH}_2\text{PO}_4$  for use as a carrier buffer in ultra-sensitive liquid chromatography. *J. Chrom. Sci.* 8:581.
- Stabursvik, E. and Martens, H. 1980. Thermal denaturation of proteins in *postrigor* muscle tissue as studied by differential scanning calorimetry. *J. Sci. Food Agric.* 31:1034.
- Stanley, D.W., Pearson, G.P. and Coxworth, V.E. 1971. Evaluation of certain physical properties of meat using a universal testing machine. *J. Food Sci.* 36:256.
- Stanley, D.W., McKnight, L.M., Hines, W.G.S., Usborne, W.R. and Deman, J.M. 1972. Predicting meat tenderness from muscle tensile properties. *J. Texture Stud.* 3:51.
- Stromer, M.H., Goll, D.E. and Roth, L.E. 1967. Morphology of rigor-shortened bovine muscle and the effect of trypsin on pre- and *postrigor* myofibrils. *J. Cell Biol.* 34:431.



Swift, C.E. and Berman, M.D. 1959. Factors affecting the water retention of beef. 1. Variations in composition and properties among eight muscles. *Food Technol.* 13:365.

Takahashi, K., Fukazawa, T. and Yasui, T. 1967. Formation of myofibrillar fragments and reversible contraction of sarcomeres in chicken pectoral muscle. *J. Food Sci.* 32:409.

Vaccari, A. and Maura, G. 1978. Effects of drugs on the extracellular spaces of smooth muscle in vitro. *Pharmacol. Res. Comm.* 10:675.

Webb, N.B., Kahlenberg, O.J., Naumann, H.D. and Hedrick, H.B. 1967. Biochemical factors affecting beef tenderness. *J. Food Sci.* 32:1.

Whiting, R.C. 1980. Calcium uptake by bovine muscle mitochondria and sarcoplasmic reticulum. *J. Food Sci.* 45:288.

Wierbicki, E., Kunkle, L.E., Cahill, V.R. and Deatherage, F.E. 1956. Post mortem changes in meat and their possible relation to tenderness together with some comparisons of meat from heifers, bulls, steers, and diethylstilbestrol treated bulls and steers. *Food Technol.* 10:80.

Winger, R.J. and Pope, C.G. 1980-81. Osmotic properties of post-rigor beef muscle. *Meat Sci.* 5:355.



## V. Appendices

### A. Mobile phase

In choosing the buffer systems used for the chromatography of ATP and its degradation products several factors were considered. The first was to avoid a high concentration of halides which can corrode the stainless steel parts of the pumps. For this reason the procedure of Riss *et al.* (1980) was avoided. The small amount of KCl in buffer A was retained to aid in the elution of UV impurities in the phosphate buffers. The problem of UV impurities in phosphate buffers when using gradient elution with a pellicular anion exchange column was reported by Shmukler (1970). The method suggested for purifying the phosphate buffer involved the passage of the buffer over Dowex 1-X8 columns. Purification of the Dowex 1-X8 column having an eluant  $A_{254} < 0.005$  was impossible and for this reason the procedure was abandoned. An Amberlite XAD-2 column was prepared in which the eluant  $A_{254}$  was less than .005. A 70% reduction in UV absorbance was achieved after passage of a 0.5 M  $\text{KH}_2\text{PO}_4$  (HPLC grade) buffer through this column. However, the use of this buffer did not overcome the problem of irregularities on the baseline when the gradient reached about 0.4 M  $\text{KH}_2\text{PO}_4$  after the column had been used about 2 weeks. It was found that after the first regeneration of the new column (according to the Whatman procedure) the UV impurities were removed by simply injecting 100  $\mu\text{L}$  of 0.1 M



EDTA and running buffer A through the column overnight at 0.7 mL/min. When a 0.015 M phosphate buffer without the KCl was used, little improvement in column performance occurred. With the KCl the recovery of column performance was excellent and a procedure was developed with KCl retained in buffer A.

Another problem faced was the separation of NAD, AMP and IMP. The major factor affecting their separation is the pH of buffer A. If the pH is 4.5, AMP and IMP overlap; a reduction in the pH to 3.7 results in the overlap of NAD and AMP. A pH of 4.1 allows all three components to be well resolved under the conditions chromatographed. It can be seen from the standard deviations of the retention times (Table V.1) for NAD and AMP of samples chromatographed at approximately 1 hr intervals, that the positions of these two peaks move about considerably. Clearly, the column is not equilibrated. In fact the retention times for NAD and AMP are approximately 6.95 and 9.5 min for a well-equilibrated column. Resolution of NAD, AMP and IMP can be obtained with repeat injections of less than 1 hr (although the retention times of NAD and AMP in particular are much shorter), but 1 hr was chosen as a convenient time interval for column equilibration, sample preparation and reinjection.



Table V.1 Retention times of ATP degradation products<sup>1</sup>

Compound	Retention Time <sup>2</sup>
Inosine	2.22±0.05
Hypoxanthine	2.43±0.09
Nicotinamide adenine dinucleotide	6.30±0.33
Adenosine 5'-monophosphate	8.10±0.46
Inosine 5'-monophosphate	12.17±0.12
Inosine 5'-diphosphate	20.64±0.23
Adenosine 5'-diphosphate	21.02±0.20
Adenylosuccinic acid	22.60±0.23
Adenosine 5'-triphosphate	30.38±0.15
Inosine 5'-triphosphate	29.44 <sup>3</sup>

<sup>1</sup>This table has previously been published by Currie et al. (1982).

<sup>2</sup>The mean retention time of 10 chromatograms of muscle extracted at different times postmortem. Values are the means of the retention times ± standard deviation.

<sup>3</sup>The retention time of a prepared standard.



## B. Treatment of acid extracts

The first procedure followed was that of Davey and Gilbert (1976) using 1 N NaOH to readjust the 0.5 M HClO<sub>4</sub> extract to pH 7.0. The second procedure attempted was that of Chen *et al.* (1977) where the perchloric acid extract is neutralized with KOH and the precipitated perchlorate salt removed by filtration. The third procedure was the dilution of a more concentrated 10% TCA extract (1:1) and injection with the hope that the TCA peak would not interfere. The final procedure adopted was that of Khym (1975), as discussed by Chen *et al.* (1977) and Riss *et al.* (1980), in which a 0.5 M tri-n-octylamine/Freon 113 solution (A) was used to extract the acids from the nucleotides. Equal volumes of solution A and the acid-extracted nucleotides were mixed in a screw cap test tube and the contents centrifuged to promote layer separation. The top, aqueous phase contained the nucleotides. No pH adjustments were required since the pH values of the extracts were consistently between 4 and 6 (Chen *et al.*, 1977). With perchloric acid extracts, 3 layers were visible; the top was the aqueous layer, the middle consisted of perchlorate-tri-n-octylamine complex and the bottom was Freon 113. The procedure utilizing the tri-n-octylamine/Freon 113 solution to remove the salts was chosen for the reasons outlined below.

When ATP measurements (enzymatic) were made previously in this laboratory, the extraction of the nucleotides was



according to the procedure of Lester and Gilbert (1976) in which a 0.5 M  $\text{HClO}_4$  extract was made and the solution neutralized with NaOH. However, the injection of a neutralized perchloric acid extract is not suitable for HPLC analysis on a SAX column since IMP is resolved into two peaks (a sharp initial peak and a broad second peak). By varying the pH of a standard IMP perchlorate solution, different ratios of two and sometimes even three peaks of IMP were observed. No problems with neutralized solutions of the other extracted components were apparent.

The removal of the interfering perchlorate ion was attempted by its precipitation using KOH instead of NaOH to adjust the pH to neutrality, thus forming the insoluble potassium perchlorate salt (Chen *et al.*, 1977). This procedure did not seem to remove all of the perchlorate ion since the problem of a dual peak for IMP was not overcome.

When a standard solution of IMP in 10% TCA was chromatographed, the IMP was a sharp single peak. A diluted 10% extract of meat was injected, but the broad TCA peak interfered with the quantitation of AMP. However, the IMP peak was sharp and well resolved, suggesting that the perchlorate ion was the reason for the double IMP peak.

It was found that 0.5 M tri-n-octylamine/Freon 113 solution removes either TCA or perchloric acid from the nucleotides so that no problems with the symmetry of the peaks are encountered. Extraction of the acids from standard solutions have shown excellent recovery, with values in the



order of that reported by Chen et al. (1977). In assessing the recovery of ATP and its degradation products from meat, a comparison of four extract preparations was made: injections of a 0.5 M HClO<sub>4</sub> extract without acid extraction, a 0.5 M HClO<sub>4</sub> extract with acid extraction (0.5 M tri-n-octylamine/Freon 113), a 10% TCA extract without acid extraction and a 10% TCA extract with acid extraction (0.5 M tri-n-octylamine/Freon 113). With the exception of AMP in the 10% TCA extract without acid extraction, all the concentrations of ATP and its degradation products in the original meat sample ( $\mu$ mole/g) could be compared. The areas of the two IMP peaks from the HClO<sub>4</sub> extract were totalled to obtain the concentration of IMP in this extract. All the values obtained were within the standard deviation found for repeated perchloric acid extractions of a meat sample followed by acid extraction and quantitation of ATP and its degradation products. In other words, errors produced from the lack of uniformity of the meat sample (e.g. fat, collagen levels), integration errors, and treatment of the extracts (e.g. length of time in the liquid extract before injection) were all greater than differences contributed by the method of extraction.

### C. ATP metabolites

Figures V.1 through V.24 present the results obtained from the HPLC analysis of samples from carcasses 7 to 18. The data for each carcass consist of two graphs. The first

Figure V.1. Concentration profile of ATP metabolites [ATP (●-●-●), ADP (▼-▼-▼) and IMP (▲-▲-▲) vs time postmortem] for carcass 7. Each datum point represents a single determination.

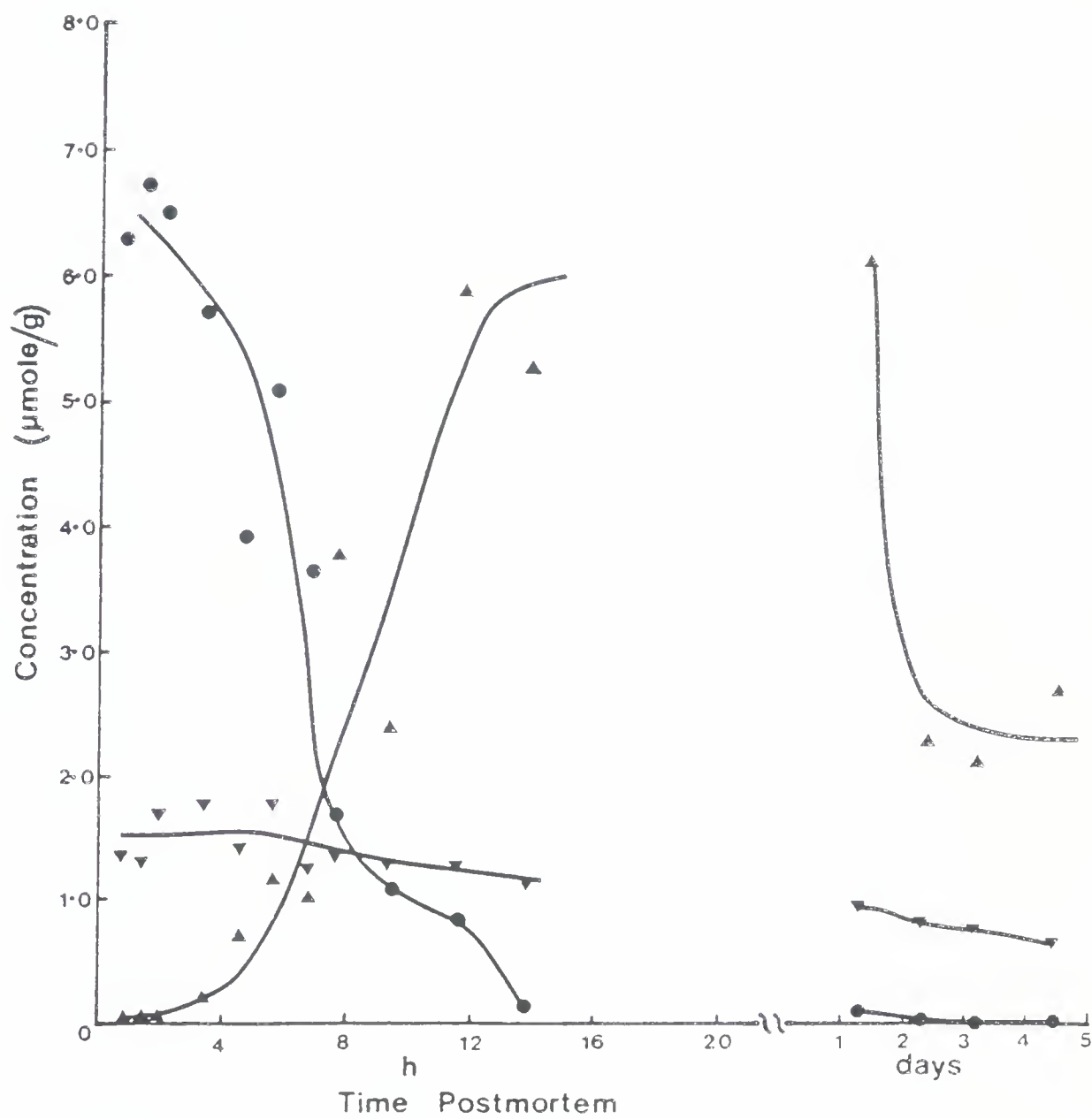


Figure V.2. Concentration profile of ATP metabolites [inosine (●-●-●) and hypoxanthine (■-■-■) vs time postmortem] for carcass 7. Each datum point represents a single determination.

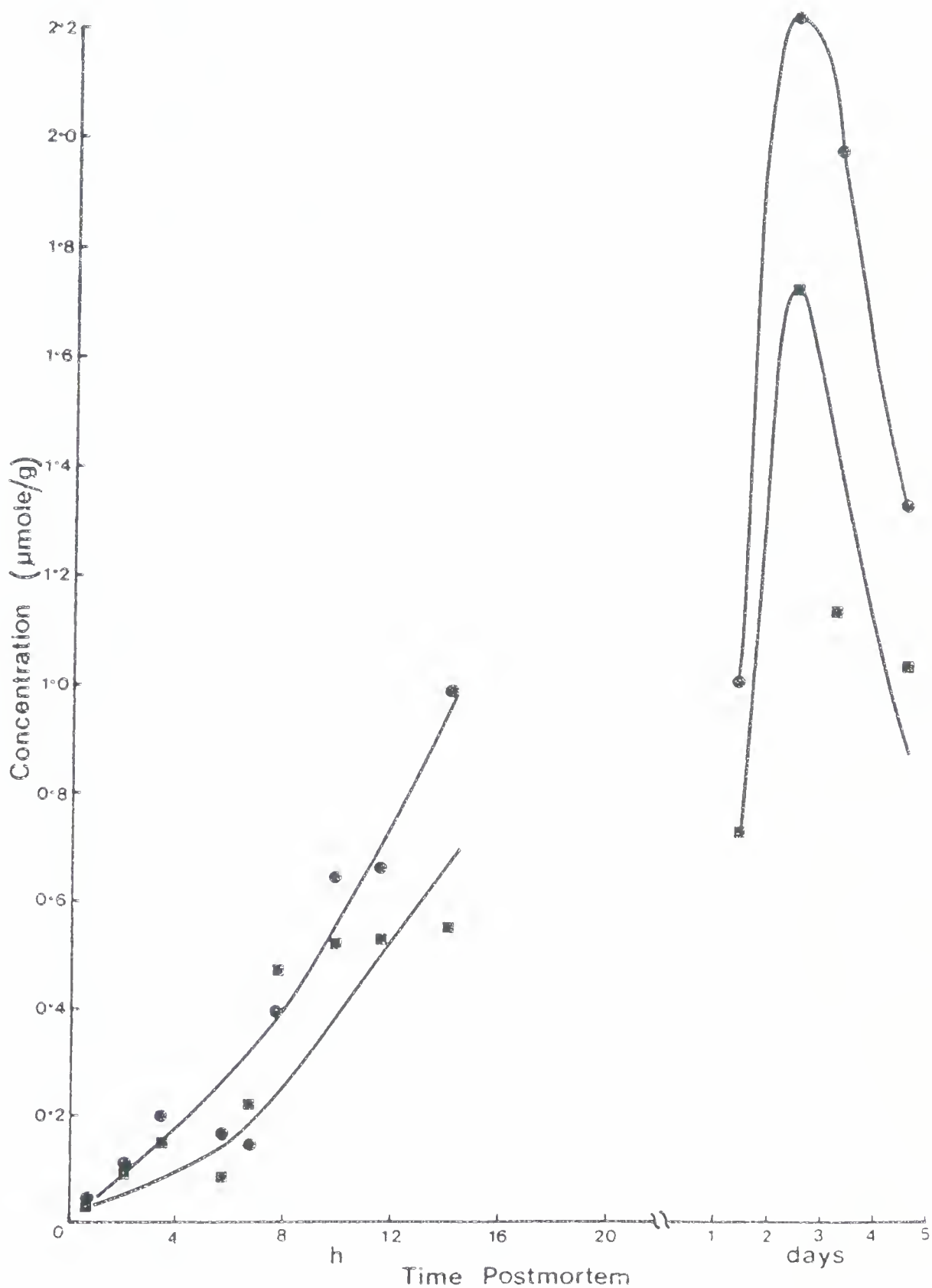


Figure V.3. Concentration profile of ATP metabolites [ATP (●-●-●), ADP (▼-▼-▼) and IMP (▲-▲-▲) vs time postmortem] for carcass 8. Each datum point represents a single determination.

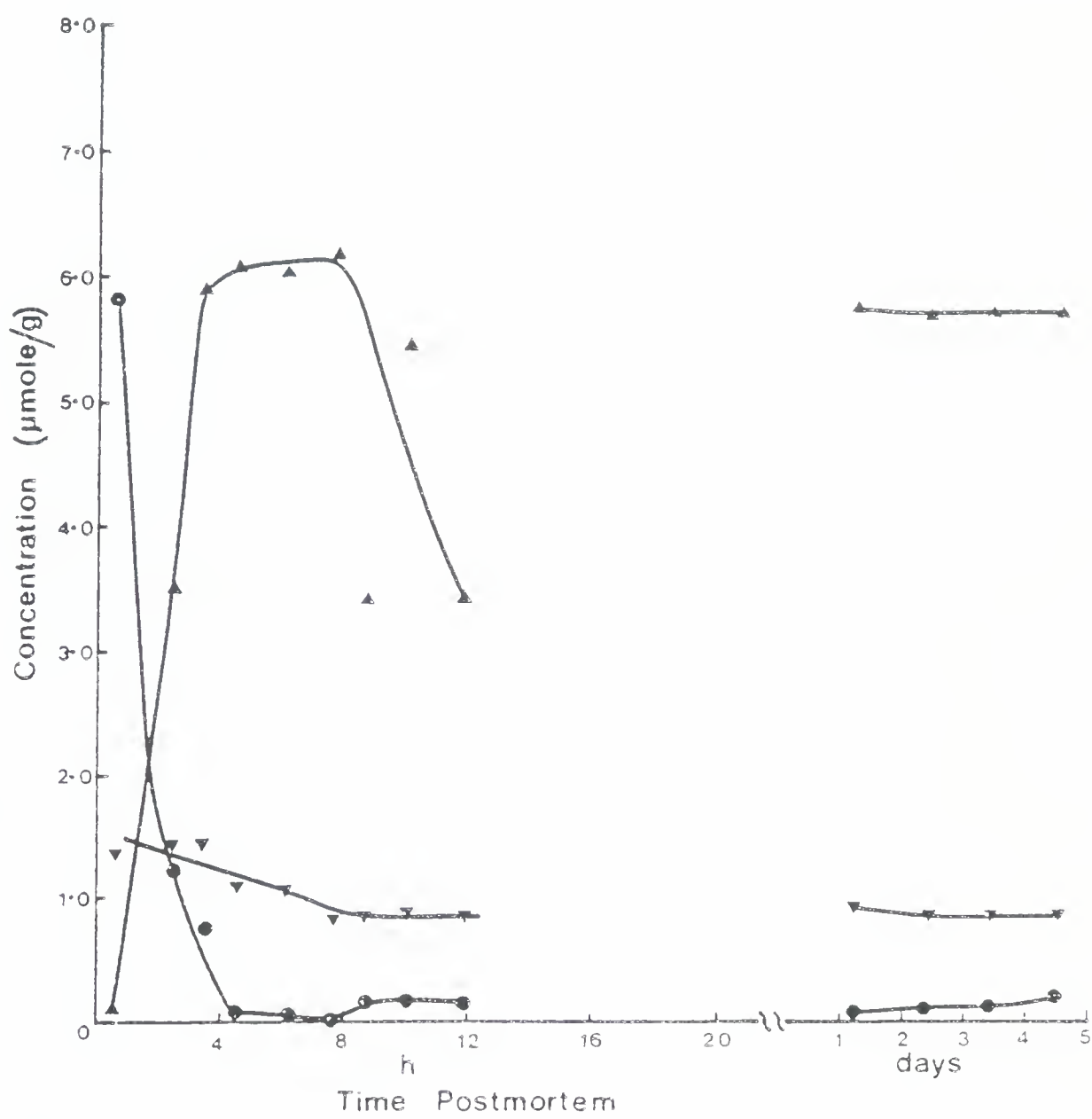


Figure V.4. Concentration profile of ATP metabolites  
[inosine (•-•-•) and hypoxanthine (■-■-■) vs time  
postmortem] for carcass 8. Each datum point represents a  
single determination.

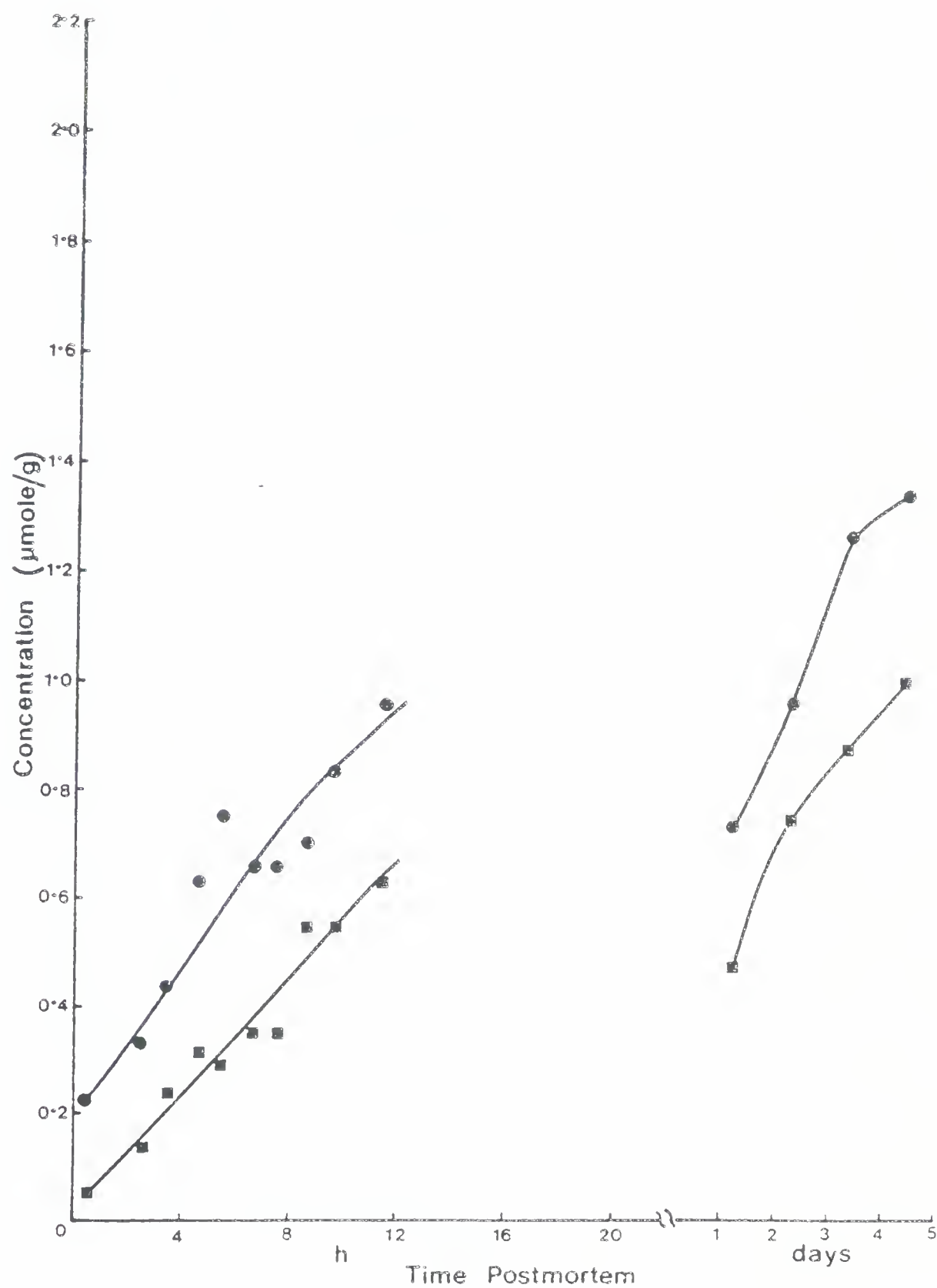


Figure V.5. Concentration profile of ATP metabolites [ATP (●-●-●), ADP (▼-▼-▼) and IMP (▲-▲-▲) vs time postmortem] for carcass 9. Each datum point represents a single determination.

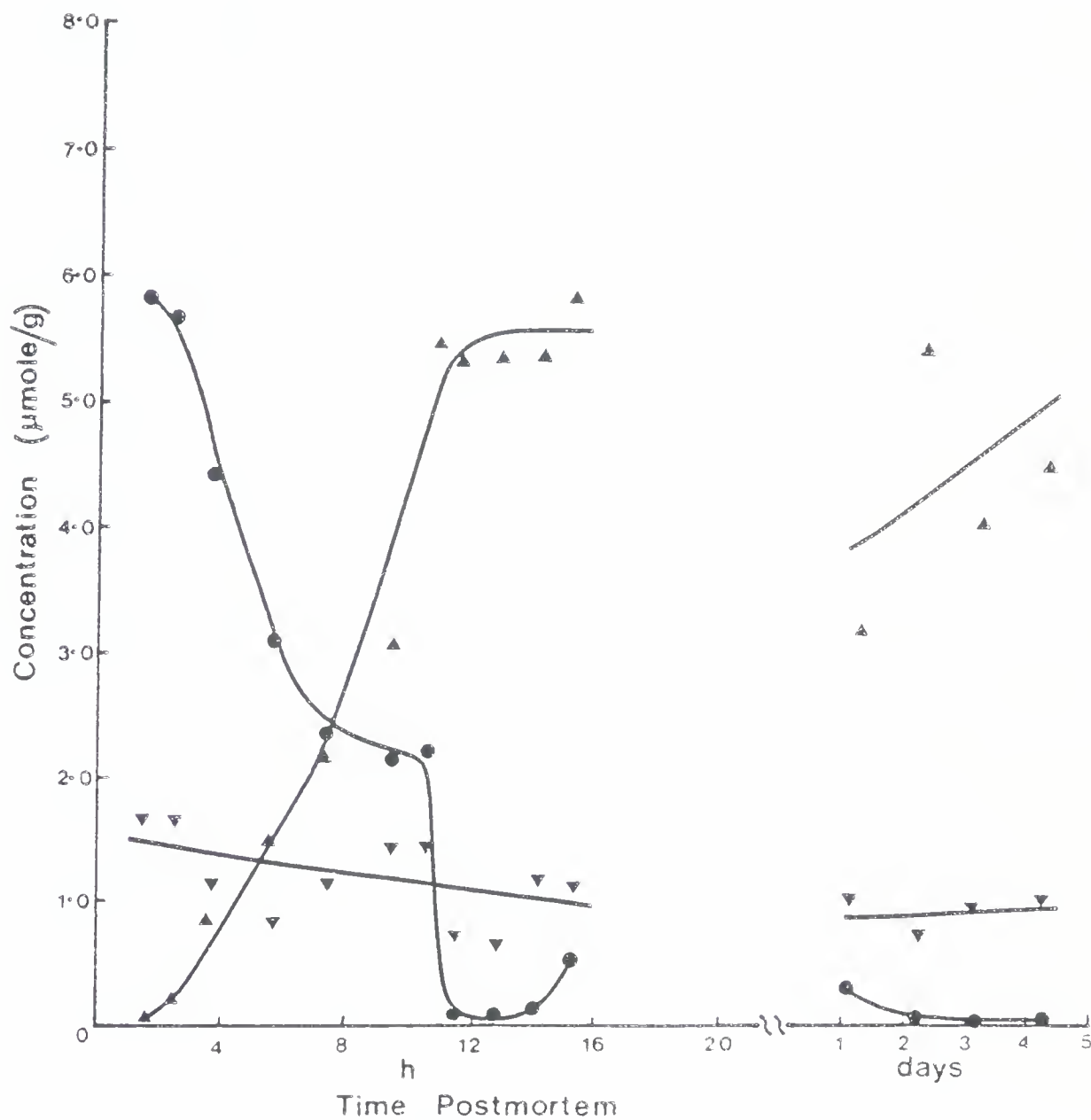


Figure V.6. Concentration profile of ATP metabolites [inosine (●---●) and hypoxanthine (■---■) vs time postmortem] for carcass 9. Each datum point represents a single determination.

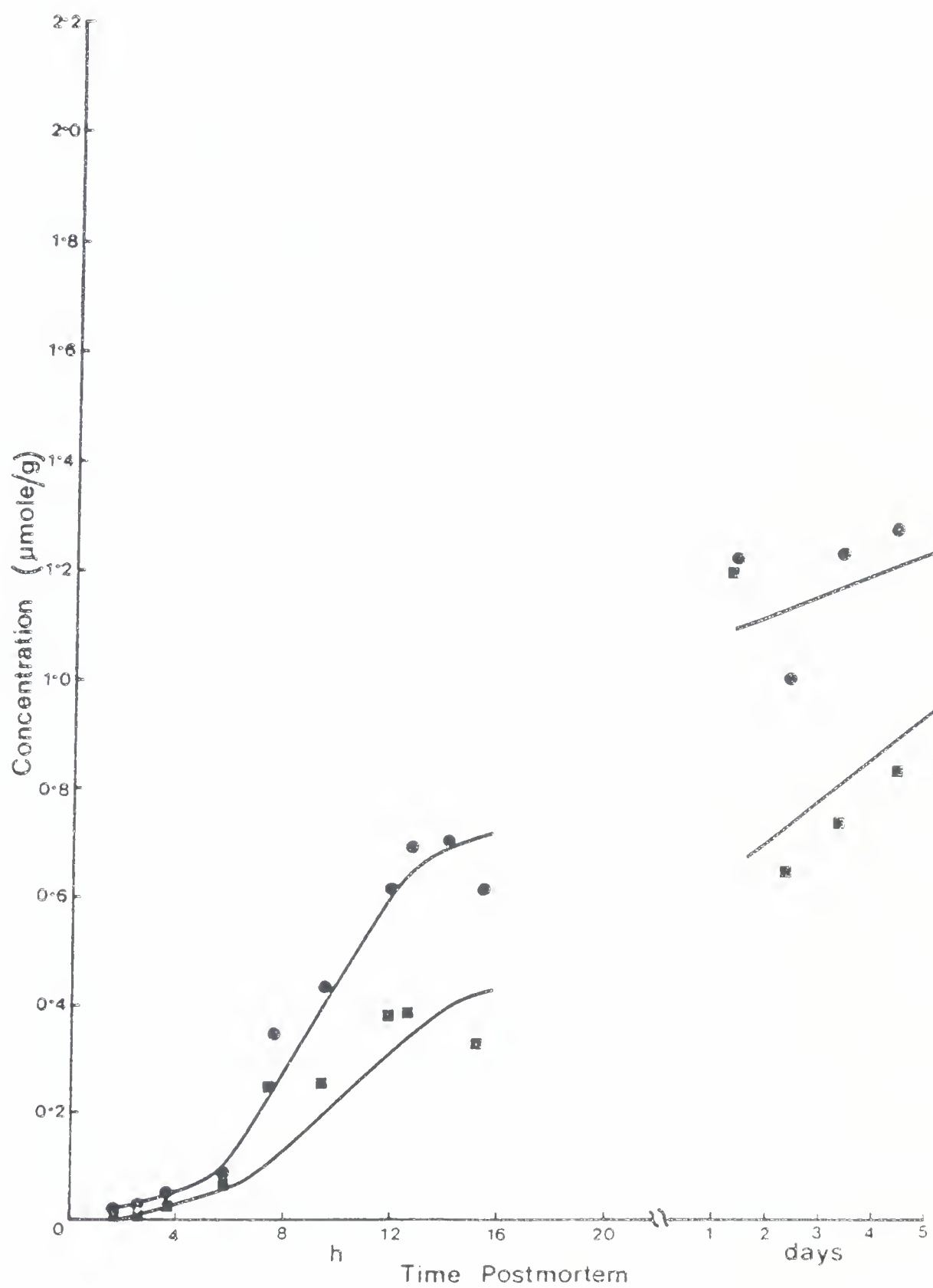


Figure V.7. Concentration profile of ATP metabolites [ATP (●-●-●), ADP (▼-▼-▼) and IMP (▲-▲-▲) vs time postmortem] for carcass 10. Each datum point represents a single determination.

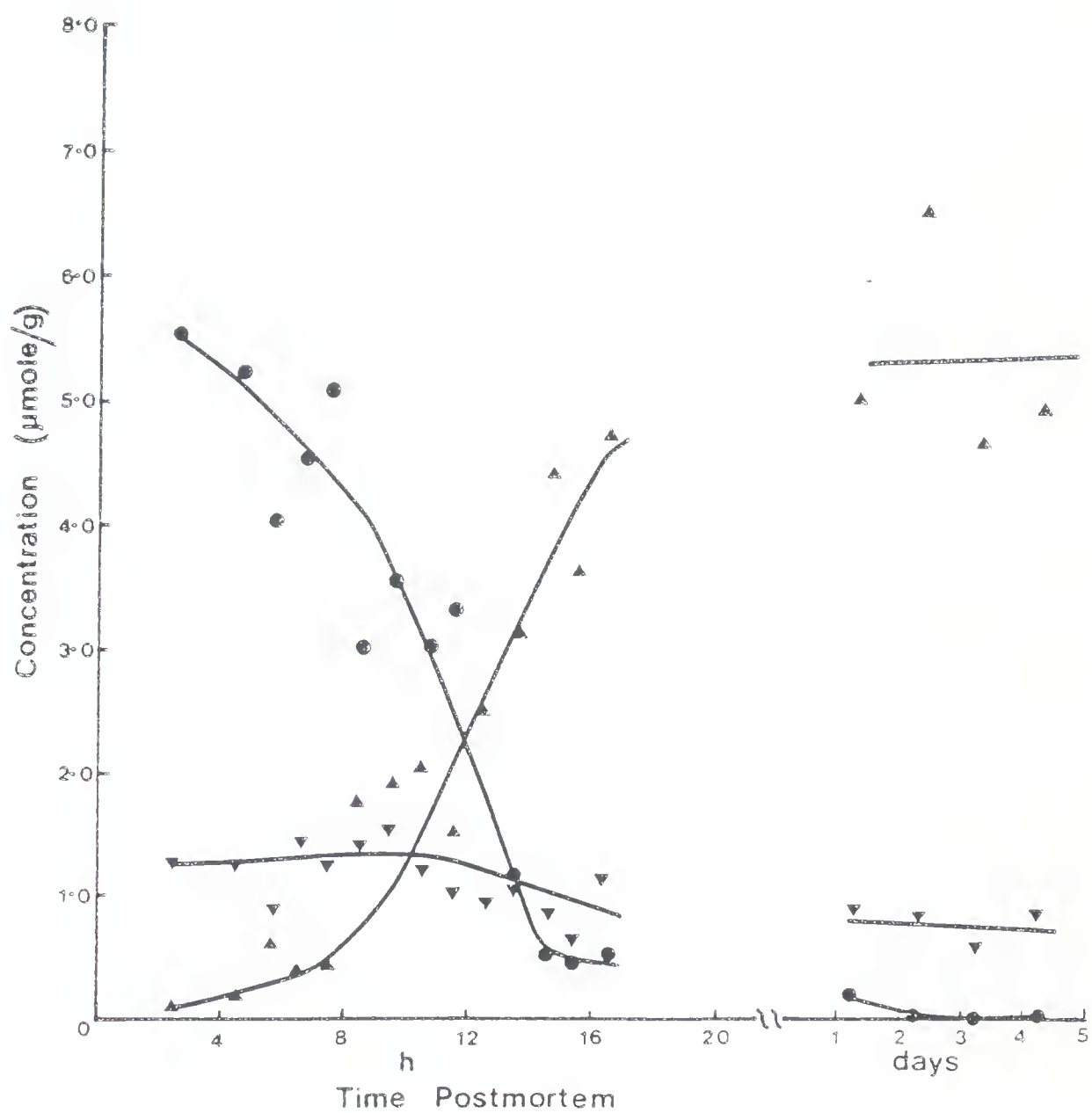


Figure V.8. Concentration profile of ATP metabolites [inosine (•---•) and hypoxanthine (■---■) vs time postmortem] for carcass 10. Each datum point represents a single determination.

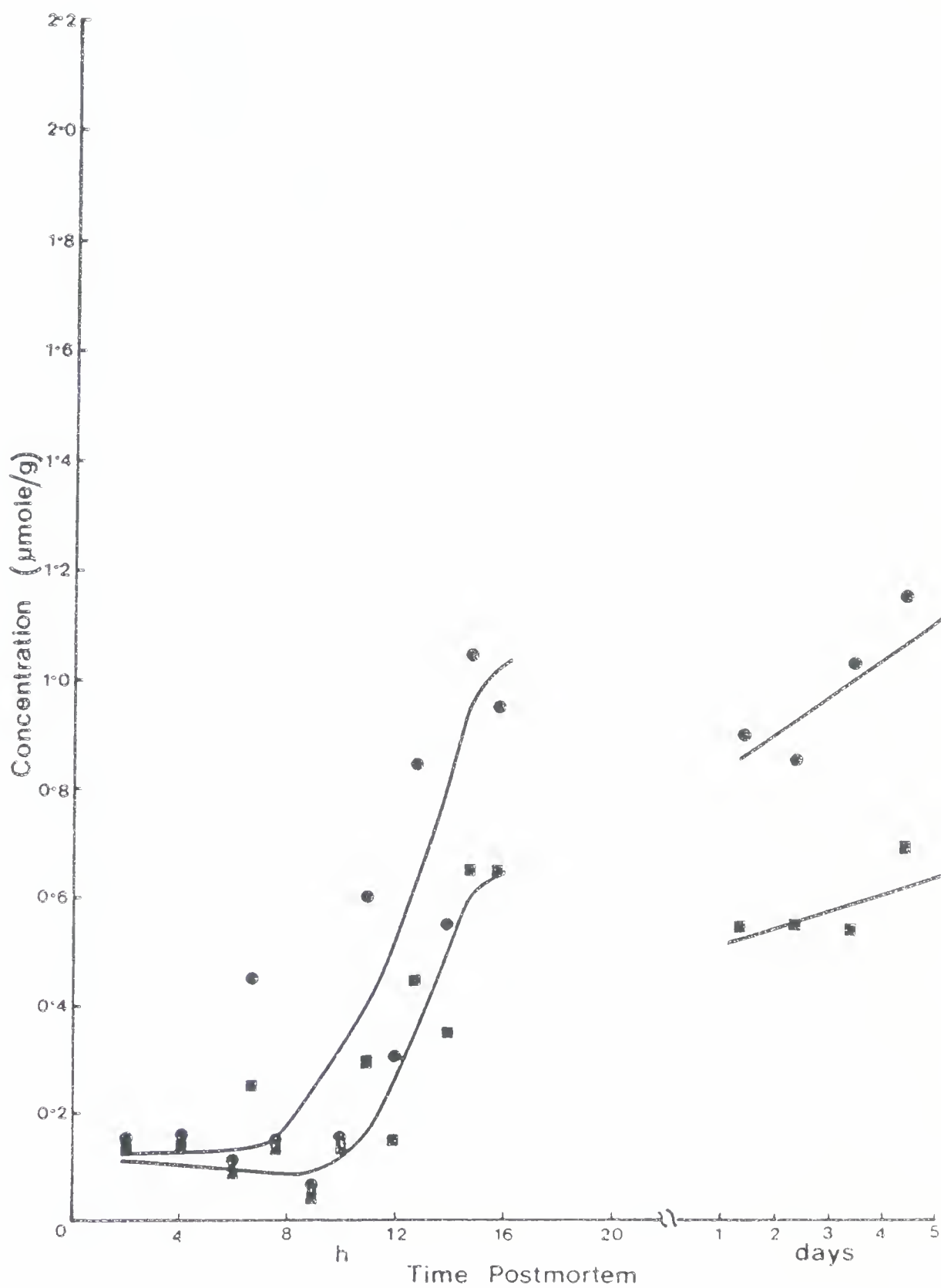


Figure V.9. Concentration profile of ATP metabolites [ATP (●-●-●), ADP (▼-▼-▼), IMP (▲-▲-▲) and NAD (■-■-■) vs time postmortem] for carcass 11. Each datum point represents a single determination.

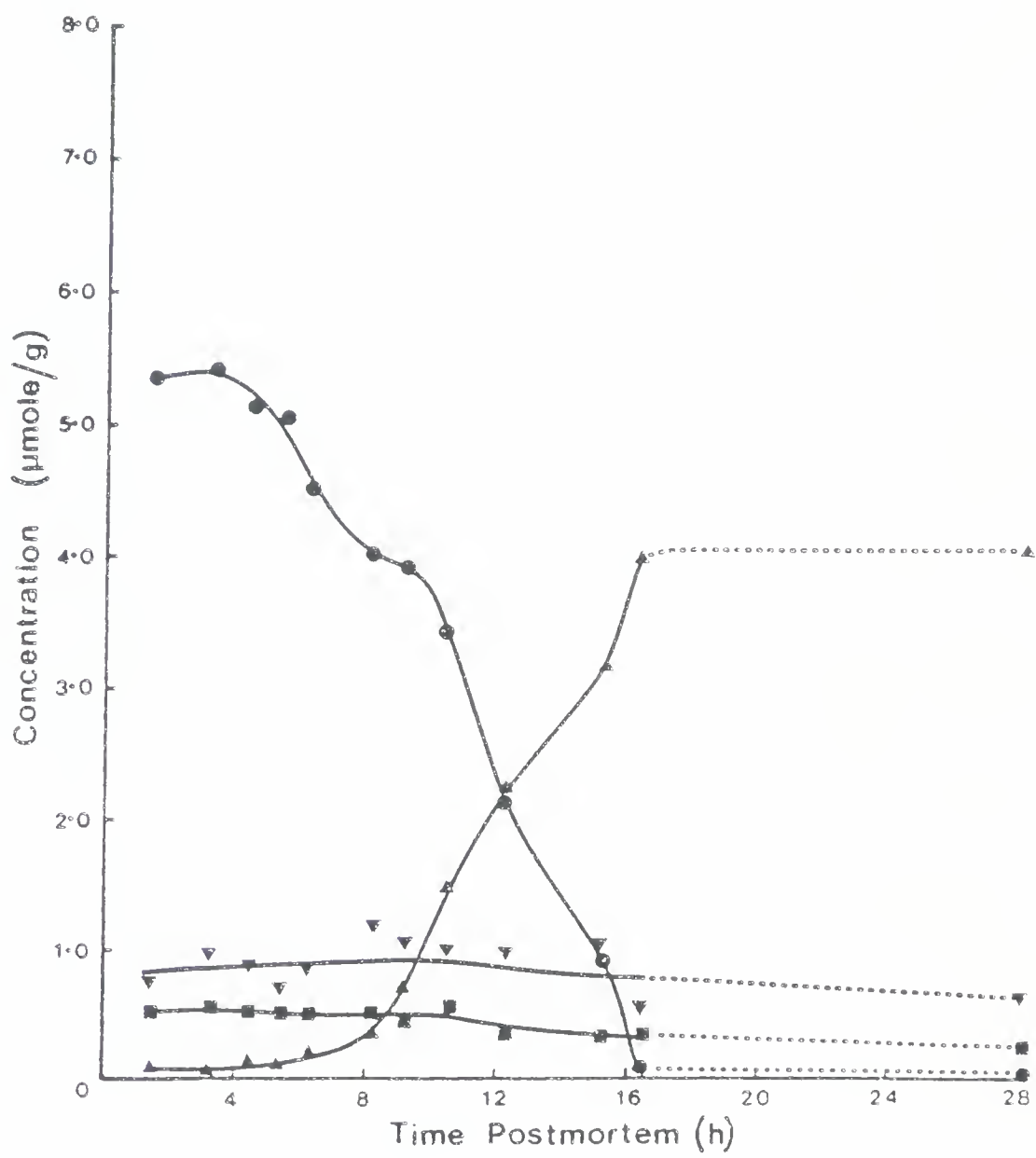


Figure V.10. Concentration profile of ATP metabolites [inosine (•-•-•), hypoxanthine (■-■-■) and AMP (▲-▲-▲) vs time postmortem] for carcass 11. Each datum point represents a single determination.

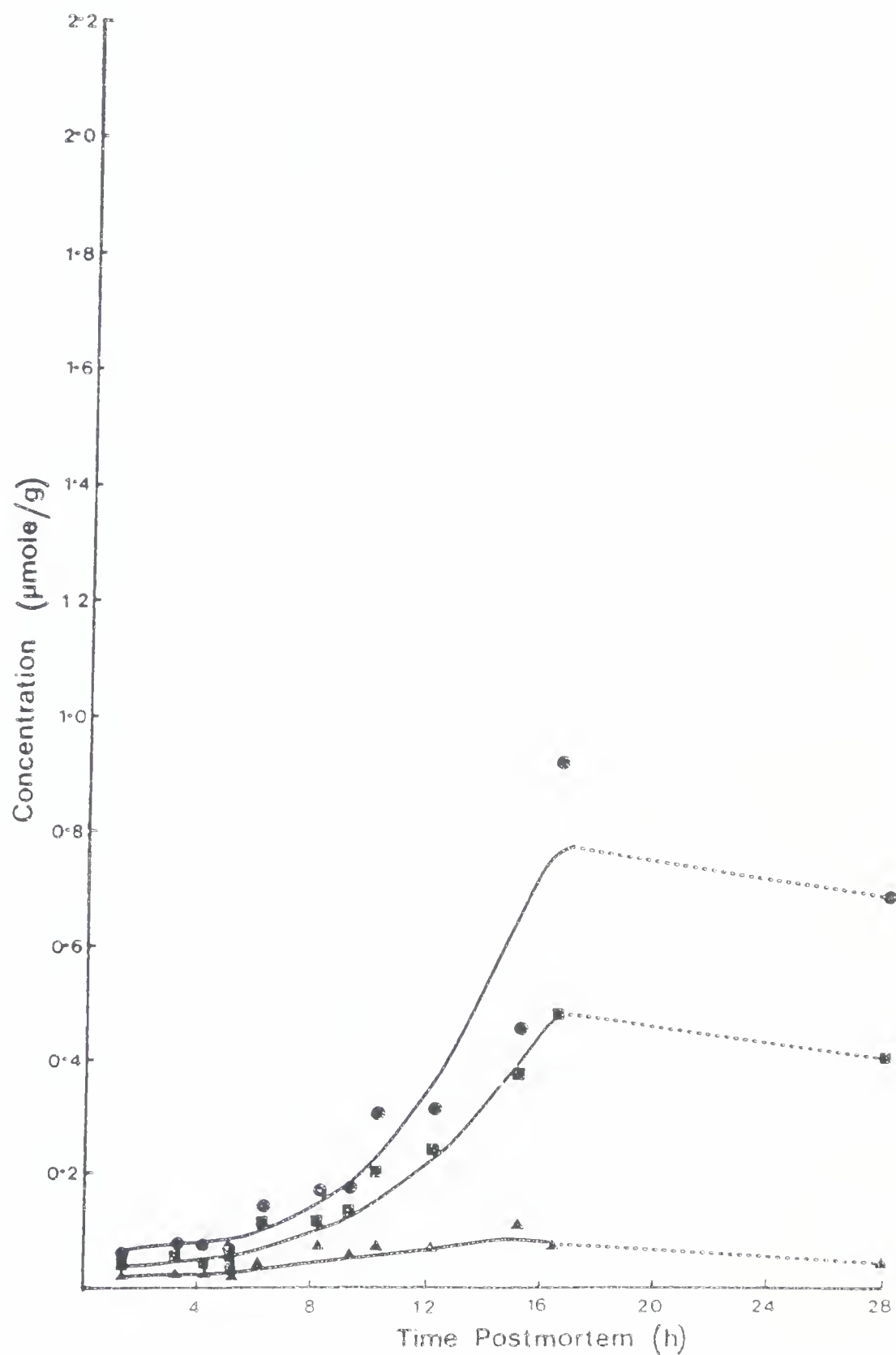


Figure V.11. Concentration profile of ATP metabolites [ATP (●-●-●), ADP (▼-▼-▼), IMP (▲-▲-▲) and NAD (■-■-■) vs time postmortem] for carcass 12. Each datum point represents a single determination.

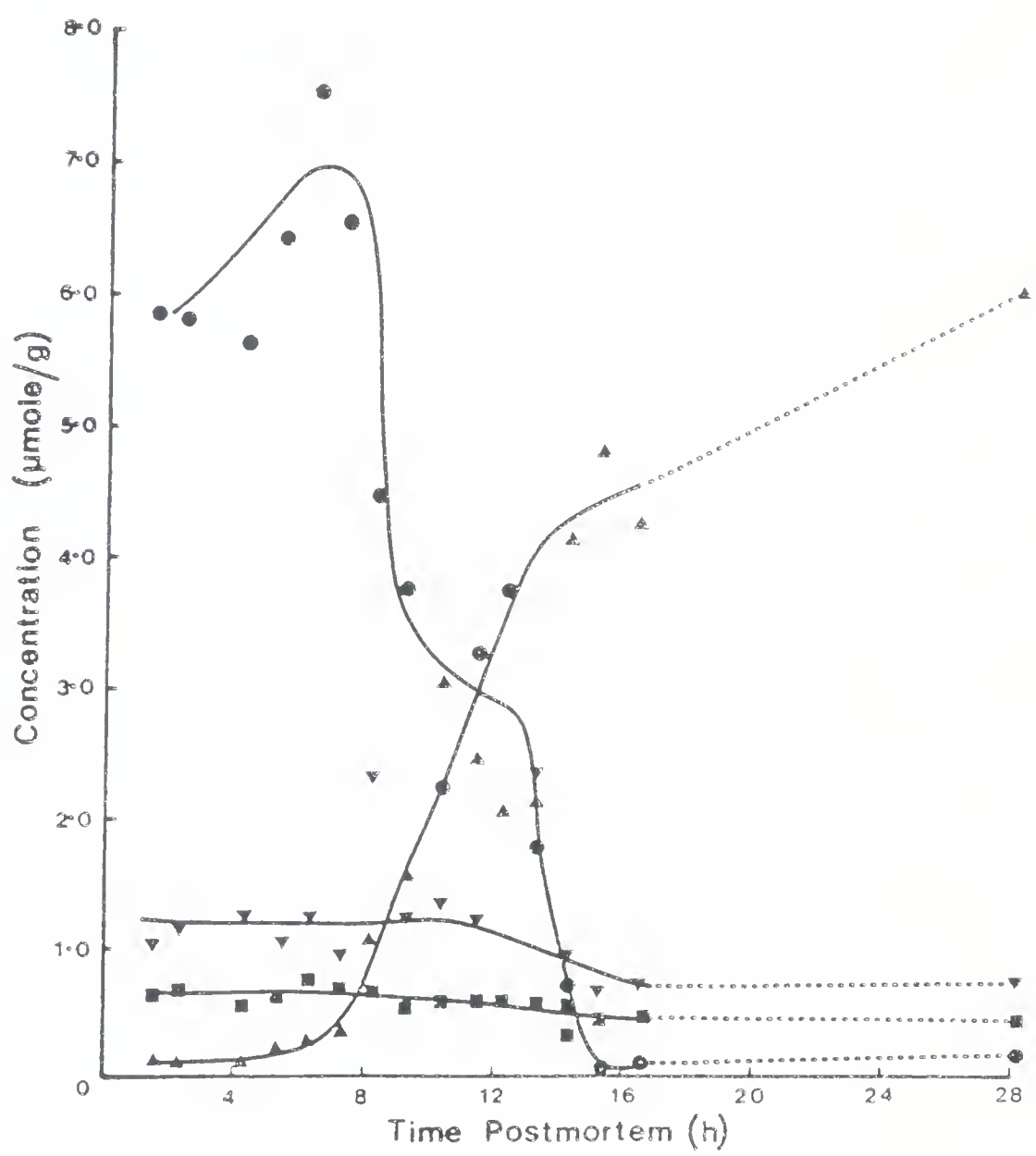


Figure V.12. Concentration profile of ATP metabolites [inosine (●-●-●), hypoxanthine (■-■-■) and AMP (▲-▲-▲) vs time postmortem] for carcass 12. Each datum point represents a single determination.

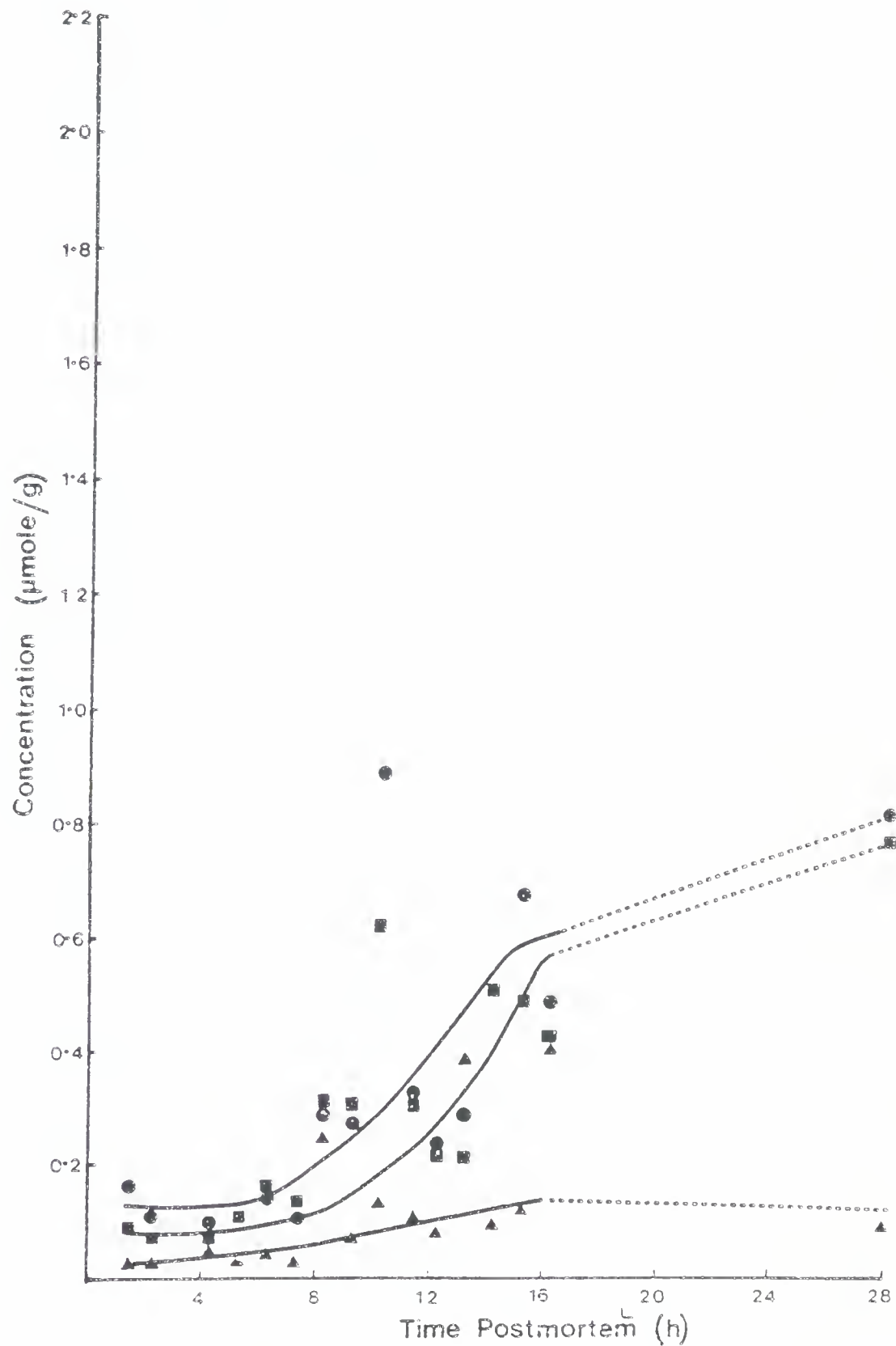


Figure V.13. Concentration profile of ATP metabolites [ATP (●-●-●), ADP (▼-▼-▼), IMP (▲-▲-▲) and NAD (■-■-■) vs time postmortem] for carcass 13. Each datum point represents a single determination.

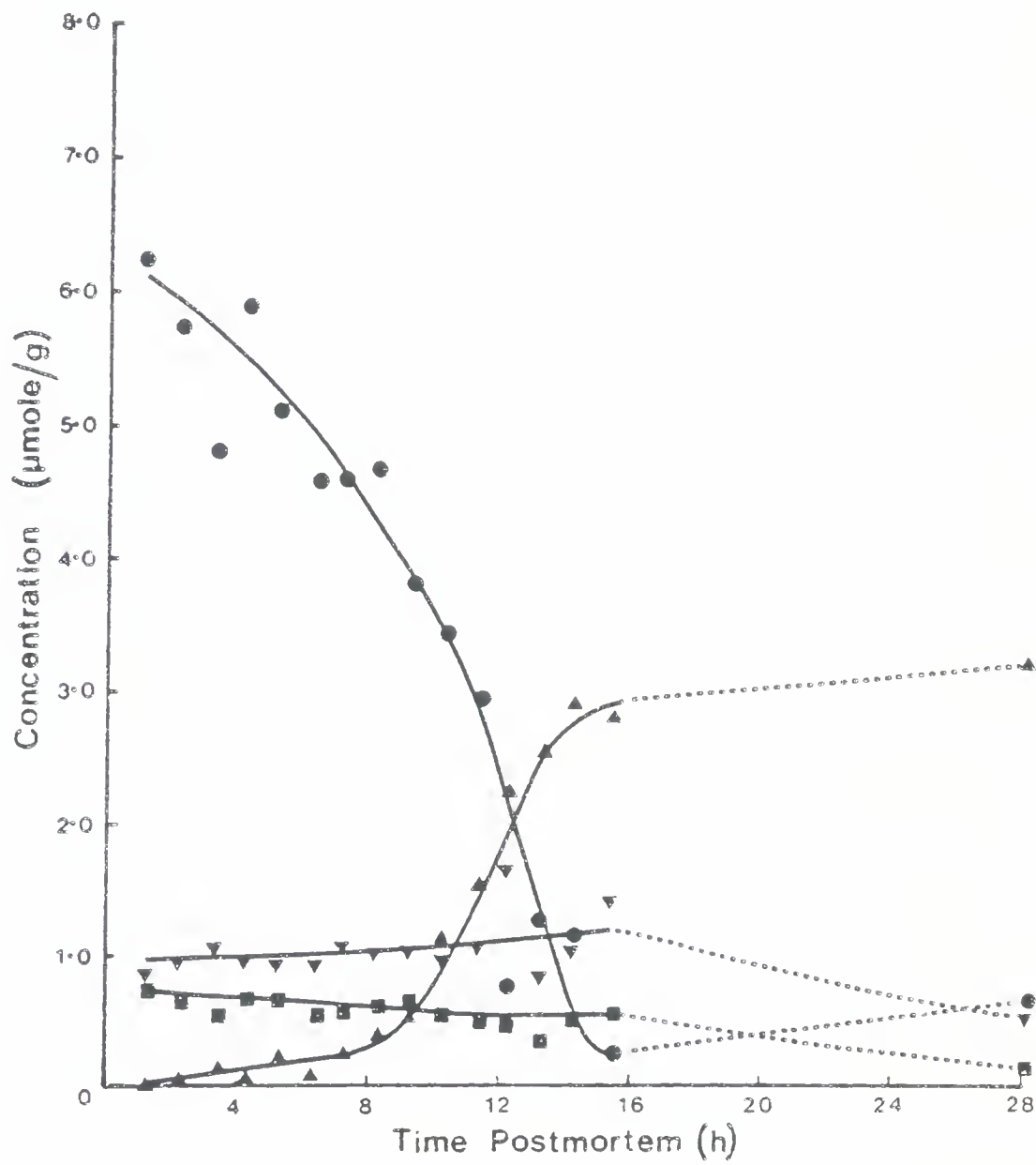


Figure V.14. Concentration profile of ATP metabolites [inosine (•-•-•), hypoxanthine (■-■-■) and AMP (▲-▲-▲) vs time postmortem] for carcass 13. Each datum point represents a single determination.

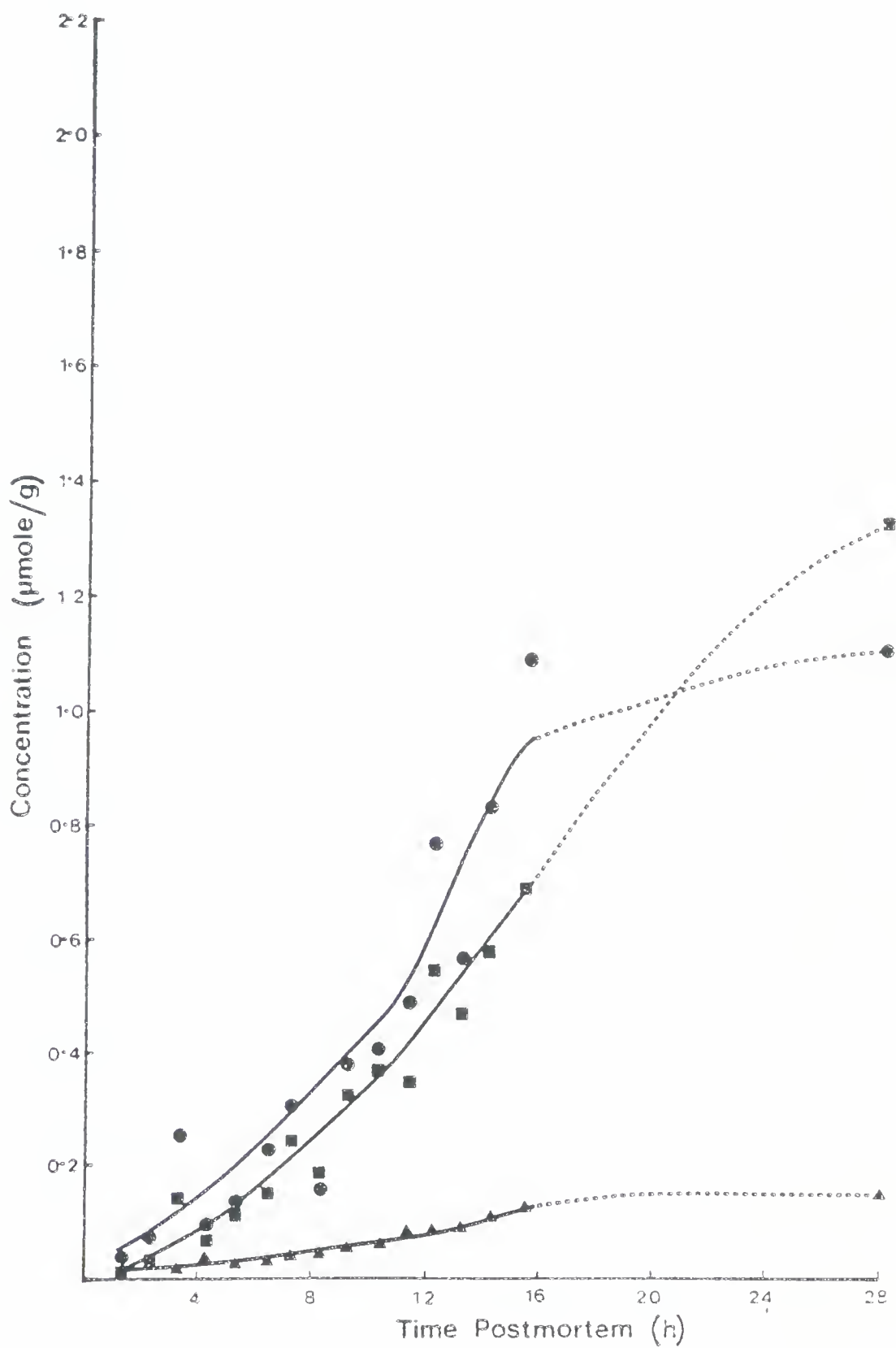


Figure V.15. Concentration profile of ATP metabolites [ATP (●-●-●), ADP (▼-▼-▼), IMP (▲-▲-▲) and NAD (■-■-■) vs time postmortem] for carcass 14. Each datum point represents a single determination.

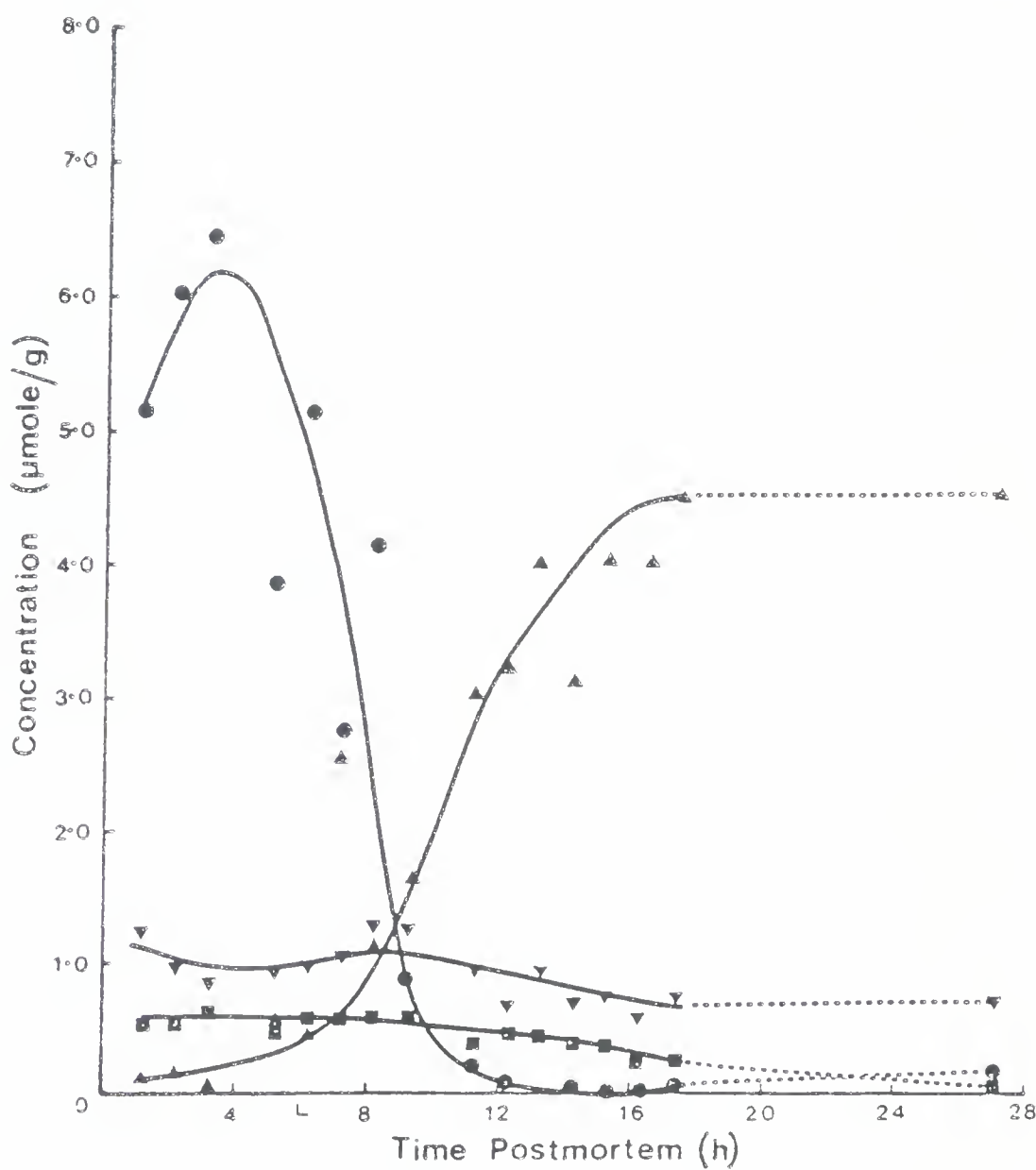


Figure V.16. Concentration profile of ATP metabolites [inosine (●-●-●), hypoxanthine (■-■-■) and AMP (▲-▲-▲) vs time postmortem] for carcass 14. Each datum point represents a single determination.

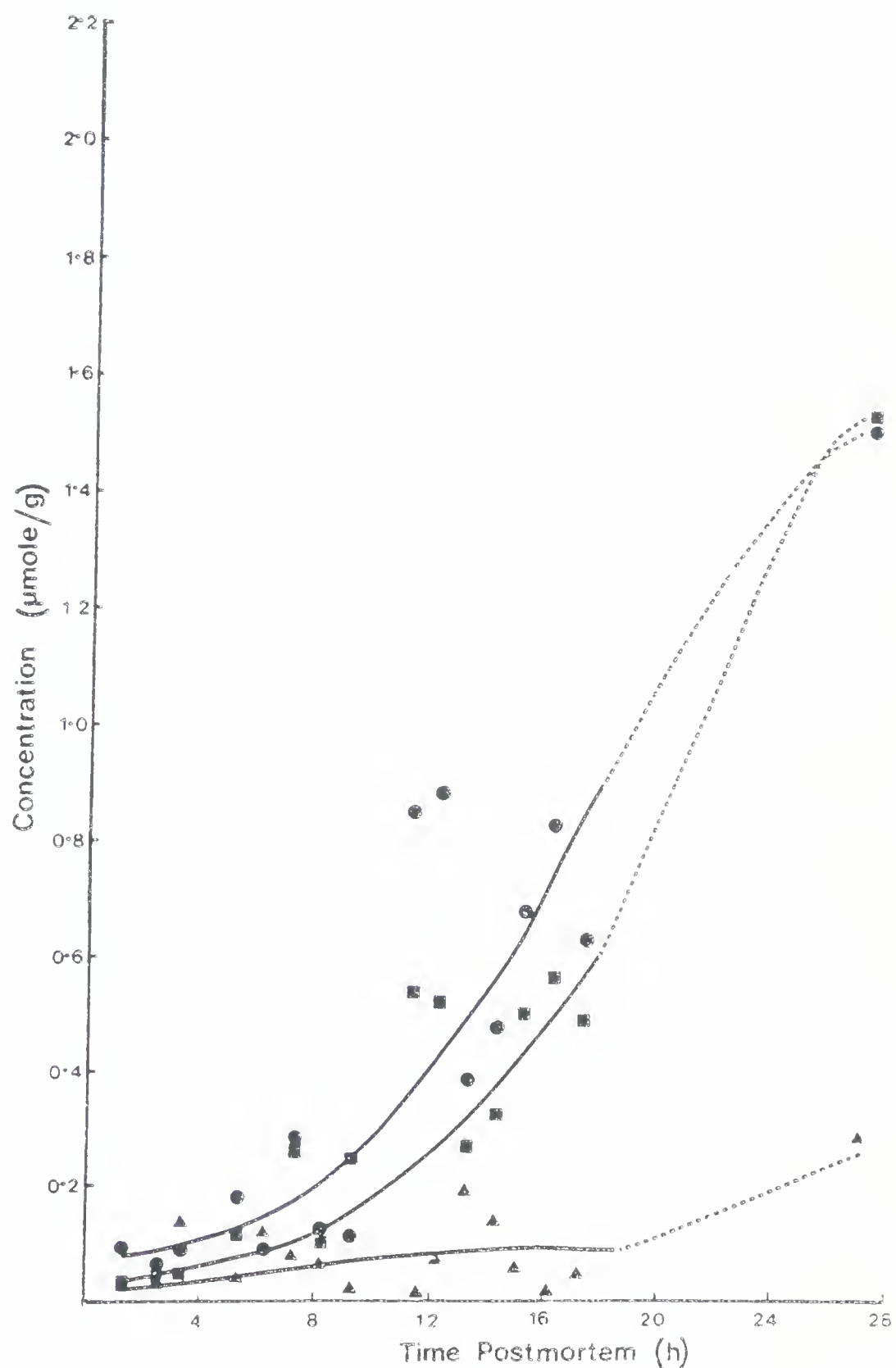


Figure V.17. Concentration profile of ATP metabolites [ATP (●-●-●), ADP (▼-▼-▼), IMP (▲-▲-▲) and NAD (■-■-■) vs time postmortem] for carcass 15. Each datum point represents a single determination.

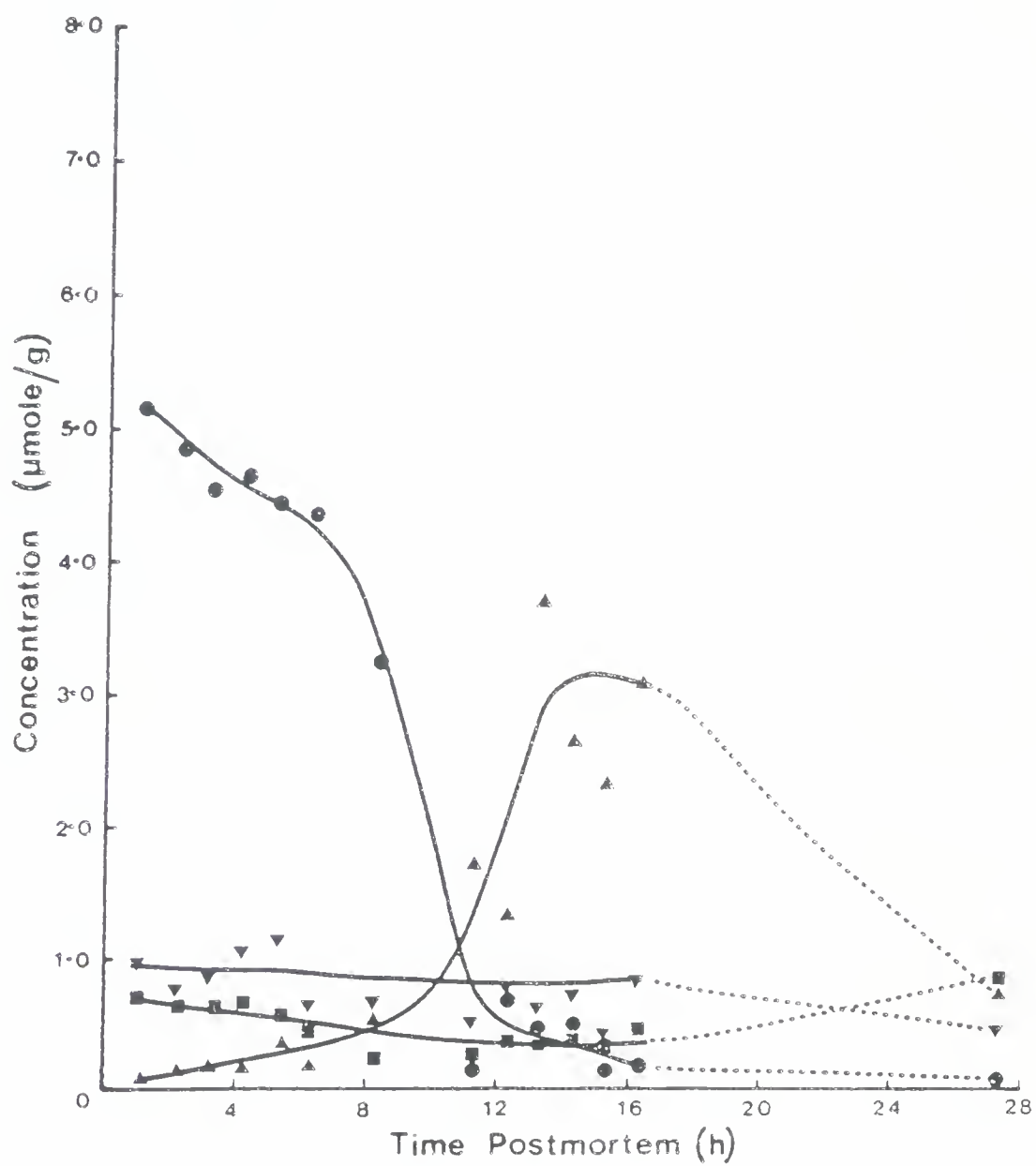


Figure V.18. Concentration profile of ATP metabolites [inosine (●-●-●), hypoxanthine (■-■-■) and AMP (▲-▲-▲) vs time postmortem] for carcass 15. Each datum point represents a single determination.

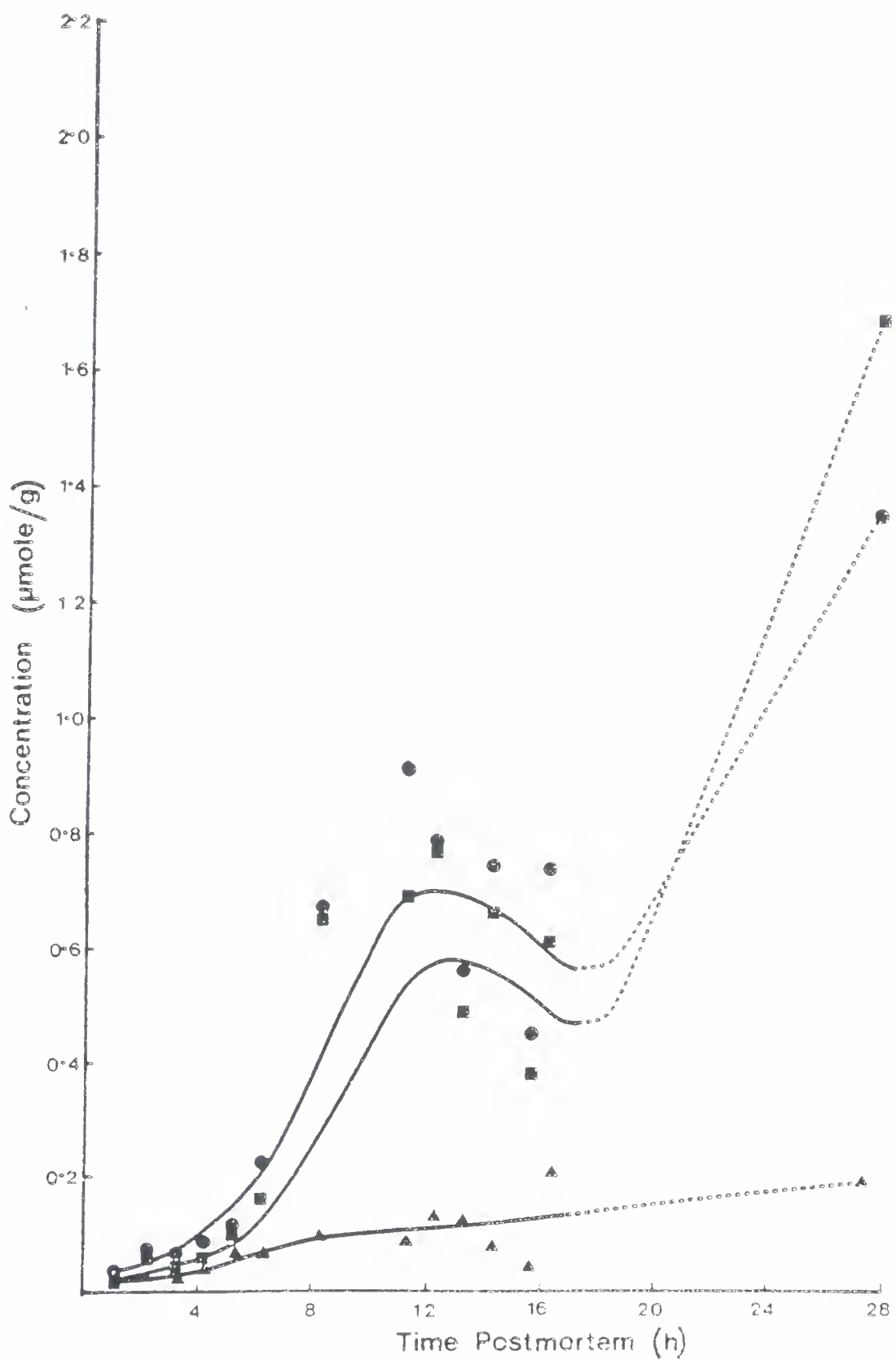


Figure V.19. Concentration profile of ATP metabolites [ATP (●-●-●), ADP (▼-▼-▼), IMP (▲-▲-▲) and NAD (■-■-■) vs time postmortem] for carcass 16. Each datum point represents a single determination.

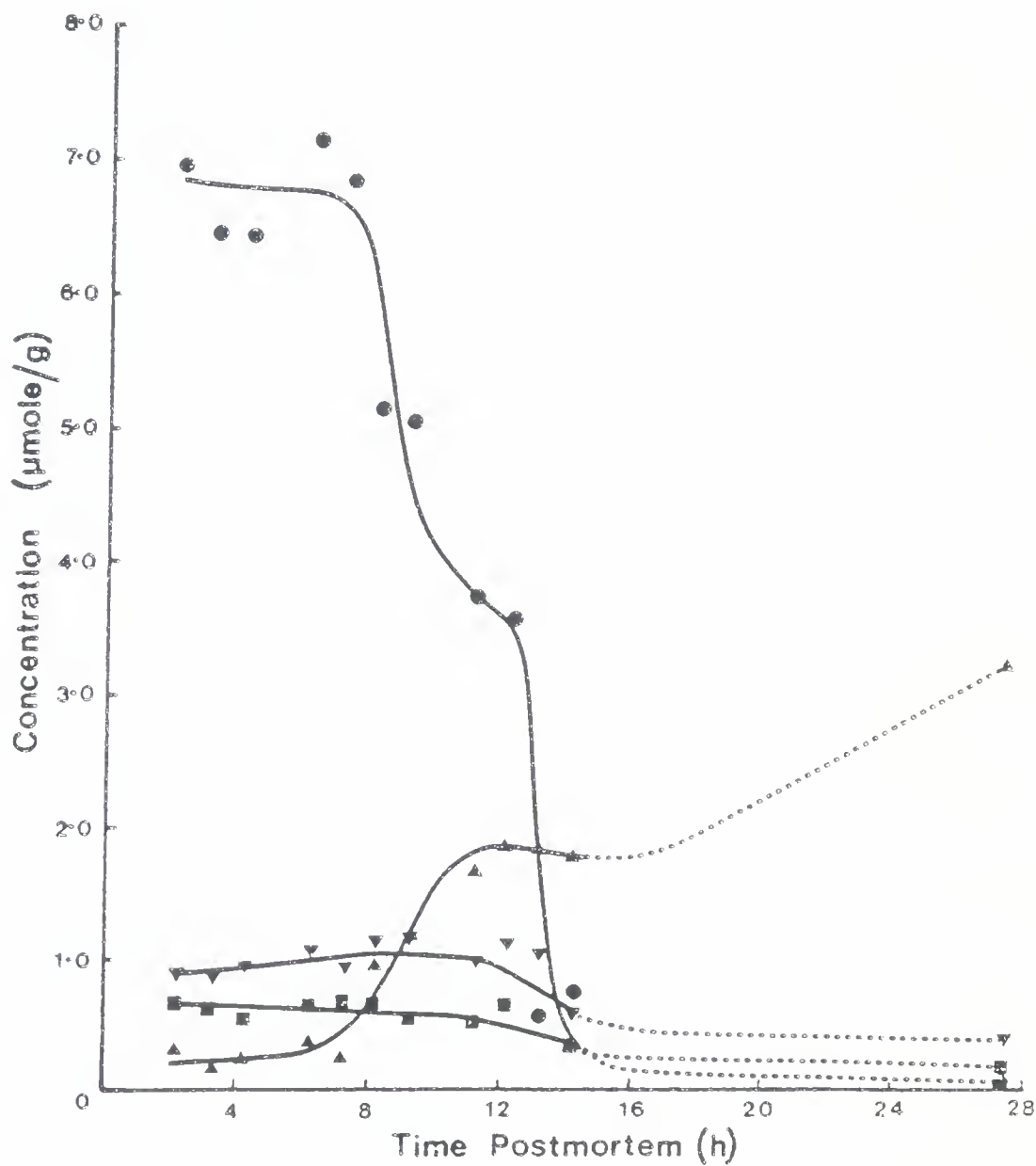


Figure V.20. Concentration profile of ATP metabolites [inosine (●-●-●), hypoxanthine (■-■-■ and AMP (▲-▲-▲) vs time postmortem] for carcass 16. Each datum point represents a single determination.

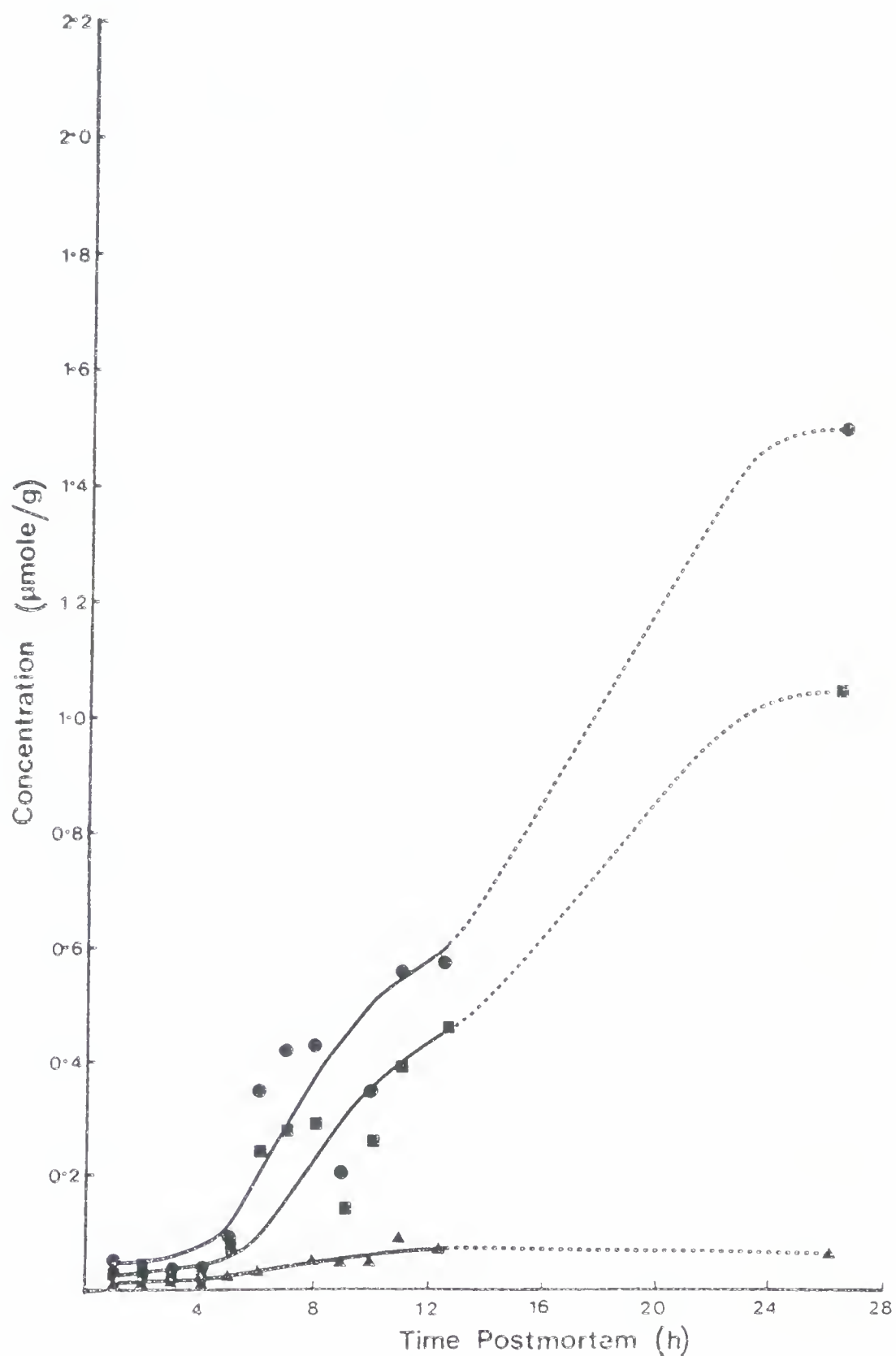


Figure V.21. Concentration profile of ATP metabolites [ATP (●-●-●), ADP (▼-▼-▼), IMP (▲-▲-▲) and NAD (■-■-■) vs time postmortem] for carcass 17. Each datum point represents a single determination.

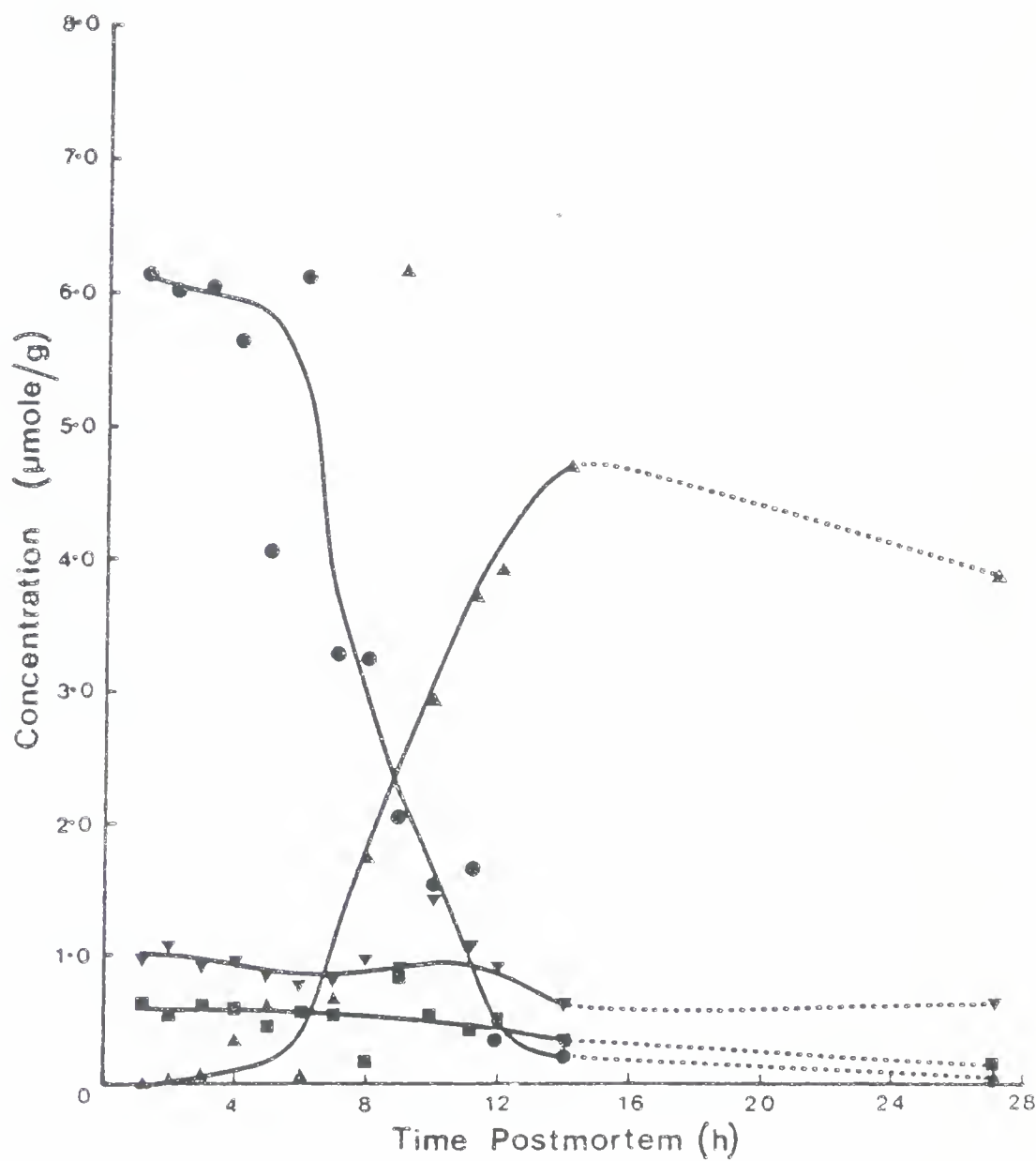


Figure V.22. Concentration profile of ATP metabolites [inosine (●-●-●), hypoxanthine (■-■-■) and AMP (▲-▲-▲) vs time postmortem] for carcass 17. Each datum point represents a single determination.

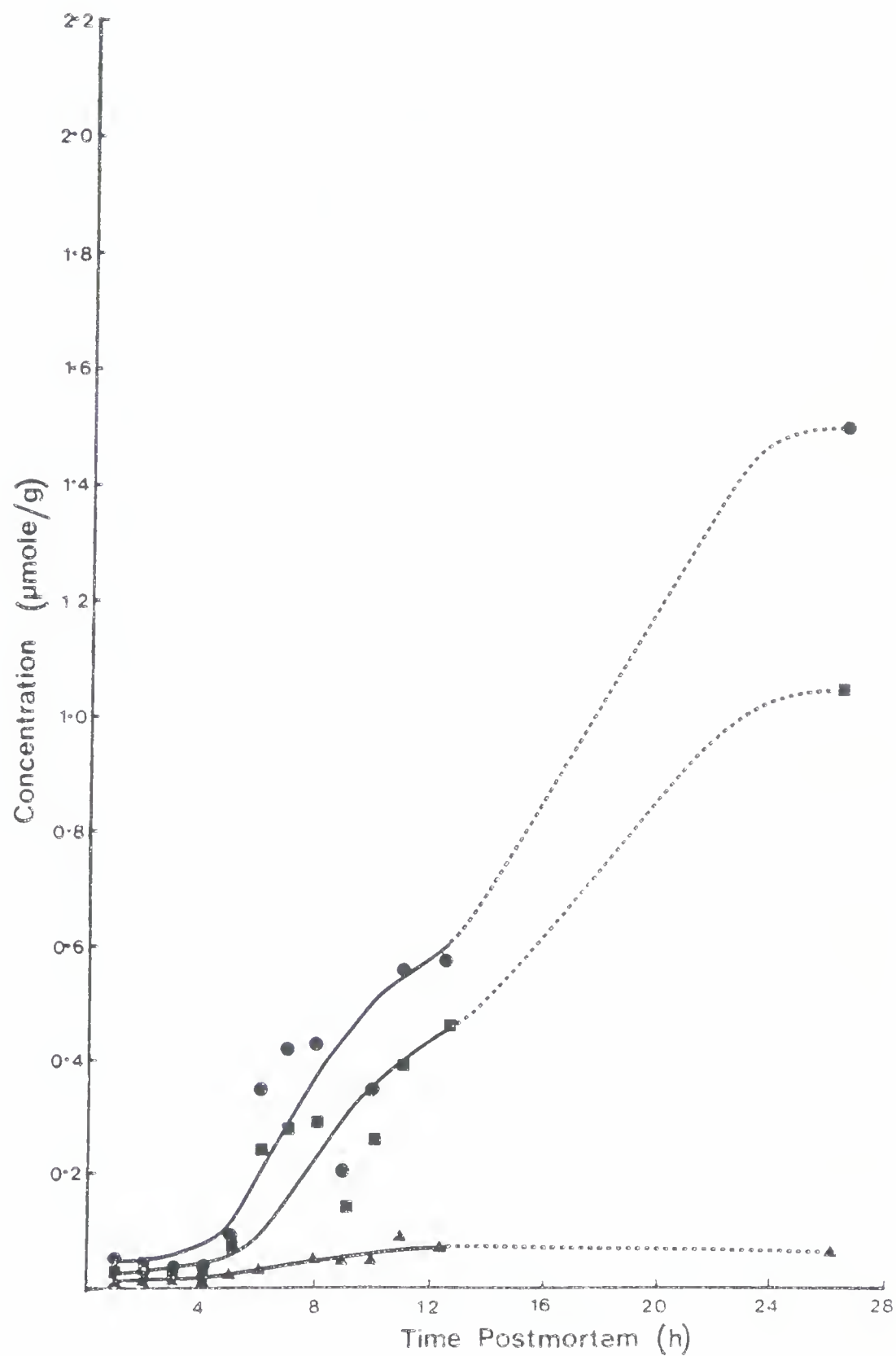


Figure V.23. Concentration profile of ATP metabolites [ATP (●-●-●), ADP (▼-▼-▼), IMP (▲-▲-▲) and NAD (■-■-■) vs time postmortem] for carcass 18. Each datum point represents a single determination.

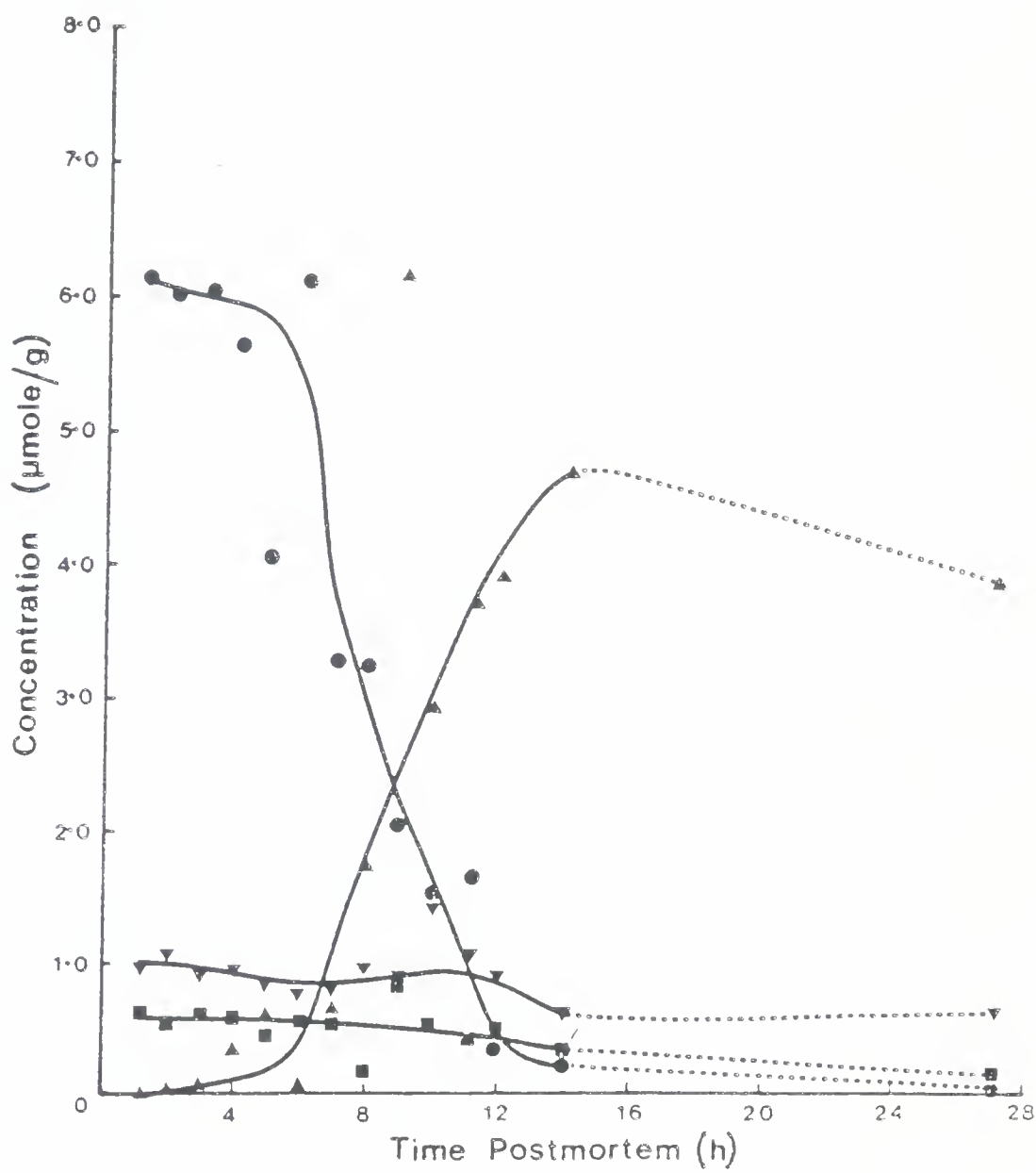
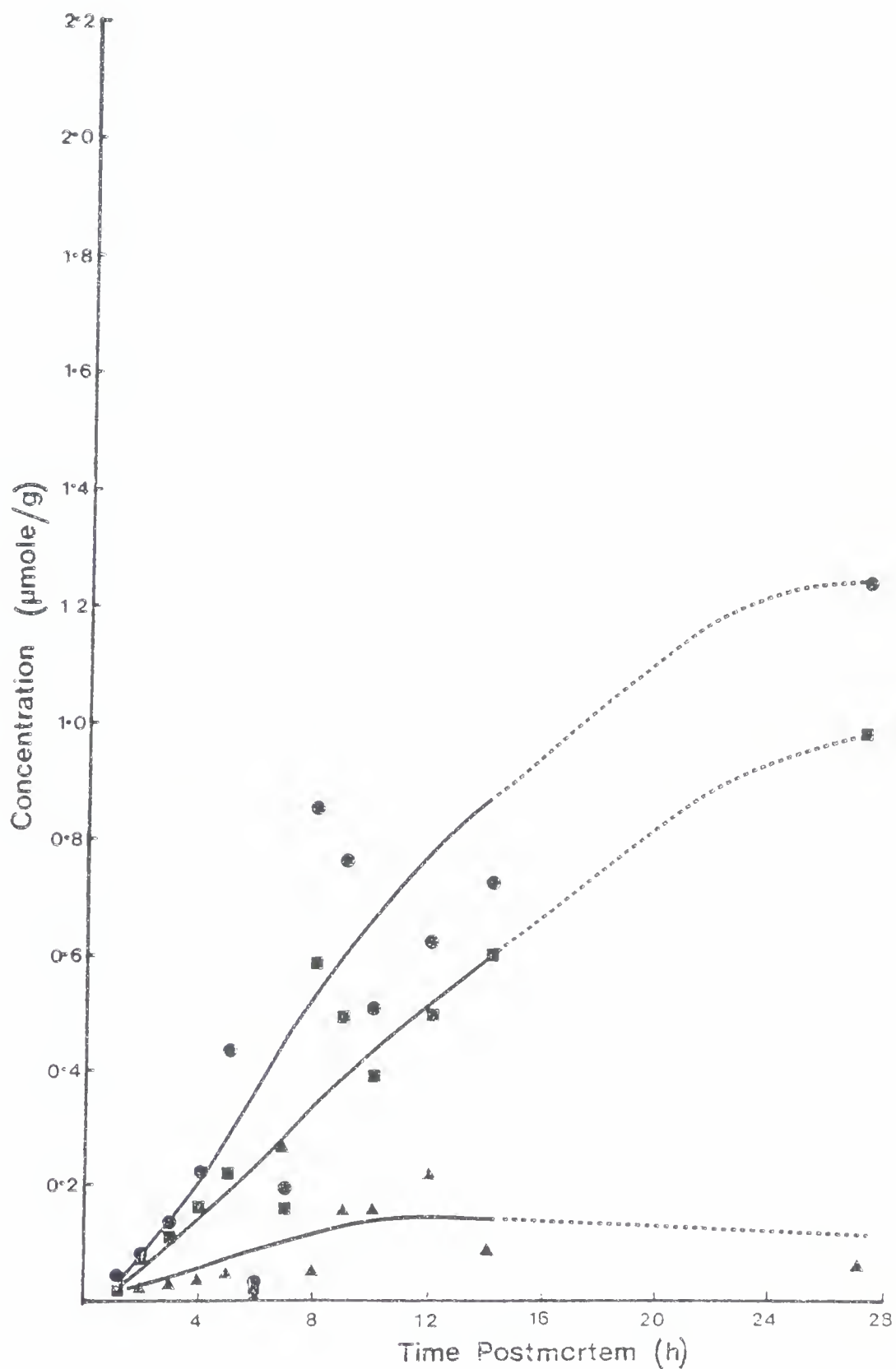


Figure V.24. Concentration profile of ATP metabolites [inosine (●-●-●), hypoxanthine (■-■-■) and AMP (▲-▲-▲) vs time postmortem] for carcass 18. Each datum point represents a single determination.





graph is a plot of concentration ( $\mu\text{mole/g}$ ) versus time postmortem of ATP (adenosine-5'-triphosphate), IMP (inosine-5'-monophosphate), ADP (adenosine-5'-diphosphate) and NAD (nicotinamide adenine dinucleotide). The second graph is a plot of concentration ( $\mu\text{mole/g}$ ) versus time postmortem of inosine, hypoxanthine and AMP (adenosine-5'-monophosphate). Carcasses 7-10 were first analysed when NAD and AMP had not been resolved. For this reason those two components are not plotted in Figures V.1-V.8.

GTP (guanosine-5'-triphosphate), IDP (inosine-5'-diphosphate) and GMP (guanosine-5'-monophosphate) were not plotted since normally their contents were low. GTP was usually about 0.090-0.100  $\mu\text{mole/g}$  and would be absent at 28-30 hr. IDP increased from less than 0.02  $\mu\text{mole/g}$  near slaughter to reach a concentration of 0.100  $\mu\text{mole/g}$  near rigor. Bendall and Davey (1957) also reported more IDP at the later stages of rigor but it was undetectable by 28 hr. GMP increased from undetectable levels to concentrations in the region of 0.08-0.100  $\mu\text{mole/g}$  at 28-30 hr. Naguno and Matsuo (1979) mixed 0.5 g of GMP (disodium salt) with 50 g beef, 150 g water and 4 g NaCl. They reported that 125.2 g of water per 50 g of meat were retained in the treated ground meat, compared to 24.7 g water per 50 g of meat in the control. Thus, about 7  $\mu\text{mole}$  of GMP/g of a ground meat slurry were capable of increasing the water holding capacity 5-fold. A comparison of the GMP concentration at 28 h and the maximum expressed juice did not reveal a significant



correlation ( $r=0.041$ ) in the present study. The expressed juice was determined using a very high centrifuge pressure so that small differences in WHC could not be detected. For this reason the results reported here cannot be considered conclusive.

The initial ATP concentrations of carcasses 7-18 ranged from about 5.2-6.9  $\mu\text{mole/g}$ . This range encompasses the initial postmortem ATP concentration of 5.5 and 5.7  $\mu\text{mole ATP/g}$  from the sternomandibularis and longissimus dorsi, respectively, reported by Bendall (1973). The early postmortem ATP concentration of different carcasses was found to increase, remain constant or fall rapidly within the early postmortem period. Sample 16 was extraordinary in that the ATP concentrations were greater than 6.5  $\mu\text{mole/g}$  for 7 hr. The other extreme, carcass 8, had an ATP concentration of 0.1  $\mu\text{mole/g}$  within 4.5 hr. The ATP concentration in this sample did not remain low but rose again near 8 hr. This increase seemed to correlate with the prolonged gradual pH fall which continued for 20 hr postmortem. Carcasses 9 and 13 also reflected similar changes in the ATP concentration in that the concentrations reached a minimum and then rose. The pH fall recorded was exceptionally long. The pH was still falling at 28 hr for carcass 9 and carcass 13 was not at the ultimate pH until 24 hr. Carcass 10 never reached a minimum ATP concentration early postmortem, but the concentration remained relatively high near rigor (about 0.5  $\mu\text{mole/g}$ ) for several hours and



was still 0.2  $\mu\text{mole/g}$  at 28 hr. The pH of carcass 10 was still falling at 36 hr, the longest pH fall recorded in this study. These observations could be explained as a result of prolonged glycolysis. The glycolytic activity within the cell could maintain the ATP concentrations or increase the ATP level in the muscle with a concomitant reduction in pH. The isometric tension recorded for carcasses 9 and 10 peaked at 12.4 and 17.5 hr, respectively. This may suggest the muscle ATP hydrolases were inactivated for some reason, allowing the ATP concentrations to increase in the muscle as glycolysis continued.

The isometric tension for carcass 13 was near maximum at 18 hr ( $60 \text{ g/cm}^2$ ), although the ultimate tension was not reached until 23 hr ( $61.5 \text{ g/cm}^2$ ). This may indicate the myofibrillar ATPase was inhibited (but not inactivated as in the previous two samples). The ATPase in the muscle would be capable of maintaining an isometric tension but it would be inadequate to increase the tension. This would allow ATP levels in the muscle to increase as glycolysis continued since the ATP hydrolases would not be rapidly utilizing the ATP generated.

ADP concentrations were also similar to those recorded by Bendall (1973) of about 1  $\mu\text{mole/g}$ . Bendall (1973) indicates the calculated free ADP concentration should only be 0.03  $\mu\text{mole/g}$ . Thus, the ADP determined must have originated from ADP bound to actin monomers in the thin filament and to myosin or ADP compartmentalized in the



mitochondria and sarcoplasmic reticulum. The ADP concentrations were fairly constant during the prerigor period and then fell near rigor. For samples where the ATP concentrations were near initial values for a few hours (carcasses 10, 11, 16 and 17) there was a slight increase in ADP concentration before falling. Bendall (1973) observed the ADP levels continued to fall until the concentration was about 0.5-0.7  $\mu\text{mole/g}$ , which is the amount calculated to be bound to actin. For many samples in this study these values of ADP were reached within 28 hr.

AMP concentrations were initially below those reported by Newbold and Scopes (1967). Initial values of AMP for carcasses 11-18 varied between 0.005-0.025  $\mu\text{mole/g}$ . Newbold and Scopes (1967) reported an initial AMP concentration of 0.2  $\mu\text{mole/g}$ .

Bendall (1973) explained a plateau in glycolysis as "probably" a result of the deamination of AMP. AMP is required as a cofactor for phosphorylase and for phosphofructokinase to promote glycolysis. In the current observations AMP concentrations were initially low and increased as rigor progressed. These results seem to contradict the earlier observations. With respect to AMP, the data support the observations of Berman and Kench (1973) in their studies of the malignant hyperthermia syndrome in pigs. They found a rapid decline in ATP and creatine phosphate; ADP was unaffected, as with our measurements, but AMP and IMP accumulated. Berman and Kench (1973) concluded



that glycogenolysis was accelerated not only by the depletion of ATP but by the accumulation of AMP. When the AMP levels in this study were compared to the rate of pH fall ( $r=0.245$ ; d.f.=6), time to ultimate pH ( $r=-0.169$ ; d.f.=6) and ultimate pH ( $r=0.432$ ; d.f.=6), no significant correlations were found. It is unlikely the  $\text{HClO}_4$  extracted AMP concentrations reflect the free AMP concentrations in the muscle. Bendall (1973) calculated that the initial AMP concentrations should be about  $3 \times 10^{-5}$   $\mu\text{moles/g}$ , but the initial AMP concentrations determined were much higher (about  $1.5 \times 10^{-2}$   $\mu\text{mole/g}$ ). It is probable that AMP, like ADP, is bound or compartmentalized, thus altering its free concentration in the cytoplasm. It would be reasonable to expect the higher AMP concentrations near rigor would increase the free AMP levels, but the above mentioned problem may cloud the results and thus not confirm the suggestion of Berman and Kench (1973) that glycolysis is accelerated by an accumulation of AMP.

Bendall (1973) reported NAD concentrations of 0.4-0.5  $\mu\text{mole/g}$  in beef muscle. Newbold and Scopes (1967) found that NAD concentration fell during rigor and in the postrigor period. Both these observations have been confirmed in this study. The inability to determine the oxidation state of NAD precludes any opportunity to comment on the  $\text{NAD}^+$  or  $\text{NADH}$  concentrations at different times in the postmortem muscle.

The deamination of AMP leads to the formation of IMP and ammonia. The absorbance ratios at the wavelengths



250:258 nm and the calculation of R values (Honikel *et al.*, 1981) have often been used to assess the rate of ATP degradation and the onset of rigor. With this absorbance ratio method the relative concentrations of the adenine nucleotides to IMP and inosine are measured. For many carcasses the fall in ATP is paralleled with a rise in IMP, inosine and hypoxanthine levels. However, the changes that each of the nucleotides undergo cannot be assessed with the absorbance ratio method. Several differences in the metabolism of IMP are seen in the results obtained. The IMP levels of carcasses 7, 8, 10 and 12 are all greater than 5  $\mu\text{mole/g}$  by rigor or 28 hr. The inosine and hypoxanthine concentrations are relatively low during the same time period, less than 1.0 and 0.7  $\mu\text{mole/g}$ , respectively. For several other carcasses, most notably 13, 14, 15 and 16, the IMP levels were low, less than 5.0  $\mu\text{mole/g}$ , and the inosine and hypoxanthine concentrations were greater than 1.0  $\mu\text{mole/g}$ . The remainder of the carcasses had IMP, inosine and hypoxanthine values were somewhere in between these levels, although overlapping of some values did occur. These results reveal interesting differences in the mechanism activating or inhibiting these transitions. Calkins *et al.* (1982), in their sequential determination of inosine and IMP using enzymes, reported very large differences in the rate of reaction converting IMP to inosine between electrically stimulated and nonstimulated muscle samples. The factors contributing to these differences were not determined. The



variations in the concentrations of IMP, inosine and hypoxanthine between carcasses in this study infer that some factors affecting the conversion rates are also present in the *in situ* muscle.

The conversion of IMP to inosine and finally to hypoxanthine does not reflect the stoichiometric relationship predicted. For example, the IMP levels for carcass 9 dropped from 5.7 to 3.6  $\mu\text{mole/g}$ . This reflects the conversion of 2.1  $\mu\text{mole}$  of IMP to inosine and hypoxanthine. During the same time period (12-36 hr postmortem) only 1.45  $\mu\text{mole}$  of additional inosine and hypoxanthine were formed. Calkins *et al.* (1982) suggested from their data that IMP is catabolized beyond hypoxanthine. The inconsistencies in the conversion noted above would support their conclusion.

Lawrie (1979) has indicated that meat is organoleptically at an optimum when the hypoxanthine level has reached 1.5-2.0  $\mu\text{mole/g}$ . He stated that these levels can be attained by 30-40 hr at 20°C. Carcasses 14 and 15 had attained these levels by 28 hr but none of the other carcasses were this high by this time. Carcass 7 was at 1.75  $\mu\text{mole/g}$  by 54 hr and then fell again as the carcass aged. These results reveal that considerable variability in nucleotide metabolism exists between carcasses.

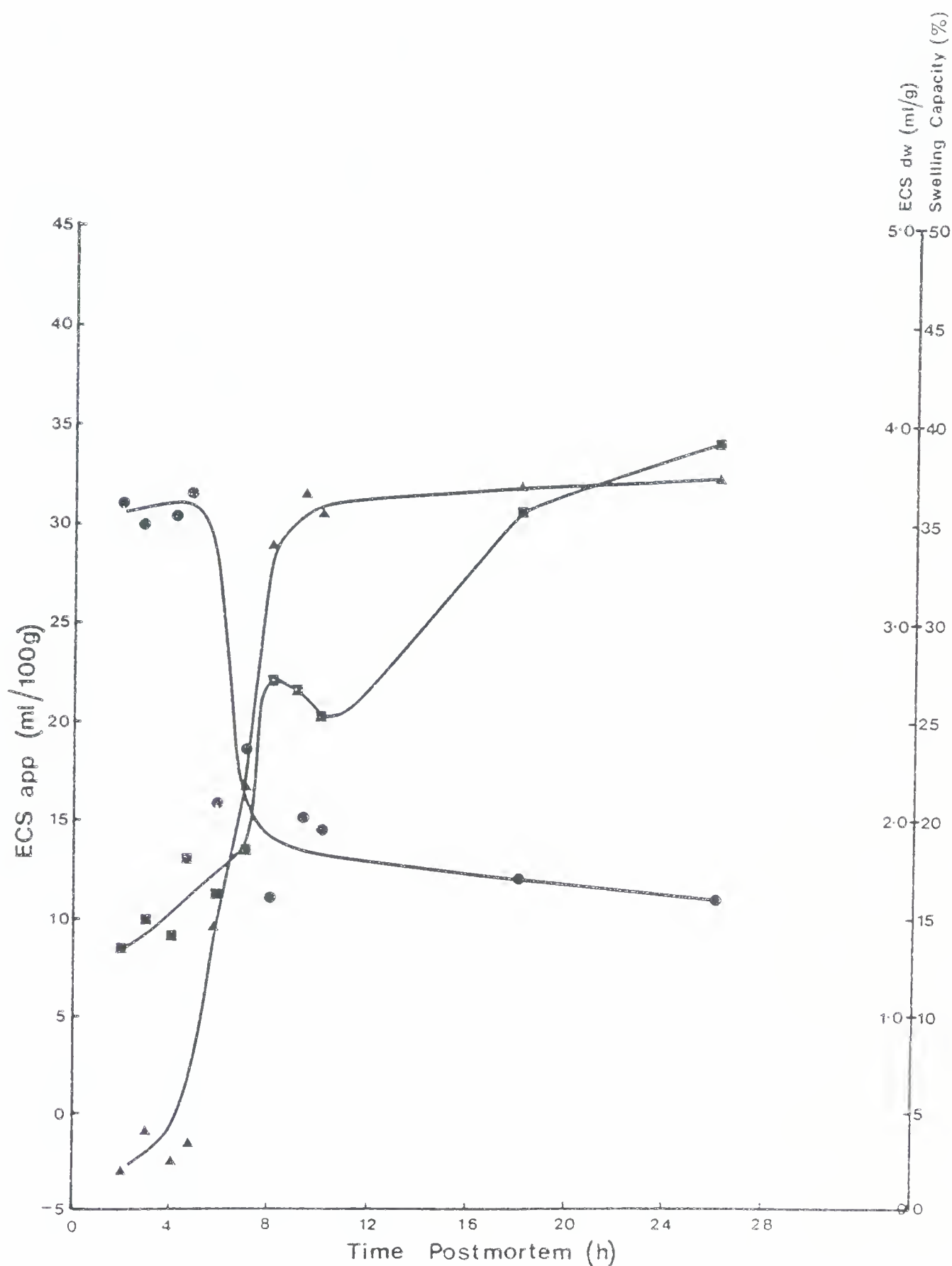


#### D. Carcass 4 ( $\Delta T_1 = 0.098$ sec)

The NMR  $T_1$  profile (Figure III.34) for carcass 4 was very similar to that of carcass 15, except that  $T_1$  did not fall postrigor. The only additional data collected on this carcass were pH fall (Figure III.1) and ECS (Figure V.25). The ECS app was very low initially (2.5 mL/100 g), suggesting a high intrafibre water affinity, which would contribute to a low  $T_1$ . But within 5 hr the swelling capacity dropped and the ECS app rose dramatically. A careful examination of the ECS data indicates that, although ECS app increased greatly when the swelling capacity fell, the ECS dw changed very little (compare 4.8 and 5.6 hr postmortem). As mentioned in section III-C on the discussion of ECS measurements, this would mean the reduction in swelling capacity was almost completely due to a loss of water from the ICS. This would suggest that in the muscle in the NMR tube the water would have rapidly moved into the ECS, contributing to the sudden rise in the NMR  $T_1$  values. By 8 hr postmortem the ECS dw values were high, suggesting permeation of the fibre by inulin as a result of membrane failure. This part of the reason for the rapid rise in  $T_1$  values could be due to membrane failure and free movement of water into the ECS.

In this carcass the pH fall was very rapid (1.33 pH units/hr). This likely contributed to the early formation of crossbridges and the tightening of the interfilamental spacing, resulting in an early loss of swelling capacity and

Figure V.25. Carcass 4. Plot of swelling capacity (•-•-•) vs time postmortem; the standard deviation is 2-15% (ave. 9%) of the mean. Plot of ECS dw (■-■-■) vs time postmortem; the standard deviation is 3-15% (ave. 10%) of the mean. Plot of ECS app (▲-▲-▲) vs time postmortem; the standard deviation is 5-25% (ave. 18%) of the mean.





a reduction of the intrafibre water affinity. If the contraction initiated at this time was fueled by glycolysis until 16 hr, the extent of the contraction could be considerable. The interfilamental spacing may be so tight that it would be impossible to restore the high intrafibre water affinity (ECS app) measured early prerigor. It may be for this reason that no reduction in  $T_1$  was measured postrigor.

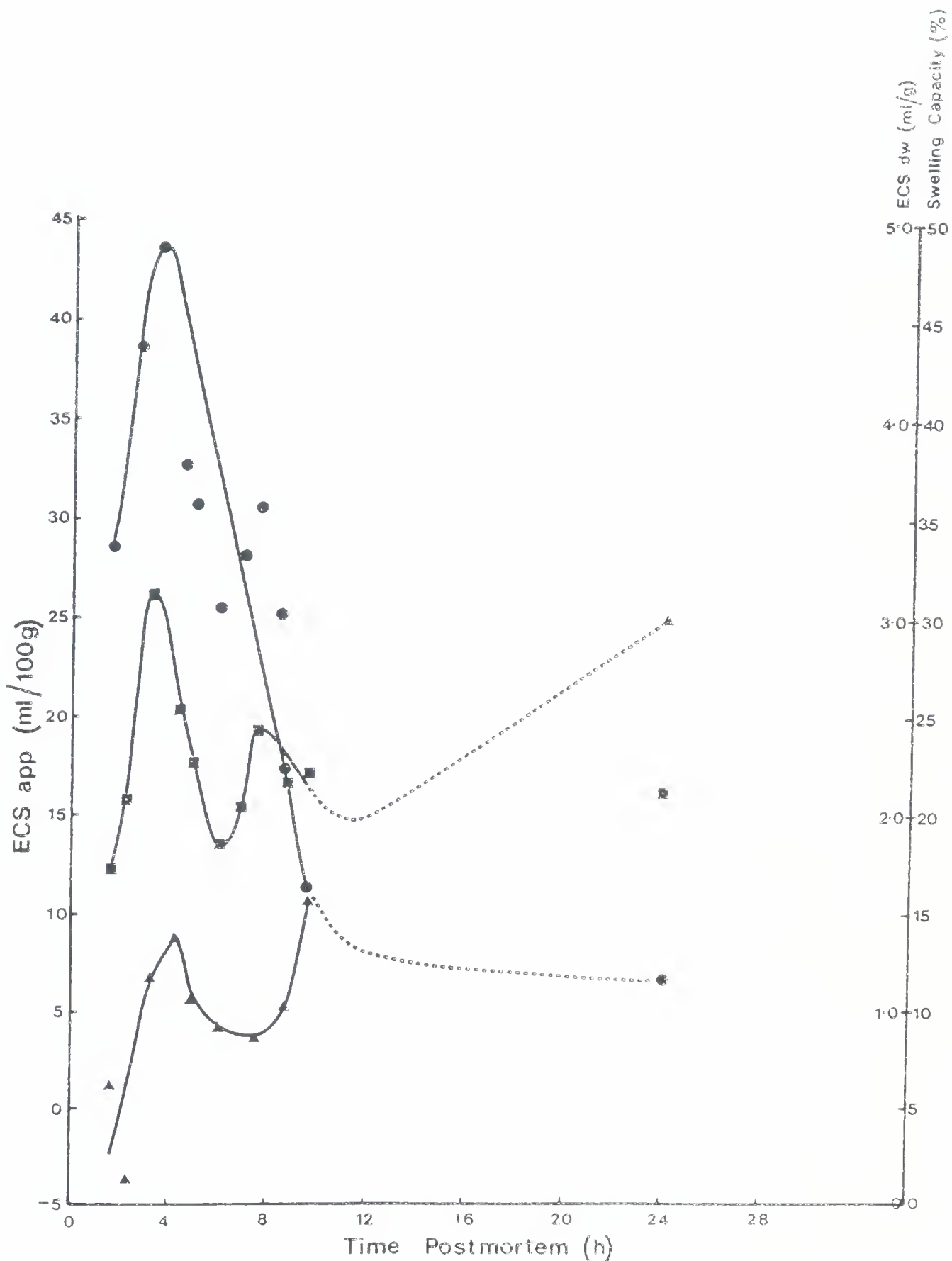


### E. Carcass 5 ( $\Delta T_1=0.038$ sec)

The collection of the  $T_1$  data (Figure III.34) did not begin until 3.5 hr. However, it appears that the  $T_1$  rose quite quickly initially, plateaued between 4 and 8 hr, and then increased again to peak at 12 hr postmortem. The slope postpeak was -0.00174 sec/hr. The ECS data (Figure V.26) show an initially high intrafibre water affinity (ECS app -2.5 mL/g) which is rapidly lost (rising ECS app and ECS dw). At 4 hr the ECS app falls, showing an increase in the intrafibre water affinity. This parallels the plateau in the  $T_1$  values observed between 4 and 8 hr postmortem. After approximately 8 hr the ECS data began to rise steeply, as would be expected from a similar rise in  $T_1$  data.

The pH data (Figure III.1) show a relatively low rate of pH fall (0.36 pH units/hr), attaining the ultimate pH at 11 hr.

Figure V.26. Carcass 5. Plot of swelling capacity (•-•-•) vs time postmortem; the standard deviation is 2-20% (ave. 10%) of the mean. Plot of ECS dw (■-■-■) vs time postmortem; the standard deviation is 2-30% (ave. 10%) of the mean. Plot of ECS app (▲-▲-▲) vs time postmortem; the standard deviation is 2-15% (ave. 9%) of the mean.



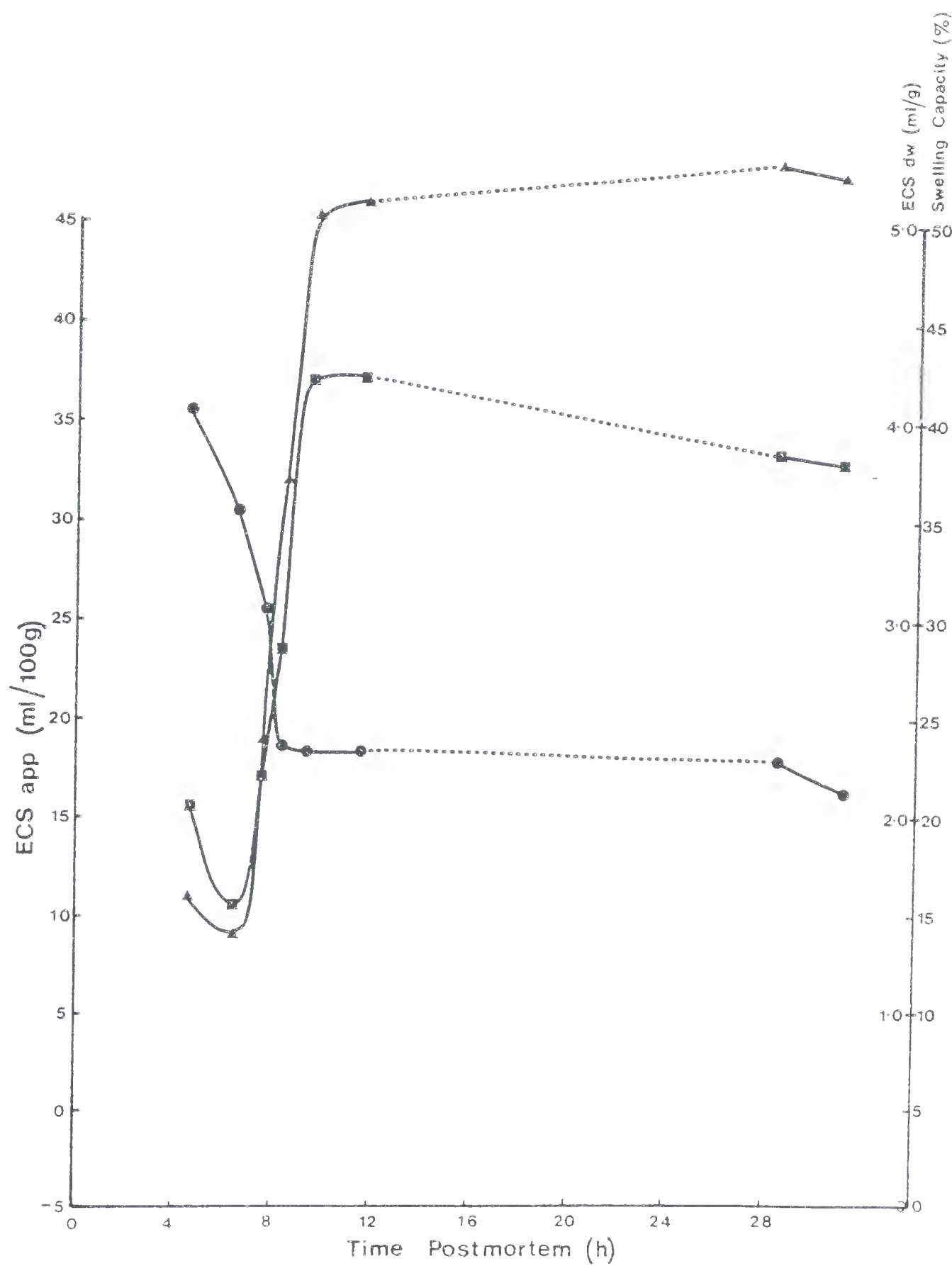


#### F. Carcass 6 ( $\Delta T_1 = 0.038$ sec)

The  $T_1$  profile (Figure III.34) consists of a rise in  $T_1$  until 4 hr, a plateau between 4 and 6 hr, and then a rise in  $T_1$  to peak at 8.5 hr. The slope postpeak was -0.00199 sec/hr. The ECS data (Figure V.27) were not obtained early prerigor, but the first data collected indicated a low intrafibre water affinity (ECS app 11 mL/g). The ECS app fell briefly ( $\approx 4-6$  hr) and then quickly rose.

The small change in  $\Delta T_1$ , and the high ECS app suggest a carcass having a low intrafibre water affinity throughout rigor development. These results imply that a small  $\Delta T_1$  may not be a characteristic of a carcass having a high intrafibre water affinity. If the intrafibre water affinity is initially low, then the initial  $T_1$  will be high and the relative loss of intrafibre water affinity will be smaller, resulting in a small  $\Delta T_1$ . The  $T_1$  slope postpeak (slope = -0.00199) demonstrates an improvement in the intrafibre water activity.

Figure V.27. Carcass 6. Plot of swelling capacity (●-●-●) vs time postmortem; the standard deviation is 2-29% (ave. 19%) of the mean. Plot of ECS dw (■-■-■) vs time postmortem; the standard deviation is 2-15% (ave. 7%) of the mean. Plot of ECS app (▲-▲-▲) vs time postmortem; the standard deviation is 3-35% (ave. 15%) of the mean.



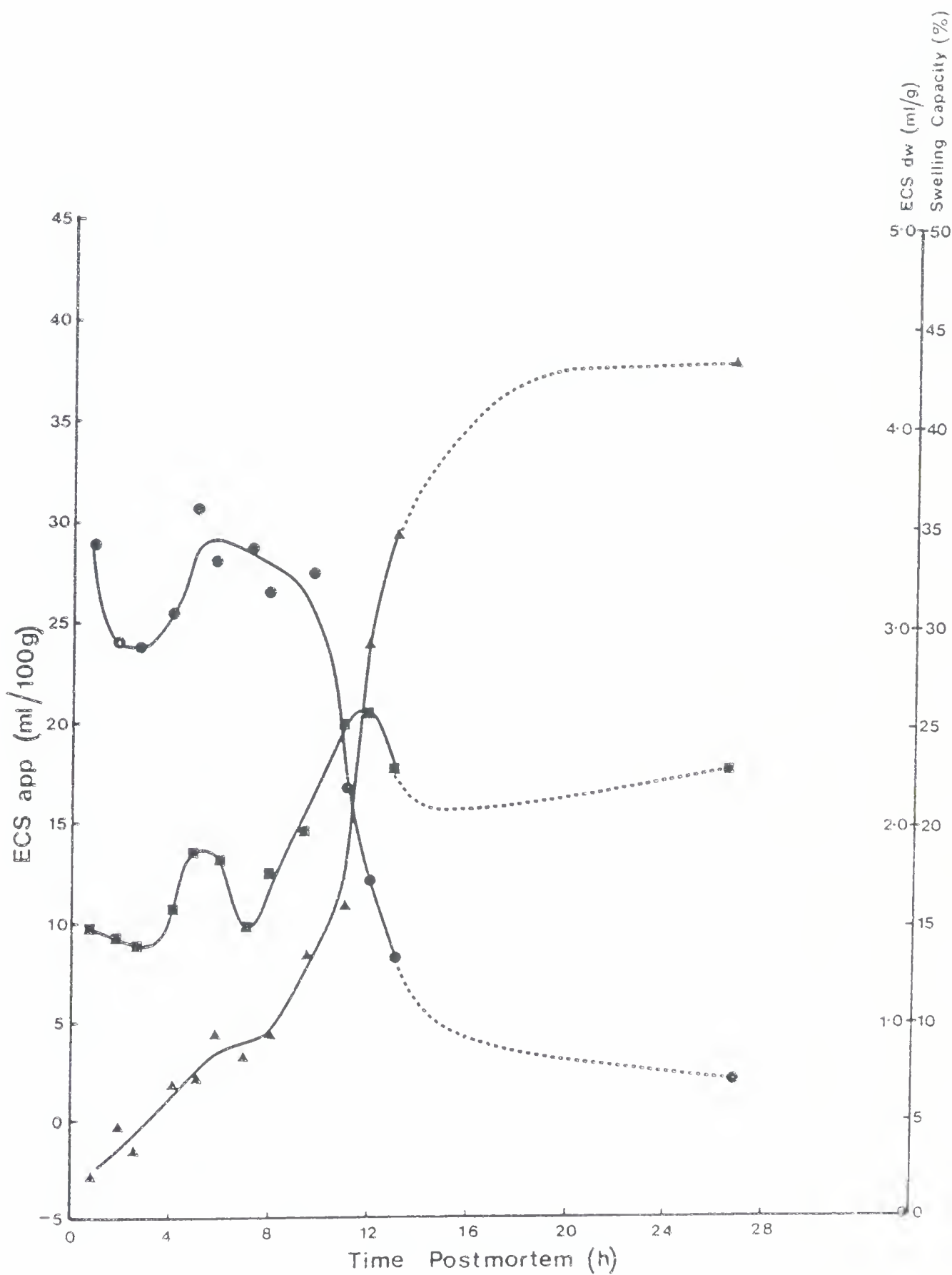


### G. Carcass 7 ( $\Delta T_s = 0.017$ sec)

The peak  $T_s$  (7.5 hr) occurred when the ATP was high ( $>1.5 \mu\text{mole/g}$ ). The ATP concentration (Figure V.1) reached normal postrigor values ( $0.05 \mu\text{mole/g}$ ) at 14 hr. Based on this information, it would appear that the major fall in the  $T_s$  (Figure III.35) would have occurred during the time isometric tension (if measured) would have been developing. This observation and the rise in the  $T_s$  values postrigor are comparable to carcass 14 in that the interfilamental distances would likely have been very small.

The ECS data (Figure V.28) show a rapid loss of intrafibre water affinity. The ECS app is low (high intrafibre water affinity) initially, but the intrafibre water affinity was never regained.

Figure V.28. Carcass 7. Plot of swelling capacity (●-●-●) vs time postmortem; the standard deviation is 2-60% (ave. 24%) of the mean. Plot of ECS dw (■-■-■) vs time postmortem; the standard deviation is 2-14% (ave. 9%) of the mean. Plot of ECS app (▲-▲-▲) vs time postmortem; the standard deviation is 1-40% (ave. 11%) of the mean.





H. Pearson's correlation coefficients from parameters  
obtained from carcasses 9-18

Table V.2 contains the correlation coefficients of 36 variables. A correlation is significant if p is less than 0.05. The 36 variables are:

V2 -- ultimate pH

V3 -- pH at 1 hr

V4 -- rate of pH decline

V5 -- time (hr) to ultimate pH

V6 -- maximum isometric tension (g/cm<sup>2</sup>)

V7 -- time (hr) to maximum isometric tension

V8 -- time (hr) of initial isometric tension increase

V9 -- initial T<sub>1</sub>, (s)

V10 -- peak T<sub>1</sub>, (s)

V11 -- time (hr) to peak T<sub>1</sub>,

V12 -- time (hr) to T<sub>1</sub>, plateau

V13 -- pH at peak T<sub>1</sub>,

V14 -- initial postpeak T<sub>1</sub>, slope

V15 -- second postpeak T<sub>1</sub>, slope

V16 -- moisture (%)

V17 -- Initial ECS app (mL/100 g)

V18 -- time (hr) to initial ECS app pH

V19 -- ECS app (mL/100 g) initial pH

V20 -- time (hr) to post initial peak ECS app minimum

V21 -- postpeak ECS app (mL/100 g) minimum

V22 -- time (hr) to ECS app of 15 mL/100 g



V23 -- postrigor ECS app (mL/100 g)  
V24 --  $\Delta T_1$ ,  
V25 -- initial expressed juice (%)  
V26 -- time (hr) to 10% expressed juice  
V27 -- postrigor expressed juice (%)  
V28 -- time (hr) to beginning of first  $T_1$  slope  
V29 -- time (hr) to second postpeak  $T_1$  slope  
V30 -- initial swelling capacity (%)  
V31 -- time (hr) for swelling capacity to fall to 20%  
V32 -- postrigor swelling capacity (%)



Table V.2 Pearson's correlation coefficients of 36 selected variables from carcasses 9-18

	V2	V3	V4	V5	V6	V7	V8	V9	V10	V11	V12
V2	1.0000 ( 9 ) P= .223	.2913 ( 9 ) P= .097	-.4737 ( 9 ) P= .020	-.2144 ( 9 ) P= .001	-.3784 ( 9 ) P= .440	.0970 ( 9 ) P= .106	-.5832 ( 9 ) P= .365	.1408 ( 9 ) P= .094	.2631 ( 9 ) P= .056	-.3123 ( 9 ) P= .154	-.0799 ( 9 ) P= .393
V3	.2913 ( 9 ) P= .097	1.0000 ( 0 ) P= .036	-.6192 ( 9 ) P= .001	-.6849 ( 9 ) P= .001	.4580 ( 9 ) P= .440	.1338 ( 9 ) P= .466	.1355 ( 9 ) P= .364	.4798 ( 9 ) P= .070	.5615 ( 9 ) P= .095	-.3824 ( 9 ) P= .048	-.1054 ( 9 ) P= .071
V4	-.4737 ( 9 ) P= .097	-.6192 ( 9 ) P= .036	1.0000 ( 0 ) P= .001	.8590 ( 9 ) P= .001	.0594 ( 9 ) P= .156	-.0332 ( 9 ) P= .214	-.2000 ( 9 ) P= .172	-.5291 ( 9 ) P= .109	-.4777 ( 9 ) P= .145	.5844 ( 9 ) P= .033	.5281 ( 9 ) P= .017
V5	-.2144 ( 9 ) P= .289	-.6849 ( 9 ) P= .020	.8590 ( 9 ) P= .001	1.0000 ( 0 ) P= .001	-.3794 ( 9 ) P= .156	.3014 ( 9 ) P= .214	-.3561 ( 9 ) P= .172	-.4532 ( 9 ) P= .109	-.3947 ( 9 ) P= .145	.6306 ( 9 ) P= .048	.6988 ( 9 ) P= .071
V6	-.3784 ( 9 ) P= .157	.4580 ( 9 ) P= .106	.0594 ( 9 ) P= .440	-.3794 ( 9 ) P= .156	1.0000 ( 0 ) P= .156	-.1927 ( 9 ) P= .309	.4870 ( 9 ) P= .390	.2591 ( 9 ) P= .250	.3147 ( 9 ) P= .204	.1642 ( 9 ) P= .336	.1801 ( 9 ) P= .321
V7	.0970 ( 9 ) P= .402	.1338 ( 9 ) P= .365	-.0332 ( 9 ) P= .466	.3014 ( 9 ) P= .214	-.1927 ( 9 ) P= .309	1.0000 ( 0 ) P= .391	.1076 ( 9 ) P= .391	.3927 ( 9 ) P= .147	.4962 ( 9 ) P= .086	.3698 ( 9 ) P= .163	.6782 ( 9 ) P= .021
V8	-.5832 ( 9 ) P= .048	.1355 ( 9 ) P= .364	-.2000 ( 9 ) P= .302	-.3561 ( 9 ) P= .172	.4870 ( 9 ) P= .090	.1076 ( 9 ) P= .391	1.0000 ( 0 ) P= .391	.5644 ( 9 ) P= .055	.4972 ( 9 ) P= .085	-.1416 ( 9 ) P= .358	-.3779 ( 9 ) P= .157
V9	.1408 ( 9 ) P= .359	.4798 ( 9 ) P= .094	-.5291 ( 9 ) P= .070	-.4532 ( 9 ) P= .109	.2591 ( 9 ) P= .250	.3927 ( 9 ) P= .147	.5644 ( 9 ) P= .055	.9434 ( 0 ) P= .000	.9434 ( 9 ) P= .000	-.0264 ( 9 ) P= .473	-.2162 ( 9 ) P= .288
V10	.2631 ( 9 ) P= .246	.5615 ( 9 ) P= .056	-.4777 ( 9 ) P= .095	-.3947 ( 9 ) P= .145	.3147 ( 9 ) P= .204	.4962 ( 9 ) P= .086	.4972 ( 9 ) P= .085	1.0000 ( 0 ) P= .000	1.0000 ( 9 ) P= .000	-.1050 ( 9 ) P= .394	-.1144 ( 9 ) P= .384
V11	-.3123 ( 9 ) P= .206	-.3824 ( 9 ) P= .154	.5844 ( 9 ) P= .048	.6306 ( 9 ) P= .033	-.1642 ( 9 ) P= .336	.3698 ( 9 ) P= .163	-.1416 ( 9 ) P= .358	.9434 ( 9 ) P= .473	-.0264 ( 9 ) P= .394	.7072 ( 9 ) P= .016	.7072 ( 9 ) P= .016
V12	-.0799 ( 9 ) P= .419	-.1054 ( 9 ) P= .393	.5281 ( 9 ) P= .071	.6988 ( 9 ) P= .017	.1801 ( 9 ) P= .321	.6782 ( 9 ) P= .021	-.3779 ( 9 ) P= .157	-.2162 ( 9 ) P= .288	-.1144 ( 9 ) P= .384	.7072 ( 9 ) P= .016	1.0000 ( 0 ) P= .016

(COEFFICIENT / CASES) / SIGNIFICANCE) n. n IS PRINTED IF A COEFFICIENT CANNOT BE COMPUTED



Table V.2 (cont.) Pearson's correlation coefficients of 36 selected variables from carcasses 9-18

	V2	V3	V4	V5	V6	V7	V8	V9	V10	V11	V12
V13	.8254 ( P= .003	.4733 ( P= .098	-.3637 ( P= .167	-.1443 ( P= .355	-.1882 ( P= .313	.2151 ( P= .289	-.3415 ( P= .183	.2064 ( P= .297	.4265 ( P= .125	-.4252 ( P= .126	-.0263 ( P= .473
V14	.2852 ( P= .228	-.2687 ( P= .241	.0176 ( P= .482	-.0547 ( P= .444	-.1651 ( P= .335	-.6075 ( P= .040	-.4625 ( P= .104	-.7042 ( P= .016	-.6288 ( P= .034	-.5757 ( P= .051	-.3711 ( P= .162
V15	.3831 ( P= .153	-.5229 ( P= .073	.0510 ( P= .448	.3096 ( P= .208	-.7687 ( P= .007	-.0170 ( P= .483	-.6220 ( P= .036	-.6198 ( P= .036	-.5892 ( P= .046	.0585 ( P= .440	.1629 ( P= .337
V16	.3326 ( P= .190	.5632 ( P= .056	-.3491 ( P= .177	-.1811 ( P= .320	.1817 ( P= .319	.7261 ( P= .012	.3074 ( P= .210	.6480 ( P= .028	.8433 ( P= .002	-.0967 ( P= .402	.2086 ( P= .294
V17	-.4418 ( P= .116	.4682 ( P= .100	-.0674 ( P= .431	-.4859 ( P= .091	.8650 ( P= .001	-.3444 ( P= .181	.3758 ( P= .158	-.0292 ( P= .470	-.0157 ( P= .484	-.3660 ( P= .165	-.2483 ( P= .259
V22	.2619 ( P= .247	2026 ( P= .300	.1661 ( P= .334	.3775 ( P= .157	.0456 ( P= .454	.8125 ( P= .003	-.1155 ( P= .383	.1851 ( P= .316	.4244 ( P= .126	.1398 ( P= .360	.6641 ( P= .024
V23	-.3759 ( P= .158	.2876 ( P= .226	-.3404 ( P= .184	-.2925 ( P= .222	.0761 ( P= .423	.4063 ( P= .138	.3805 ( P= .155	.3210 ( P= .199	.1703 ( P= .330	.3119 ( P= .206	.2269 ( P= .278
V24	.3933 ( P= .146	.3363 ( P= .187	.0406 ( P= .459	.0839 ( P= .415	1837 ( P= .318	.3571 ( P= .172	-.1144 ( P= .384	-.0379 ( P= .461	.2946 ( P= .220	.2952 ( P= .219	.2464 ( P= .261
V25	.6425 ( P= .030	.7648 ( P= .202	-.6153 ( P= .038	-.4578 ( P= .106	.0814 ( P= .417	.2815 ( P= .231	-.0591 ( P= .440	.3637 ( P= .167	.5549 ( P= .059	-.2952 ( P= .219	.2464 ( P= .261
V26	.0238 ( P= .476	-.3174 ( P= .202	.6490 ( P= .028	.7520 ( P= .009	-.0344 ( P= .465	.4143 ( P= .133	-.2279 ( P= .277	-.2544 ( P= .254	-.0352 ( P= .464	-.6236 ( P= .339	-.1159 ( P= .057
V27	.5630 ( P= .056	.4255 ( P= .126	.0630 ( P= .436	.0922 ( P= .407	.1941 ( P= .308	.3591 ( P= .170	-.3157 ( P= .203	.1698 ( P= .117	.4388 ( P= .435	.0635 ( P= .331	.3765 ( P= .158

(COEFFICIENT / (CASES) / SIGNIFICANCE) " . " IS PRINTED IF A COEFFICIENT CANNOT BE COMPUTED



Table V.2 (cont.) Pearson's correlation coefficients of 36 selected variables from carcasses 9-18

	V2	V3	V4	V5	V6	V7	V8	V9	V10	V11	V12
V28	-.4104 ( P= .135	-.4123 ( P= .134	.6777 ( P= .021	.6180 ( P= .037	.0501 ( P= .335	-.1205 ( P= .378	-.2951 ( P= .220	-.3302 ( P= .192	.8305 ( P= .002	.5153 ( P= .076	
V29	.7239 ( P= .013	.6530 ( P= .027	-.7044 ( P= .016	-.5628 ( P= .056	-.1397 ( P= .360	-.0492 ( P= .450	-.3529 ( P= .175	.0108 ( P= .489	.1330 ( P= .366	-.6810 ( P= .021	
V30	-.0848 ( P= .414	.3366 ( P= .187	.0431 ( P= .456	-.1165 ( P= .382	.1547 ( P= .345	-.3524 ( P= .175	-.4474 ( P= .112	-.3312 ( P= .191	-.4261 ( P= .125	.0879 ( P= .411	
V31	.2400 ( P= .266	.3530 ( P= .175	.0266 ( P= .473	.2585 ( P= .250	.0153 ( P= .484	.8239 ( P= .003	-.1332 ( P= .366	.1311 ( P= .368	.3563 ( P= .172	.0617 ( P= .437	
V32	-.0292 ( P= .470	.7062 ( P= .016	-.1522 ( P= .348	-.2138 ( P= .290	.3685 ( P= .163	.0834 ( P= .415	-.0024 ( P= .498	.0128 ( P= .487	.1210 ( P= .378	.6810 ( P= .147	
V33	.1624 ( P= .338	.1579 ( P= .342	-.1283 ( P= .371	-.2856 ( P= .227	.2041 ( P= .299	-.1588 ( P= .341	-.3074 ( P= .210	-.0101 ( P= .490	-.0945 ( P= .404	.1250 ( P= .202	
V34	-.0652 ( P= .434	-.3143 ( P= .204	-.2305 ( P= .275	-.1809 ( P= .320	.1590 ( P= .341	.0771 ( P= .422	.1022 ( P= .396	.0844 ( P= .414	-.0812 ( P= .418	.3165 ( P= .258	
V35	.1550 ( P= .345	.0180 ( P= .482	.1915 ( P= .310	.4636 ( P= .103	-.4219 ( P= .128	.4934 ( P= .087	-.5284 ( P= .070	.0044 ( P= .496	-.0517 ( P= .447	.6478 ( P= .028	
V36	-.3152 ( P= .203	-.0675 ( P= .431	.2564 ( P= .252	.1711 ( P= .330	.4697 ( P= .100	.4613 ( P= .104	.3139 ( P= .204	.3639 ( P= .167	.3517 ( P= .176	.7542 ( P= .009	
V37	-.0408 ( P= .458	.2723 ( P= .238	-.3706 ( P= .162	-.5647 ( P= .055	.6240 ( P= .035	-.0816 ( P= .417	.6596 ( P= .025	.4708 ( P= .099	.5340 ( P= .068	.6020 ( P= .042	

(COEFFICIENT / (CASES) / SIGNIFICANCE) " . " IS PRINTED IF A COEFFICIENT CANNOT BE COMPUTED



Table V.2 (cont.) Pearson's correlation coefficients of 36 selected variables from carcasses 9-18

	V13	V14	V15	V16	V17	V22	V23	V24	V25	V26	V27
V2	.8254 (-.9) P=.003	.2852 (-.9) P=.228	.3831 (-.9) P=.153	.3326 (-.9) P=.190	-.4418 (-.9) P=.116	.2619 (-.9) P=.247	-.3759 (-.9) P=.158	.3933 (-.9) P=.146	.6425 (-.9) P=.030	-.0238 (-.9) P=.476	.5630 (-.9) P=.056
V3	-.4733 (-.9) P=.098	-.2687 (-.9) P=.241	-.5229 (-.9) P=.073	.5632 (-.9) P=.056	.4682 (-.9) P=.100	.2026 (-.9) P=.300	.2876 (-.9) P=.226	.3363 (-.9) P=.187	.7648 (-.9) P=.007	-.3174 (-.9) P=.202	.4255 (-.9) P=.126
V4	-.3637 (-.9) P=.167	.0176 (-.9) P=.482	.0510 (-.9) P=.448	-.3491 (-.9) P=.177	-.0674 (-.9) P=.431	.1661 (-.9) P=.334	-.3404 (-.9) P=.184	.0406 (-.9) P=.459	-.6153 (-.9) P=.038	.6490 (-.9) P=.028	.0630 (-.9) P=.436
V5	-.1443 (-.9) P=.355	-.0547 (-.9) P=.444	.3096 (-.9) P=.208	-.1811 (-.9) P=.320	-.4859 (-.9) P=.091	.3775 (-.9) P=.157	-.2925 (-.9) P=.222	.0839 (-.9) P=.145	-.4578 (-.9) P=.106	.7520 (-.9) P=.009	.0922 (-.9) P=.407
V6	-.1882 (-.9) P=.313	-.1651 (-.9) P=.335	-.7687 (-.9) P=.007	.1817 (-.9) P=.319	.8650 (-.9) P=.001	.0456 (-.9) P=.454	.0761 (-.9) P=.423	.1837 (-.9) P=.318	.0814 (-.9) P=.417	-.0344 (-.9) P=.465	.1941 (-.9) P=.308
V7	.2151 (-.9) P=.289	-.6075 (-.9) P=.040	-.0170 (-.9) P=.483	.7261 (-.9) P=.012	-.3444 (-.9) P=.181	.8125 (-.9) P=.003	.4063 (-.9) P=.138	.3571 (-.9) P=.172	.2815 (-.9) P=.231	.4143 (-.9) P=.133	.3591 (-.9) P=.170
V8	-.3415 (-.9) P=.183	-.4625 (-.9) P=.104	-.6220 (-.9) P=.036	.3074 (-.9) P=.210	.3758 (-.9) P=.158	-.1155 (-.9) P=.383	.3805 (-.9) P=.155	-.1144 (-.9) P=.384	-.0591 (-.9) P=.440	-.2279 (-.9) P=.277	-.3157 (-.9) P=.203
V9	.2064 (-.9) P=.297	-.7042 (-.9) P=.016	-.6198 (-.9) P=.036	.6480 (-.9) P=.028	-.0292 (-.9) P=.470	.1851 (-.9) P=.316	.3210 (-.9) P=.199	-.0379 (-.9) P=.461	.3637 (-.9) P=.167	-.2544 (-.9) P=.254	.1698 (-.9) P=.331
V10	.4265 (-.9) P=.125	-.6288 (-.9) P=.034	-.5892 (-.9) P=.046	.8433 (-.9) P=.002	-.0157 (-.9) P=.484	.4244 (-.9) P=.126	.1703 (-.9) P=.330	.2946 (-.9) P=.220	.5549 (-.9) P=.059	-.0352 (-.9) P=.464	.4388 (-.9) P=.117
V11	-.4252 (-.9) P=.126	-.5757 (-.9) P=.051	.0585 (-.9) P=.440	-.0967 (-.9) P=.402	-.3660 (-.9) P=.165	.1398 (-.9) P=.360	.3119 (-.9) P=.206	-.2952 (-.9) P=.219	-.6236 (-.9) P=.035	.1613 (-.9) P=.339	.0635 (-.9) P=.435
V12	-.0263 (-.9) P=.473	-.3711 (-.9) P=.162	.1629 (-.9) P=.337	.2086 (-.9) P=.294	-.2483 (-.9) P=.259	.6641 (-.9) P=.024	.2269 (-.9) P=.278	.2464 (-.9) P=.261	-.1159 (-.9) P=.383	.5606 (-.9) P=.057	.3765 (-.9) P=.158

(COEFFICIENT / (CASES) / SIGNIFICANCE) " . " IS PRINTED IF A COEFFICIENT CANNOT BE COMPUTED



Table V.2 (cont.) Pearson's correlation coefficients of 36 selected variables from carcasses 9-18

	V13	V14	V15	V16	V17	V22	V23	V24	V25	V26	V27
V13	1.0000 ( 9 ) P= .	.1355 ( 9 ) P= .364	.0760 ( 9 ) P= .423	.6043 ( 9 ) P= .041	-.3039 ( 9 ) P= .212	.4781 ( 9 ) P= .095	-.4754 ( 9 ) P= .097	.7129 ( 9 ) P= .015	.8610 ( 9 ) P= .001	.2626 ( 9 ) P= .247	.7270 ( 9 ) P= .012
V14	.1355 ( 9 ) P= .364	1.0000 ( 9 ) P= .052	.5717 ( 9 ) P= .086	-.4964 ( 9 ) P= .397	.1014 ( 9 ) P= .233	-.2791 ( 9 ) P= .049	-.5811 ( 9 ) P= .348	.1514 ( 9 ) P= .460	.0390 ( 9 ) P= .460	.0754 ( 9 ) P= .423	-.1222 ( 9 ) P= .377
V15	.0760 ( 9 ) P= .423	.5717 ( 9 ) P= .052	1.0000 ( 9 ) P= .	-.3221 ( 9 ) P= .198	-.5688 ( 9 ) P= .054	-.0755 ( 9 ) P= .423	-.1689 ( 9 ) P= .489	.0108 ( 9 ) P= .327	-.1733 ( 9 ) P= .428	.0707 ( 9 ) P= .428	-.0889 ( 9 ) P= .410
V16	.6043 ( 9 ) P= .041	-.4964 ( 9 ) P= .086	-.3221 ( 9 ) P= .198	1.0000 ( 9 ) P= .	-.0773 ( 9 ) P= .421	.7333 ( 9 ) P= .011	.1347 ( 9 ) P= .365	.6793 ( 9 ) P= .021	.7037 ( 9 ) P= .016	.2509 ( 9 ) P= .257	.6659 ( 9 ) P= .024
V17	-.3039 ( 9 ) P= .212	.1014 ( 9 ) P= .397	-.5688 ( 9 ) P= .054	-.0773 ( 9 ) P= .421	1.0000 ( 9 ) P= .	-.1495 ( 9 ) P= .350	.2102 ( 9 ) P= .293	.0444 ( 9 ) P= .455	.0809 ( 9 ) P= .418	-.2030 ( 9 ) P= .300	-.1050 ( 9 ) P= .394
V22	.4781 ( 9 ) P= .095	-.2791 ( 9 ) P= .233	-.0755 ( 9 ) P= .423	.7333 ( 9 ) P= .011	-.1495 ( 9 ) P= .350	1.0000 ( 9 ) P= .	-.0657 ( 9 ) P= .433	.7320 ( 9 ) P= .012	.4793 ( 9 ) P= .094	.7583 ( 9 ) P= .008	.6862 ( 9 ) P= .020
V23	-.4754 ( 9 ) P= .097	-.5811 ( 9 ) P= .049	-.1689 ( 9 ) P= .332	.1347 ( 9 ) P= .365	.2102 ( 9 ) P= .293	-.0657 ( 9 ) P= .433	1.0000 ( 9 ) P= .	-.4051 ( 9 ) P= .138	-.1332 ( 9 ) P= .366	-.5120 ( 9 ) P= .078	-.3447 ( 9 ) P= .181
V24	.7129 ( 9 ) P= .015	.1514 ( 9 ) P= .348	.0108 ( 9 ) P= .489	.6793 ( 9 ) P= .021	.0444 ( 9 ) P= .455	.7320 ( 9 ) P= .012	-.4051 ( 9 ) P= .138	1.0000 ( 9 ) P= .024	.6639 ( 9 ) P= .	.6061 ( 9 ) P= .040	.8067 ( 9 ) P= .004
V25	.8610 ( 9 ) P= .001	.0390 ( 9 ) P= .460	-.1733 ( 9 ) P= .327	.7037 ( 9 ) P= .418	.0809 ( 9 ) P= .094	.4793 ( 9 ) P= .008	-.1332 ( 9 ) P= .366	.6639 ( 9 ) P= .024	1.0000 ( 9 ) P= .	.0800 ( 9 ) P= .419	.5631 ( 9 ) P= .056
V26	.2626 ( 9 ) P= .247	.0754 ( 9 ) P= .423	.0707 ( 9 ) P= .428	.2509 ( 9 ) P= .257	-.2030 ( 9 ) P= .300	.7583 ( 9 ) P= .008	-.5120 ( 9 ) P= .078	.6061 ( 9 ) P= .040	.0800 ( 9 ) P= .419	1.0000 ( 9 ) P= .	.4533 ( 9 ) P= .109
V27	.7270 ( 9 ) P= .012	-.1222 ( 9 ) P= .377	-.0889 ( 9 ) P= .410	.6659 ( 9 ) P= .024	-.1050 ( 9 ) P= .394	.6862 ( 9 ) P= .020	-.3447 ( 9 ) P= .181	.8067 ( 9 ) P= .004	.5631 ( 9 ) P= .056	.4533 ( 9 ) P= .109	1.0000 ( 9 ) P= .

(COEFFICIENT / CASES) / SIGNIFICANCE) " . " IS PRINTED IF A COEFFICIENT CANNOT BE COMPUTED



Table V.2 (cont.) Pearson's correlation coefficients of 36 selected variables from carcasses 9-18

	V13	V14	V15	V16	V17	V22	V23	V24	V25	V26	V27
V28	-.3591 ( .9) P= .170	-.3504 ( .9) P= .177	.1144 ( .9) P= .384	-.2355 ( .9) P= .270	-.3034 ( .9) P= .213	-.0992 ( .9) P= .400	.0823 ( .9) P= .416	-.1837 ( .9) P= .318	-.6368 ( .9) P= .031	.1123 ( .9) P= .386	.0401 ( .9) P= .459
V29	.7281 ( .9) P= .012	.3863 ( .9) P= .151	.2011 ( .9) P= .301	.2937 ( .9) P= .221	.0662 ( .9) P= .433	.0977 ( .9) P= .401	-.0980 ( .9) P= .401	.4158 ( .9) P= .132	.8345 ( .9) P= .002	-.2270 ( .9) P= .278	3267 ( .9) P= .194
V30	-.1823 ( .9) P= .319	.0851 ( .9) P= .414	-.1170 ( .9) P= .382	-.4672 ( .9) P= .101	.4110 ( .9) P= .135	-.2793 ( .9) P= .233	.2139 ( .9) P= .290	-.3249 ( .9) P= .196	-.0608 ( .9) P= .438	-.3039 ( .9) P= .212	-1151 ( .9) P= .384
V31	.4675 ( .9) P= .101	-.2669 ( .9) P= .243	-.0516 ( .9) P= .447	.7170 ( .9) P= .014	-.0521 ( .9) P= .447	.9533 ( .9) P= .000	.1125 ( .9) P= .386	.6983 ( .9) P= .017	.5667 ( .9) P= .054	.6207 ( .9) P= .036	.6014 ( .9) P= .042
V32	.3319 ( .9) P= .190	-.0509 ( .9) P= .448	-.4759 ( .9) P= .096	.2670 ( .9) P= .243	.5359 ( .9) P= .067	.3074 ( .9) P= .210	.0667 ( .9) P= .432	.3683 ( .9) P= .164	.6101 ( .9) P= .039	.1271 ( .9) P= .372	.2190 ( .9) P= .285
V33	-.2725 ( .9) P= .238	-.0107 ( .9) P= .489	.1249 ( .9) P= .374	-.2150 ( .9) P= .289	.2018 ( .9) P= .301	-.2229 ( .9) P= .282	.3544 ( .9) P= .174	-.2987 ( .9) P= .217	-.2343 ( .9) P= .271	-.4576 ( .9) P= .106	.0954 ( .9) P= .403
V34	-.5414 ( .9) P= .065	-.0242 ( .9) P= .475	.3671 ( .9) P= .164	-.2190 ( .9) P= .285	-.0972 ( .9) P= .402	-.2762 ( .9) P= .235	.5272 ( .9) P= .071	-.5123 ( .9) P= .078	-.4512 ( .9) P= .110	-.4342 ( .9) P= .120	-4212 ( .9) P= .128
V35	.0416 ( .9) P= .458	-.4392 ( .9) P= .117	.1254 ( .9) P= .374	.0178 ( .9) P= .482	-.4300 ( .9) P= .123	.3393 ( .9) P= .185	.2932 ( .9) P= .221	-.1850 ( .9) P= .316	-.0606 ( .9) P= .438	.1621 ( .9) P= .338	.1592 ( .9) P= .341
V36	-.3965 ( .9) P= .144	-.4602 ( .9) P= .105	-.3838 ( .9) P= .153	.2433 ( .9) P= .263	.2418 ( .9) P= .265	.4425 ( .9) P= .115	.3257 ( .9) P= .195	-.0365 ( .9) P= .463	-.2362 ( .9) P= .270	.2965 ( .9) P= .218	.0883 ( .9) P= .410
V37	.0668 ( .9) P= .432	.0721 ( .9) P= .427	-.4599 ( .9) P= .105	.3739 ( .9) P= .160	.5039 ( .9) P= .082	.0598 ( .9) P= .439	-.0800 ( .9) P= .419	.2608 ( .9) P= .248	.3202 ( .9) P= .199	-.0505 ( .9) P= .449	0337 ( .9) P= .466

(COEFFICIENT / (CASES) / SIGNIFICANCE) n . n IS PRINTED IF A COEFFICIENT CANNOT BE COMPUTED



Table V.2 (cont.) Pearson's correlation coefficients of 36 selected variables from carcasses 9-18

	V28	V29	V30	V31	V32	V33	V34	V35	V36	V37
V2	-.4104 ( .9) P= .135	.7239 ( .9) P= .013	-.0848 ( .9) P= .414	.2400 ( .9) P= .266	-.0292 ( .9) P= .470	.1624 ( .9) P= .338	-.0652 ( .9) P= .434	.1550 ( .9) P= .345	-.3152 ( .9) P= .203	-.0408 ( .9) P= .458
V3	-.4123 ( .9) P= .134	.6530 ( .9) P= .027	.3366 ( .9) P= .187	.3530 ( .9) P= .175	.7062 ( .9) P= .016	.1579 ( .9) P= .342	-.3143 ( .9) P= .204	.0180 ( .9) P= .482	-.0675 ( .9) P= .431	.2723 ( .9) P= .238
V4	.6777 ( .9) P= .021	-.7044 ( .9) P= .016	.0431 ( .9) P= .456	.0266 ( .9) P= .473	-.1522 ( .9) P= .348	-.1283 ( .9) P= .371	-.2305 ( .9) P= .275	.1915 ( .9) P= .310	.2564 ( .9) P= .252	-.3706 ( .9) P= .162
V5	.6180 ( .9) P= .037	-.5628 ( .9) P= .056	-.1165 ( .9) P= .382	.2585 ( .9) P= .250	-.2138 ( .9) P= .290	-.2856 ( .9) P= .227	-.1809 ( .9) P= .320	.4636 ( .9) P= .103	.1711 ( .9) P= .330	-.5647 ( .9) P= .055
V6	-.1649 ( .9) P= .335	-.1397 ( .9) P= .360	.1547 ( .9) P= .345	.0153 ( .9) P= .484	.3685 ( .9) P= .163	.2041 ( .9) P= .299	-.1590 ( .9) P= .341	-.4219 ( .9) P= .128	.4697 ( .9) P= .100	.6240 ( .9) P= .035
V7	.0501 ( .9) P= .449	-.0492 ( .9) P= .450	-.3524 ( .9) P= .175	.8239 ( .9) P= .003	.0834 ( .9) P= .415	-.1588 ( .9) P= .341	.0771 ( .9) P= .422	.4934 ( .9) P= .087	.4613 ( .9) P= .104	-.0816 ( .9) P= .417
V8	-.1205 ( .9) P= .378	-.3529 ( .9) P= .175	-.4474 ( .9) P= .112	-.1332 ( .9) P= .366	-.0024 ( .9) P= .498	-.3074 ( .9) P= .210	.1022 ( .9) P= .396	-.5284 ( .9) P= .070	.3139 ( .9) P= .204	.6596 ( .9) P= .025
V9	-.2951 ( .9) P= .220	.0108 ( .9) P= .489	-.3312 ( .9) P= .191	.1311 ( .9) P= .368	.0128 ( .9) P= .487	-.0101 ( .9) P= .490	.0844 ( .9) P= .414	.0044 ( .9) P= .496	.3639 ( .9) P= .167	.4708 ( .9) P= .099
V10	-.3302 ( .9) P= .192	.1330 ( .9) P= .021	-.4261 ( .9) P= .366	.3563 ( .9) P= .125	.1210 ( .9) P= .172	-.0945 ( .9) P= .378	-.0812 ( .9) P= .404	-.0517 ( .9) P= .418	.3517 ( .9) P= .176	.5340 ( .9) P= .068
V11	.8305 ( .9) P= .002	-.6810 ( .9) P= .021	.0879 ( .9) P= .411	.0617 ( .9) P= .437	-.3916 ( .9) P= .147	.3165 ( .9) P= .202	.2489 ( .9) P= .258	.6478 ( .9) P= .028	.4126 ( .9) P= .134	-.6020 ( .9) P= .042
V12	.5153 ( .9) P= .076	-.2405 ( .9) P= .266	.1693 ( .9) P= .331	.6810 ( .9) P= .021	.1250 ( .9) P= .374	.0971 ( .9) P= .402	-.0639 ( .9) P= .435	.7542 ( .9) P= .009	.3706 ( .9) P= .162	-.5897 ( .9) P= .046

(COEFFICIENT / (CASES) / SIGNIFICANCE) " . " IS PRINTED IF A COEFFICIENT CANNOT BE COMPUTED



Table V.2 (cont.) Pearson's correlation coefficients of 36 selected variables from carcasses 9-18

	V28	V29	V30	V31	V32	V33	V34	V35	V36	V37
V13	-.3591 ( . 9) P= .170	.7281 ( . 9) P= .012	-.1823 ( . 9) P= .319	.4675 ( . 9) P= .101	.3319 ( . 9) P= .190	-.2725 ( . 9) P= .238	-.5414 ( . 9) P= .065	.0416 ( . 9) P= .458	-.3965 ( . 9) P= .144	.0668 ( . 9) P= .432
V14	-.3504 ( . 9) P= .177	.3863 ( . 9) P= .151	.0851 ( . 9) P= .414	-.2669 ( . 9) P= .243	-.0509 ( . 9) P= .448	-.0107 ( . 9) P= .489	-.0242 ( . 9) P= .475	-.4392 ( . 9) P= .117	-.4602 ( . 9) P= .105	.0721 ( . 9) P= .427
V15	.1144 ( . 9) P= .384	.2011 ( . 9) P= .301	-.1170 ( . 9) P= .382	-.0516 ( . 9) P= .447	-.4759 ( . 9) P= .096	.1249 ( . 9) P= .374	.3671 ( . 9) P= .164	.1254 ( . 9) P= .374	-.3838 ( . 9) P= .153	-.4599 ( . 9) P= .105
V16	-.2355 ( . 9) P= .270	.2937 ( . 9) P= .221	-.4672 ( . 9) P= .101	.7170 ( . 9) P= .014	.2670 ( . 9) P= .243	-.2150 ( . 9) P= .289	-.2190 ( . 9) P= .285	.0178 ( . 9) P= .482	.2433 ( . 9) P= .263	.3739 ( . 9) P= .160
V17	-.3034 ( . 9) P= .213	.0662 ( . 9) P= .433	.4110 ( . 9) P= .135	-.0521 ( . 9) P= .447	.5359 ( . 9) P= .067	.2018 ( . 9) P= .301	-.0972 ( . 9) P= .402	-.4300 ( . 9) P= .123	.2418 ( . 9) P= .265	.5039 ( . 9) P= .082
V22	-.0992 ( . 9) P= .400	.0977 ( . 9) P= .401	-.2793 ( . 9) P= .233	.9533 ( . 9) P= .000	.3074 ( . 9) P= .210	-.2229 ( . 9) P= .282	-.2762 ( . 9) P= .235	.3393 ( . 9) P= .185	.4425 ( . 9) P= .115	.0598 ( . 9) P= .439
V23	.0823 ( . 9) P= .416	-.0980 ( . 9) P= .401	.2139 ( . 9) P= .290	.1125 ( . 9) P= .386	.0667 ( . 9) P= .432	.3544 ( . 9) P= .174	.5272 ( . 9) P= .071	.2932 ( . 9) P= .221	.3257 ( . 9) P= .195	-.0800 ( . 9) P= .419
V24	-.1837 ( . 9) P= .318	.4158 ( . 9) P= .132	-.3249 ( . 9) P= .196	.6983 ( . 9) P= .017	.3683 ( . 9) P= .164	-.2987 ( . 9) P= .217	-.5123 ( . 9) P= .078	-.1850 ( . 9) P= .316	-.0365 ( . 9) P= .463	.2608 ( . 9) P= .248
V25	-.6368 ( . 9) P= .031	.8345 ( . 9) P= .002	-.0608 ( . 9) P= .438	.5667 ( . 9) P= .054	.6101 ( . 9) P= .039	-.2343 ( . 9) P= .271	-.4512 ( . 9) P= .110	-.0606 ( . 9) P= .438	-.2362 ( . 9) P= .270	.3202 ( . 9) P= .199
V26	.1123 ( . 9) P= .386	-.2270 ( . 9) P= .278	-.3039 ( . 9) P= .212	.6207 ( . 9) P= .036	.1271 ( . 9) P= .372	-.4576 ( . 9) P= .106	-.4342 ( . 9) P= .120	.1621 ( . 9) P= .338	.2965 ( . 9) P= .218	-.0505 ( . 9) P= .449
V27	.0401 ( . 9) P= .459	.3267 ( . 9) P= .194	-.1151 ( . 9) P= .384	.6014 ( . 9) P= .042	.2190 ( . 9) P= .285	.0954 ( . 9) P= .403	-.4212 ( . 9) P= .128	.1592 ( . 9) P= .341	.0883 ( . 9) P= .410	.0337 ( . 9) P= .466

(COEFFICIENT / CASES) / SIGNIFICANCE " . " IS PRINTED IF A COEFFICIENT CANNOT BE COMPUTED



Table V.2 (cont.) Pearson's correlation coefficients of 36 selected variables from carcasses 9-18

	V28	V29	V30	V31	V32	V33	V34	V35	V36	V37
V28	.1.0000 ( . 0) P= .	-.6065 ( . 9) P= .040	.0986 ( . 9) P= .400	-.1549 ( . 9) P= .345	-.3147 ( . 9) P= .204	.0903 ( . 9) P= .408	-.0504 ( . 9) P= .449	.3704 ( . 9) P= .162	-.0262 ( . 9) P= .473	-.6566 ( . 9) P= .026
V29	-.6065 ( . 9) P= .040	1.0000 ( . 0) P= .	.2149 ( . 9) P= .289	.2610 ( . 9) P= .248	.4803 ( . 9) P= .094	.0334 ( . 9) P= .466	-.2326 ( . 9) P= .273	-.0579 ( . 9) P= .441	-.5407 ( . 9) P= .065	.0784 ( . 9) P= .420
V30	.0986 ( . 9) P= .400	.2149 ( . 9) P= .289	1.0000 ( . 0) P= .	-.1070 ( . 9) P= .392	.5078 ( . 9) P= .080	.4437 ( . 9) P= .114	-.1531 ( . 9) P= .347	.4409 ( . 9) P= .116	-.1590 ( . 9) P= .341	-.4782 ( . 9) P= .095
V31	-.1549 ( . 9) P= .345	.2610 ( . 9) P= .248	-.1070 ( . 9) P= .392	1.0000 ( . 0) P= .	.4839 ( . 9) P= .092	-.2009 ( . 9) P= .302	-.2780 ( . 9) P= .234	.3972 ( . 9) P= .144	.3300 ( . 9) P= .192	-.0167 ( . 9) P= .483
V32	-.3147 ( . 9) P= .204	.4803 ( . 9) P= .094	.5078 ( . 9) P= .080	.4839 ( . 9) P= .092	1.0000 ( . 0) P= .	-.2728 ( . 9) P= .238	-.6744 ( . 9) P= .022	.1244 ( . 9) P= .375	-.1358 ( . 9) P= .363	.0448 ( . 9) P= .454
V33	.0903 ( . 9) P= .408	.0334 ( . 9) P= .466	.4437 ( . 9) P= .114	-.2009 ( . 9) P= .302	-.2728 ( . 9) P= .238	1.0000 ( . 0) P= .	.6054 ( . 9) P= .041	.2129 ( . 9) P= .291	.2943 ( . 9) P= .220	-.1225 ( . 9) P= .376
V34	-.0504 ( . 9) P= .449	-.2326 ( . 9) P= .273	-.1531 ( . 9) P= .347	-.2780 ( . 9) P= .234	-.6744 ( . 9) P= .022	.6054 ( . 9) P= .041	1.0000 ( . 0) P= .	-.0130 ( . 9) P= .487	.3879 ( . 9) P= .150	.0834 ( . 9) P= .415
V35	.3704 ( . 9) P= .162	-.0579 ( . 9) P= .441	.4409 ( . 9) P= .116	.3972 ( . 9) P= .144	.1244 ( . 9) P= .375	.2129 ( . 9) P= .291	-.0130 ( . 9) P= .487	1.0000 ( . 0) P= .	.1471 ( . 0) P= .352	-.7744 ( . 9) P= .006
V36	-.0262 ( . 9) P= .473	-.5407 ( . 9) P= .065	-.1590 ( . 9) P= .341	.3300 ( . 9) P= .192	-.1358 ( . 9) P= .363	.2943 ( . 9) P= .220	.3879 ( . 9) P= .150	.1471 ( . 9) P= .352	1.0000 ( . 0) P= .	.3330 ( . 9) P= .190
V37	-.6566 ( . 9) P= .026	.0784 ( . 9) P= .420	-.4782 ( . 9) P= .095	-.0167 ( . 9) P= .483	.0448 ( . 9) P= .454	-.1225 ( . 9) P= .376	.0834 ( . 9) P= .415	-.7744 ( . 9) P= .006	.3330 ( . 9) P= .190	1.0000 ( . 0) P= .

(COEFFICIENT / (CASES) / SIGNIFICANCE) " " IS PRINTED IF A COEFFICIENT CANNOT BE COMPUTED



Table V.2 (cont.) Pearson's correlation coefficients of 36 selected variables from carcasses 9-18

	V18	V19	V20	V21	V18	V19	V20	V21
V2	.0701 (-.8) P=.434	-.4766 (-.8) P=.114	.2325 (-.8) P=.289	-.5587 (-.8) P=.073	V13 .2320 (-.8) P=.289	-.6262 (-.8) P=.046	.3845 (-.8) P=.172	-.6948 (-.8) P=.026
V3	.2945 (-.8) P=.238	.4420 (-.8) P=.135	.2424 (-.8) P=.281	.5141 (-.8) P=.094	V14 -.2466 (-.8) P=.277	.2858 (-.8) P=.245	-.4468 (-.8) P=.132	.0988 (-.8) P=.408
V4	-.0631 (-.8) P=.441	-.1221 (-.8) P=.386	-.1120 (-.8) P=.395	-.2481 (-.8) P=.276	V15 .2629 (-.8) P=.264	-.3525 (-.8) P=.195	.0043 (-.8) P=.496	-.4760 (-.8) P=.115
V5	.2179 (-.8) P=.301	-.4378 (-.8) P=.137	.2484 (-.8) P=.276	-.5524 (-.8) P=.076	V16 .4075 (-.8) P=.157	-.3448 (-.8) P=.200	.6032 (-.8) P=.055	-.1221 (-.8) P=.386
V6	-.3064 (-.8) P=.229	.6032 (-.8) P=.055	-.2500 (-.8) P=.274	.6729 (-.8) P=.032	V17 -.1118 (-.8) P=.396	.9153 (-.8) P=.001	-.2454 (-.8) P=.278	.9280 (-.8) P=.000
V7	.6931 (-.8) P=.027	-.3849 (-.8) P=.172	.8542 (-.8) P=.003	-.2568 (-.8) P=.269	V22 .6067 (-.8) P=.053	-.2674 (-.8) P=.396	.8283 (-.8) P=.005	-.2401 (-.8) P=.283
V8	-.2711 (-.8) P=.257	.2057 (-.8) P=.312	-.1723 (-.8) P=.341	.4621 (-.8) P=.123	V23 .6196 (-.8) P=.049	.2777 (-.8) P=.260	.4724 (-.8) P=.117	.4565 (-.8) P=.126
V9	-.1515 (-.8) P=.360	-.2456 (-.8) P=.278	.2799 (-.8) P=.250	-.0184 (-.8) P=.483	V24 .4816 (-.8) P=.112	-.1403 (-.8) P=.370	.3072 (-.8) P=.228	-.1520 (-.8) P=.359
V10	-.0744 (-.8) P=.430	-.2912 (-.8) P=.241	.3463 (-.8) P=.199	-.0580 (-.8) P=.446	V25 .4806 (-.8) P=.112	.1529 (-.8) P=.358	.6049 (-.8) P=.054	.2071 (-.8) P=.311
V11	.3134 (-.8) P=.224	-.5772 (-.8) P=.065	.3236 (-.8) P=.216	-.5779 (-.8) P=.065	V26 .1886 (-.8) P=.327	-.2506 (-.8) P=.274	.3702 (-.8) P=.182	-.3378 (-.8) P=.205
V12	.7451 (-.8) P=.016	-.2350 (-.8) P=.287	.6721 (-.8) P=.032	-.3000 (-.8) P=.234	V27 .2309 (-.8) P=.290	-.4338 (-.8) P=.140	.2864 (-.8) P=.245	-.4707 (-.8) P=.118

(COEFFICIENT / CASES) / SIGNIFICANCE " " IS PRINTED IF A COEFFICIENT CANNOT BE COMPUTED



Table V.2 (cont.) Pearson's correlation coefficients of 36 selected variables from carcasses 9-18

	V18	V19	V20	V21
V28	.1144 ( P= .393	-.4122 ( P= .199	-.1827 ( P= .273	-.4503 ( P= .130
V29	.3468 ( P= .264	.2522 ( P= .005	.1547 ( P= .437	.1789 ( P= .335
V30	.2622 ( P= .005	.5730 ( P= .437	.0500 ( P= .001	.3860 ( P= .171
V31	.8246 ( P= .005	-.0672 ( P= .437	.9049 ( P= .001	-.0471 ( P= .456
V32	.4614 ( P= .123	.7259 ( P= .019	.3399 ( P= .204	.6612 ( P= .035
V33	.0376 ( P= .465	.1110 ( P= .396	-.0296 ( P= .472	.0621 ( P= .442
V34	.0217 ( P= .480	-.1379 ( P= .372	.0975 ( P= .409	-.0088 ( P= .492
V35	.6511 ( P= .038	-.3311 ( P= .210	.7480 ( P= .015	-.4286 ( P= .143
V36	.0516 ( P= .452	.0366 ( P= .466	.4518 ( P= .129	.1435 ( P= .367
V37	-.5058 ( P= .099	.3277 ( P= .213	-.2384 ( P= .284	.5050 ( P= .099

(COEFFICIENT / (CASES) / SIGNIFICANCE) " " IS PRINTED IF A COEFFICIENT CANNOT BE COMPUTED













B30406